Environmentally friendly tools for the removal of emerging pollutants from natural matrices

Presentata da: ENRICO BUSCAROLI

SUMMARY

LIST OF ACRONYMS

5

AA	acetic anhydride
A.U.	arbitrary unit
ADI	acceptable daily intake
AMR	anti-microbial resistance
BTEX	benzene, toluene, ethyl benzene and xylenes
C6	*n*-hexane
CP	cross polarization
d	day/days
DAD	diode array detector
DMF	N,N-dimethylformamide
DTPA	diethylenetriaminepentaacetic acid
DW	dry weight
EtOH	ethanol
FA	fulvic acids
FID	flame ionization detector
FT-IR	Fourier transform infrared spectroscopy
GC	gas chromatography
h	hour/hours
HA	humic acids
HM	heavy metal
IUPAC	international union of pure and applied chemistry
LC	liquid chromatography
MAS	magic angle spinning
MCM-41	Mobil composition of matter No. 41
MeCN	acetonitrile
MePh	toluene
MeOH	methanol
min	minute/minutes
MOAH	mineral oil aromatic hydrocarbons

5

MOHs	mineral oil hydrocarbons
MOSH	mineral oil saturated hydrocarbons
MS	mass spectrometry detector
MW	molecular weight
NAPL	non-aqueous phase liquid
NMR	nuclear magnetic resonance spectroscopy
PDA	4-(phenyldiazenyl)aniline
POP	persistent organic pollutants
RT	room temperature
s	second/seconds
SBA-15	Santa Barbara amorphous material No. 15
SC	sulfachloropiridazine
SD	sulfadiazine
SEM	scanning electron microscopy
SM	sulfametazine
SMX	sulfamethoxazole
SS	solid state
T	temperature
TGA	thermogravimetric analysis
UV-vis	ultraviolet – visible spectroscopy
VOC	volatile organic compounds
WWTP	water treatment plant / waste water treatment plant

AIM OF THE THESIS

In this work of thesis, some sustainable remediation techniques for the decontamination of natural matrices have been developed and valued, considering their effectiveness and sustainability. Four different projects concerning sustainable remediation are pointed out and discussed. The original intent shared by these projects is to develop innovative solutions for emerging pollution cases, representing a workable alternative for companies and authorities dealing with contamination of water bodies, wastewaters, sediments, sludge and recyclable byproducts (such as paper pulp).

Some porous synthetic silica materials, commonly used in catalysis, have been studied, valued and adapted for use in pollutant decontamination, thanks to a fruitful collaboration with Prof. Leonardo Marchese of DiSIT (Department of Sciences and Technological Innovation of Università del Piemonte Orientale A. Avogadro) which co-tutored this PhD thesis and offered the essential know-how on the material development.

In the first project (chapter 2) dealt by the present thesis, synthetic high silica (>200 SiO_2/Al_2O_3 ratio) faujasite (Y) used for antibiotics sorption from waste waters (exhausted zeolite) was tested for regenerability: the intent reported was to investigate the possibility to reuse the Y zeolites for the same environmental application (antibiotic sorption from waste water) after solvent desorption or thermal regeneration. As reported in the attached paper, the tested high silica Y has been regenerated with thermal treatments; the most effective (and less costing) temperature and treatment time was determined and the regenerated zeolite was reused for many sorption – regeneration cycles. Another successful option, a solvent desorption, was also validated [1].

In the second project (chapter 3), the heavy hydrocarbons contamination of recycled paper and paperboard – with particular attention to food-contact paperboard – was accounted. The aim of the project was developing a hydrocarbon-specific sorbent material suitable to be used during industrial processes of paper recovery and recycling. In this project, some highly hydrophobic mesoporous materials were tested, adapted and modified for their utilisation in paper mills. The most effective sorbent, capable to retain up to 184% of its dry weight, was a modified (trimethylsilylated-) MCM-41 mesoporous silica. Its capacity to adsorb and retain hydrocarbons from highly wet pulp in paper mill-like conditions were successfully tested in a pilot-scale plant, and the utilization of the said material was patented [2]. In addition, a paper

has been published, reporting the behaviour of the sorbent mixed to waste paper and its ability to retain the hydrocarbons and to limit their migration to food [3].

In the third project (chapter 4), a case study on the heavy metal removal from water sediments is presented. This was the only project where it was not used a synthetic material, but a $CaCl_2$ mild sediment washing technique in order to remove Cu and Zn from a contaminated sediment of a land reclamation consortium canal. Among other washing techniques (e.g. EDTA, hydrochloric acid), $CaCl_2$ washing is supposed to be cheap, to have minor impact on a soil structure and to be less dangerous for operators. In the study presented the treatment efficacy to remove heavy metals is assessed, as well as an aggregate structural stability evaluation post-treatment.

During the research period abroad conducted by the candidate, thanks to a fruitful collaboration with Prof. Francesco Di Renzo of the École Nationale Superieure de Chimie de Montpellier (ENSCM), a multidisciplinary project (chapter 5) on humic substances could begin. The aim of the project was to use humic and humic-like substances (possibly recovered from sustainable sources) for water remediation, exploiting their sorbent capacity to retain pollutants, or facilitate their degradation.

1. INTRODUCTION

Water, soil and land pollution, as well as food contaminations, are serious threats to human health and living, if not a consistent danger for all the biosphere. Containing the spread of undesired or noxious compounds coming from anthropic activities, or cleaning the already polluted or endangered environment is not only a duty toward ourselves and the future generations, but an undisputable necessity.

In the last decades, an increasing awareness has led both the public opinion and the policy-makers (especially in western countries) to care more about the quality and safety of food production and its industry, along with even more pressing requests for a clean environment. As a matter of fact, at a global scale, ensuring and pursuing these needs is one of the most important goals in many countries' government policies, international treaties and communitarian strategies.

Another emerging critical aspect of environmental, food and agriculture legislation is the sustainability of pertinent productions and exploitation [4, 5]. Water bodies preservation, soil fertility maintenance, waste treatment and recycling, organic agriculture and food, manure disposal, sustainable livestock production, etc. are only few instances of many trending topics of great interest for decision makers, local or big producers, large-scale retail traders and end-consumers [6, 7].

In this context, porous synthetic materials can have a strategic role in contaminant removal application. Their effectiveness is granted by the possibility to produce sorbent materials extremely specific to a target pollutant (or class of pollutants); and the reproducibility of their production process (synthesis) can lower their costs. In addition, their production is not extremely relying on fossil chemicals (contrarily to plastics and hydrocarbon polymers) and most of these materials can be recycled after regeneration treatments.

1.1. SYNTHETIC POROUS MATERIALS FOR ENVIRONMENTAL REMEDIATION

In the past, material such as wooden sawdust, chips, straws, clay and sand, sponges and fabric have been always used to remove undesired substances or clarify liquids. The advancements of chemistry and physics during 18th and 19th century made possible to study sorption processes in terms of adsorption enthalpy, surface tension, capillarity, specific surface and intermolecular interaction, which are basic concepts in the field of Material Science.

Yet, the idea to "capture" contaminant molecules using synthetic materials specifically designed and synthesized for that purpose is quite recent, and could be made possible by material characterization techniques such as X-ray diffraction and modern chemical synthesis.

Most of the materials (only few examples are reported in the next pages) available for environmental remediation and research at the present were initially developed for catalysis. One of the first environmental application of a catalysis in history can be found in the catalytic converter, an instrument for the control of gaseous emission of internal combustion engines, which reduce noxious tailpipe gases (e.g. CO, NOx, uncombusted hydrocarbons...). In the past decades, many synthetic materials originally produced to facilitate chemical reaction in industry were adapted and tested for drug delivery, drug uptake, imaging and environmental application. The sorption capacity, pore distribution and surface chemistry of such materials can lead to several different applications, which will be shortly listed in this chapter.

Furthermore, synthetic porous materials have the great advantage to be built, adapted and specifically modified for a desired purpose. Non-synthetic porous materials (such as activated charcoal, bentonite, natural zeolite...) do not always possess the same adjustability.

Porous synthetic materials can be produced in different forms (powder, microbeads, monoliths, pellets), different composition (mostly Si, Al, but also Mn, Cr, C oxides...) and structure (amorphous or crystalline). The porosity is most relevant property of such materials. Essential is the presence of pores, channels, cavities or interstices with a depth higher than their width. The different kind of pores are briefly shown in Figure 1

It is common, inside the very same material, to find pores very different in size. The International Union of Pure and Applied Chemistry (IUPAC) distinguish three different pore size scales:

- Micropores – <2 nm (mean water OH bond length: 0,097 nm, glucose is ca. 1 nm)

- Mesopores – from 2 to 50 nm (mean immunoglobulin dimension: 10 nm)

- Macropores – pores larger than 50 nm
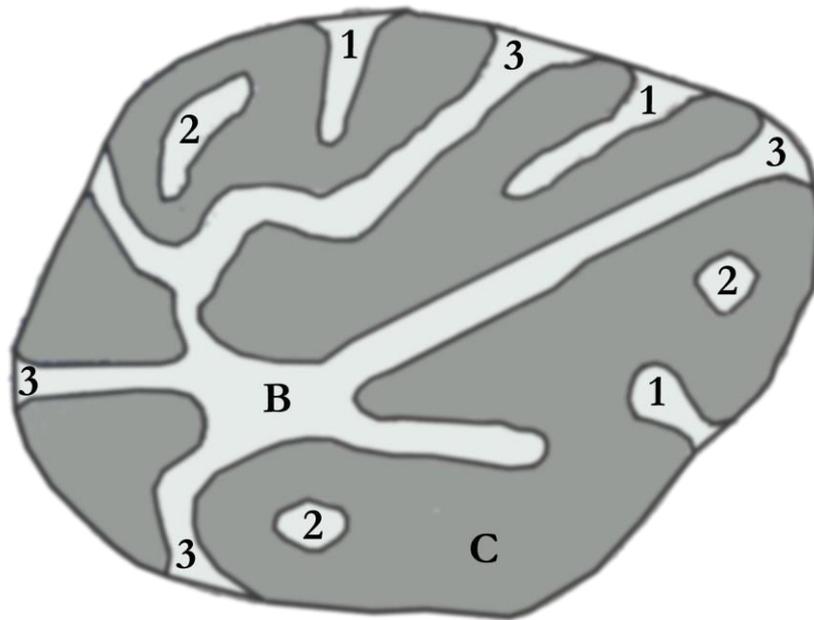
Figure 1: Example of a section of a porous material particle.
A: outer space – B: inner volume – C: solid volume
1: closed pores – 2: inaccessible pores – 3: open pores

Pores can have different size and accessibility, and can be either located on the particle's outer surface or be part of an extensive channel system internal to a particle. Pore size is often indicated as a mean diameter: most of porous materials, especially the amorphous ones (e.g. fumed silica), have a rather large pore size range. Only templated materials, such as synthetic zeolites, have uniform (unimodal or ordered) size of pores. In Figure 2 are shown two possible pore distributions.

Density of a porous material can be considered "true" (considering mass and volume of the solid network only), "apparent" (considering also the closed and inaccessible pores) and "bulk" (considering also the open pores and inter-particle voids. Pore volume V_p is often intended as the volume of the whole pore system, but it is also possible to measure the volume of a specific class of pores only (e.g. macropores volume, mesopores volume and micropores). Porosity can be described as the apparent volume fraction constituted by open

and/or closed pores (inter-particle voids are not considered). Furthermore, the specific surface area is related to all inner (accessible/detectable) and outer surfaces per mass unit. Many physical characterization techniques are available to assess the textural properties of solids such as density, porosity, specific surface area, and pore size [8]. Some of these properties can be measured in several ways. Here is a non-exhaustive list [9, 10]:

- Stereology and microscopy observations: consists on the direct observation of a material sample. Material samples are prepared and observed through Scanning or Transmission microscopy. Repeated observations and measurements, once processed statistically can return mean particle size and mean pores size. Despite this method seems not precise and time-consuming, in some cases it has shown a huge accuracy, since it is not based upon a physical model, but only on observation.

- Scattering radiation techniques are a group of non-destructive analysis routinely used to determine the physical structure and properties of a sample. A porous solid scatters an electromagnetic beam depending on the wavelength and its pores size. The angular distribution and the intensity of the scattered beam gives information on the surface area and the porosity. Different monochromatic beams of X-rays, light or neutron beams can be used, depending on the material to characterize. X-Ray Diffraction analysis (XRD) belongs to this technique family, for the assessment of reticular structure of crystalline solids (e.g. zeolites and zeotypes).

- Pycnometry is the measurable volumetric displacement of a liquid penetrating into a solid's open pores. The displaced volume is used to calculate the apparent density of the solid. Both the liquid and the solid have to be degassed.

- Gas adsorption is the most exploited conservative technique, which provides insightful information on specific surface and pore distribution. Monolayer sorption isotherms of probe gases such as N_2 or Ar are registered with volumetric or gravimetric methods at the boiling points (77 K for N2 and 87 for Ar) preceded and followed by material outgassing. The Brunauer-Emmett-Teller (BET) model derives the surface area and pore distribution from the obtained curve. The only limit of this quick, accurate and automatic techniques is the assessment of microporosity. Inside micropores the interactions between sorbate molecules make them condensate inside pores, making monolayer model inapplicable.

- Mercury porosimetry is a destructive (considered so) technique in which at a very well-controlled temperature, pressured mercury is pushed into the degassed sample. As the

pressure applied increases, the mercury enters smaller pores (up to 3.5 nm). Correlating the applied pressure and volume reduction, is it possible to derive a volumetric distribution of pores (once again, micropores are excluded).
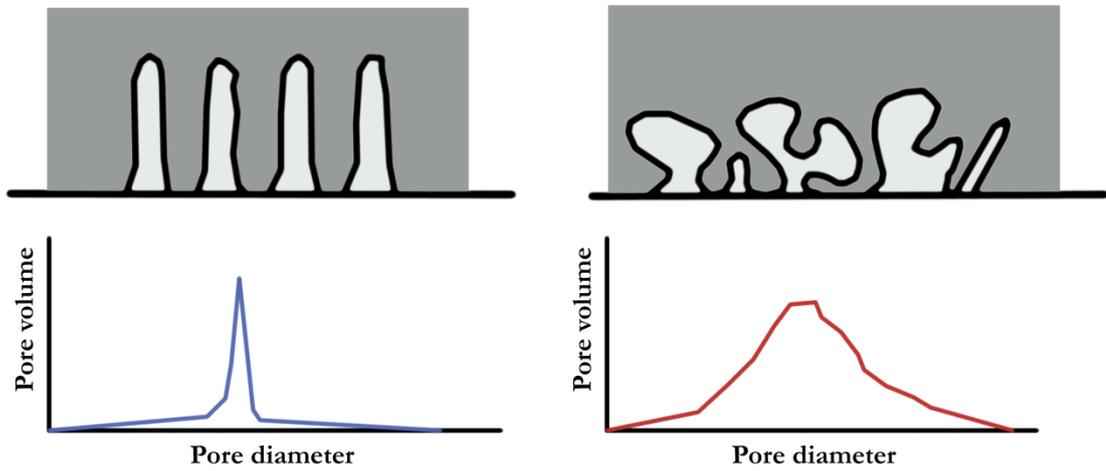
Figure 2: Two examples of pore distribution. On the left, a unimodal distribution of uniform pores (ordered porosity). On the right, a unimodal heterogeneous distribution

1.2. MESOPOROUS SILICAS

The first procedure to produce mesoporous silicas was patented in 1970, but only during the nineties these materials were deeply studied and produced. Notable examples of mesoporous amorphous structures with ordered porosity are the M41S material family, synthesized by Mobil corporation in 1992 (now ExxonMobil corp.). These are MCM-41, MCM-48 and MCM-50 (MCM is the acronym for Mobil Composition of Matter), and they have a monomodal pore size range between 2 and 10 nm. University of Santa Barbara subsequently developed another amorphous silica with ordered mesopores (4.6-30 nm pore size), with the name of SBA-15 (Santa Barbara Amorphous type material no. 15). Beside the pore size, both M41S and SBA15 materials have high specific surface and an amorphous, rigid structure stable in water and most organic solvents.

According to IUPAC, mesopores can space from 2 to 50 nm. Molecules entering such pores can only move in the pore cavity by surface diffusion or Knudsen diffusion (typical for molecules diffusing via gas in pores shorter than their free path). On the contrary to macroporous systems, bulk diffusion and viscous flow are not usually possible in mesopores cavity. As the superficial silanol functions are acidic (with a resulting $pKa \approx 6.8$) [11] they are easily deprotonated in water. [12]

Mesoporous silicas are usually synthesized in hydrothermal conditions with the aid of amphiphilic molecules forming micelles in a water solution, which serve as a template for the silica structure. Subsequently, the silica source is added and starts to polymerize around the template. After the polymerization is concluded, the template is removed by calcinations and/or extraction in slightly acidic alcoholic solution. The use of different surfactants at different concentrations affects the framework structure of the material (e.g. for the M41S, different cetyltrimethylammonium bromide concentrations are used to obtain MCM-41, MCM-48 or MCM-50).

Mesoporous materials have been extensively studied in the last two decades. Their amorphous silica surface can be modified by adding organic moieties [12, 13] and even metal catalysts nanoparticles [14, 15], thus increasing enormously the versatility of their use. Significant applications, apart from catalysis, have been experimented and reviewed. Few notable advances can be mentioned on gas storage improvement [16], sorption of heavy metal and radionuclide complexes [17, 18], drug delivery [19, 20] and contaminant removal from wastewater [21].

1.3. ZEOLITES

Zeolites, meaning literally "boiling stones" from the greek term ζέω λίθος, are aluminosilicates (3D tectosilicates) with a crystalline microporous structure. Their small pores (<1 nm) can host small molecules and cations. The term refers to both naturally occurring and synthetic zeolites. Their crystal structure is composed by silica made of *tetrahedra* sharing the bonded oxygens in regular 3-dimensional patterns, where silicon atoms are partially substituted by aluminium. The result is a regular and extensive channels-and-cages network which constitutes the microporous architecture. The possible crystalline frameworks are theoretically millions, but only 232 have been discovered or synthesized and catalogued so far. Each of these is identified by a unique code of three letters (e.g.: MOR, FAU, SOD, BRE...). The zeolite general formula is

$$M^n_{x/n}Si_{1-x}Al_xO_2 \cdot yH_2O$$

In which:

- M is a cation (Na^+, K^+, Li^+, Ag^+, NH_4^+, H^+, Ca^{2+}, Ba^{2+}) and n the cation positive charge
- X is the number of Al atoms substituting silicons in the reticulum. According to Loewensteins rule, two Al atoms cannot share an oxygen, since a reticulum with a Al-O-Al bond would not be a zeolite. Thus, only less than half of the Si atoms can be substituted by Al ($x < 0.5$). The ratio $(1-x)/x$ is the Si/Al ratio, which must be higher than 1 for the same reason. The higher is the ratio, the more organophilic the zeolite is, since the less is the number of negative charges that have to be balanced by counter cations.

Cations present in the micropore system can be easily exchanged, making low Si/Al zeolites ideal for ion exchange applications (e.g. water softening) and catalytic processes, but also drinkable water remediation [22], VOC sequestration and cleavage [23] and even the containment of environmental spread of radioactive elements [24]. The uniformity of their porous structure make them ideal molecular sieves [25].

Zeolite synthesis is commonly performed in basic sol-gel medium under hydrothermal conditions using silicate and aluminate salts, pH regulators, water and organic templates. Synthetic zeolites are incredibly adaptable and versatile materials, owing to their possibility to be tuned during their preparation. In fact, synthesis conditions can be modified (e.g. changing Si/Al ratio, templating agent, pH, temperature, counter-ion...) to obtain different frameworks with different surface affinity.

Faujasite
[FAU]
Zeolite X and Y

Mordenite
[MOR]

ZSM-5
[MFI]
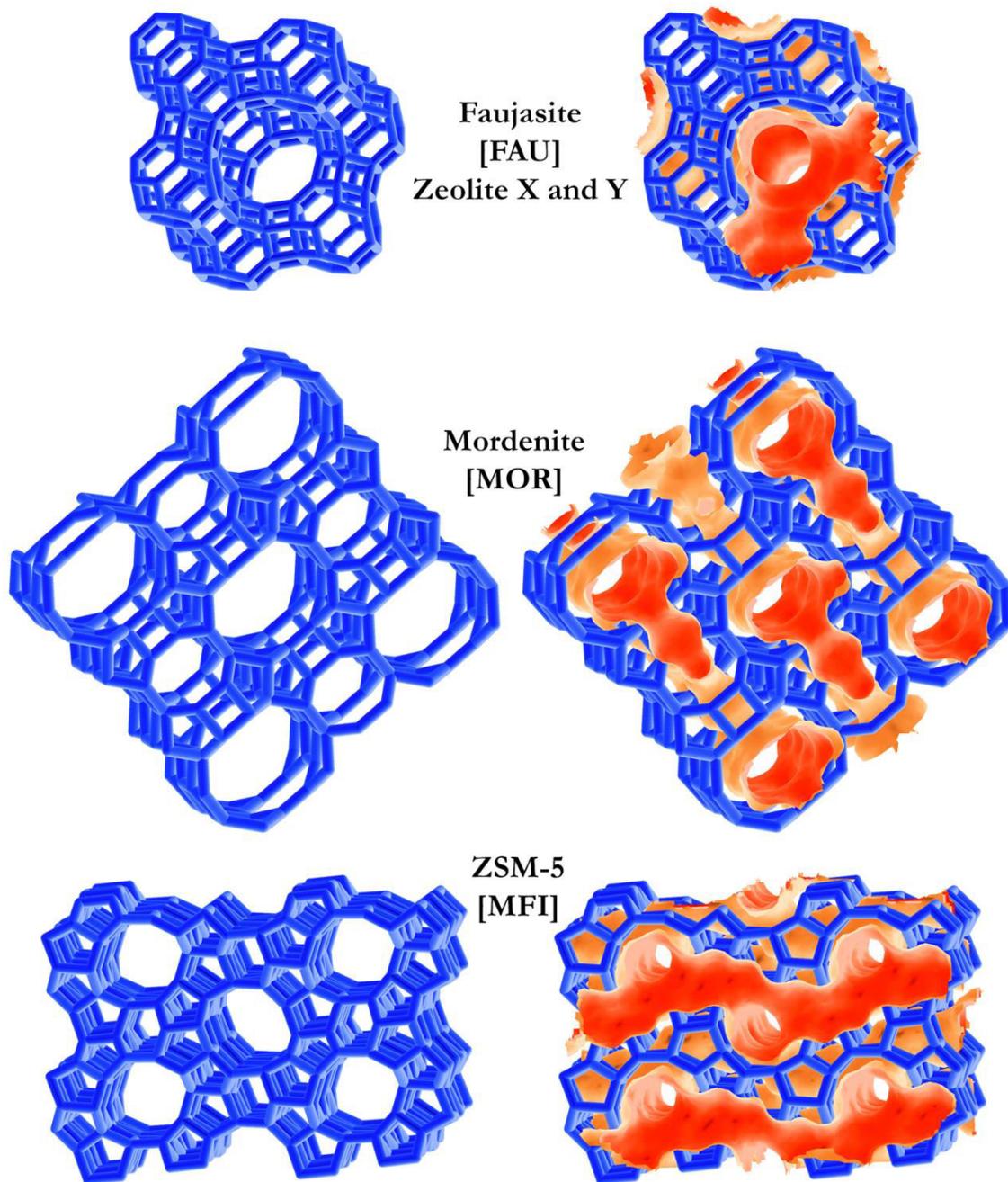
Figure 3: Framework of faujasite, mordenite and MFI structures (left) with their channel/cage system highlighted (right). The framework code is in square brackets.

2. Physico-chemical regeneration of high silica Y zeolite after adsorption of sulfonamide antibiotics from water.

2.1. INTRODUCTION

The presence and consequences of drug molecules in the hydrosphere, due to human activities, has been addressed in environmental chemistry as one of the most worrying problem threatening human and ecosystem's health. Anti-inflammatory, antibiotics, contraceptives and hormones, beta-blockers are only a few examples of pharmaceuticals detectable in surface waters or hospital wastewaters. Exposure to these chemicals on organisms, apart from showing toxic activities dependant on dose and composition [26, 27], may have other more severe consequences, as it will be discussed in this chapter.

Antibiotics are an extremely important class of drugs, whose discovery in the 20th century completely revolutionised the treatment of bacterial infections, and therefore medicine [28].

2.1.1. Anti microbial resistance and animal husbandry

Without considering those destined to human consumption, one third of European antibiotics demand is covered by animal productions and veterinary use [29]. Administering antibiotics to livestock has various purposes: i) treatment and prevention of bacterial-caused diseases such as mastitis in cattle and E. coli infection in poultry ii) prophylactic treatment during stressful phases of the production cycle (e.g. weaning or transport) iii) extensive utilisation as growth promoter (especially in USA, whilst Europe progressively banned this practice since 2003) for swine and poultry production [30, 31].

Once delivered their pharmaceutical activity, antibiotics are normally excreted by the organism through faeces and urine. Excreted compounds aregenerally altered by metabolic processes [27, 32], which transform the molecule in different compounds (e.g.: by conjugation, hydrolysis, oxidation...). Though, this is not true for particular classes of antibiotics such as sulfonamides, which are excreted mainly unaltered or in reversible forms [33, 34].

The most serious risk connected to the massive use of antibiotics and their spread into the environment is represented by the insurgence of anti-microbial resistance (AMR). Occurring of AMR has been documented, reviewed and described extensively in the last decades. Risks and consequences to this phenomenon take place in two possible ways:

- Animal exposure to antibiotics leads to the selection of antibiotic-resistant pathogens directly into the animal organism (or human patient), and resistant pathogens outbreak among close individuals, causing diseases untreatable with that molecule [35, 36].
- Antibiotic dispersed into the environment cause, at a local level, the selection of antibiotic-resistant *microbiota*: point sources (usually manure, sewer, urban wastes, waterstreams) of a recalcitrant antibiotic cause ecological disruption throughout all the living organisms of the food chain, and possibly back to the individuals treated by that molecule in first place [31, 37, 38]. For this particular reason, it is of primary relevance to keep monitoring the presence of resistant strains in the environment, as potential pool of AMR genes [39, 40]. Even drinking water, in the past, was found to contain immune bacteria [41, 42].

Antibiotics have been used in human and veterinary medicine for more than 60 years ensuring the health of both animals and humans [43]. As a consequence of the selective pressure exerted by antibiotics and the spread of difficult-to-treat multi-drug resistant (MDR) pathogens observed during last two decades, it is now a common opinion that their use has to be strictly controlled in human and veterinary (farm animal and pets) settings to avoid selection and spread of resistant bacteria. In the EU, 25000 patients die annually as a result of infections caused by these superbugs with about 1.5 billion € annually of estimated costs [44]. Animals and animal wastes are a potential reservoir of multi-resistance genes that can be transmitted directly or indirectly to humans through contact and food consumption [45]. Moreover, scientific literature highlights the transmission of AMR bacteria from livestock effluents/manure to food of animal origin and into the water-soil system with increasing health risk [46]. In microorganisms, AMR is a natural defence mechanism realized through genetic modifications triggered to survive the drug action. In several conditions, the genetic material bearing AMR can be shared among different bacterial species through horizontal gene transfer, like bacterial conjugation and the so-called "R-plasmids" [47]. AMR spreads up as a favourable phenotype by the selective pressure caused by the antibiotic occurrence in specific contexts as hospitals and livestock farming. Since antibiotics are life-saving drugs for

humans and animals (in many situations the same molecule is used for both), it is of utmost importance to limit their administration when they are strictly necessary and to prevent their environmental spreading as much as possible. The AMR issue has been publicly recognized by the World health Organization (WHO), as well as the Council and the European Parliament, and the EU Commission [48, 49].

2.1.2. Sulfonamides antibiotics

Sulfonamides antibiotics (sulfa drugs) are synthetic derivatives of sulfanilamide used in medicine since 1930' for their bacteriostatic effect. They have been (and still are) used widely to treat infections caused by bacteria, fungi and protozoa in human therapy, animal husbandry and aquaculture [50]. Sulfa drug's structure is reported in Figure 4: R2 is generally an heterocyclic group (or an hydrogen in the case of sulfanilamide). They serve as competitive inhibitors of dihydropteroate synthase, an enzyme involved in the microbial folate (vitamin B9) synthesis. These drugs inhibit the growth of microorganisms but do not kill them directly. Sulfa drugs do not affect human and animals since they acquire folate by diet.
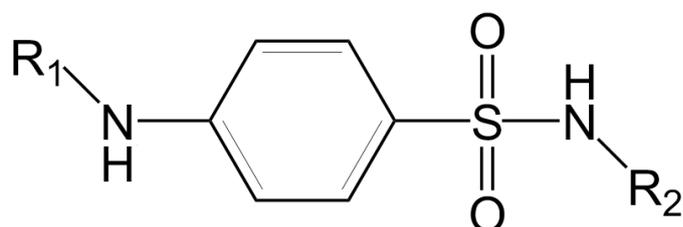
Figure 4: Base structure of sulfonamide antibiotics. R2 is generally an heterocyclic group

Microorganisms can develop AMR by being exposed to sulfonamides: the resistance mechanism involved is called *bypass*, since a metabolic alternative pathway can eventually be adopted by microorganisms to synthesize folate and continue their growth [51].
These molecules are recalcitrant and chemically stable in manure, where they can be found abundantly (up to 20 mg kg^{-1} in some conditions [52]) and where they still carry out residual bacteriostatic activity until the manure is spread into soil [53]. Pasture grazing also produces the same effect. Once in soil, they may remain unaltered for even months [33, 34].
In liquid dejections they are excreted as a N-aniline acetyl conjugates which are spontaneously transformed back again into the parent compounds [54]. In addition, due to

their weak acidity (pK$_a$ 4-7), they are anionic in the pH range 4.5-8.5 (as it is the case of soil water, liquid dejections, surface waters, etc…). Owing to the net negative charge of soil, they result only partially adsorbed by soil, thus sensibly mobile along soil section and in natural waters[55-57]. Thiele-Bruhn and co-workers evaluated the sorption to soil particles of five sulfa drugs (namely sulfanilamide, sulfadimidine, sulfadiazine, sulfadimethoxine, and sulfapyridine) in different soil profiles, confirming that adsorption was highly pH-dependent and generally higher for molecules with more aromatic group and electronegative moieties [58]. For the five sulfonamides were found a Freundlich sorption coefficient (k$_F$) spacing 0.5 to 6.5 and $1/n = 0.76$, the nonlinearity of fitting curves was hypothesized to be due to specific molecular interaction. These findings were confirmed by Schwarz et al. [59], which underlined the importance of H-bondings and dipole-dipole interactions for the sorption of sulfonamides into soil humic matter.

Bearing an amino group and a sulfonamide hydrogen, all sulfa drugs have at least two proton acceptor/donor moieties. Below pH 2-3 the amino group nitrogen is associated into a –NH$_3^+$ function, whilst above pH 4-8 the sulfonamide hydrogen can dissociate from the –SO$_2$-N$^{(-)}$-R group. The exact pK$_a$ values depend on the presence of other functional group capable to lower/raise the two pK$_a$s. Nevertheless, for natural water's pH and soil solutions, most of sulfa drugs assume a negatively charge.

As these antibiotics are massively used, their input rate in the environmental systems is higher compared to their very low biodegradation rate: their persistence guarantees in this way they could continue to exert pressure to indigenous *microbiota* for long time. Another critic scenarios is often represented by open aquaculture plants in which fish is treated with sulfonamides, making the spread of resistant pathogens in fresh waters likely (if not certain, depending on the fish farm waste water management). Sulfonamides are in fact authorized for use in aquaculture for the treatment of furunculosis and enteric redmouth disease [60]. Not only they can induce AMR on bacteria causing diseases to farm fish, but on environment indigenous *microbiota* too, through plasmide exchanges (conjugation) [61-64].

Additional details on risk assessments and real cases contamination are summarized in more recent reviews on the topic [35, 36]. In this work of thesis (project A), an efficient sorbent for water remediation from sulfa drugs, high silica faujasite (zeolite Y) was tested for physical and chemical regeneration after the sorption of four sulfonamides.

2.1.3. State of art

Wastewater treatment plants (WWTP) can fail to achieve a satisfactory removal or degradation of sulfonamides antibiotics from sewage effluents [65, 66]. Fish farms and hospitals water treatment plants, along with slurry collecting pools in animal farms, represent critical points source of antibiotics. Therefore, in order to prevent antibiotics dissemination, comprehensive monitoring activities and risk analysis have to be established for these sites, even plant modification or post-treatments.

Biological degradation has many limitations for sulfonamide degradation, as these drugs are not easily retained by activated sludge (due to their anionic nature at neutral-basic pHs) or do not represent a convenient carbon source for microorganisms [67]. In addition, sulfa drugs retained by the microbial film (i.e. activated sludge) are not always degraded, thus they continue to carry on their AMR-inducing activity [68]. Chemical methods such as photo-degradation, photo-oxidation and photo-Fenton are much more effective, but they often require chemical reagents input (such as $FeCl_3$, H_2O_2 or persulfate salts [69]).

Sorption approaches have been taken into account much more frequently in the last years. Favorable sorbents revealed to be activated charcoal, biochar, carbon nanotubes or modified carbon nanotubes, clay minerals and zeolites (especially) [67]. Particularly, sulfa drug aqueous sorption into synthetic zeolites presents many advantages [70-72]:

- Certain high silica framework type are highly specific to host sulfonamides molecules in their pore system with an irreversible adsorption.
- Dissolved organic matter do not occlude the zeolite pores. On the contrary, some small organic molecules can make the sulfonamide sorption even more favourable through the formation of a stable guest-guest adduct within the zeolite cage [73].
- Zeolite structure is greatly stable, reproducible and cheap to synthesize
- The solid crystalline structure could bear harsh physical/chemical regeneration treatment, making possible to be reused.

2.1.4. Aim of the project

Despite there are several research activities on the physico-chemical treatments to degrade sulfonamides [69, 74, 75], as well as on the regeneration of sorbent materials used for sulfa drug removal from water (e.g.: spent activated charcoal) [76], the possibility to regenerate spent high silica zeolites used for sulfonamides sorption remains to be established.

This project aims to evaluate different techniques to regenerate hydrophobic high silica zeolite Y (faujasite) in order to dispose/destroy the sorbate and reuse the sorbent for further water treatment cycles. In this study, photolysis, Fenton-like reactions, thermal oxidation and solvent desorption were tested on sulfonamide-loaded zeolites Y. The considered sulfonamide molecules, chosen for their diversified chemical structure, were sulfadiazine (SD), sulfamethazine (SM), sulfachloropyridazine (SC) and sulfamethoxazole (SMX), as reported in Figure 5.
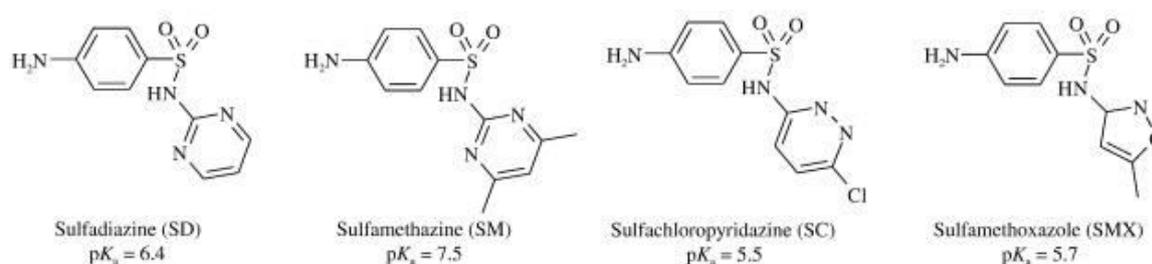
Figure 5: structure and pKa of the four considered sulfa drugs.

Stock solutions of each selected molecules were prepared with both deionised water and filtered river water; high silica zeolite Y samples were loaded with each different sulfonamide stock solution. Photodegradation, Fenton-like reaction, thermal degradation and chemical desorption trials were hence performed. To assess their efficacy, infrared spectroscopy (FT-IR) and thermo-gravimetric analysis (TGA) were carried out on treated zeolites.

After treatments, zeolite samples were subsequently analysed by X-ray diffraction (XRPD) to assess if those processes altered their structure. Repeated sorption trials were also performed on successfully regenerated zeolite samples.

This study represents the prosecution of an in-depth mineralogical study on the same thermally treated zeolite [77].

2.2. MATERIALS AND METHODS

- SD, SM, SC and SMX were purchased from Sigma-Aldrich (USA). Powdered Y type faujausite high silica (200 SiO_2/Al_2O_3 mol:mol ratio) zeolite (HSZ-390HUA) was purchased from Tosoh Corp. (Japan).

- Stock solutions of each sulfonamide at their maximum solubility were prepared both in Milli-Q® water (Merck KGaA, Germany) and natural river water. This which was sampled from the Italian river Reno in Bologna province, filtered to 0.22 μm (Millipore-Merck, Germany) and characterised before use. Concentration of the stock solutions were analysed by High Performance Liquid Chromatography with a Diode Array Detector (HPLC-DAD).

- Samples of zeolites loaded with each single sulfonamide were obtained by adding stock solution aliquotes to weighed amount of zeolite powder, using enough solution to completely load the zeolite. Maximum loading capacities of zeolite Y for the considered sulfonamides were assessed by HPLC-DAD and were: 15, 21, 26, 24% on zeolite dry weight (DW) for SD, SM, SC and SMX respectevely. The quantitative analysis, confirmed experimental results already obtained in literature [70, 72].

- Photolisis was performed through an artisanal rotative Rayonet reactor equipped with 4 mercury lamps (Rayonet RPR-2537, USA). The photolisys was tested for 10, 30 and 60 min at 271 nm wavelenght for SC-loaded zeolite samples and 254 nm for the other sulfonamides. The quartz vessel inside the reactor contained 10 mL of acqueous suspension with 20 mg of loaded zeolite. Photolysis of sulfonamides solutions without zeolite were carried out as control. Constant magnetic stirring and external ventilation assured homogeneus irradiation and avoided overheating. After the desired amount of time, the zeolite samples were hence removed from the reactor, filtered, air-dried and analysed by TGA and FT-IR to evaluate if any reaction products was left.

- Fenton-like reaction tests took place in beakers in which 20 mg of loaded zeolites were suspended in 10 ml $FeCl_3$ solution (two concentrations were tested, 10 and 40 mmol L^{-1}) and stirred for 2 h at 3000 rpm. H_2O_2 solution (200 or 600 mmol L^{-1}) was added drop by drop until gas production stopped. The pH was monitored to remain <2 throughout the reaction. After 6 h the stirring was stopped and the suspension was left quiet for 2 additional hours. Zeolite was hence filtered and air-dried for TGA and FT-IR analysis.

- Thermal treatments were performed at five different temperature (400, 450, 500, 550 and 600 °C) for 1 to 8 h, using 40 mg of SD, SM, SC or SMX loaded zeolite (from both deionised and river water) in a Carlo Erba static lab furnace.

- For the solvent-assisted extraction it has been used water, acetonitrile and methanol in pure form or in different mixture combination. Solubility of the four sulfonamide in each solvent (or solvent mixture) was preliminary assessed. Sulfonamide-loaded samples of zeolites (both by deionised and river water) were suspended in 5 mL of each mixture and kept magnetically stirring at ca. 400 rpm for 1, 5, 10, 20 and 30 minutes. Zeolite was hence filtered and air-dried for further analysis, whilst spent solvent was analysed by HPLC-DAD after dilution to prevent detector saturation.

- Infrared spectra (FT-IR) of treated zeolites in the form of self-supporting pellets obtained with a mechanical press (SPECAC, UK) were registered with a Tensor27 spectrophotometer (Bruker, USA) equipped with a KBr sample cell connected with a vacuum line (residual pressure ca. 10^{-2} Pa).

- XRPD diffraction patterns of the thermally treated zeolite were registered with a Bruker D8 Advance Diffractometer (USA).

- HPLC analysis were performed by a Jasco (USA) chromatografic set-up consisting in a pump, eluent degaser, an autosampler, a Water Spherisorb C8 column, a column heater and a DiodeArray detector.

- Thermogravimetric analyses were operated with a TGDTA92 thermic balance (Setaram, FR). The system was calibrated with the transition temperature of indium.

2.3.   RESULTS AND DISCUSSION

- Photolysis: half life time in deionised water solution at 254 nm of the pure sulfonamides were determined to be 12, 39, 16 and 60 minutes for SD, SM, SC, SMX respectively, as expected from similar works available in literature [75, 78]. Photolysis tests for sulfonamide-loaded zeolite, though, revealed that after an hour treatment, more than 90% of the sorbed material remained unaltered. TGA-DTG analysis of loaded zeolites treated with photolysis, compared to an untreated sample, showed that most of the sorbed organic mass was still present inside the zeolite. Further IR analysis confirmed the treatment inefficacy as the spectra of control and samples exposed to photolysis were not significantly different. Photolysis was thus not considered a viable option to regenerate sulfonamide-loaded zeolite Y.

- Fenton-like reaction: the degradation of the four sulfonamides in deionised water solution revealed to be rapid, with half-life time of only few seconds at all the Fe^{3+} and H_2O_2 concentrations tested. Nevertheless, the same reaction operated for 60 min on sulfonamides trapped in the zeolite cage was unsatisfactory for all the reagent concentrations and for all sulfonamides (according to TGA/DTG analysis and FT-IR spectra). TGA analysis showed that the organic residue on the Fenton-like treated zeolites was always above 88% of the initial loading; over more, the derivative of the thermograms (DTG) showed an additional endothermic peak at higher temperatures, comparing to sulfonamide thermal pattern. This seemingly suggested that more thermally stable reaction products formed as the oxygen radicals and the trapped sulfonamides partially reacted. A poor and slow diffusion of •OH and •OOH radicals inside the loaded zeolite was hypothesized to explain the poor efficacy of the treatment [74].

- Thermal treatment: owing to the notable thermal stability of high silica zeolite in air [79-81], the most efficient treatment setting was established, in order to completely degrade loaded sulfonamides using as few energy consumption as possible. A temperature of 500 °C and a treatment duration of 4 hours revealed to give the best performances in the static air furnace used for these treatment, degrading all the sorbed sulfonamides (according to IR analysis, as well as TGA reported in Figure 6).
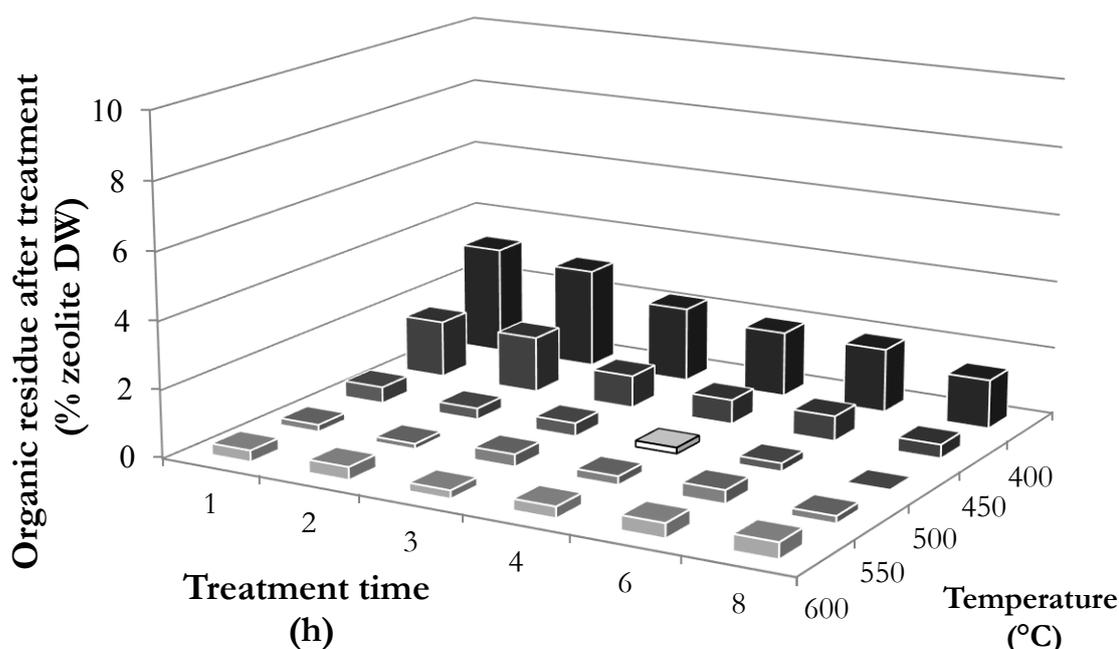
Figure 6: organic residue left on zeolite after thermal treatment at different temperature and for different treatment time

XPRD patterns of bare, loaded and regenerated zeolite were also registered, revealing that its crystalline structure is "flexible" enough to undergo a slight deformation when loaded of sulfonamides (resulting in cell parameter modification), but when regenerated, the original diffraction pattern and cell parameters seems to be resumed again. Additional sorption trials were then performed: in all cases, loading capacity of zeolite Y for each of the selected sulfonamide was not altered after up to 3 cycles of loading/regeneration. For SMX the cycles were extended up to 7: in that case the loading capacity after regeneration was never altered as well.

- Solvent-assisted desorption: water, methanol and acetonitrile were used pure, in binary or ternary mixtures. Samples of sulfonamide-loaded zeolites were exposed for 30 minutes to the selected solvents. Water was not able to desorb sulfonamides from zeolite Y significantly, confirming the irreversibility sorption nature of sulfa drugs by water. Acetonitrile alone was only able to extract ca. 60% of loaded SMX, whereas was not able to desorb the other three (more than 89% remained inside its structure).
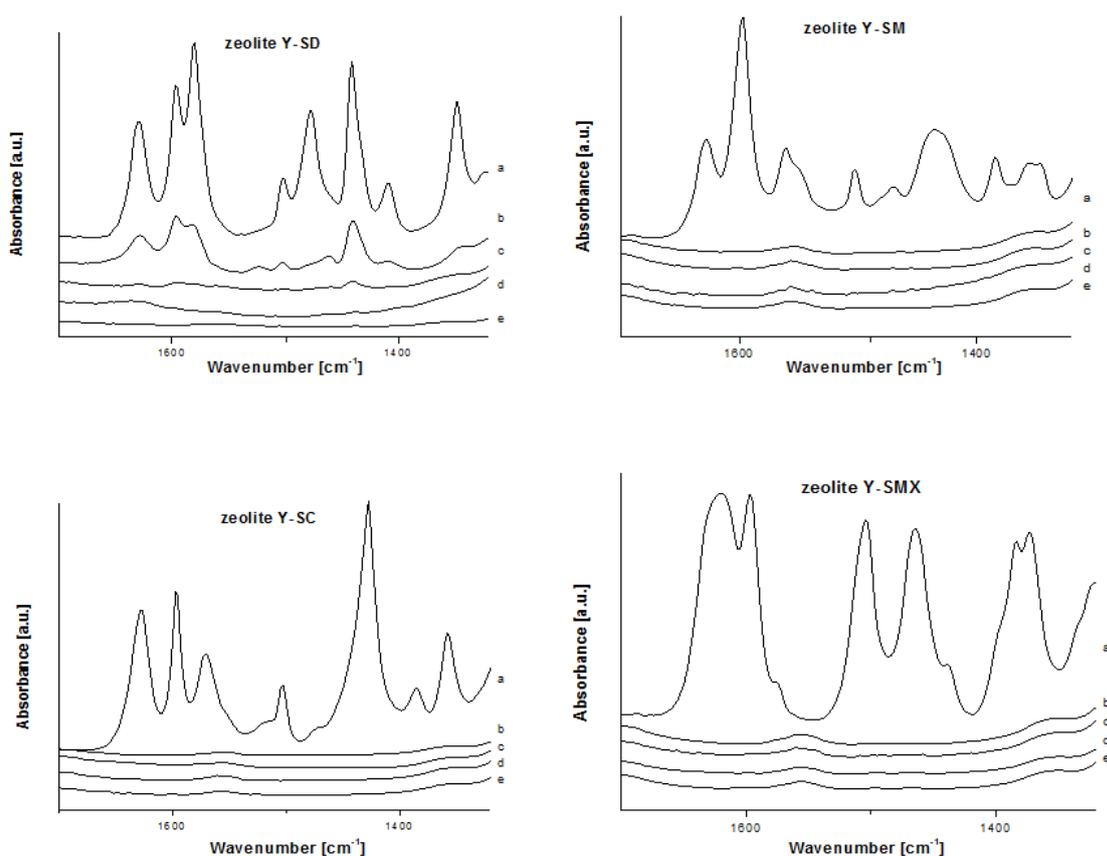
Figure 7: FT-IR spectra of high silica zeolite Y loaded with SD, SM, SC SMX before (a) and after extraction with CH₃CN/CH₃OH/H₂O = 33/33/33 (*V/V/V*) ratio with the extraction durations for (b) 1, (c) 5, (d) 10, and (e) 20 min.

Pure methanol was not able to effectively remove sulfonamides either, nor were able the methanol:acetonitrile binary mixtures. The best extraction was obtained with a 1:1:1 (pH 6 water, acetonitrile, methanol) ternary mixture, which succeeded to extract 92% of the loaded sulfonamides on average. In Figure 7 are reported the IR spectra of loaded zeolite samples before and after extraction by the ternary mixture at different times (1, 5, 10 and 20 minutes). For all the sulfonamide, the desorption equilibrium is quickly achieved (after 1 minute), with the only exception of sulfadiazine, which desorbs more slowly. This was explained by the occurrence into the zeolite cages of the bulky SD-SD dimer as demonstrated in previous works [82, 83].

2.4.   CONCLUSIONS

Among all the regeneration treatments tested, the solvent extraction with the acetonitrile/water/methanol ternary mixture, as well as a 4 h thermal treatment at 500° successfully removed sulfonamides antibiotics from high silica zeolite Y, allowing thus its reuse for water treatment.

Solvent extraction removed in a single step 92% on average of the loaded sulfonamides, thus suggesting that a comprehensive recirculating extraction-distillation apparatus could be set for a continuous extraction of loaded zeolites and recycling of the extracting solvent mixture. Alternatively, a thermal regeneration can achieve a complete oxidation of the organic matter in the most efficient way. Further studies shall be aimed to apply these treatments at pilot-scale conditions, using zeolites loaded from real wastewaters, in order to establish the performances of this technique and improve it.

3. Trimethylsilylation of mesoporous MCM-41 for the decontamination of recycled paper pulp from mineral oil hydrocarbon

3.1. INTRODUCTION

Recycled cellulose, a material commonly considered safe and sustainable, may suffer from severe contamination from heavy hydrocarbon [84-87].

Offset printing is one of the cheapest and most common technique for paper and paperboard printing. The ink pigment is dissolved in solvent mixture composed of medium and heavy hydrocarbons (C15-C40), with up to 20% aromatics ("technical grade" mineral oil). As the most volatile fraction evaporates, the pigment fixates on the cellulose substrate. Nevertheless, not all the mineral oil printing solvent is removed: high boiling hydrocarbons (still present in the commonly used offset oil) do not evaporate and remain physically adsorbed into paperboard. As a consequence, freshly printed paperboard and recycled cellulose end up containing up to hundreds mg kg^{-1} of hydrocarbons [88, 89].

Mineral oils used for offset printing have a heterogeneous composition and can contain both saturated and aromatic hydrocarbons. Mineral Oil Saturated Hydrocarbons (MOSH) consist in heavy paraffins (C24-C40) and lower boiling hydrocarbons (C12-C24) and also a certain amount (<20% in technical grade oils, as specified above) of alkylated aromatic hydrocarbons (the aromatic component is called MOAH, or Mineral Oil Aromatic Hydrocarbons) [90]. A refined mixture, which does not contain any aromatics, is often called "white" mineral oil, but it is not much used in printing since it is not cost-effective.

The main risk represented by mineral oil hydrocarbons (MOH) in cellulose is their tendency to migrate via gas phase from paper and paperboard to undesired targets, as foodstuff in paper-based food packaging. Although vapour pressure of medium and high boiling MOH is extremely low (it would be inappropriate to refer to evaporation), due to their non-polar nature and absence of strong intermolecular interactions, C16-24 MOH have enough mobility to migrate from cellulose to other material present nearby [91-93]. This is particularly relevant when using paper or paperboard packaging for food contact: it has been demonstrated that food packed into MOH contaminated paperboard packaging, when it is not protected by further specific barriers, can contain up to hundreds of mg kg^{-1} of

hydrocarbons, depending on: i) paperboard initial contamination; ii) storage time and temperature (though MOHs migration may occur even at -20°C); iii) characteristics of the food (fat-rich, dry, high specific surface foods accumulate more hydrocarbons) [94].

Paper recycling is without doubt an essential resource in order to keep cellulose fibres a sustainable and renewable commodity [88, 95]. However, the quality and safety of such material should not be taken as granted. Due to the particular structure and composition of cellulose fibres, many other contaminants (apart from mineral oil, the most common) may end up into the recycling process and, eventually, in the end-user recycled product of packaging. This is the case of diisopropylnaphtalene (contained in the ink microcapsules of carbonless copy paper), phthalates (plastifiers contained by glues and plastics present in the recycling paper mill, potential endocrine disruptors) and photoinitiators [96, 97].

All kinds of the most common paper products, such as corrugated cardboard, paperboard, paper and tissue are made from cellulose fibres, obtained from various sources. As shown in Figure 8, cellulose is a polysaccharide polymer made of D-glucoses units linked together by β(1→4) glycosidic bond; this bond makes the structure result in a straight chain without any coiling or branching (unlike starch polymers) and a length spacing from 300 and 10000 glucose units, depending on the organism who produces it (e.g. trees, cotton, hemp, bacteria...).
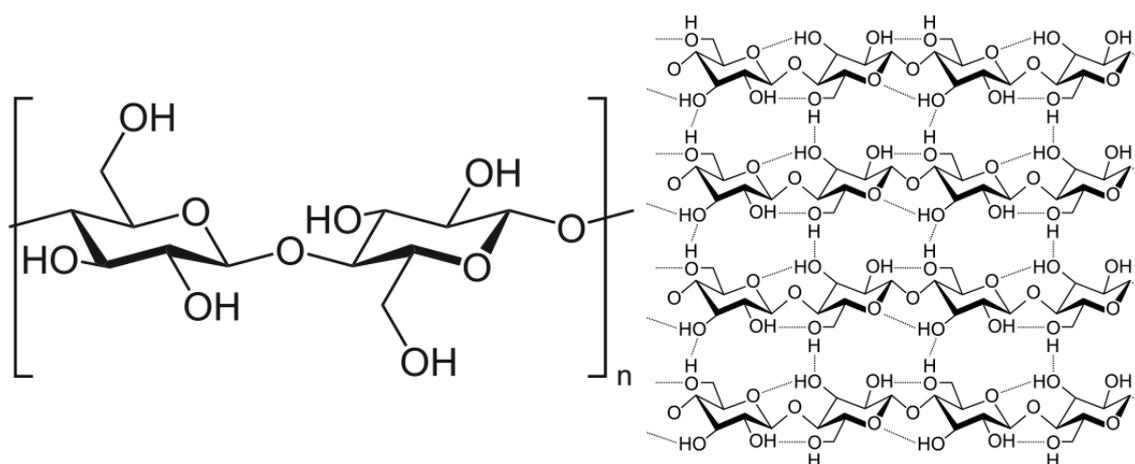
Figure 8: Polimeric nature of cellulose and inter-polymer H-bondings

Compared to other glucose polymers, such as amylose or amilopectin, cellulose has a much higher crystalline state: the presence of three –OH functional group per monomer, which is disposed "symmetrically" to the adjacent glucoses, makes each single polymer chain prone to merge with many others thanks to a large number of H-bonds (as seen in Figure 8), forming

microfibrils. Many of these joint structures compose a single cellulose fibre; where both crystalline and amorphous parts are generally present [98], as shown in Figure 9.
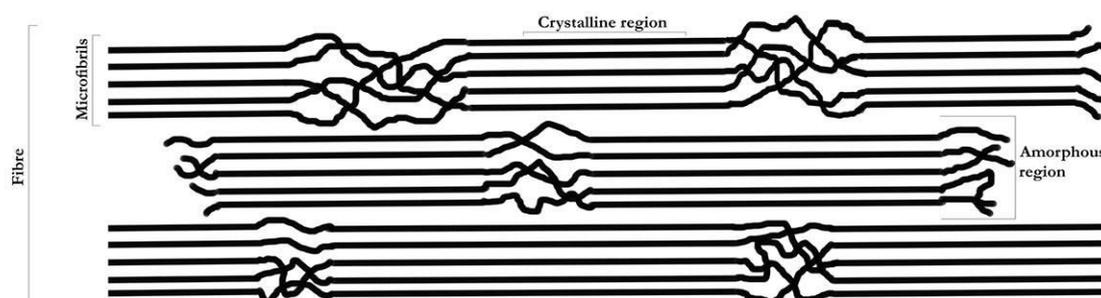
Figure 9: Supramolecular structure of cellulose polymer into microfibrils and fibres "glued" together by H-bonds.

Crystalline regions are rigid, non porous bundles of polymers, whilst in the amorphous parts the polymer bundle is more loose, thus offering elasticity and porosity to the whole fibre. Cellulose extraction process contributes significantly to alter the structure of fibres by breaking them down and creating amorphous "degraded" regions. Recycling cellulose hence does not totally preserve their structure, and degrades the overall quality of fibres, this is why some fresh virgin paper pulp needs to be added to recycled pulp in most cases.

Cellulose pulp for paper making (both freshly extracted from primary sources and recycled) consists in a wet dispersion of cellulose fibres of different length and crystallinity grade. Depending on the product of interest, additives are subsequently added, such as binders, fillers, pigments or sizing agents. Some common fillers thoroughly present in most paper and paperboard products are calcium carbonate, kaolin, titanium dioxide, chalk or talc [99].

Sheets are formed by a paper-making machinery, which is fed by the abovementioned pulp. The machinery dries and presses the suspended pulp, and the wet sheet is then hot-air dried. Before being printed and transformed into the end-product, additional finishing or coating processes can take place. Despite the possible presence of hydrophobic additives (e.g. polyethylene), it is not wrong to assume that most of the molecules contained in paper are polar, thus it is not surprising that hydrocarbons weakly adsorbed on the paper fibres could have enough mobility via gas to migrate to more organophilic medium such as food's fat.

30

3.1.1. Analytical challenges

Mineral oil hydrocarbons are a vast group of aliphatic and aromatic hydrocarbons spacing from C15 to C40 [100, 101]. Mineral oil used for industrial application, even when the most refined formulations are concerned, contains millions possible isomeric forms. Literature reports that the structural isomers of *n*-tetradecane are 1858, growing exponentially as carbon atoms are added (computational studies found 14490245 possible isomers for C24 and 493782952902 for C35 [102]). This is a major issue, considering the quantitative analysis for such a large amount of possible molecules with very similar boiling point.

Normally, the quantitative analysis on single hydrocarbons is performed by separating analytes via GC chromatography and measuring the electronic response of a proper detector – usually a Mass Spectrometer detector (GC/MS). For targeting DIPN or specific phthalates or photoinitiators, this analytical techniques is sufficiently precise and reliable. For mineral oil, though, the detector response of the GC/MS does not consist in resolved peaks but in a large "hump" containing most of the analytes. Even trying to integrate such chromatogram does not result in a reliable quantification for those molecules, since ideally the response factor for each targeted ion is impossible to predict.

A much more reliable technique[103-106] was developed in Kantonales labor of Zurich by Grob and co-workers. Briefly, a dedicated LC-GC/FID is fed with a sample extract (from food or packaging) containing an Internal Standard (IS). A LC capillary reverse phase column retains or slows down all the slightly polar compounds (such as DIPN or MOAHs, the aromatic fraction of mineral oil), whilst MOSH (Mineral Oil Saturated Hydrocarbons) being nonpolar are immediately eluted. The LC eluate containing MOSHs, MOAHs, the IS and other analytes is transferred to the GC/FID system by an on-line large volume injection. The so-composed system presents the following advantages: i) LC run produces a more accurate separation of analytes, preventing undesired molecules to enter the GC; ii) the Flame Ionisation Detector, even if obsolete, can bear high concentration of analytes, has a very good linearity response for all hydrocarbons and no integration adjustments are required.

Furthermore, the heterogeneous composition of mineral oil is even more problematic when it comes to defining toxicity assessments and legislation limits, as it will be showed in the next paragraphs.

3.1.2. Health concerns and risk assessment

As previously stated, since mineral oil is a complex mixture of compounds, standard toxicological assessments are not available. Still, many studied evaluated short and long term effect of exposure to mineral oil and similar hydrocarbon mixtures, or considering specific hydrocarbon fractions like MOAH or heavy paraffin singularly.

Aromatic component of mineral oil virtually does not contain Polyciclic Aromatic Hydrocarbons (PAHs), but no condensed molecules with several alkyl substituents to the aromatic ring and lower boiling point. Still, MOAHs have mutagenic and carcinogenic effects [107], thus pose a serious threat to human health. Food grade mineral oil (so-called "white oil") does not contain any MOAHs, but technical grade mineral oil used for offset printing and lubrication does (ca. 20%) [108].

Many studies on oral exposure confirm that heavy paraffin (>C35) are not absorbed by human intestine, thus ingestion produces no relevant effects on health. Lower-boiling saturated hydrocarbons, though, are far from being considered safe [109]. Evidences from studies on human indicate that medium-chain hydrocarbons (C16-C35) are assimilated and accumulate into human tissue [110, 111]. Moreover, non-oral expositions (such as contact) can induce autoimmune response or aggravate different ones in human and rat studies [109, 112]

3.1.3. Paper decontamination from mineral oil and controversies

Since food safety authorities first began to study possible food contaminations by hydrocarbon coming from paperboard packaging, roughly at the beginning of nineties, many studies on the topic have been issued, confirming the possible risk and assessing serious contamination cases of consumer's food product. Despite that, the regulatory process to limit the phenomenon has not properly followed. As stated in the previous paragraph, the main cause for this is the difficulty to assess properly which fraction(s) of mineral oil poses a threat to human's health and how, being mineral oil a complex mixture of many different hydrocarbons, and as a consequence the difficulty to define clearly *what exactly* has to be regulated.

At present, no European regulation is in place, only local rules on food or packaging additives. It must be said that while the use of technical grade mineral oil rich in MOAHs in food industry is banned virtually anywhere, it is NOT banned in printing industry. Therefore,

the risks of hydrocarbons migrations from packaging are not always properly taken into account. The Joint FAO/WHO Expert Committee on Food Additives (JECFA) issued in 2002 a temporary ADI for medium and low viscosity white oils (without MOAHs) [113], which has been withdrawn in 76th JECFA monographs (2012) [114, 115]. At the present, the International Agency for Research on Cancer (IARC) and the World Health Organization special agency consider low/mildly refined mineral oils (such as technical oils containing up to 30% MOAHs) as group 1 carcinogens (definitely carcinogenic to humans), whilst the highly refined ones such as white oil and food grade oil as group 3, as they are not suspected to be carcinogenic, but still there are insufficient evidences to prove their safety [116]. On the other hand, Food Standards Agency (FSA)[117] of UK published in 2011 a survey on hydrocarbon migration to food, concluding that consumers have no need to change their dietary habits. For United States Food and Drug Administration (FDA) white mineral oil for food industry and packaging is a Generally Recognized As Safe product (GRAS), and its use in food processing is less limited than most of EU countries [118].

On the contrary, the European Food Safety Agency (EFSA) and its expert panel on the topic, deputed to gather and produce documentation for European lawmakers, have always endorsed a EU regulation process. In 2010 EFSA released a call on scientific data, and in 2012 it followed an opinion on the topic, expressing that "background exposure to MOSH via food in Europe was considered of potential concern" [119]. The German Bundesinstitut für Risikobewertung (BfR), has not the intention to underestimate the risk represented by exposure to MOHs and has released a recommendation in 2010 saying that "minimizing the exposure to hydrocarbons via migration from contaminated paperboard food packaging is a priority" [120]. Moreover, in 2014 BfR issued the third draft on mineral oil ordinance, hence preparing to adopt a very specific legislation on food-contact packaging.

The Federal Ministry of Food, Agriculture and Consumer Protection has presented a new draft ordinance on mineral oils (22nd ordinance amending the food contact material, regulation of 24 July 2014). According to the draft, contact material for food made from recycled paper must not exceed 24 mg of MOSH and 6 mg of MOAH per kg of paper, paperboard or cardboard. Other two significant aspects of this draft are: i) the carbon range of MOSH and MOAH for which the limit is established does depend on the characteristics of the storage and the food products contained therein; ii) materials exceeding these thresholds may still be put on market provided that it is demonstrated that migration of hydrocarbons in food does not exceed 2 mg of MOSH and 0.5 mg of MOAH per kg of food. The Council of Europe is currently working on a "Technical Guidelines on Paper and

Paperboard" draft, which uses the same limits and principles (there is still debate, though). Even though Council of Europe guidelines are not legally binding, once the drafts will be officialised, they will be likely assumed as derogatory legislation source by the member states [121].

European bodies' interest on the matter seems to strongly suggest that hydrocarbons content in food packaging is going to undergo some sort of regulation. So far, packaging producers and food retailers decided autonomously to use only virgin fibres to produce food-contact paperboard, thus consuming more wood as primary resource. Despite that, the need to obtain a safe and clean recycled paper pulp should not be postponed.

In this PhD thesis, a modified mesoporous silica is assessed to stabilise MOH directly in wet paper pulp, paving the way to its use (as recoverable pellet/monolites) for hydrocarbon removal in paper mills, to obtain clean pulp in a sustainable way.

Note: the following part (3.1.4. to 3.4.) is intended as a short summary of the published paper and the patent reported at the end of the thesis as Attachment 8.2. and 8.3.

3.1.4. State of art

As largely discussed in the introduction, food contact packaging and more generally, paper and paperboard, may contain up to several hundred mg kg^{-1} of mineral oil hydrocarbon, eventually migrating to food via gas phase.

In the last few years, as the public interest and the scientific research on the matter grew, packaging producers and food retailers began to deal with mineral oil contaminants in paperboard, anticipating law regulations and enquiries from consumers' associations. Corporate strategies and needs (not always compatible with sustainability issues) aimed to find a quick, effective and easy solution to avoid the presence of mineral oil in food contact products. Many possible solutions have been adopted or discussed among stakeholders, none of them, though, seems to be immune to criticism. As few notable examples, Barilla group S.p.A., as well as COOP Italia S.c.a.r.l. adopted cardboard packaging with virgin fibres only for their branded products. This approach, apart from the cost raise, does not represent a sustainable option, as increases the demand for freshly produced fibre, instead of valorising recycled cellulose.

Other strategies involve material coupling: packaging paperboard is actually composed by different thin layers of paper or paperboard and possibly plastic, as briefly shown in Figure

10. Packaging products with a single (or double) outer plastic coating are already produced and offered to retailers. Unfortunately, not all the plastics serve as a barrier preventing MOH migration: polypropylene (PP) and polyethylene (HDPE and LDPE) are permeable to hydrocarbons [86, 122-124]. Some polyvinyl alcohols (PVOH), polyacrilates and polyesters in a recent study showed unacceptable permeability too [122].
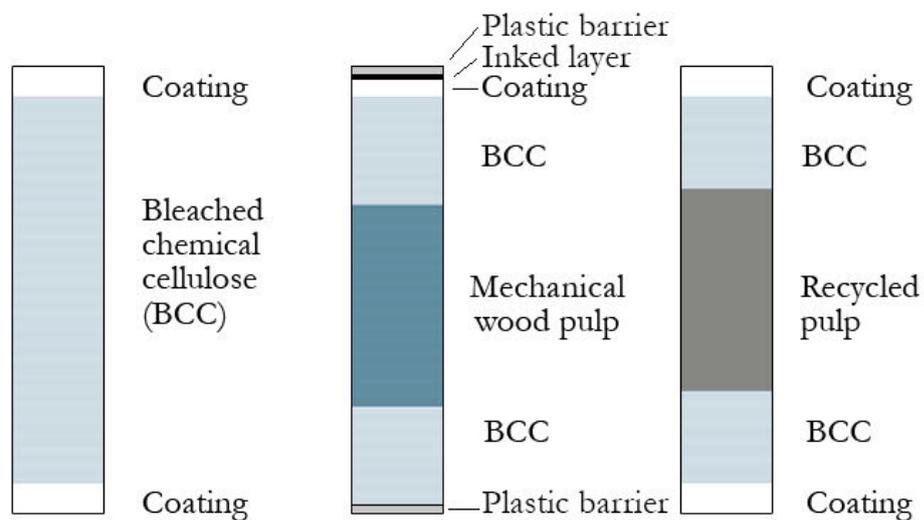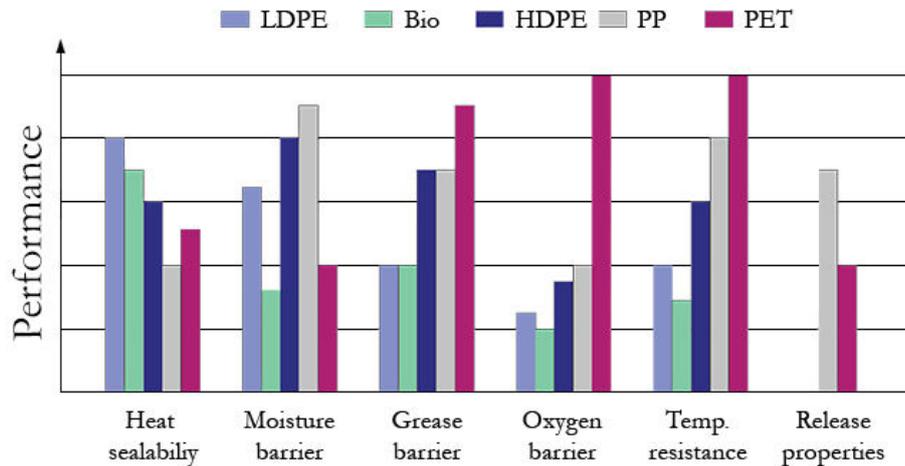
Figure 10, TOP: Technical characteristics and performances of some plastic layers commonly used for coupled paperboard packaging, as declared by the producer. LDPE: low density polyethylene – Bio: bioplastic – HDPE: high density polyethylene – PP: polypropylene – PET: polyethylene terephtalate. Modified from Iggesund paperboard, Sweden
BOTTOM: three sections of paperboard for different purpose. On the left: a simple paperboard sheet for graphics and drawing. On the right: a paperboard sheet with a unbleached recycled inner layer. In the centre, a typical food-contact paperboard

Only polar polymers such as polyamines and polyethylene terephtalate (PA and PET respectively) can be considered safe functional barriers towards MOH. Nevertheless, these are not always the optimal product choice (e.g.: due to poor water resistance) [124]. Moreover, a plastic layer coupled to cardboard is an additional post-consumer waste that needs to be disposed of. Similarly, Smurfit Kappa has released a cardboard with a inner activated carbon layer which significantly prevents MOH migration to foodstuff, retaining hydrocarbons [122]. Despite the successful idea, much more interesting and valuable would be to produce clean recycled paper in the first place. This could be achieved by i) governance bodies progressively dissuading offset printing and promoting MOH-free techniques ii) improve and optimise waste paper collection for recycling iii) removing hydrocarbons directly from the paper mill were waste paper is macerated.

Considering this last option, no solutions appeared to be easily viable to recycled paper producers at the research or technical level. Achieving hydrocarbons removal from recycled paper pulp, made possible by specific sorbent materials, would represent a huge step in improving the quality of recycled cellulose products.

3.1.5. Aim of the project

Once paper, paperboard and cardboard are collected as urban or industrial wastes, they are packed and transferred to recycling plants. Raw material is hence mashed in water and screened. At this point, recycled paper pulp is produced, but still many treatments are usually performed (e.g.: pigment removal) and an additional step to remove hydrocarbons contaminant can be implemented. The aim of this project is: i) to find an efficient synthetic sorbent versatile, cost-effective and easy to produce; ii) test its efficacy in paper mill conditions, and evaluate at which recycling stage it is more profitable to intervene; iii) assess in which form the sorbent phase should be added (e.g.: powder, pellet, monoliths...) and perform decontamination tests.

Several synthetic sorbents were tested in a preliminary screening for mineral oil sorption capacity. The most effective one was added to recycled paper pulp in its powder form and not removed later. The additivated pulp was hence used to produce recycled paper. Analyses of mineral oil were performed at each production step and compared to a non-additivated control pulp. Finally, a migration test on a food (semolina) and on a food simulant (TENAX®) was carried out.

During this project, an industrial patent has been deposited [2] and a research paper has been published on the Journal of European Food Research and Technology [3].

3.2.   MATERIALS AND METHODS

- A technical mineral oil mixture was chosen for the preliminary sorption tests: Paraset 32 H was purchased from Petrochem Carless, UK. The mixture had density of 836 g L^{-1}, a boiling point of 278-315 °C, a vapour tension <0.04 kPa and an aromatics content of 12.5% on weight.
- <u>Sorbent materials</u> used for the preliminary sorption tests are listed in Table 1 and were chosen owing to their: i) high specific surface area (SSA) ii) high water stability iii) hydrophobic properties iv) white or pale colour. With the only exception of Davisil silica (purchased from Sigma-Aldrich), the materials were synthesized or modified according to the method cited in the table.

Sorbent Materials	Source	Particle size (µm)	Pore size (nm)	SSA ($m^2 g^{-1}$)	MOH adsorption (% dw)
SiO₂-Davisil	Sigma-Aldrich	150-250	6.0	605	<1
Porous alumina	[125]	5-10	3-8	450	<1
Saponite SAP-20	[126]	<2	0.10-10	216	2.0
Saponite SAP-110	[126]	<2	0.1-10	369	≥1
Saponite SAP-150	[126]	<2	0.1-10	314	≥1
SBA-15	[127]	0.5-0.6	8	757	<1
Platelet SBA-15	[128]	0.2-0.3	~8.5	733	≥1
*iso*butyl-SBA15	[129]	<1	8.1	659	137
Trimethylsilyl-SBA15	[130]	<1	6.5-15	690-1040	318
Trimethylsilyl-MCM41	[130]	<1	2.5	729	184

Table 1: list of materials tested for their MOH sorption capacity expressed as percentage of their dry weight

- For <u>SBA-15-isobutyl synthesis and derivatization</u> a modified method reported by Etgar et al. [129] was followed: the SBA-15 mesoporous silica previously prepared [127] was derivatized through post-synthesis grafting of isobuthyl groups. 1 g ca. of material was dried in vacuum at 200 °C for 2 h. Under N_2 atmosphere, 100 ml of anhydrous toluene were added as solvent, followed by 0.50 ml isobutyl-(trimethoxy)silane

$[(CH_3)_2CHCH_2Si(OCH_3)_3]$ (97%, Sigma-Aldrich). The suspension was left stirring for 20 h at 50 °C. The sample was then filtered, collected, and characterised.

- Synthesis and derivatization of trimethylsylil SBA-15 and trimethylsilyl MCM-41 (SBA-15-$Si(CH_3)_3$ and MCM-41-$Si(CH_3)_3$): The materials have been synthesized using a modified procedure reported by Batonneau and co-workers [130]. Surface functionalization of both MCM-41 and SBA-15 followed afterwards, briefly described as follows.
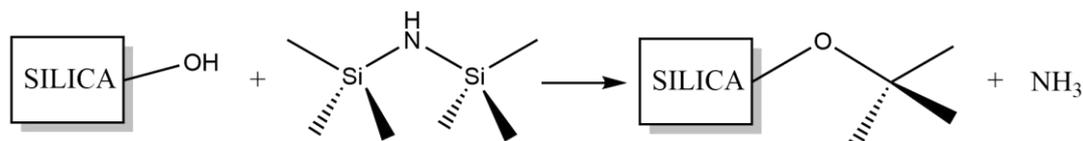
Distinctly, 2 grams of each material were put into a three-neck round-bottom flask and dehydrated at 200 °C for 2 h. The solid was hence cooled down at room temperature (RT) in nitrogen atmosphere, and 40 ml of anhydrous toluene were added as solvent (Carlo Erba, analytical grade). Subsequently, 2 mmoles of hexamethyldisilazane (99.9%, Sigma-Aldrich) were slowly added as reagent, and the suspension was heated to 110 °C. After 3 h, the derivatized material was filtered, recovered and dried at 40°C overnight. The materials were finally characterized.

- Screening of sorbent materials: the sorbent materials in Table 1 were tested for their MOH sorption capacity in water suspension. 50 mg of each material were weighed and put into 5 mL vial. 1.5 mL of deionised water were added, and finally 0.35 mL of Paraset 32H mineral oil mixture.

The three phases suspension was left stirring at RT overnight, then stopped. After 1 hour to rest, the mineral oil possibly floating as supernatant was removed with a cotton swab; the suspension was hence centrifuged and dried for 24h at 40°C. Sorbent materials loaded so were subsequently analysed by TGA/DTG and FT-IR.

- Recycled paper pulp production and enrichment: highly MOH contaminated paper pulp was produced using five "fresh" copies of "Il Giornale" italian newspaper (issue of October the 22nd, 2014). Simulating recycling processes, 50 g of shredded newspaper were put in a laboratory fibre disintegrator ("pulper") along with 1200 mL of mains water at 40°C. Half of the pulp was additivated with 0.5 g of synthetic sorbent powder (MCM-41-$Si(CH_3)_3$ was chosen as the most effective sorbent: pulp samples enriched with this material will be called from now on "enriched pulp") whilst the other half was used as control. An aliquot of both was sampled for MOH analysis
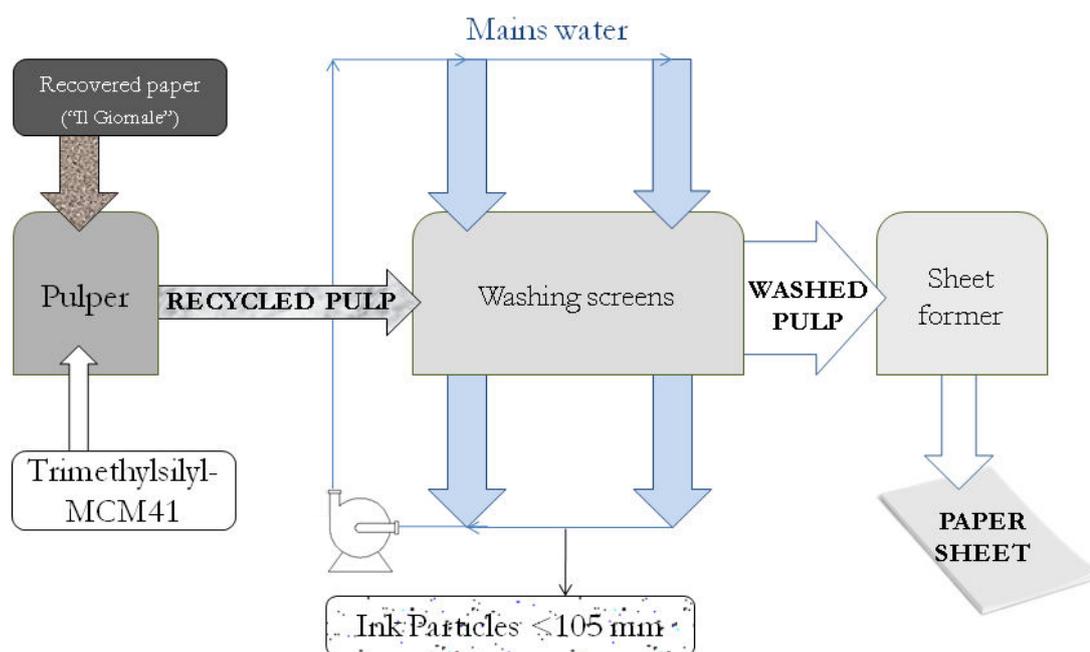
Figure 11: Scheme depicting the process adopted to produce sheets of washed, recycled cellulose starting from newspaper as raw material

- Washing test on enriched pulp: enriched and control pulp were placed in a Sommerville type fractionator used to simulate washing (or screening) process which recycled pulp usually undergoes in recycling plants. The washing cell was equipped with a fine screen (0,105 mm or 150 mesh) on a vibrating bottom. As water flowed through the unit, the (most of) cellulose fibres were retained by fine screen and vigorously washed by the water stream; the feeding water flow was measured as 4.7 L min^{-1} for 15 min. Washed treated pulp and washed control pulp were then sampled for MOH analysis. After this stage, MCM-41-Si(CH$_3$)$_3$ particles were still present in the pulp and visible to the naked eye.

- Recycled paper sheet production: washed treated pulp and washed control pulp were used to produce paper sheets of 140 g m^{-2} in a Rapid Kothen equipment (Estanit, Germany): briefly, the machinery suspends fibres in large water volumes, filter them under vacuum and dry them at 93°C and 63 mbar for 10 min. Treated and control sheets were sampled for MOH content and used for food migration trials. Even after this final stage, treated paper sheets still had visible particles of MCM-41-Si(CH$_3$)$_3$ on it.

- >C12 MOH analysis on cellulose samples (namely: newspaper, treated shredded pulp, control shredded pulp, treated washed pulp, control washed pulp, treated sheet, control sheet) were performed using EPA8015D 2003 method on hexane extracts obtained as

reported by Lorenzini and coworkers [85]. The extraction consisted in weighing about 1g (in dry weigh) of wet sample was added with 25 mL of ethanol in sealable glass flasks (glass or teflon caps required) and shaken for an hour. 20 mL of analytical *n*-hexane were subsequently added and left shaking overnight. Agitation was stopped and the samples left for 1 h to sediment; 10 mL of milliQ water was added to facilitate the hexane extract collection. The extracts were hence analysed following the EPA8015D 2003 method, consisting in GC-FID quantification of heavy hydrocarbons (C>12). The extract was directly injected after a filtration on syringe. Results obtained by this analysis, despite not being particularly precise, may safely be compared each other.

- The treated and the control paper sheets produced were also used in <u>food migration tests</u>. Semolina flour and TENAX® (by Supelco) were selected as reference food [131] for this test. Samples of treated or control paper were sealed in glass jar with aluminum caps along with semolina or TENAX® (1:5 mass/mass ration between paper and food target) and kept for 15 days at 40°C to simulate and magnify storage conditions [122, 132]. Migration tests were conducted in duplicate. Paper sheets samples were analyzed before and after the migration tests. Semolina and TENAX ® were only analyzed after the test since both were certified MOH-free. MOSH and MOAH analysis for the migration test samples are described hereafter.

- In-depth <u>analysis on MOAH and MOSH</u> contained in the migration test samples were accounted on COOP Italia and performed by Mérieux NutriSciences (Accredia lab 0144, Tuscany 016) in according to internal method 004 MPP FCM040. After extracting the paperboard or food samples (similarly as described above) the extracts were injected in a on-line HPLC-GC/FID system similar to which is described in section B.1.3. of the present chapter. HLPC stationary phase performed a pre-separation of MOSH and MOAH, which were then injected in the on-line GC/FID system, concentrated by solvent evaporation and revealed by Flame Ionisation Detector. This analysis can be safely considered more accurate than the MOH analysis described in the previous paragraph, as the latter: i) do not discriminates MOSH and MOAH, but considers the whole non-halogenated hydrocarbons above C12 ii) may suffer from sample contamination and is generally considered less precise.

3.3.   RESULTS AND DISCUSSION

- Sorption screening and thermal analysis of the material reported in Table 2 revealed that Davisil silica, porous alumina, all the saponite samples and the non-derivatized SBA-15 samples did not show capacity to adsorb MOH dispersed in aqueous phase. On the contrary, *iso*-butyl-SBA15, trimethylsilyl-MCM41 and trimethylsilyl-SBA15 showed favourable sorption capacity (retaining 137%, 184%, 318% of MOH on dry weight respectively). Sorption values were obtained examining thermo-gravimetric curves by TGA/DTG. The porous materials dispersed in water with MOH adsorbed both water and mineral oil. Water sorption was revealed in TGA by a weight loss at temperature <150°C in almost all the materials, whilst MOH loading was revealed by a weight loss at roughly 200-300°C. Derivatized materials such as *iso*-butyl-SBA15, trimethylsilyl-MCM41 and trimethylsilyl-SBA15 also showed a further weight loss at higher temperatures, due to the degradation of alkyl functions grafted onto the surfaces. In the case of trimethylsilyl-SBA15, though, this weight loss partially overlapped to the loss caused by MOH volatilisation, roughly at 300°C. This overlapping not only resulted in an inaccurate quantification of loaded MOH on trimethylsilyl-SBA15, but also resulted in the impossibility to thermally regenerate that material (and reuse it) without the risk to alter the organic functions bonded therein. Trimethylsilyl-MCM41 was hence preferred for subsequent project stage (paper mill tests) as it presented a significant sorption capacity to MOH (184% on its DW) as well. For sake of brevity, TGA and FT-IR spectroscopic studies are here omitted.

- MOH analysis on wet pulp samples from paper mill trial are briefly reported as follows (reported value have a <25% error). Starting from a newspaper containing 3125 mg kg^{-1} >C12 hydrocarbons, recycled paper pulp was produced in presence of trimethylsilyl-MCM41 and in absence of it. After 10 minutes in the pulper, the MOH content of the control (638.5 mg kg^{-1} DW) and trimethylsilyl-MCM41 enriched pulp (961.5 mg kg^{-1} DW) was considerably reduced with respect to the newspaper (3125 mg kg^{-1}). Seemingly, the mechanical action carried out by the pulper unit at 40°C was sufficient to desorb ca. two thirds of the MOH. It has to be noted that the newspaper was printed few hours earlier: it is likely that most of hydrocarbons contained therein were low boiling C12-C18. The concentration of MOH in the recycled pulp sample with the additive was 50% higher than the control pulp, owing to the presence of trimethylsilyl-MCM41 and its chemical affinity for hydrocarbons (as revealed by the screening tests). It was therefore

safely assumed that the sorbent additive retained significantly the hydrocarbons and prevented evaporation. This tendency was confirmed after the washing process, as washed pulps contained 503 and 616 mg kg^{-1} of MOH on their DW for control and enriched pulp respectively. Moreover, even after the sheet formation, in which fibres undergo heating and vacuum for 10 minutes, the MOH content of enriched samples were higher with respect to the control (286 and 236 mg kg^{-1} respectively) These results confirmed the high affinity of trimethylsilyl-MCM41 and its capability to adsorb and retain MOH from wet paper pulp, and strongly validated the hypothesis to use the material in a recoverable form (e.g.: pellets or monoliths) in order to use it to remove hydrocarbons from recycling paper pulp.

- <u>MOSH and MOAH migration analysis</u>: Recycled sheets obtained after washing in presence and in absence of trimethylsylil-MCM41 were put in a sealed jar with semolina flour or Tenax® under accelerated migration conditions at 40 °C for 15 days. Table 3 reports the concentration of MOH as the sum of migrating (≤C24) aliphatic (MOSH) and aromatic (MOAH) hydrocarbons, referred to the dry weight of the sample before and after migration test. The hydrocarbon >C24 are omitted, since according to literature their migration to food is negligible [93, 133]. As reported in Table 3, before the migration test, the MOH content of the enriched paper sheet was 272 mg kg^{-1} on DW whilst the control was 220 mg kg^{-1} on DW (25% more).

The ratio between MOAH and MOSH, interestingly, is very similar in both enriched and control paper before and after migration test, indicating that: i) MOAH and MOSH migrate at the same ratio; ii) trimethylsilyl-MCM41 shows similar affinity for the saturated and aromatic fractions. After the migration test, the control sheet <u>loss</u> MOH down to the 40% of the initial amount (92.0 mg kg^{-1} on DW) whilst a conspicuous amount was found in the semolina flour (20.4 mg kg^{-1} on DW). On the contrary, the enriched recycled sheet, with trimethylsilyl-MCM41 powder even after 15 day was still 88% of the initial amount (239.0 mg kg^{-1} on DW) and only 4.3 mg kg^{-1} were found in the flour (roughly, one fifth of the mineral oil migrated in absence of the additive).

Results concerning migration to Tenax, on the other hand, were not satisfying, as food simulant samples resulted highly contaminated: the sample kept in contact with enriched paper sheet and that kept in contact with the control sheet were 33.4 and 24.1 mg MOH kg^{-1} on DW, respectively, Table 2.

SAMPLES	MOSH C≤24	MOAH C≤24	MOH C≤24
Initial concentration			
Enriched paper sheet	210.0 ± 37.0	62.0 ± 15.0	272.0 ± 52.0
Control paper sheet	168.0 ± 28.0	52.0 ± 10.0	220.0 ± 38.0
Migration at day 15			
On semolina flour			
Enriched paper sheet	188.0 ± 33.0	51.0 ± 12.0	239.0 ± 45.0
Control paper sheet	70.0 ± 12.0	22.0 ± 5.0	92.0 ± 17.0
Semolina on enriched paper sheet	3.1 ± 0.8	1.2 ± 0.3	4.3 ± 1.1
Semolina on control paper sheet	15.9 ± 4.3	4.5 ± 1.2	20.4 ± 5.5
On Tenax®			
Enriched paper sheet	40.0 ± 6.0	16.0 ± 4.0	56.0 ± 10.0
Control paper sheet	32.0 ± 10.0	15.0 ± 4.0	47.0 ± 14.0
Tenax® on enriched paper sheet	23.5 ± 6.3	9.9 ± 2.7	33.4 ± 9.0
Tenax® on control paper sheet	18.3 ± 5.0	5.8 ± 1.6	24.1 ± 6.6

Table 2: MOSH and MOAH analysis on migration test samples, MOH column is the sum of MOSH and MOAH. All values are referred to DW.

This could be partially explained by the regular polymeric structure of Tenax®, which is often questioned to be fully representative of foodstuff [134]. Seemingly, its presence in much larger amount (1 g) with respect to the sorbent particles (ca. 10 mg) impaired the retention capacity of the derivatized MCM41. Still, as far as the only semolina flour migration test is addressed, the results were fully satisfactory.

3.4. CONCLUSIONS

This preliminary study was fundamental to elucidate adsorbent properties of trimethylsilyl-MCM41 in paper mill conditions for MOH removal. The meaningful insights on this sorbent capacity to retain MOH during all the recycled pulp production and cleaning stages paved the way to its utilisation in recoverable form, object of an on-going study. Moreover, thanks to these results the utilisation of this material for hydrocarbon removal in the recycled pulp production has been patented as a genuine innovation developed by some of the inventors, which also co-authored the attached paper (attachment 8.3.).

In this study, hydrophobic sorbent materials with high specific surface were initially screened for their capacity to adsorb MOH dispersed in aqueous phase. Trimethylsilyl-MCM41 was

selected owing to its high loading capacity (184% on DW) and stability at 300°C (allowing to be thermally regenerated). This material was added in powder form to recovered waste paper and recycled pulp was produced. The pulp was subsequently washed and the washed pulp was finally used to produce recycled sheet for a food migration test. Trimethylsilyl-MCM41 powder was not removed during the entire recycling processes, and powder particles were still present in recycled paper sheet.

Mineral oil content (MOH >C12) of recycled pulp, washed pulp and recycled paper sheets containing trimethylsilyl-MCM41 was always higher in recycled pulp, washed pulp and recycled sheet (+50.6, +22.5 and +21.2%, respectively) with respect to the control samples. The MOH stabilization by the additive was confirmed by the test on MOH migration to food. In this test, MOH content of additivated recycled paper sheet was significantly higher (+160%) with respect to the control, after 15 days at 40°C in contact with semolina flour. Moreover, semolina kept stored with paper enriched with trimethylsilyl-MCM41 had 78.9% less hydrocarbons compared to semolina kept with control paper (4.3 instead of 20.4 mg kg^{-1} on DW)

According to our findings, trimethylsilyl-MCM41 has been able to retain successfully MOH in wet conditions (during recycling paper production) and also in dry conditions (during migration tests), preventing MOH from migrating into flour. It is prone to be regenerated thermally, and suitable to be synthesized in pellets or monoliths. In following research steps the sorbent in the form of monoliths will be added and removed from the pulper, and thermally regenerated after use in order to produce MOH-free recycled paper.

4.   CaCl$_2$ sediment washing for *in situ* Cu and Zn decontamination: effect on wet aggregate stability and DTPA-extractable metal content

4.1.   INTRODUCTION

Persistent organic pollutants (POPs) and organic contaminants in general, even the most recalcitrant ones, can always be converted to water, carbon dioxide and anhydrides [135]. Heavy metals (HM), instead, may be only transformed in different chemical species of the same element, but cannot be permanently degraded (unstable nuclides, like ^{235}U or ^{210}Po, are the only exceptions) [136].

The non-canonical term "heavy metal" refers to those elements, generally transition metals or metalloids, with density higher than 5 g cm^{-3} [137]. Some of them, especially those located in the 4th period of periodic table, are essential micronutrients to plant and animal nutrition like Fe, Cu, V, Mn and Zn [138]. The very same elements, though, can form toxic chemical species, like MnO$_4^-$, V$_2$O$_5$, Cr(VI) and show toxicity at high doses [136, 139]. Other HM have no significant biological role and are simply toxic elements (e.g. Hg, Pb, Cd). Heavy metal environmental accumulation endangers soil, water and atmosphere quality. All transition metals, if assimilated in excess, can potentially catalyse the formation of reactive oxygen species (O$_2^-$ •, HO•) which can damage DNA and RNA of living cells [140]. Moreover, most of them have several ways to explicate toxicity and are prone to accumulate along the food chain. Their environmental monitoring and pollution prevention is thus a priority for most industrialized areas [141].

Environmental contamination of As, Pb, Cd, Hg, and Cr poses serious threat to the food chain, due to their widespread use, their toxicity levels [142] and potential bioaccumulation. In the human body, these five elements show great affinity towards organic sulphur of biological molecules. Once in the bloodstream, they can severely disrupt proteins functionality (e.g. substitution of the S-coordinated metal ion cofactor of metalloproteins such as hemoglobin) and hence the related metabolism. Both Cr(VI) and Hg organic species are heavily toxic [143]. Cr(VI) and As are carcinogens, alkylated Hg and Pb cause serious damages to brain tissue, and Cd leads to a degenerative bone syndrome. Having been

extensively used as fuel additive, Pb is the most prevalent environmental contaminant and, despite tetraethyl lead was banned in most of the industrialised countries by the early 2000s, still Pb concentration is significantly high [97].

Other metal elements known for their hazardous nature are Mn, Co, Ni, Cu, Zn, Se, and Ag, with particular respect to copper and zinc, which are the most conspicuous contaminants associated with electronic wastes (e-wastes).

Heavy metals form approximately the 5% of the earth's crust weight (95% of which is iron), as they are naturally present in rocks and ores or as inclusions in minerals. Eruption, tectonic movements, rock erosion, sediment transportation by superficial waters and paedogenesis disseminate them to soils, generally as insoluble oxihydroxides, sulphides or as clay inclusions. Then, plant exudates or microorganisms can partially mobilize heavy metals to metabolise them as micronutrients, entering thus into the biological cycles of living organisms. In general, each one of these elements has its own biogeochemical cycle, in which the metal changes place, form and oxidation state. Human activities have great impact in altering these cycles: from bronze age (roughly 3000 BC), excavation and smelting of tin and copper, to recent use of rare earths as semiconductors or engineered nanomaterials, heavy metals have been massively extracted, used, collected and reused [136, 144-146].

Today, sustainable waste management and heavy industry risk assessment have great potential to prevent and reduce any incorrect disposal or dissemination of potentially toxic metals into the environment. Many mechanical and electronic products commercially available to consumers contain several metal components, many of which contain highly toxic elements, precious metals or rare earths (the so called "technology metals") [147, 148]. Neither the metals contained in end-user product, nor those used by heavy industry can always be completely recycled, and the huge demand and production increase for electronic devices contributed to make the electronic waste management a global crisis [149, 150]. Lead, copper and zinc contamination in top soils and water sediments seems to be ever present in most industrialized areas [151]. Despite most of the metals contamination coming by e-waste are scarcely mobile downward the soil profile, they can be mobilized and assimilated by plants through radical exudates, thus entering the food chain, especially zinc [152].

Apart from wastes, human industrial activities are also mainly responsible for environmental pollution and toxic-level exposure cases: mining, smelting, galvanisation, industrial processes, use in agriculture, combustion are only few notable example activities [139, 153-155]. Even if most of heavy metal species do not migrate easily along soil and do not dissolve easily in water, they can be transported by water, as associated to soil particle eroded and transported

by ditches and canals. In general, they are not volatile (with a few exceptions like H_3As and $Hg(0)$ and $Hg(I)/(II)$ organic forms) but can nonetheless be transported in the atmosphere with the most fine combustion residues, the so called PM10 and PM2.5 (particulate matter with diameter <10 and <2.5 μm respectively) [156].

Trace heavy metals in soil and sediments can be extracted and analysed in several ways. Government laws and risk assessment prescriptions usually require total metal analysis or pseudo-total metal analysis. For these analyses a soil extraction with one (pseudo-total extraction) or more (in case of total metal extraction) strong mineral acids (HF, *aqua regia*, boiling HNO_3, $HClO_4$...) is required, usually through a microwave-assisted digestion. Acid extracts are then analysed by atomic absorption spectrometry or inductively coupled plasma spectrometry. This is the most easy and fast extraction technique, even if it does not give information about the potential risk associated to heavy metal availability to *biota* but only about their total concentration as intrinsic hazardousness. Other analyses, based on organic chelants as extractants (such as diethylenetriaminepentaacetic acid or ethylenediaminetetraacetic acid, DTPA and EDTA respectively) can mimic the biological extraction process, thus giving information on how much metal can be mobilised and uptaken by plants at their interface with soil (rhizosphere) [157, 158]. Unfortunately, this analysis does not return any detailed information about the chemical environment of a metal species, and thus it does not give information on how the mobility of the metal could change under different soil conditions.

A more accurate analysis, often referred as metal speciation, consists in the analysis of sequential extractions of the same matrix, using different extractants (progressively stronger), which mobilize only the metals bound to a specific soil fraction. A first sequential extraction was set up by Tessier and co-workers in 1979 [159] and it has been extensively used or adapted in environmental research [160] especially. The most widespread version of this analysis returns metal concentration upon the following fraction: i) mobilized metal cations adsorbed on the soil exchange sites; ii) metals precipitated as carbonates; iii) metals bonded to Mn oxides and hydroxides; iv) metals bonded to Fe oxides and hydroxides; v) metal sulphides or bound to organic compounds; vi) metals contained into mineral reticulum and unavailable to biological processes: the residual fraction. Since metal speciation is a particular expensive and time-consuming analysis, it is not usually performed for simple monitoring.

Finally, isotopic analysis can sometimes give information on the geological origin of a particular metal, and evaluate if a contamination is anthropogenic or allochthonous. A

relation between the metal concentration of fine grain size of soil (e.g. fine silt and clay) and the anthropogenic origin of the contamination can be observed [161].

4.1.1. Heavy metal contamination in water sediments

Estuaries, rivers, canals and ditches receive rainwater and suspended particle drained from the territory, as well as water treatment plants (WTP) effluents, urban drainage water and even illegal wastes. Due to their progressive sedimentation of mineral and organic suspended particles, water courses (and their terminal segment, estuaries) are notable examples of environmental sinks of heavy metal contaminants [162]. Nevertheless, both rivers and artificial water courses flowing through inhabited land have to be managed to maintain their hydraulic functionality. A periodic re-sectioning or re-shaping of the watercourse bed is necessary to prevent an excessive amount of sediments to be deposited, hence reducing the hydraulic section and facilitating floods.

Water sediment's management is a necessary practice which produces thousands ton of wet sediments as by-product: for vast basins and large navigable rivers this activity is conducted on large scale with heavy trailing suction dredger or similar machines, capable to move thousands of cubic metres of material per load. Sediments dredged in this way are routinely monitored for pollutants according to good environmental protection practices imposed by governments and by determining the material quality for its use in civil engineer or for construction industry.

Considering though the whole territory of a drainage basin, the majority of it consists of areas whose waters are collected by small canals and ditches, as it is the case of cultivated land, city outskirts, etc. These are usually the rural areas managed by land reclamation agencies, which are deputed to monitor, manage and maintain the drainage canal network, as it will be presented in the case study.

4.1.2. Burana reclamation consortium case study

Note: this section contains reference from government bodies technical reports and workshops redacted in Italian language [163-166]

For the purpose of this thesis, the canal sediments management of Italian Burana reclamation consortium were considered. The typical sediment management issue is related to territories located in the city outskirts receiving urban wastewaters from small inhabited centres. These waters are rich in fine particulate matter containing typical

anthropogenic/industrial contaminants (such as heavy metal, PCBs, hydrocarbons etc.) in traces, not enough to be treated further. As the canals depth seldom exceeds the metre, and the flow rate are kept low, suspended material in waste water effluents tends to sediment quickly along the canal.

Furthermore, receiving low water flow rates, they do not need their sediments to be dredged frequently (e.g. once every ten years on average), since few material deposits. Thus, when sediments are dredged from small canals next to urban centres, they can suffer mild heavy metal contamination caused by ten years of material sedimentation.

Uncontaminated material excavated from canal bed is usually used *in situ* as soil amendment, or for canal bank shaping. According to the current Italian law, Dlgs 3/4/2006 n. 152, even if only one contaminant is present in concentration higher than national threshold [167], all the excavated material cannot be used for these purposes (may still be used in industrial sites, though). This results in: i) a huge increment of the operational costs, due to the material movement and stocking; ii) an unsustainable loss of valuable soil, due to the fact that there are no alternatives to landfill disposal of the excavated material.

Despite many ex-situ treatments are technically available for sediment remediation, practically they are not feasible, since the material amount is relatively small and contamination levels are generally not too severe. Plus, the benefits from doing so do not repay the costs afforded, so the only solution is simply disposing the dredged material into landfills. In this work of thesis (project C), a sediment washing by *in-situ* treatment with $CaCl_2$ solution is proposed and evaluated as a more sustainable option to avoid transportation and disposal of mildly polluted sediments. Such treatment would be relatively safe and less impacting compared to other chemical washings (also not justified by the pollutants concentration levels). If this technique was capable to reduce the metal content to less than the threshold limits, the on-site reuse of dredged sediments would be feasible.

4.1.3. State of art

Heavy metals can be often released from urban waste water treatment plants (WWTP) to superficial waters. Once they have been disseminated through water bodies, they can i) remain suspended, bound or sorbed to fine mineral particulate and be transported along the water body ii) remain soluble due to the formation of organic complexes with the dissolved organic matter in particular pH conditions iii) or precipitate [168-171].

Metal elements occurring in soil or in water (or at their interface, like water sediments) present different solubility, mobility, bioavailability or exchangeability according to their nature, their chemical framework, pH, redox potential and the presence of specific enzymes, plants and microorganisms [172-174]; as a good rule of thumb, the more mobile a metal is, the higher is its assimilation by the *biota*. As a consequence, the only presence (expressed as total concentration) of a potentially toxic element does not necessarily result in a high availability to organisms [175, 176]. Due to this complexity of *equilibria* determining the bioavailability of heavy metals in soil and water bodies, policy-makers tend to undervalue the *risk* (intended as likelihood) of their most noxious effects, but their intrinsic *hazardousness*. This is why environmental risk assessment policies on heavy metal contamination use the total or pseudo-total concentration as operative parameter, and not their mobility or bioavailability [177, 178] (pseudo-total metal analysis are performed with a one-step strong mineral acid and have a good approximation of the "real" total value, which is obtainable by multiple strong acid extractions). Italian regulation on heavy metal contaminated materials and sites suits well this policy, since only total or pseudo-total content analyses are requested by law [167, 179-181].

As specified in the introduction (III.1.3.1.), the necessary dredging of water sediments from canals – operated routinely to maintain their functionality – produces high amounts of sediments potentially contaminated with heavy metals. The European directive 2000/60/CE does not report any specific limit for metals in water sediments: therefore, member states usually apply the thresholds for heavy metals in soil [177]; this is also the case of Italy [167]. In case water sediments exceeded these limits for even just one metal, dredged sediment must not be used *in-situ* (e.g. for their bank shaping or agricultural amendment of fields) and must be transported and disposed in landfill, which is not to be considered a sustainable

management and therefore avoided, if possible [178]. Thus, the need to implement and test – along with land reclamation technicians and local lawmakers – feasible in-situ treatments for moderately contaminated sites.

In literature, many soil/sediment treatments are available [182-185]: they are usually based on extraction or immobilization of the heavy metal. The first ones, based on chemical extractants, called *sediment washing,* are aimed to mobilize a metal in order to remove it; on the other hand, the second ones are aimed to make it permanently unavailable. Since the goal considered is removing metals from dredged sediments exceeding a threshold defined by law, only the first will be considered [186]. Acidic HCl washing of sediment, for instance, cause a strong pH drop which i) decreases the matrix negative charges mobilizing sorbed metal cations; ii) dissolves or disaggregates some soil component (e.g. amorphous aluminum/iron oxides/hydroxides and carbonates); iii) causes the formation of chlorinated metal species more mobile than metal hydroxides.

Far less drastic, a $CaCl_2$ washing instead is able to displace the metals exchangeable fraction with low impact on soil pH and structure [187]. Sometimes these two techniques are combined [188]. Over more, $CaCl_2$ washing has already been tested for the remediation of cultivated soils polluted with Cd [187, 189, 190]. Among several other acidic or saline washings, 0.1 M $CaCl_2$ treatment was proven ideal to remove Cd from paddy fields in Japan [187, 189]. In this series of scientific publications, a consistent Cd removal was obtained (mainly affecting its exchangeable component), observed as a decreased Cd content on harvested rice. Soil fertility was also restored with no visible effect on crops by soil amending.

4.1.4. Aim of the project

In the present study, a $CaCl_2$ washing was performed on freshly-sampled contaminated sediments to test its capacity to remove heavy metals. The aim was to evaluate the possibility to use this treatment to decontaminate dredged sediments *in-situ*, and eventually use the cleaned sediment as stable material for canal bank shaping or field spread, possibly after corrective amendment [191].

Sediments from a canal belonging to Burana land reclamation consortium were collected in three different points, at increasing distance from a municipality WWTP drain. The three sediments were characterised for their physico-chemical properties and their metal content (pseudo-total and DTPA-extractable). A saline $CaCl_2$ treatment was hence performed on the

fresh sediments, and the most contaminated was sequentially extracted to evaluate the metal speciation through the different soil fractions. Texture and aggregate stability were then assessed for the washed sediments.

A scientific paper containing the research outcomes of this project was produced and submitted to Chemosphere

4.2.   MATERIALS AND METHODS
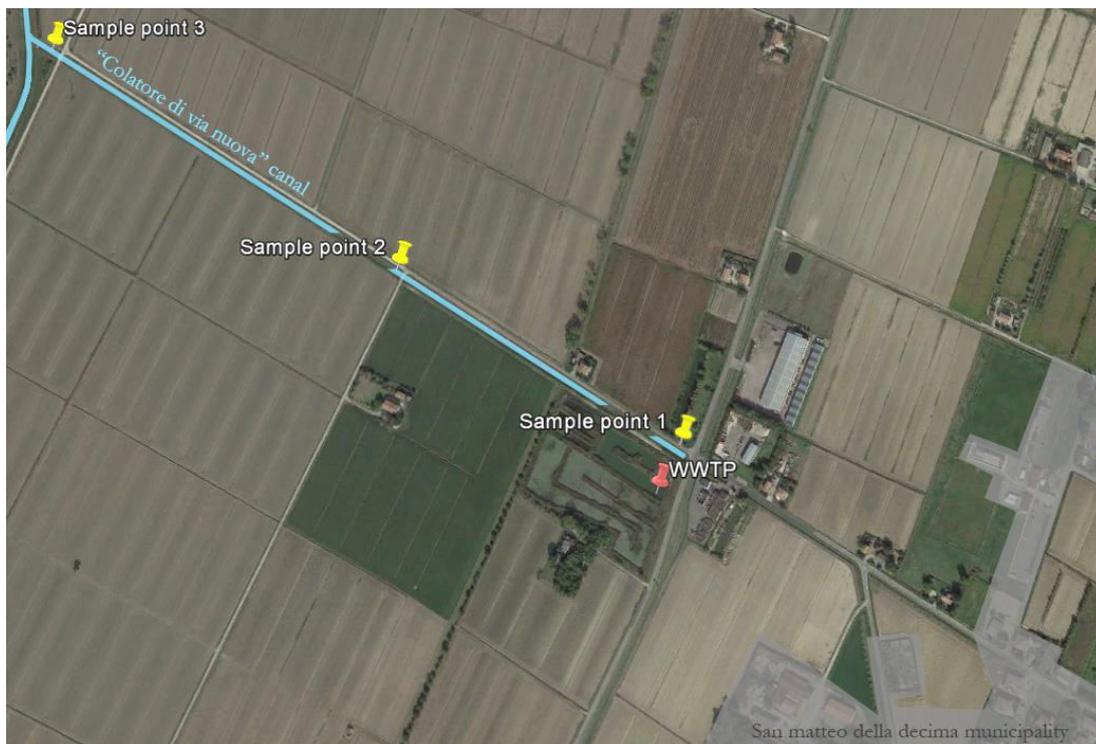
Figure 12: Satellite picture of the sample points. The distance between point is ca. 385 m and 450 m from point 1 to 2 and 2 to 3 respectively

- Sediment samples were collected from three distinct points along a water canal near San Matteo della Decima, Bologna (Italy) during the summer of 2013. Sediment samples points 1, 2 and 3 were located at coordinates 11°13'10.2"E 44°42'57.1"N, 11°12'55.6"E 44°43'04.3"N, and 11°12'38.7"E 44°43'12.5"N respectively (datum WGS84). The canal, belonging to Burana land reclamation consortium area, serves to convoy treated wastewaters coming out from a 7000 population equivalent plant (WWTP). Samples

were called S1, S2 and S3 respectively. All samples were sieved fresh (without altering their water content) at 5 mm, homogenized and stored at 4°C or deep-frozen at -18°C.

- <u>Moisture content and volatile solids</u> content were determined on fresh homogenized samples as a mass loss after a drying at 105°C for 24h and at 550°C for 4h sequentially. All the other <u>physical and chemical characterisations</u> were determined after air-drying of sediments at RT, homogenization through a ball mill (Retsch, Germany) and sieving at 2 mm. In Table 3 the official method used for the characterisation are listed.

Analysis	Method	Instrument
pH of soil solution	ISO 10390	Crison pH-probe (Spain)
Electric conductivity of soil solution (EC)	ISO 11265	Radiometer conductivity meter (Denmark)
Total organic carbon (TOC)	ISO 14235	Flash 2000 CHNS-O analyzer (USA)
Total nitrogen (TN) and **Total sulphur** (TS)	ISO 11261	Flash 2000 CHNS-O analyzer (USA)
Total carbonates	ISO 10693	-
Trace metals, pseudo-total (aqua regia and microwave digestion + ICP analysis)	ISO 12914	Scientific microwave oven (Milestone, USA)
	ISO 22036	Spectro Arcos, Inductively Coupled Plasma - Optical Emission Spectrometer (Germany)
DTPA-extractable metals	ISO 14870 [158]	Spectro Arcos, Inductively Coupled Plasma - Optical Emission Spectrometer (Germany)

Table 3: List of characterisation analysis performed on the sampled sediments, the official ISO method adopted and the instrument used for each of it.

- <u>Calcium chloride washing treatment</u> was performed using $CaCl_2 \cdot 2H_2O$ (Merck) and deionised water to prepare a 0.5 M solution. 250 mL of this solution was added to 100 g (expressed as dry mass) of fresh 500 mL polypropylene centrifugation tubes. These were agitated for 6 h at RT in an horizontal shaker, then centrifuged. The supernatant was discarded, and subsequently the washed sediments were re-suspended in deionised water and centrifuged again. This last step was repeated several times (4 to 5) until restoring their original EC value, in order to remove all the charges in excess.

- <u>Sequential extraction and metal speciation</u>: after lyophilisation, sediments were sequentially extracted following a modified procedure reported by Tessier et al [159]:

  - Fraction I: Exchangeable metals. 1.4 g of lyophilized sediment were extracted with 20 mL of 1 M of NH_4COOCH_3 (ammonium acetate) solution at pH 7.0 for 2 h at RT.

- Fraction II: Metals precipitated with carbonates. The residue from fractionation I was extracted with 30 ml of 1 M NH_4COOCH_3 (ammonium acetate) solution at pH 4.8 for 6 h at RT under continuous stirring.

- Fraction IIIa: Metals bound to Mn oxides. Residue from fractioning II was extracted with 30 mL of a NH_4OH (ammonium hydroxide) solution at pH 3.0 and microwave-digested at 630 W for 50 min up to 100 °C and 344 kPa.

- Fraction IIIb: Metals bound to Fe oxides. Residue from fractioning IIIa was estracted with 50 mL of $(NH_4)_2C_2O_4$ (ammonium oxalate) buffered at pH 2.7 with oxalic acid and microwave-digested at 630 W in three steps (each of them consisting in 60 min up to 130 °C and 344 kPa).

- Fraction IV: Metals bound to organic matter and sulfides. Residue from fractioning IIIb was extracted with 15 mL of 6% H_2O_2 (hydrogen peroxide) at pH 8, microwave-digested at 250 W for 25 min up to 40 °C and 202.6 kPa, then for 25 min up to 60 °C and 202.6 kPa, and finally for 60 min up to 80 °C and 344 kPa. After cooling, 15 mL of 6% hydrogen peroxide at pH 2 were added and the three-steps microwave-digestion at 250 W was repeated. After cooling, 10 mL of 3.2 M ammonium acetate solution (pH 2.9) were added and the suspension was agitated for 30 min;

- Fraction V: Residual metals. Residue from fractioning 4 was dried at 105 °C for 24 h. 0.1 g of dried sample were extracted with 5 mL of Milli-Q water, 3 mL of *aqua regia* and 1.5 mL of HF (48% solution), microwave-digested at 630 W by a two-steps program (60 min and then 20 min up to 170 °C and 962 kPa). After cooling, 5 ml of a saturated H_3BO_3 solution were added and microwave digested using the same two-steps program. Digestions were carried out by a CEM MDS-2000 microwave oven, using Teflon vessels. Finally, each extract was filtered and then analyzed its total metal content by ICP-EOS (ISO 12914, ISO 22036).

- <u>Sediment particle size distribution and clay dispersible ratio</u>. The particle size distribution of two subsamples of each sediments was determined by the pipette method [192] utilising two dispersants: (i) $(NaPO_3)_6$ solution (sodium hexametaphosphate) and (ii) deionised water. In both cases, the particle size classes [193] determined were: coarse sand (2.0-0.2 mm), fine sand (0.20-0.05 mm), coarse silt (0.05-0.02 mm), fine silt (0.02 mm-2 µm), and clay (<2 µm). The samples textural class was defined on the basis of the

(NaPO$_3$)$_6$ data [193]. The <2 μm fractions obtained were named as sodium-dispersible clay (SDC) and water-dispersible clay (WDC). The dispersivity of the clay fraction was evaluated using the clay dispersion ratio (CDR =WDC/SDC × 100).

- Wet structural stability of sediment samples [194] was evaluated on dry sediments re-wet at their original water content (63.7, 62.9 and 54.1% for S1, S2 and S3, respectively) after 1 d of incubation, in order to simulate the original condition. 10 g of each sample were wet-sieved at 0.2 mm for 10 and 60 min by a mechanical machinery. The material remaining on the sieves was then dried and weighed. The amount of stable material (i.e., the fraction that maintained its size >0.2 mm) was then corrected for its content of coarse sand (determined after H$_2$O$_2$ oxidation according to van Reeuwijk [195]) and skeleton grains (obtained after further samples wet sieving to 2 mm). The wet structural stability index (WSS%) was calculated as follows:

$$\text{WSS\%} = \frac{\text{weight retained} - \text{weight of coarse sand} - \text{weight of skeleton grains}}{\text{total sample weight} - \text{weight of coarse sand} - \text{weight of skeleton grains}} \cdot 100$$

4.3. RESULTS AND DISCUSSION

- Sediment characterization revealed some similarities with illuvial silty carbonatic agricultural soils abundant in the area were samples have been collected. Nevertheless, the amount of total organic carbon (9.62, 8.22 and 5.52% for S1, S2 and S3 respectively) exceeds typical soil values. Physical and chemical characterisation of the samples is reported in Table 4.

Parameter (unit)	**Sediment samples**		
	S1	**S2**	**S3**
Moisture (% fw)	63.7	62.9	54.1
Volatile solids (% dw)	14.1	13.9	7.2
pH-H$_2$O	7.49	7.78	8.24
pH-CaCl$_2$	7.29	7.34	7.81
EC (dS m^{-1})	1.09	0.56	0.55
TOC (% DW)	9.62	8.22	5.52
TN (% DW)	0.49	0.4	0.25
TS (%DW)	0.56	0.64	0.61
Total carbonates (% DW)	13.3	13.4	9.04
Textural class	silt loam	silt loam	clay

Table 4: Characterisation of sediment samples (fw: fresh weigth, dw: dry weight)

Interestingly, the amount of organic matter in the sediment decreased, as the distance of the sample point from the WWTP discharge increased (9.62, 8.22 and 5.52% for sediments 1, 2 and 3 respectively, Table 4). A similar tendency can be observed for the total carbonates (13.3, 13.4 and 9.04 respectively, Table 4).

- The determination of pseudo-total metals, reported in Table 5, confirmed that the sediment of "Colatore di via Nuova" canal suffered to different extent of copper and zinc contamination, with higher concentrations in the two sample points closer to the WWTP drain.

	Sediment sample			Dlgs 152/2006 threshold limits	
Metal	**S1**	**S2**	**S3**	**A**	**B**
As	4.60±0.06	4.76±0.28	4.83±0.17	20	50
Be	1.12±0.11	1.44±0.11	2.00±0.23	2	10
Cd	0.56±0.01	0.56±0.01	0.24±0.01	2	15
Co	10.0±0.1	11.9±0.3	15.5±0.1	20	250
Cr	73.2±2.3	82.9±5.9	96.6±11.3	150	800
Cu	**197±1**	**174±5**	**69.8±1.8**	120	600
Hg	0.48±0.01	0.48±0.01	<LOQ	1	5
Ni	46.6±0.2	52.6±1.5	63.3±0.3	120	500
Pb	85.2±1.7	94.7±2.8	30.5±2.2	100	1000
Sb	2.68±0.1	2.16±0.2	1.64±0.1	10	30
Se	1.44±0.01	1.08±0.04	<LOQ	3	15
Sn	**1.62±0.09**	**1.70±0.07**	**1.51±0.05**	1	350
Tl	0.79±0.02	**0.96±0.68**	0.89±0.19	1	10
V	57.3±4.4	72.7±6.6	94.6±16.4	90	250
Zn	**494±3**	**481±5**	**166±2**	150	1500

Table 5: Metal pseudototal content for sediments 1, 2 and 3 (S1, S2 and S3).
For each element are the two respective treshold limits (A and B).
Exceeding values in bold character.

Italian law on excavated material establishes, for each possible contaminant, two different sets of limits: "A" and "B". "A" applies for excavated material, which has to be used in residential or green areas (as defined by local municipality), while "B" applies to industrial areas only. Since the purpose of this thesis is using the dredged sediments *in situ*, and the sediments are excavated from a non-industrial area, limits "A" apply.

A decreasing tendency (similar to those registered for carbonates and organic matter, Table 5) can also be observed for copper, zinc total content. It should be noted that

since have been sampled only three points along the canal, any assumption of correlation between a physical o chemical parameter and the position (in this case, the distance from the WWTP) should be taken with caution. Interestingly, cadmium, copper and lead DTPA-extractable ratios increase in S3, suggesting those metals in sediments of the first two sample points can be found prevalently in precipitated, non-available forms.

- The effect of CaCl$_2$ washing was first registered analysing the pseudo-total metal content of washed and untreated sediments. Once it was assessed that the most significant reduction of Zn and Cu was obtained for S1, an in-depth metal speciation was performed on washed ad unwashed sediments, in order to elucidate the cation exchange mechanism. For the sake of brevity, in Figure 13 are briefly reported the reduction of Cu and Zn assessed by pseudo-total metal analysis, in Table 6 the DTPA-extractable metal content and in table 7 are reported the metal content of the different geochemical fractions (speciation) for sediment 1 only.

In the preliminary pseudo-total metal analysis, the CaCl$_2$ treatment obtained a copper reduction of 25.8, 20.7 and 19.8% for sediments S1, S2 and S3 respectively (Figure 13): promising, yet insufficient to bring the copper content below its law limit for green and residential areas (120 mg kg^{-1}) in any of the three sediments. Moreover, zinc reduction was sensible for S1 but not significant for S2 and S3, and still far from reducing zinc below its limit "A" (150 mg kg^{-1}).
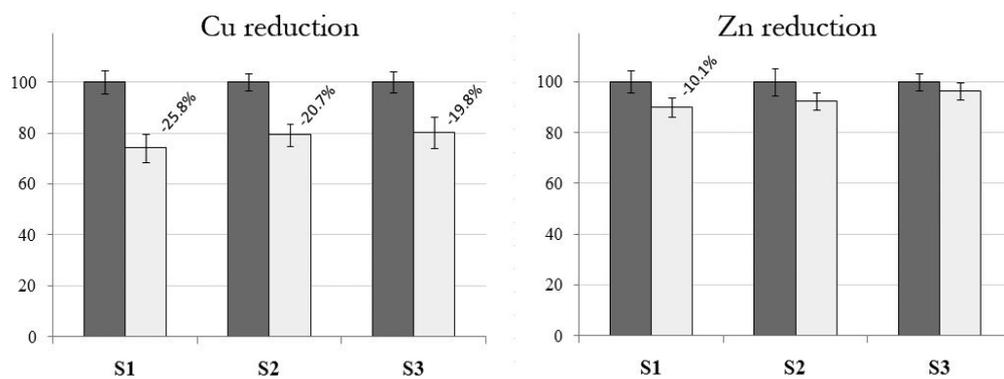
Figure 13: Cu and Zn reduction, expressed as a percentage, before and after CaCl$_2$ washing for all the three sediments

- The effect of CaCl$_2$ washing was also assessed by <u>DTPA extractable trace metal analysis</u>. In Table 6 the DTPA-extractable concentration of each metal is reported before and after the saline treatment on fresh sediments. In addition, this analysis was also repeated on the same sediments after they were air-dried and kept stored for one year. This

analysis was performed in order to have additional clues on the mobility of metal cations present in sediments after the dredged material be exposed to atmosphere.

Trace Metal	S1	S2	S3	S1	S2	S3
	Control Sediment samples					
	Fresh			*One year air dry stored*		
Cd	0.21±0.01 (38%)	0.21±0.01 (38%)	0.15±0.01 (63%)	0.18±0.01 (31%)	0.16±0.03 (26%)	0.03±0.01 (10%)
Co	0.57±0.06 (6%)	0.56±0.05 (5%)	0.50±0.04 (3%)	0.58±0.01 (5%)	0.51±0.02 (4%)	0.40±0.01 (2%)
Cr	0.14±0.01 (<1%)	0.14±0.01 (<1%)	0.14±0.01 (<1%)	<LOQ	<LOQ	<LOQ
Cu	24.6±1.0 (12%)	26.4±1.1 (15%)	18.7±0.5 (27%)	68.2±0.8 (35%)	71.4±1.2 (41%)	27.5±0.5 (39%)
Ni	2.14±0.02 (5%)	1.80±0.01 (3%)	1.61±0.01 (3%)	2.70±0.05 (6%)	2.10±0.07 (4%)	1.79±0.06 (3%)
Pb	11.9±0.5 (14%)	14.5±0.2 (14%)	7.90±0.10 (26%)	13.8±0.1 (16%)	16.9±0.1 (18%)	9.84±0.03 (26%)
Zn	60.6±2.2 (12%)	44.6±2.1 (9%)	10.8±0.5 (7%)	101.0±0.2 (20%)	71.8±0.2 (15%)	17.9±0.2 (12%)
	CaCl$_2$ washed sediment samples					
	Fresh			*One year air dry stored*		
Cd	0.08±0.01 (38%)	0.09±0.01 (38%)	0.03±0.01 (63%)	0.10±0.01 (20%)	0.08±0.01 (18%)	0.03±0.01 (11%)
Co	0.45±0.06 (6%)	0.44±0.04 (5%)	0.33±0.04 (3%)	0.30±0.01 (3%)	0.29±0.01 (2%)	0.27±0.01 (2%)
Cr	<LOQ	<LOQ	<LOQ	<LOQ	<LOQ	<LOQ
Cu	20.0±1.0 (14%)	23.3±1.2 (15%)	10.3±0.5 (17%)	36.3±0.1 (25%)	39.8±0.1 (23%)	13.2±0.1 (22%)
Ni	2.14±0.02 (5%)	1.82±0.03 (3%)	1.57±0.01 (3%)	1.90±0.09 (4%)	1.60±0.05 (3%)	1.10±0.01 (2%)
Pb	13.3±0.5 (14%)	14.1±0.3 (14%)	6.76±0.10 (26%)	17.8±0.1 (21%)	21.9±0.1 (24%)	8.14±0.08 (21%)
Zn	68.9±2.51 (15%)	53.1±1.97 (13%)	15.6±0.75 (10%)	74.8±0.2 (17%)	61.9±0.2 (13%)	14.3±0.2 (9%)

Table 6: DTPA-extractable) metals for S1, S2 and S3. Their percentage on the total (reported in Table 5) is indicated in brackets

For most metals, the CaCl$_2$ washing achieved a general decrease on their DTPA-extractable fraction. Nickel fraction did not change significantly and, surprisingly, zinc fraction grew for all sediments after the saline treatment, despite the treatment reduced its total amount (Figure 13).

When the control and the treated sediments were compared after being air-dried stored for one year, a global raise in DTPA-extractable fraction was assessed for most metals,

as the joint effect of drying and oxidation is known to mobilize some metal species [196-198]. This phenomenon was particularly prominent for copper and zinc.

Nevertheless, sediments treated with $CaCl_2$ had a more contained raise, after being dried and exposed to air for a year, with the sole exception of lead. This evidence suggested that, seemingly, calcium treatment does not limit to remove metal cations from soil exchange sites, but can also remove metals from different soil fractions. In particular, water sediments exposed to air undergo important changes in their redox potential, resulting in oxidation of sulphides and organic matter accumulated underwater [199]. For this reason, calcium treatment could affect metal cation bound to these fractions. As mentioned in the second-to-last paragraphs, the organic matter present in the sampled water sediments not only is much higher compared to the average content of an agricultural soil (1-2%) but being deposited in anoxic and reductive conditions, it can be safely considered as easily oxidizable once exposed to air. A similar hypothesis could be applied to sulphurs as well.

- In order to have a better understanding on how the calcium treatment could affect the different soil fractions, a metal speciation was performed on sediment 1 (S1). According to the results reported in Table 7, copper in S1 was mainly present in its form bonded to sulphides or organic matter.

The only statistically significant reduction of copper was also found in the same fraction, in accordance with the hypothesis that the calcium treatment affects metal cations bound to sulphides and organic matter.

	Metal content (mg kg^{-1})			
	Unwashed S1		CaCl$_2$ washed S1	
Metal fraction	Cu	Zn	Cu	Zn
I – Exchangeable	0.62	16.5	0.91	15.3
II – Bound to carbonates	11.5	140	14.3	103
IIIa – Bound to Mn-oxides/hydroxides	10.2	153	10.5	155
IIIb – Bound to Fe-oxides/hydroxides	4.59	67.4	7.75	70
IV – Bound to sulphides/organic matter	113	75.3	81.8	67.3
V – Mineralogical/Not exchangeable	26.4	42.3	35.4	64.2
Sum of the above	166	495	151	475
Total content	209	552	155	496

Table 7: Metal speciation of Cu and Zn for Sediment 1 before and after saline CaCl$_2$ treatment. Errors <20%

Zinc, on the other hand, was not prevalently bound to fraction IV and its total reduction achieved by calcium treatment was consistently lower with respect to copper (Figure 13).

Zinc was mainly contained in fraction II and IIIa (precipitated with carbonates and bonded to manganese hydroxides) and the only significant decrease could be found among fraction II, as Ca^{++} ion exchanged Zn^{++} in precipitated carbonates.

Cu and Zn level for all the other fractions did not alter significantly. Minor Cu or Zn concentration raise (e.g. Cu and Zn in fraction IIIb or Cu in fraction II) in some fraction, after the calcium treatment, could be due to the fact that the copper and zinc cations displaced by calcium ion do not necessarily remain soluble (e.g. as chlorinated ionic couples) but can precipitate again as different species or, in general, undergo other chemical *equilibria* with the effect to make them immobile again.

- Sediment particle size distribution and wet aggregate stability. Pipette method for the determination of "real" particle size distribution (using $(NaPO_3)_6$ as dispersant) of the non-washed samples revealed that S1 and S2 had a silt loam texture (with S2 richer in silt), whilst S3 had a clay texture.
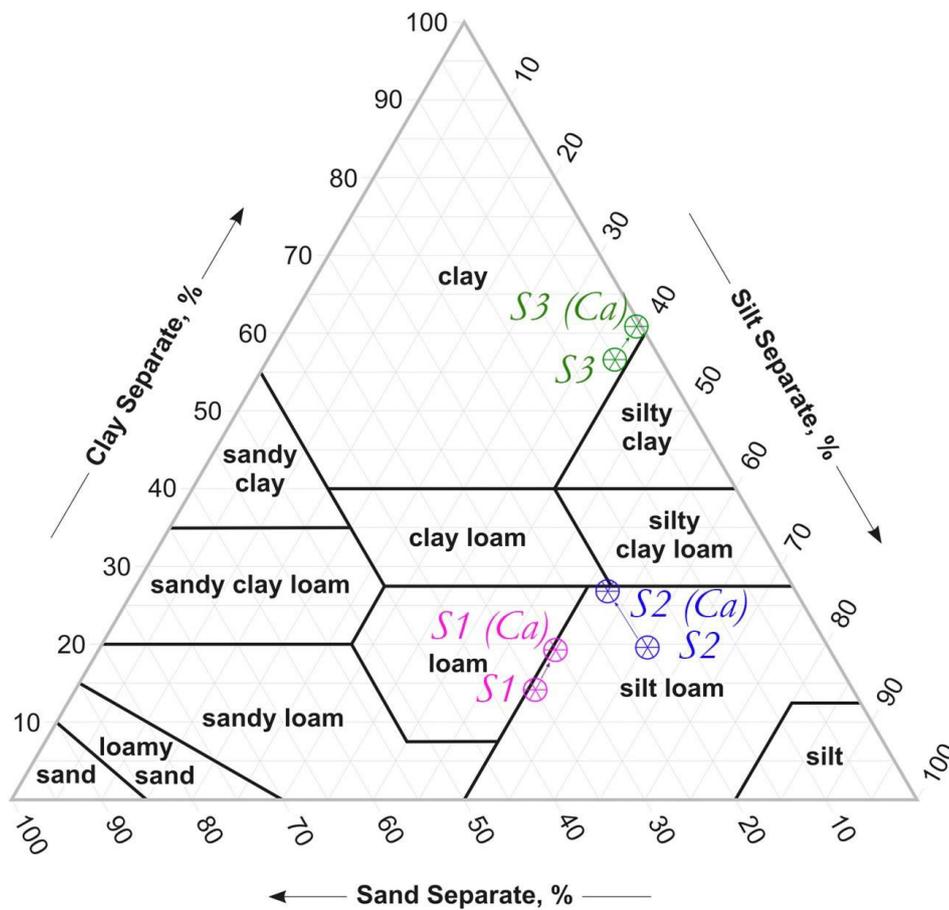
Figure 14: USDA Texture triangle containing the coordinates of the treated and untreated sediments sample. Texture triangle modified from http://schoolofpermaculture.com

Each Sediment position in the USDA soil texture triangle is reported in Figure 14. Yet again, it is possible to observe a higher presence of fine fractions (silt and clay) as the sample point distance from the WWTP increase. The effect of saline washing on texture was evaluated as well. For all treated sediments a global clay increase was registered; in S1 and S3 though, it was accompanied by a sand decrease, whilst in S2 a silt decreased.

- Clay dispersible ratio (CDR), defined as the ratio (in %) between the clay dispersed by water and the clay dispersed by $(NaPO_3)_6$ was 95.11, 49.7 and 16.3% for S1, S2 and S3 respectively: interestingly, the most clay containing sediment (S3) had most of its clay non-dispersible in water. Calcium treatment had the effect, for all the sediment samples, to increment the flocculation of clay, thus decreasing the CDR.

On the other hand, comparing the results of the stability tests for treated and untreated sediments, a general decrease in the aggregate stability (expressed as WSS%) is observed. After 10 minutes of sieving, the 60.5, 88.1 and 81.8% of S1, S2 and S3 sample respectively remained stable on the vibrating sieve, whilst it was only 33.3, 52.0 and 60.5% for the $CaCl_2$ washed sediments. Sample loss during the first 10 minutes of sieving are generally due to particle dispersion: in fact, the sediment samples with the highest CDR (S1) has the higher losses; the sample whit the lowest CDR, instead, has the lower losses. After 60 minutes of sieving, sample losses are mainly due to water abrasion, whilst losses due to dispersion are negligible: S3 samples tend to be particularly susceptible to abrasion, rather than particle dispersion. S1, on the contrary has minor losses after 60 minutes, as the particle dispersion is mainly responsible for its loss of material. In any case, calcium treatment seems to reduce water stability of sediments. This is probably due to the flocculation of clay (caused by Ca^{++} ion) and the formation of smaller, less resistant to water soil aggregates.

Sediment Sample	CDR (%)		WSS$_{10'}$ (%)		WSS$_{60'}$ (%)	
	Control	Ca-treated	Control	Ca-treated	Control	Ca-treated
S1	95.11	86.14	60.5 ± 9.2	33.3 ± 10.9	42.4 ± 7.6	36.9 ± 4.9
S2	49.7	29.2	88.1 ± 6.8	52.0 ± 9.9	67.0 ± 3.8	47.7 ± 3.4
S3	16.3	5.6	81.8 ± 8.6	60.5 ± 0.2	23.4 ± 1.8	10.3 ± 4.5

Table 8: Clay Dispersion Ratio, expressed as percentage and Wet Structural Stability (expressed after 10 and 60 m of wet sieving) of CaCl₂ washed and untreated sediment.

In conclusion, the physical effect on the soil structure of the calcium washing seems associated to a general increase in clay fraction and a decrease in the water dispersivity of

the clay particles, followed by a reduction either of the silt or the sand fraction, and a general reduction of aggregate stability in water.

4.4. CONCLUSIONS

A saline $CaCl_2$ sediment washing was tested in order to clean up water sediments dredged from a local land reclamation canal. The sampled sediments were contaminated with zinc and copper and could not be used for in-situ applications according to Italian law. The cause of the contamination was due to a municipal wastewater treatment plant serving 7000 population equivalent.

The calcium treatment was able to remove 25.8% of Cu and 10.1% of Zn from the most polluted sediment sample S1. Despite the removal of these metals was not sufficient to bring the sediment below the legally-defined contamination values, the combined results obtained from the pseudo-total metal analysis, DTPA-extractable metal analysis and metal speciation highlighted interesting evidences on $CaCl_2$ washing treatment. Copper overall reduction (assessed by pseudo-total analyses) achieved by the treatment was prevalently due to the its removal from organic matter and sulphides (fraction IV) in which copper was mainly present. Differently, zinc which was prevalently distributed in different fractions (carbonates and manganese oxihydroxides), which could not be affected decisively by the calcium washing. Exchangeable Zn and Cu (fraction I) could not be removed from the matrix by the saline washing: metal cations supposedly kept mobile by Cl^- counterions were sorbed back into exchangeable forms. In each case, copper and zinc (as well as cobalt and nickel) concentration of DTPA extract of all sediments after drying and exposure to air was reduced by the $CaCl_2$ washing.

Concerning the physical effects of the saline washing on the sediment stability, a slight increase of clay fraction was registered, along with a general decrease of water-dispersivity of clay particles. Nevertheless, overall wet aggregate stability was reduced, especially on short-term tests. As a general consideration, the sediment structure could be improved with typical soil amendments (straw, lime or biosolids) or mechanical compaction by heavy machineries.

In conclusions, saline $CaCl_2$ could be a useful tool to reduce heavy metal bonded to organic matter and sulphides in fresh water sediments, and could be an even more useful tool to stabilize Cu and Zn into bio-unavailable species when water sediments are exposed to atmosphere.

# 5.	Grafted humic acid for environmental applications

## 5.1.	INTRODUCTION

Natural soils are peculiar ecosystems. As complex natural matrices, soil can host microbial and plant life maintaining its fertility through biogeochemical cycles (nutrient uptake, transformation and release). Moreover, the soil is an extremely important buffer in ecosystems' protection, as it is a natural sink for substances undesired to superior life forms, retaining and transforming pollutants. All of these functions (carbon sink, pollutant filter, nutrient renewal) though, could not be possible without its primary, most basic, and often most underestimated function: sorption capacity.
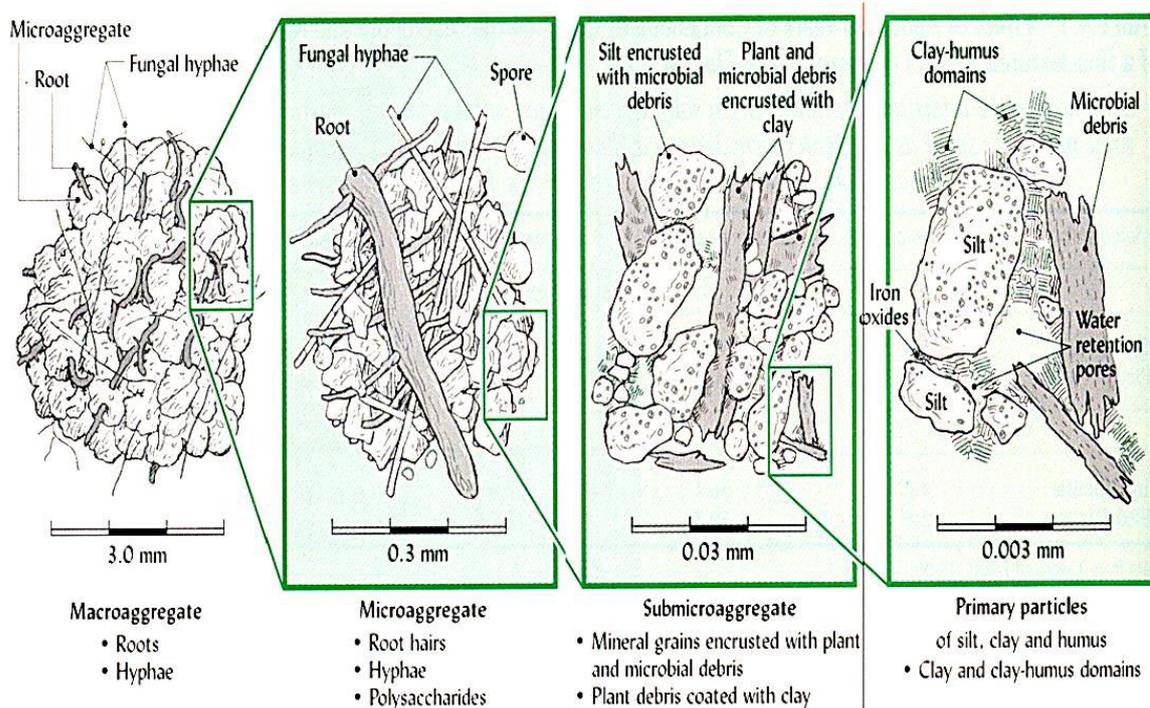
**Figure 15: Soil is a complex matrix at different scales, from the naked-eye visible scale to micro-scale. At the smallest scale, primary soil particles are an arrangement of expandable clays, humic substances and heterogeneous pores. This structure is ultimately responsible for water retention, fertility elements storage and abiotic molecular transformation. Picture from Tisdall & Oades, 1982.**

An essential role in the soil sorption capacity is carried out by soil colloids. At a micro-scale, soil is a heterogeneous material composed by a mineral and a stable organic fractions (humic substances) intimately bound. The mineral fraction is quantitatively and qualitatively variegated, as many different minerals can be present (such as carbonates, oxihydroxides, phyllosilicates...) among soil colloids. The resilient soil organic fraction, the humic fraction, is composed by organic macromolecules rich in oxygenated acidic moieties (mostly carboxyl and phenol groups). This organic fraction has been and still is difficult to isolate, study, define and catalogue. Nevertheless, it is of general knowledge that clay particles and humic substances, as well as amorphous metal oxihydroxides, are in effect the main responsible of both soil sorption capacity and degradation of pollutants.

In this context, the possibility to produce humic acids-grafted with a solid support could serve as: i) simplified model for soil particles in multidisciplinary studies; ii) to exploit humic substances sorption capacity for water contaminants[200-203]; iii) pollutant photo-degradation catalyst; iv) to exploit humic-like byproducts and wastes (e.g.: organic sludge from water treatment plants, exhausted material from bio-reactors, agro-industry sludge...) by grafting onto a solid support [204].

5.1.1. Humic acids: environmental function and sorbent properties

Humic substances are the main component of the non-living organic matter naturally occurring in soils, sediments and water bodies, from which they can be extracted [200].

Being naturally formed as a result of physico-chemical and biochemical degradation of autochthonous or allochthonous organic matter, the composition of humic substances is highly heterogeneous among different environments, as the result of multiple factors such as climate or land use. Having such a complex composition and variability [205], defining a precise molecular structure for these compounds would be unfeasible [206]. Humic acids have long been considered comparable to heterogeneous polymers or very large (10^3-10^4 Dalton) molecules. Recently, a supramolecular model is getting more and more acknowledgment [207, 208]. According to it, humic acids can be reasonably described as an heterogeneous set of organic macromolecules spacing from hundreds to not more than two thousands of Daltons, "assembled" together by intermolecular and intra-molecular interactions.

Nevertheless, it is an undoubted experimental evidence that at a small scale their structure consists in a carbon frame (both aliphatic and aromatic) with a large number of carboxylic,

phenolic and carbonyl functions [209], along with many other less abundant moieties containing sulphur and nitrogen. Due to the high number of carboxylic functions, the overall pK_a of humic acids can vary from 3 to 5; moreover, the presence of both hydrophobic and hydrophilic portions give these molecules amphiphilic properties [210, 211]. Bound to mineral fraction of soil and sediments, humic acids are strongly responsible for soil pH buffer and sorption capacity. When dissolved into water, instead, humic acids behave like colloidal surfactants. In any case, their conformation, aggregation and surface chemistry highly depends on pH and ionic strength of the aqueous solution.
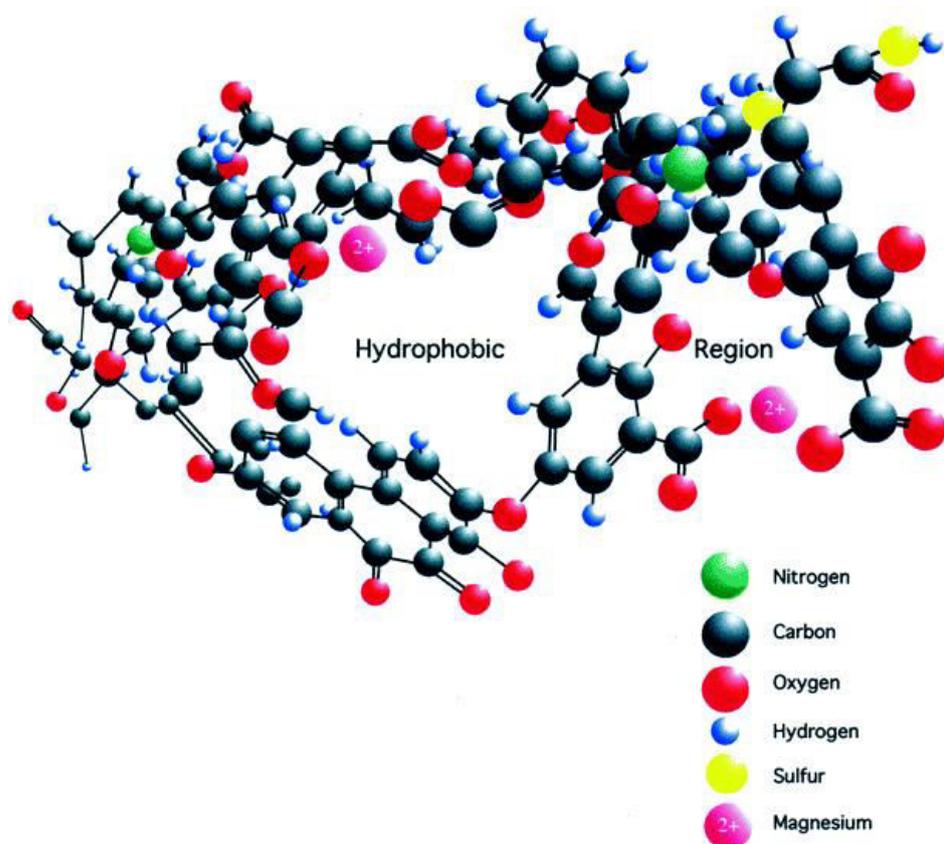
Figure 16: An example of a humic acid structure and conformation. Credits to von Wandruska and coworkers [210]

The adsorption of organic and inorganic species on humic acids has already been discussed and reported in the literature. The fate of pollutants in water courses and soil can be heavily affected by the amount and composition of humic substances dissolved or bound to soil and sediment particles [202]. The chemical interactions between pollutants and humic acids involve different mechanisms and can be affected by many factors such as saline strength, pH and chemical properties of the contaminants. Cations are easily bound on the exchange complex of the heterogeneous surface of humic acids attached to soil particle and suspended

65

in water bodies [212-215]. In fact, dissociated carboxyl groups provide a large number of negative charges, owing to the fact that the pH of agricultural soil is usually above their pK_a. In water courses as well, most of the carboxyl groups are dissociated and bound to mono or polyvalent cations. Polyvalent cations can magnify the supramolecular structure of humic acids, aggregating different humic macromolecules into bigger colloidal particles.

Many other polar interactions are involved in sorption mechanisms of pollutants on humic acids, since large number of studies have been conducted involving organic and inorganic pollutants which contain polarisable functional groups [203, 216]. The available scientific literature is hence rich in papers examining the sorption effect of humic acids on species such as cations, positively charged organic molecules and scarcely polar compounds, but still the role of nonpolar moieties of humic acids (aliphatic chains, alkyl groups, aromatic rings) in sorption mechanisms remains unclear.

As already mentioned, humic acids behave like anionic surfactants forming "pseudomicelles" and embedding nonpolar species [210], binding cations and adsorbing polar species. For environmental applications, the possibility to have humic acids immobilized onto a solid phase would be preferable to be recovered after adsorption of contaminants from the aqueous phase. The immobilization of humic acids has been addressed in the last 20 years [217-219]. Their immobilization has been achieved by polycondensation or involving the formation of chemical bonds (grafting) between humic molecules and inert material such as Merrifield resin, polymers, functionalised silica or cellulose. Such solid materials is more interesting for environmental applications in aqueous media (e.g. column filtration) as, under immobilized form, they keep some sorption properties and are easier to handle [204, 220-224]. Nevertheless, fixating these molecules into rigid solid support would inevitably modify some of their chemical moieties, prevent them from forming pseudomicelles, or dampen their supramulecular aggregation. For the very same reason, many researchers concur the humic acids bound to mineral fraction in soils be completely different after their extraction and purification with strong alkali and acids [205].

Some solid humic acids-grafted materials show an exploitable sorption capacity towards certain molecules such as pentaclorophenol and benzo[a]pyrene [220, 221, 225], and even an interesting photo-degradation activity [204].

Yet, the chemical nature of the interactions concurring in sorption mechanisms of slightly polarisable molecules is still argument of debate. In this work of thesis, soil humic components has been bound to silica material and the affinity of humic acids towards toluene, a volatile fuel-based groundwater pollutant, is addressed by different sorption trials.

5.1.2. Volatile Organic Contaminants (VOCs) in water bodies and groundwater

Pollution of the aquifer is caused by the presence of unwanted compounds and pathogens, both caused by human activities as well as by natural *phenomena*. Apart from elements naturally dissolving from minerals, such as fluorides and arsenic, contaminants may reach groundwater typically: i) by leaching through soil profile after being dispersed on the ground and ii) by direct contamination from excavation, mining sites, quarries, underground pipes, etc. In the first case, contaminants are transported by water and filtered through soil and rocks: natural attenuation, sorption and biodegradation may occur, depending on contaminant physico-chemical characteristics. In the second case, when point sources release a contaminant directly into the aquifer, attenuation mechanisms are limited; also, depending on contaminant's water solubility, pollutants may solubilise into water, form a separate phase or both, depending on solubility and local conditions [226]

The aquifer is a subterranean layer of permeable rock, fractured rock or unconsolidated material such as sand or gravel. It is underlain by non-permeable layers and saturated by water, which fills fractures and cavities. Such water naturally flows, depending on its hydraulic potential and water conductivity of rocks. When contaminants reach underground water, they spread, forming a contaminated "plume" whose amplitude and movement may vary significantly, depending on many factors (hydrogeological and chemical) which can be modelized [168]. Models simulating the diffusion of a contaminant in groundwater are a powerful tool for environment protection agencies to predict the diffusion of a noxious compound in the aquifer, and adopt the proper remediation technique [170].

BTEX contamination poses a serious threat to underground water. As reported in Table 9, benzene and toluene have a relatively high solubility in water. Toluene is toxic, while benzene is a potential carcinogen. Both molecules can be found abundantly in gasoline, kerosene and fuel.

	Molecular weight (g mol^{-1})	Boiling point (°K)	Vapour pressure* (kPa)	Partition coefficient [227] log K$_{ow}$	Solubility in water* (mg/L)
Cyclohexane	84.16	353.89	10.3	3.44	55
Benzene	78.11	353.2	10.1	2.13	1770
methylcyclohexane	98.19	374	4.93	3.61	14
Toluene	92.14	384	2.8	2.65	520
Ethylcyclohexane	112.22	405	4.13	n.a.	1.22
Etilbenzene	106.17	409	1.33	3.15	1.5

Table 9: Physico-chemical properties of some BTEX and their aliphatic counterparts
* referred to standard conditions

Benzene and toluene are the molecules, among BTEX, having the highest vapour pressure (thus highest volatility) and the highest solubility in water. Compared to their aliphatic analogues (cyclohexane, methylcyclohexane, Table 9), their solubility is much higher: this is mainly due to the delocalized electrons of the aromatic ring, which make the whole molecule significantly polarisable and susceptible to be H-bonded by water and polar moieties [228].

The most severe toluene contaminations involve the aquifer. If toluene is spilled in surface waters, due to its hydrophobicity and density, it forms a separate phase (like a petrol floating stain), which tends to evaporate. Only a small quantity dissolves into water, where it can be slowly biodegraded [229]. An aquifer contamination, instead, prevents the removal achieved by spontaneous evaporation; a floating layer of undissolved non aqueous phase liquid (NAPL) will persist over the aquifer, slowly moving along and releasing molecules in solution (spreading "plume") [230, 231].

BTEX-contaminated soil or groundwater *in-situ* remediation can be accomplished with various techniques. A deep preliminary knowledge of the morphology of the site is required such as aquifer depth, groundwater flow, presence of non-permeable clay layers, composition and vapour tension of the contaminating mixture [230].

Bioremediation can be achieved by letting BTEX to be transformed by the *microbiota* populating the unsaturated zone or groundwater: minerals, nutrients and oxygen (or other electron acceptors) can be added to promote the process (otherwise being called *intrinsic* bioremediation) [232].

On the other hand, soil vapour extraction and pump-and-treat remediation are more invasive techniques to be taken into account when bioremediation is not sufficient or for large contamination volumes.

Soil vapour extraction is a physical treatment for the remediation of volatile compounds in unsaturated zone. It is also referred to as *in situ* soil venting or vacuum extraction, and consists in mass transfer of contaminant from the solid and liquid (aqueous or non-aqueous) phases into the gas phase, with subsequent collection of the vapours (and condense) at extraction wells. This is hence treated in aboveground systems [233].

The equivalent of soil vapour extraction for the removal of contaminants in the saturated underground zone (the aquifer) is the pump-and-treat remediation. In this case, the contaminated water of the aquifer is collected from dedicated wells, pumped aboveground and treated. Generally, soil vapour extraction remediates more efficiently volatile compounds (ethylbenzene and xylenes are more volatile than benzene and toluene) contaminating only the unsaturated zone or a light insoluble NAPL floating above the saturated zone. For highly soluble or non-volatile contaminants dissolved into the saturated zone a pump-and-treat remediation plant is preferred [234].

In this work of thesis a humic acid-grafted synthetic silica is prepared and screened for its possible use on water treatment systems, evaluating and arguing its capacity to retain toluene in aqueous phase [204].

A preliminary production of a synthetic silica coated by humic substances (with sufficiently stable covalent bonding) was performed. Humic acids were purified and grafted onto a 3-aminopropyl silica gel (both were commercial) using a modified procedure proposed by Szabó and coworkers [235]. The material was characterised, tested for its stability in water and used in basic sorption tests. In the present thesis the results obtained at the time of the conclusion of the PhD program will be presented, as the interesting characteristics of the novel material can possibly lead to the start of several further research projects on the topic, such as its utilisation in photo-degradation of pollutants.

5.2.   MATERIAL PREPARATION

- Materials. Commercial sodium salt of humic acids (lot. S15539-115), commercial 3-aminopropyl silica gel (lot. SHBF5205V), anhydrous N,N-dimethylformamide, reagent grade acetic anhydride, analytical grade toluene, acetonitrile and 4-phenyldiazenylaniline (4PDA) were all from Sigma-Aldrich. 4PDA solutions were kept covered by aluminium foils to avoid trans/cis isomerisation catalyzed by UV light.

- Humic acids purification. 10 g of commercial Humic Acids as sodium salts (NaHA) have been suspended in 1 l of water at pH 11 with NaOH and stirred overnight. The suspension was hence centrifuged at 4000 g for 30 minutes, the precipitated and impurities were discarded, whilst the supernatant was collected and brought to pH 1 with a solution of HCl 1 M. The suspension was stirred for 24 hrs, and centrifuged again at the same conditions. The supernatant was discarded and the precipitated humic acids were thoroughly rinsed with a 0.01 M HCl solution and subsequently MilliQ water. The obtained product was called "Purified Humic Acids" (PHA), dried at 60 °C for 24 hrs and stored into a desiccator.

- Humic acid grafting. The procedure used was first described by Szabó and coworkers [217, 235-237]. Briefly, it involves the formation of a stable amide bond between silica's amino functions and free carboxyls of humic acid in a polar aprotic solvent able to sequestrate the condensed water (which slows the amide formation) from the reaction. Subsequently, unreacted amino functions have to be end-capped by acetylation to rule out their potential contribution to sorption. 1 g ca. of porous 3-aminopropyl silica (called from here on SiNH$_2$) were placed into a 3 necks flask and conditioned at 150°C for 4 hrs under vacuum. 300 mg of dry PHA were carefully dissolved into 30 ml anhydrous N,N-dimethylformamide (DMF) and added to the silica gel. The reaction occurred at 120 °C for 20 hrs under magnetic stirring in nitrogen atmosphere. The material was then cooled and washed thoroughly with DMF until the supernatant was transparent; then washed again with a NaCl 1 M solution until no more humic acids leaked.

- <u>Final end-capping of spare amino groups</u>. The dry material was suspended in 50 ml of DMF containing 5% acetic anhydride (AA) and stirred at room temperature for 8 hrs. Afterwards, it was filtered and washed thoroughly with: DMF, acetone, water at pH 10 and finally with deionised water.
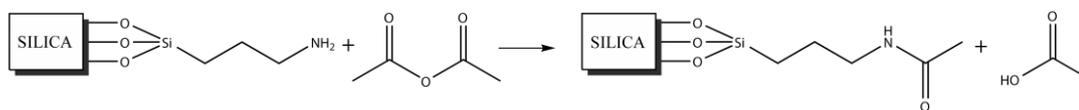
The resulting material (SiHA) was then finally dried and stored into a desiccator. Some bare $SiNH_2$ material was encapped too in order to create a reference material for comparison to SiHA. This material was called SiNCO.
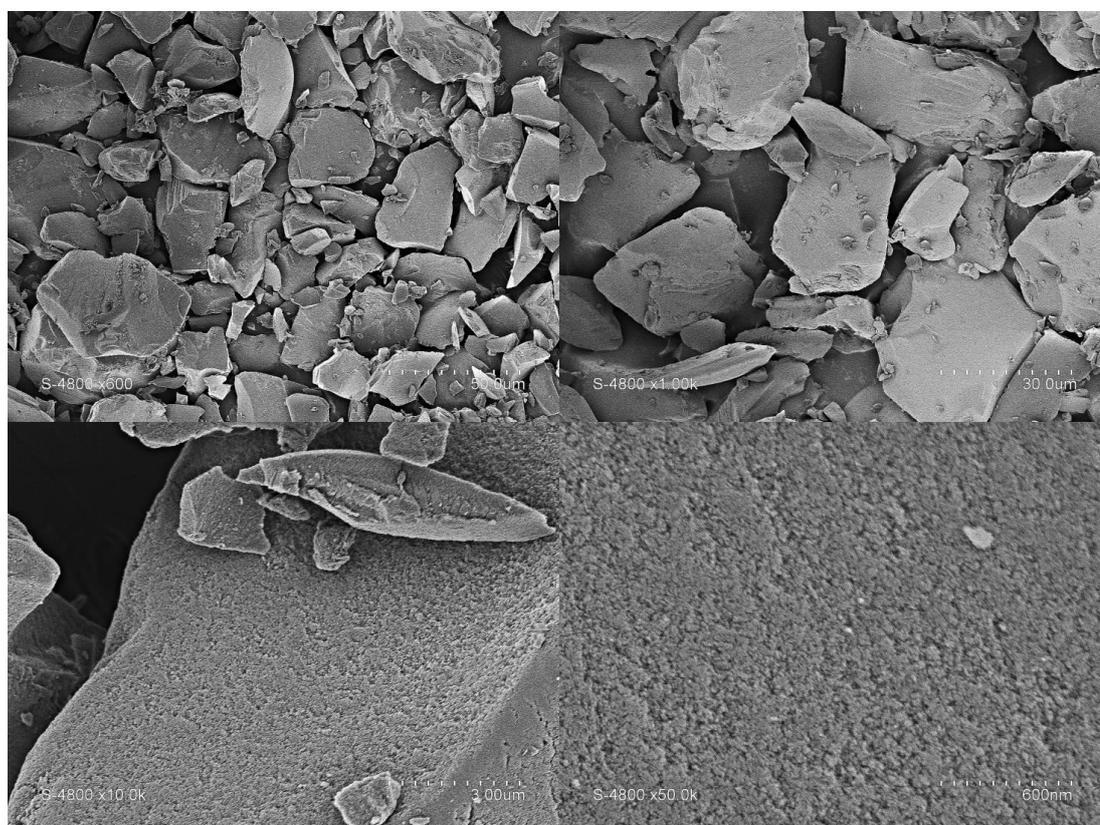
Figure 17: SEM of the humic acid grafted silica (SiHA). Thomas Cacciaguerra of the Institut Charles Gerhardt Montpellier is kindly acknowledged.

- <u>SiHA leaking test</u>. In order to assess the stability of the humic acid-grafted material in water, a "stress test" was performed following the procedure of Koopal and co-workers [217]. Briefly, a 0.05M $NaHCO_3$ stock solution was prepared. Standards for UV-vis analysis were prepared by adding known amounts of PHA to the sodium bicarbonate solution, in order to obtain a calibration curve for dissolved humic acids in the sodium bicarbonate solution. 23 mg of SiHA were washed with 10 ml of solution in a ultrasonic

bath for 5 min and centrifuged at 5000 g for 15 min. Supernatant was collected and immediately analyzed by a Lambda 35 UV-Vis spectrophotometer by PerkinElmer (USA). The procedure was repeated three times on the same SiHA sample. After the first washing, 5.2% of the grafted humics were lost from the material and 1.7% after the second one. Finally, after the third washing, no humic substances were detected. All the produced SiHA was then further washed in $NaHCO_3$ solution, in order to have a stable final product. All the characterisation analyses for SiHA refer to the material obtained after these ultimate washings.

5.3.   MATERIAL CHARACTERISATION

- The <u>nitrogen adsorption isotherms</u> on the dehydrated SiHA and $SiNH_2$ were determined with a Micromeritics TriStar 3000 instrument at 77K and the specific surface areas were calculated by the BET method.

  For $SiNH_2$, the starting material, BET calculations found 372 m^2 g^{-1} specific surface area and a specific pore volume of 0.52 cm^3 g^{-1}. The average pore diameter was calculated with the Gurvitch equations, obtaining 5.6 nm: the pore distribution curve is clearly due to a non-ordered mesoporous material (Figure 18 bottom on the next page).

  The humic acid grafted to silica (SiHA), having its surface covered with humic macromolecules, was initially thought to have its pores encumbered. Surprisingly, the material porosity of the grafted sample was reduced far less than expected, showing 316 m^2 g^{-1} specific surface, 0.38 cm^3 g^{-1} specific pore volume and an average pore diameter of 4.8 nm. It can be assumed that humic acids did not occupy the internal pore volume, but only the external surfaces. Furthermore, the pore diameter reduction could be related to the acetylation (endcapping) of 3-aminopropyl functions on the internal pores, which are not accessible to the large humic acids macromolecules.

- <u>Thermogravimetric analysis</u> and differential thermal analysis were carried out with a TGDTA92 thermic balance by Setaram (France), whilst <u>elemental analyses</u> were performed using a Flash 2000 CHNS-O analyzer (USA).

  Thermal analysis of SiHA and SiNCO (Figures 19 and 20) revealed a mass loss of -18.7 and -9.1%, respectively, in the 300-800°C temperature interval (range of organic matter decomposition), corresponding to a -19.19% and -9.99% total dry mass loss respectively (<200°C losses are mainly due to water or solvent evaporation). Subtracting the two

mass losses leads to roughly quantify the humic acid grafting as 9.2% on the dry mass of the grafted silica.

Elemental analysis of SiHA revealed that about 52% of the sample was C and 1.6% was N, indicating thus by a grafted organic material characterized by a ratio between C and N of 28.
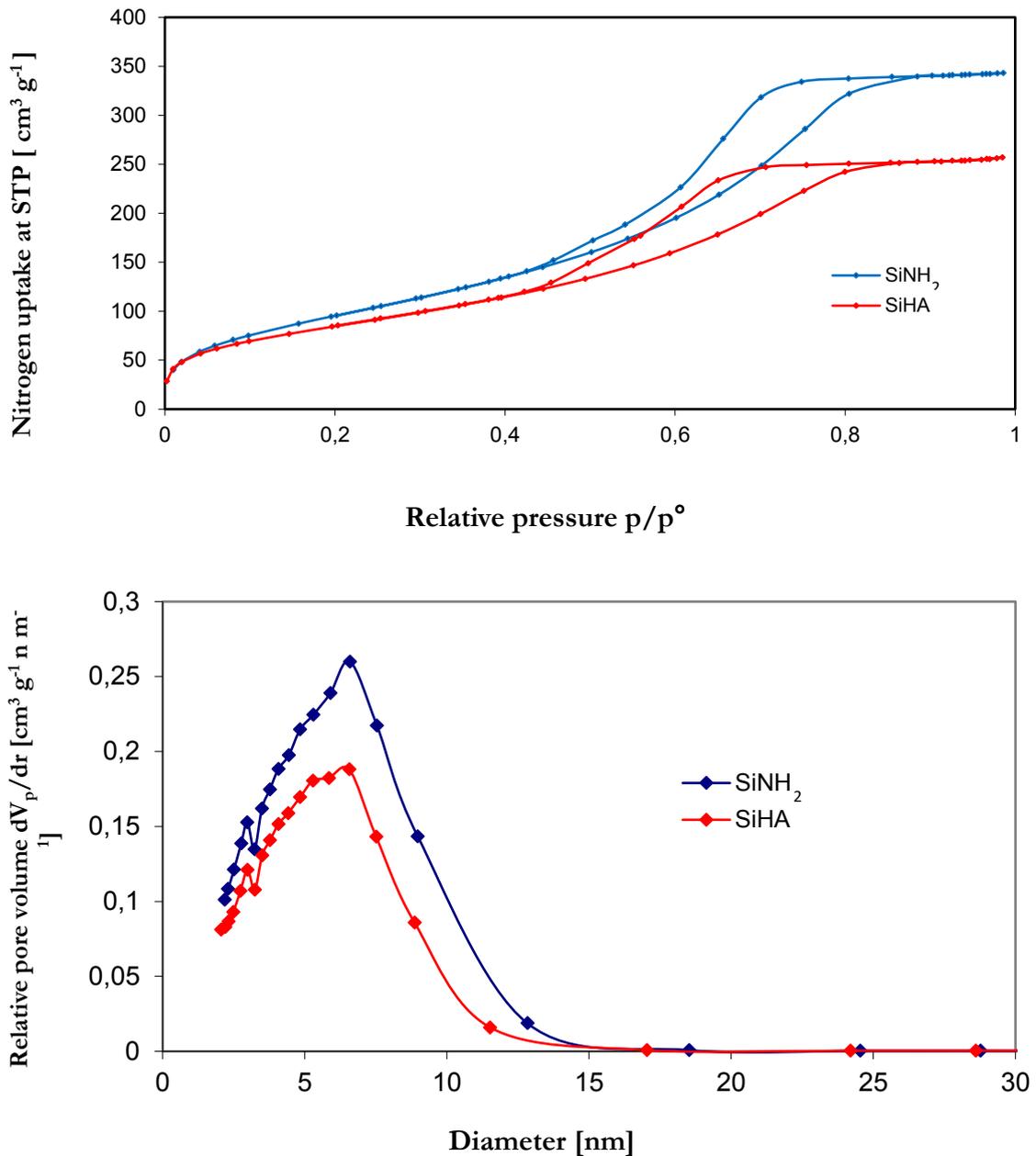
Figure 18: Nitrogen sorption isotherm (top) and pore size distribution (bottom) for starting material (SiNH$_2$) and after humic acid grafting (SiHA)
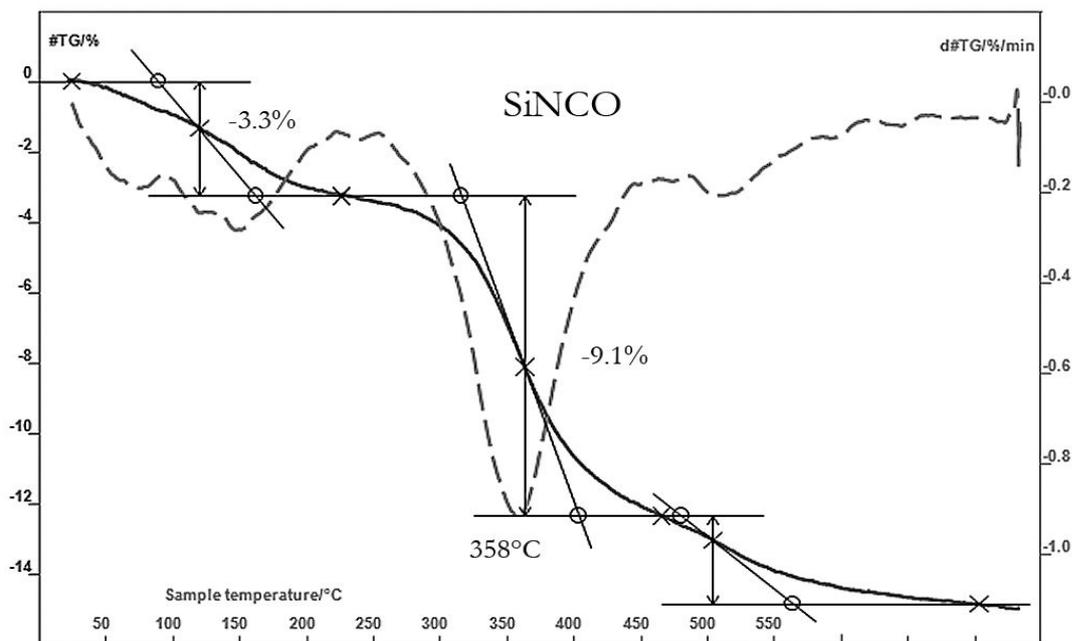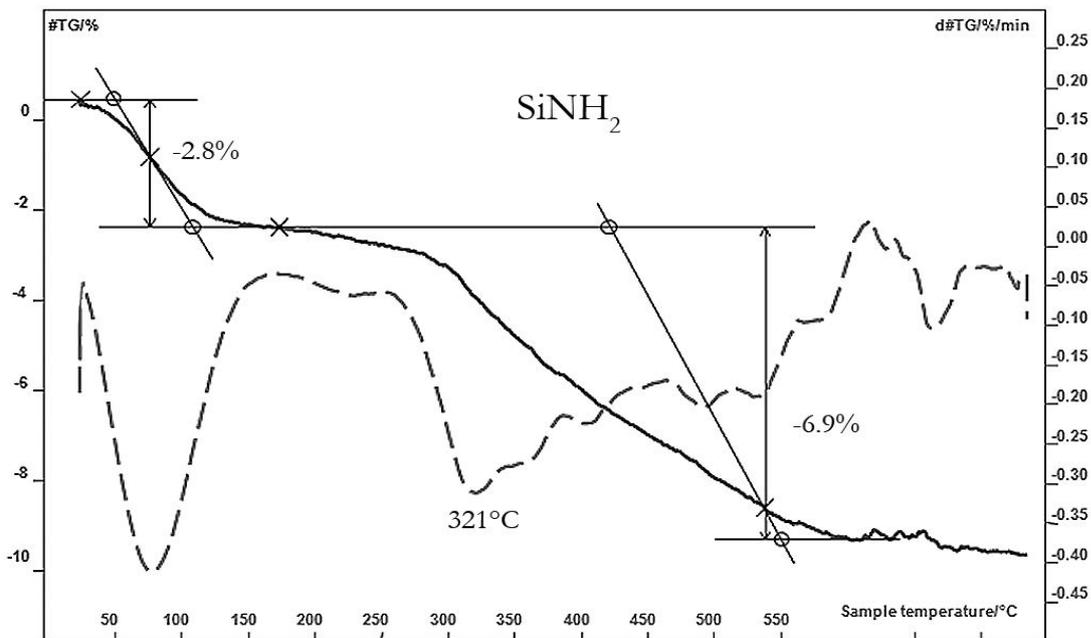
Figure 19: Thermograms of starting 3-aminopropyl silica gel (SiNH₂) and end-capped 3-aminopropyl silica gel (SiNCO). Weight loss is the bold continuous line, whilst its derivative is the dashed line

74
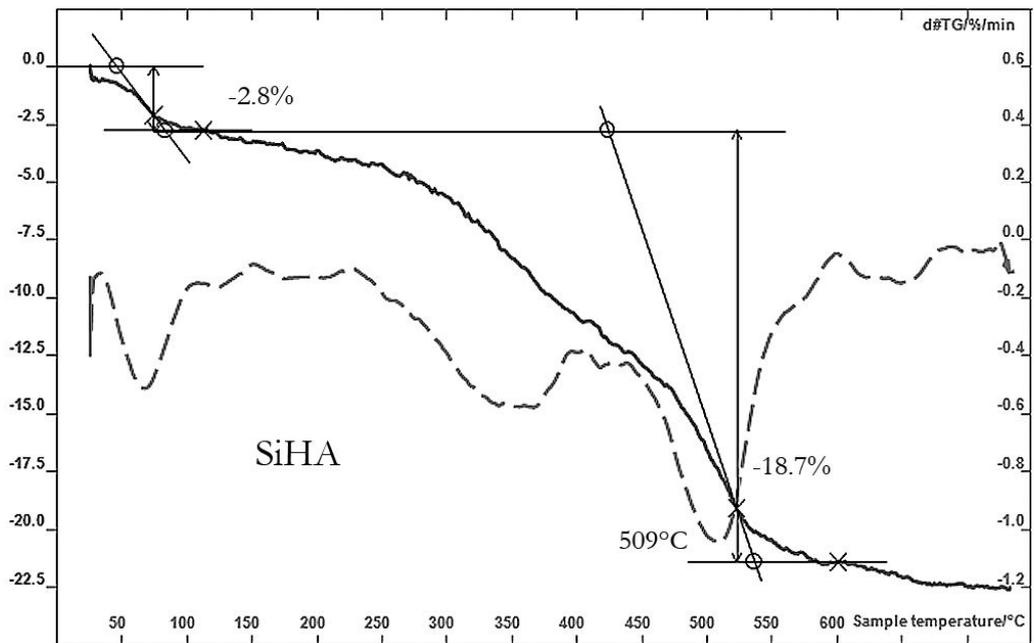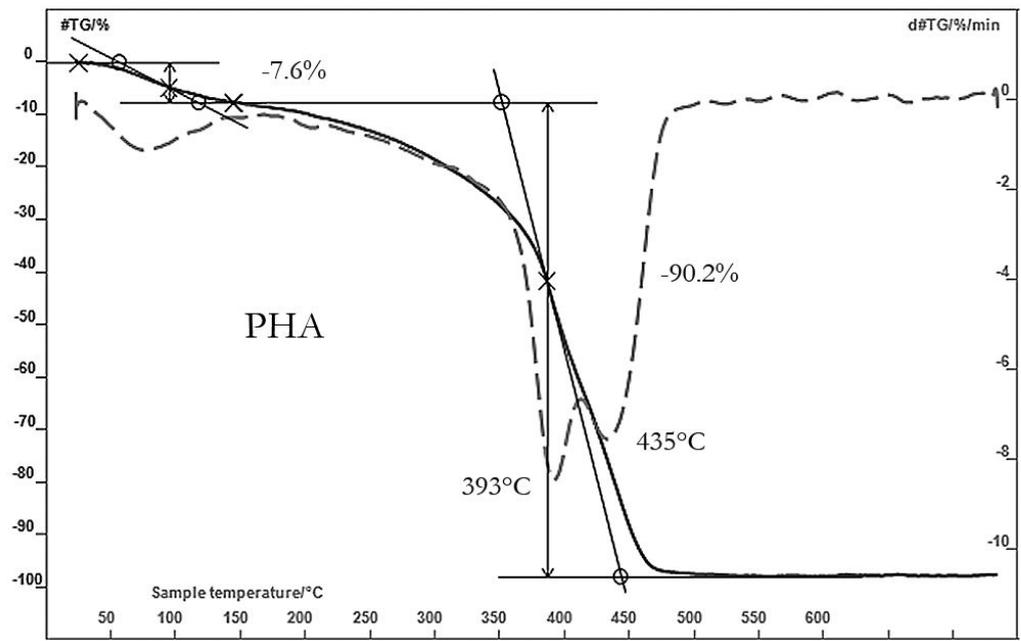
Figure 20: Thermograms of purified humic acids (PHA) and humic acid grafted, endcapped 3-aminopropyl silica gel (SiHA). Weight loss is the bold continuous line, whilst its derivative is the dashed line

- FT-IR spectra were registered with a Tensor27 (Bruker, USA): 6 mg of sample were added to 15 mg of KBr (Sigma-Aldrich, Infrared analysis certified) to produce KBr supported pellets (a press from SPECAC, UK was used). These were analysed after degasification (residual pressure of 10^{-2} Pa) obtained by a vacuum line connected to the sample holder.
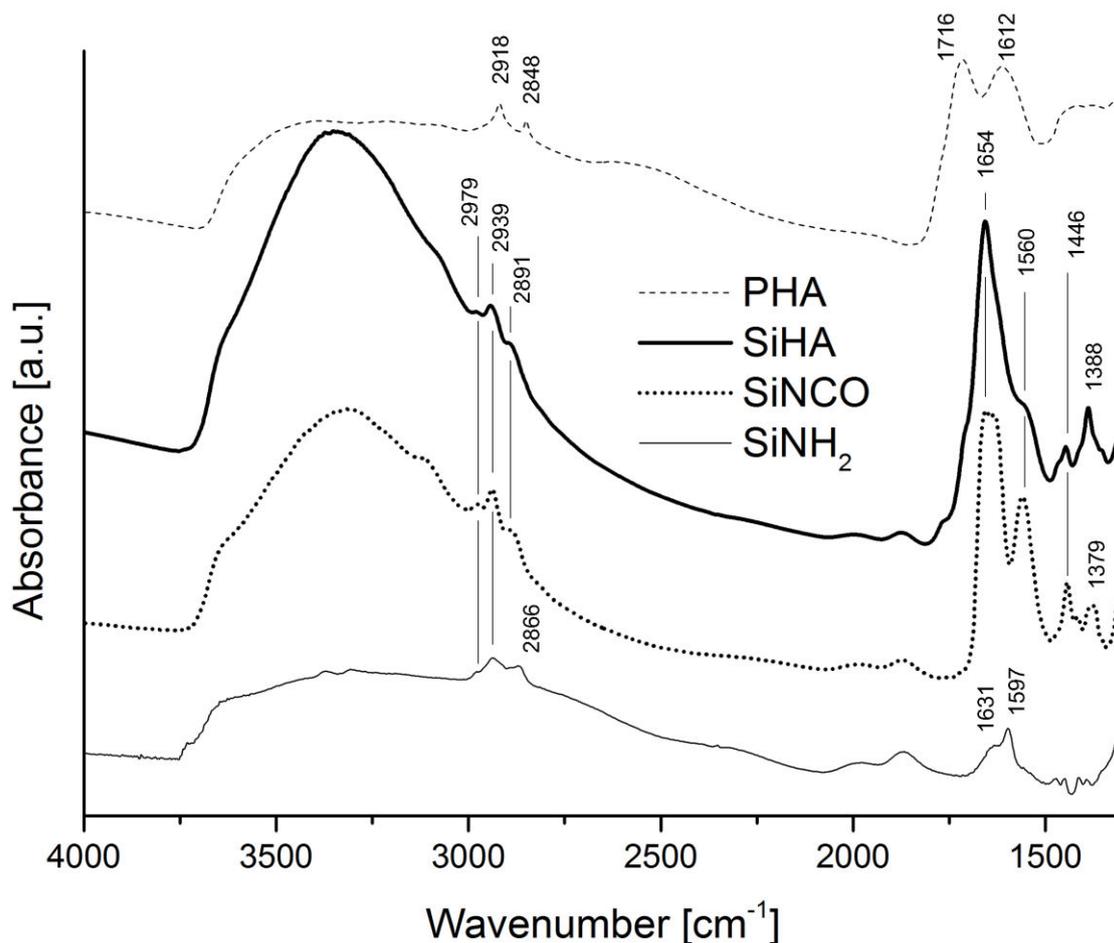
Figure 21: FT-IR spectra the starting functionalised silica (SiNH$_2$), the end-capped functionalised silica (SiNCO) and the grafted material (SiHA)

In Figure 21 the infrared spectra of SiNH$_2$, SiNCO, SiHA are reported for comparison. The spectrum of purified humic acids (PHA)) is reported as well, but due to the sample nature, intensities are not comparable to the other three spectra.

The parts of the spectra at frequencies lower than 1250 cm^{-1} were omitted due to the presence of out-of scale absorption peaks (mainly belonging to the native silicas).

SiNH$_2$ spectrum contains a sharp peak at 1597 cm^{-1} with a broad shoulder at 1631 cm^{-1}, typically related to N-H bendings of primary amines. The complex peak series at 2800-3000 cm^{-1} is assigned to the methyl and methylene C-H stretching of alkyl groups, whilst the two weak peaks in the range 3300-3400 cm^{-1} are due to the N-H stretchings of primary amines.

Spectrum of PHA, as expected, contains very broad peaks, due to the heterogeneous composition of humic acids as described in the introduction. The peaks at 2918 and 2848 cm^{-1} are assigned to alkylic C-H stretchings, the very large band at 1716 cm^{-1} to stretchings of carboxylic acids C=Ogroup, and 1612 cm^{-1} to C=O of carboxylic salts.

In the spectrum of SiHA (PHA humic acid grafted to SiNH$_2$ and end-capped), the group of peaks at 2800-3000 related to alkane C-H vibrations is visible but very different from those observed in both PHA and SINH$_2$ spectra. In addition, amine N-H stretching peaks in the range 3300-3400 cm^{-1} are not visible anymore, as expected. Carboxylic acids and salts adsorption bands seemed not visible too, possibly covered by a new strong peak at 1654 cm^{-1}. This can be related to amide C=O stretching (amides form both during humic acid grafting and both after aminopropyl end-capping: in this case 3-aminopropyl functions are converted into N-(3-propyl)acetamide functions). Mono-substituted amides have typically a strong peak at ca. 1650 and a weaker one at ca. 1560 cm^{-1}, visible in SiHA as a shoulder [238]. Two sharp peaks appeared at 1388 and 1446 cm^{-1}, possibly related to bendings of methyl group C-H. As expected, these signals are absent in SiNH$_2$ material.

SiNCO spectrum contains methylene CH vibrations at 2979 and 2939 cm^{-1}) and those of methyl groups at 2891, 1446 and 1379 cm^{-1}. Furthermore, the same strong amide peak at 1654 cm^{-1}, as well as the secondary peak at 1560 cm^{-1} of mono-substituted amides.

- <u>Cross polarisation, magic angle spinning ^{13}C nuclear magnetic resonance</u> (CP-MAS ^{13}C NMR) spectrometric analysis were conducted both at University of Montpellier 2 and at University of Piemonte Orientale, adopting similar conditions to acquire solid humic samples [239]. In Figure 22, ^{13}C NMR spectra of SiNCO, SiHA and PHA are reported. The spectrum of SiNCO consists in acetylated SiNH$_2$ (Si-CH$_2$-CH$_2$-CH$_2$-NHCOCH$_3$) and shows amide carbon nuclei at 171 ppm and four peaks below 65 ppm belonging to methyl and methylene groups of the silica.

<u>In PHA (purified humic acids) spectrum,</u> a strong peak at 33 ppm is overlapped to a broad peak below 60 ppm belonging to alkylic carbon nuclei and other large "humps" are present. Specifically, the hump centered at 160 ppm include all the many resonating

nuclei of carboxylic carbon with heterogeneous chemical environment and that centred at 129 the different aromatic carbon nuclei.
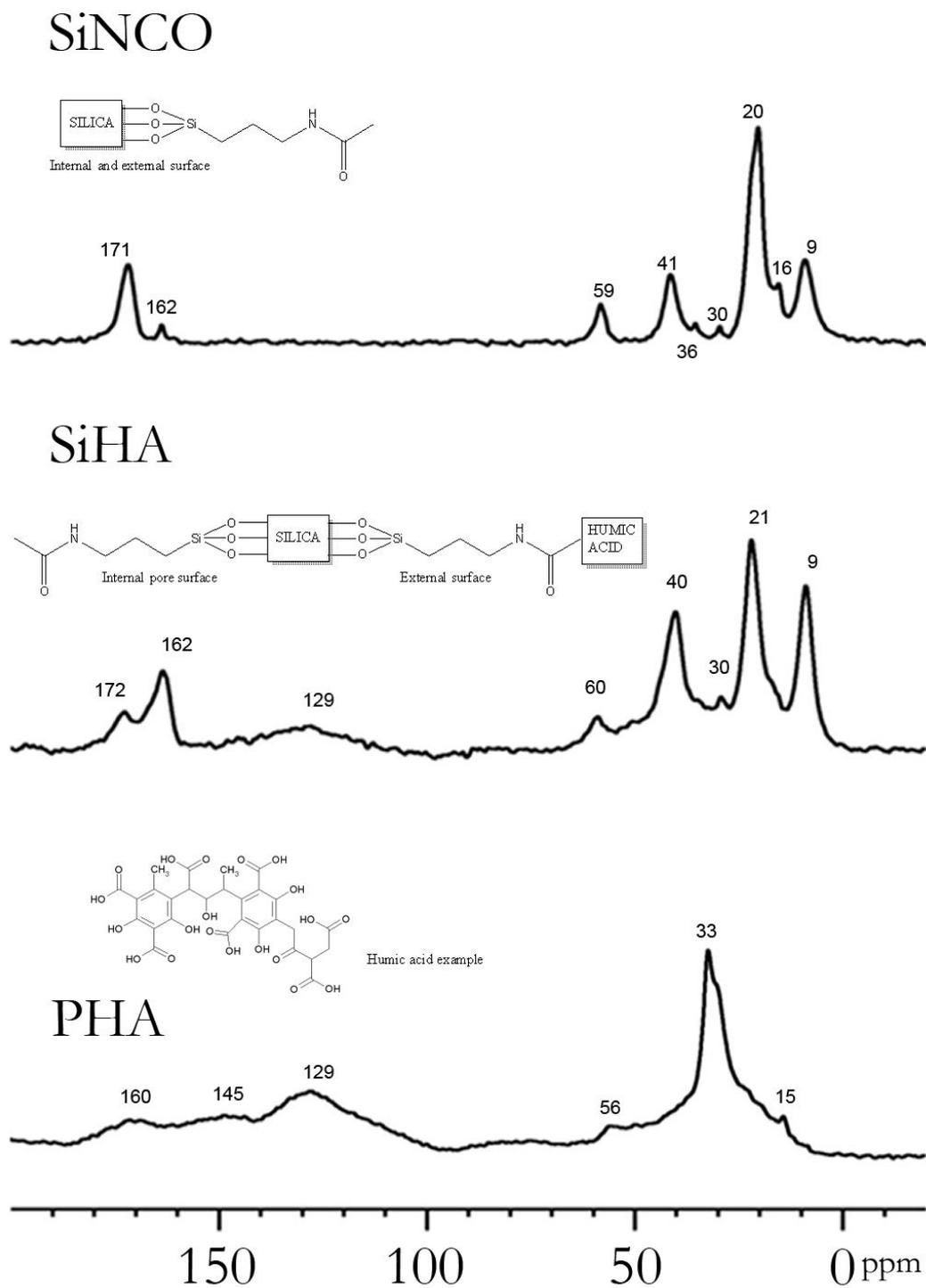
Figure 22: CP-MAS ^{13}C NMR spectra of the end-capped reference silica (SiNCO) and humic acid-grafted silica (SiHA).

In the SiHA spectrum is is possible to resemble peaks belonging to both the endcapped SiNCO and the encaped PHA: the two different amidic carbonyl are visible at 172 ppm (from SiNCO acetyl amide) and 162 ppm (from amide of grafted humic acids). The aromatic carbon region between 150 and 110 ppm of purified humic acid (PHA) is visible in the grafted material as well as the aliphatic hump below 60 ppm. The grafting of humic acids and the endcapping of the remaing amine functionalities is thus confirmed.

- As an additional experimental confirmation, a sorption test was successfully reproduced from Klavins and co-workers [220]. Briefly, 4PDA sorption tests were conducted contacting 20 mg of SiHA material (roughly corresponding to 2 mg of organics grafted) with 5 mL of 4PDA water solution at 5 mg L^{-1}at 0 and 3 M NaCl. Quantitative analyses were performed using the same PerkinElmer UV-Vis spectrophotometer. Confirming existing literature [218, 220], SiHA was able to adsorb 89.9 ± 9.4% in solution in the absence of ionic strength and 92.8 ± 5.1% at 3 M NaCl concentration.

5.4. TOLUENE SORPTION TESTS ON HUMIC ACIDS GRAFTED SILICA

The sorbent material SiHA was hence used for sorption tests of toluene from water solution. Batch tests were first run in order to construct a sorption isotherm. In addition, frontal analyses were also performed.

- Toluene solution analyses by HPLC were performed in a Waters instrument pumping a mobile phase composed by deionised water (40%) and methanol (60%) through a biphenilic Phenomenex column.
- GC-MS analyses were performed adding 500 μL of the batch tests samples to 10 mL of a saturated NaCl solution and to 20 μL of a 5.12 mg kg^{-1} fluorobenzene methanol solution. The mixture was eventually transferred in the GC-MS system through a headspace sampler. Then, the vapour pre-concentrated in the liner at 150°C was introduced in the column by a split set at a 10:1 ratio. The column (20m × 0.18mm × 1um DB624UI by Agilent) was kept at 40°C for 4 min and subsequently heated to 130°C at 15°C/min. MS ion source was kept at 230°C and the quadrupole detector at 150°C, acquiring both in full-spectrum scan and both in single ion monitoring (92 m/z).
- Batch tests were performed diluting a 200 mg kg^{-1} stock solution to prepare 10 solution standards at different concentration (2 to 200 mg kg^{-1}).
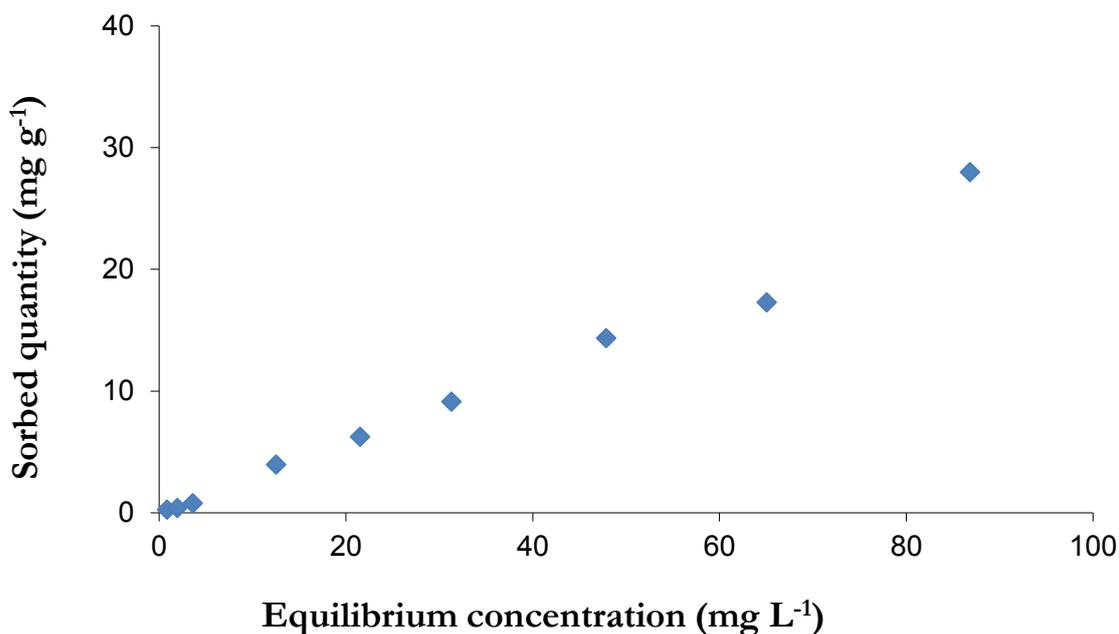
Figure 23: Adsorption isotherm of toluene on SiHA. It is possible to observe that higher toluene concentrations are needed to reach a plateau.

22 mL of each solution were contacted with 11 mg of humic acids-grafted silica gel (SiHA) and left under stirring for 24 h. After 24 hrs contact time, solutions were filtered through 0.22 μm PVDF syringe filters (EMD Millipore Millex-GV, 13 mm large) and analysed by HPLC-DAD and GC-MS. In figure 23, the adsorption isotherm of toluene on grafted silica (SiHA) is reported. In the range of toluene concentration considered, the plateau was not reached, thus meaning that the loading capacity could continue to raise for higher concentrations. In this case, no solutions at higher concentration were tested, as solutions of toluene more concentrated than 200 mg kg^{-1} tend to form separate heterogeneous phases.

- <u>Frontal analysis</u> on grafted humic acids were performed A 20 × 2 mm chromatographic column was packed with SiHA material (39.21 mg) of grafted with a 9.2% of humic acids. Solutions of toluene at 5, 10 and 20 mg kg^{-1} were prepared from the stock solution, and stored at 4°C (concentration was determined by GC-MS).

For each solution, a preliminary calibration in the HPLC system without column was performed and subsequently the breakthrough curve was assessed using the SiHA column. Mobile phase was deionised water (40%) and methanol (60%) at a flow rate of 0.5 mL min^{-1}. The results obtained by the frontal analysis are reported in Figure 24.
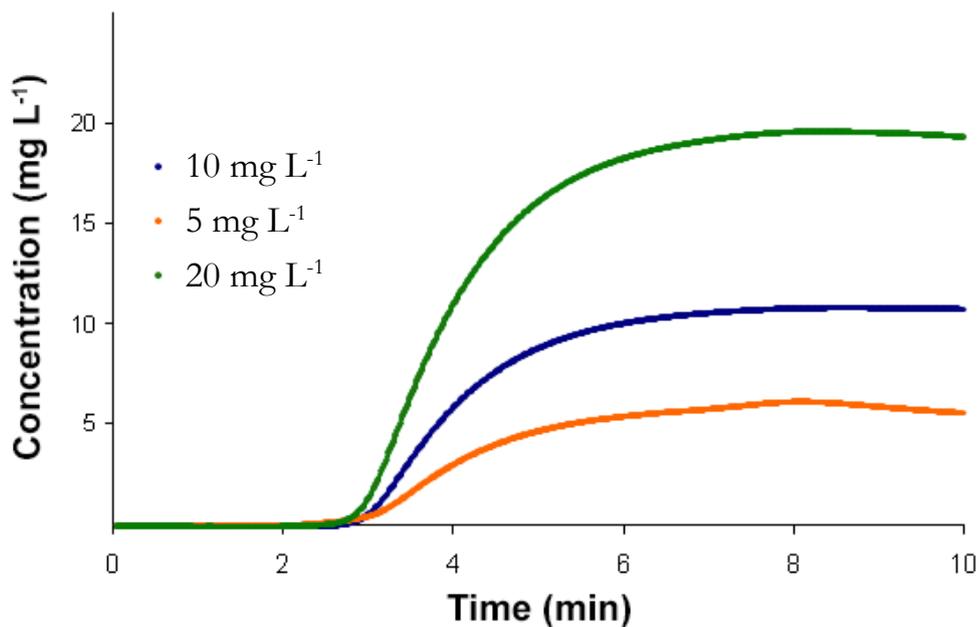
Figure 24: Breakthrough curves of toluene aqueous solution at different concentration in a SiHA packed stationary phase.

The toluene amount adsorbed by the SiHA column was calculated for each concentration (as shown in Figure 25) by finding the inflection point on the curve.
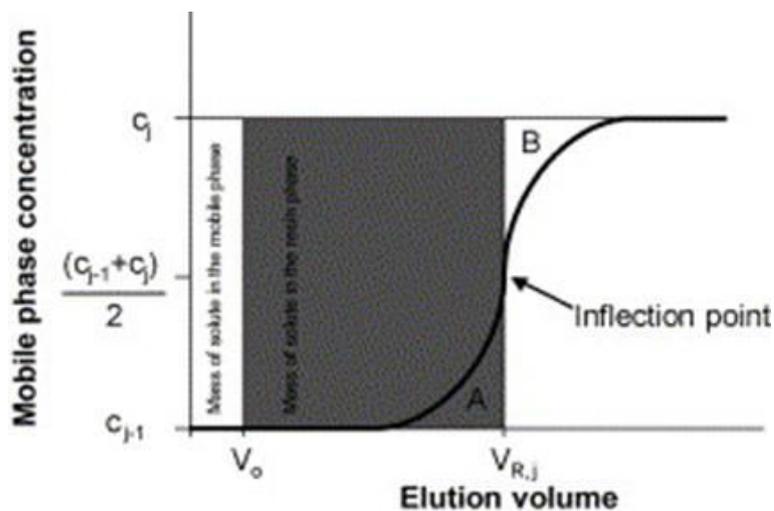
Figure 25: Calculation of sorbed quantity using the breakthrough curve

The toluene adsorption obtained by the inflection points of the breakthrough curves reported in Figure 24 was 0.82 mg g^{-1} of SiHA at the equilibrium concentration of 5 mg L^{-1}, 2.11 mg g^{-1} of SiHA at 10 mg L^{-1}, and 4.12 mg g^{-1} of SiHA at 20 mg L^{-1}. The role of the

humic acid grafted on silica in the adsorption remains to be assessed, since a sorption comparison with SiNCO material is still not available at this research stage. Though, the preliminary results obtained by the frontal analysis of SiHA column were in full agreement with those obtained by the batch adsorption trials reported in Figure 23, thus confirming the goodness of the experimental approach and indicating the grafted material as a stable organic fraction to be used for pollutant adsorption from water..

5.5. FINAL REMARKS

A humic acid grafted synthetic silica was successfully prepared using methods reported on the literature. The starting material, 3-aminopropyl silica gel had 372 m^2 g^{-1} specific surface, 10-40 μm large particles and a non-ordered mesoporosity. Humic acids grafting interested the outer surface of silica particles and was accounted for ca. 9,2 % of original silica weight. Chemical grafting was performed by amide bond formation between aminopropyl functions of silica and carboxyls of the humic molecules. The unreacted amino groups were acetylated (end-capped) using acetic anhydride. The pore system was minimally affected by the humic grafting and still maintained a certain mesoporosity (0.38 cm^3 g^{-1} specific pore volume in comparison to 0.52 cm^3 g^{-1} of the parent material).

Both the FT-IR and CP-MAS-^{13}C NMR characterisation of grafted humic acids functional groups revealed an important presence of amide groups, along with the presence of aliphatic and aromatic carbon chains. The presence of free carboxylic acids on grafted humic acids was almost negligible according to the spectroscopic techniques considered, but could be disproved by potentiometric techniques (e.g.: titration)

Humic grafting, achieved by amide bonding, was stable at RT at pH 11 and up to 3 M saline concentration.

Toluene sorption tests revealed a sensible affinity of grafted humic acids toward the hydrocarbon. Up to 4.1 mg g^{-1} of toluene were adsorbed by the material at the maximum concentration of 200 mg L^{-1}, suggesting that the sorbent properties are exploitable for these kind of contaminants. According to literature, other molecules (such as 4-nitrophenol) can also be adsorbed by similar materials [224], paving the way to several applications as sorbent for solid-liquid extraction or environmental application in water remediation.

Humic-like wastes and by-products can be used as well to prepare such materials, and their photoactivity can be exploited (once they have been immobilised on a solid support) for photo-degradation of contaminants [204].

At the present time, this project is still ongoing: different humic-like substances (humin and fulvic acids) have been successfully grafted too in the Department of Agricultural Sciences laboratories (DipSA) of the University of Bologna: named SiHu and SiFA. The characterisation of the grafted materails and their adsorption features toward toluene from water are ongoing.

6. ACKNOWLEDGEMENTS

7.   REFERENCES

1.   Braschi, I., et al., *Physicochemical regeneration of high silica zeolite Y used to clean-up water polluted with sulfonamide antibiotics.* Journal of Environmental Sciences, 2016. **43**: p. 302-312.

2.   Braschi, I., et al., *Patent application No. 102016000072535, USE OF MESOPOROUS SILICA.* 2016: Ministero per lo Sviluppo Economico, Italy.

3.   Buscaroli, E., et al., *Stabilization of mineral oil hydrocarbons in recycled paper pulp by organo-functionalized mesoporous silicas and evaluation of migration to food.* European Food Research and Technology, 2017: p. 1-14.

4.   Bardos, P., *Progress in Sustainable Remediation.* Remediation Journal, 2014. **25**(1): p. 23-32.

5.   Bardos, R.P., et al., *Sustainable remediation.* Journal of Environmental Management, 2016. **184, Part 1**: p. 1-3.

6.   Rizzo, E., et al., *Comparison of international approaches to sustainable remediation.* Journal of Environmental Management, 2016. **184, Part 1**: p. 4-17.

7.   Hou, D., P. Guthrie, and M. Rigby, *Assessing the trend in sustainable remediation: A questionnaire survey of remediation professionals in various countries.* Journal of Environmental Management, 2016. **184, Part 1**: p. 18-26.

8.   Lowell, S., et al., *Characterization of Porous Solids and Powders: Surface Area, Pore Size and Density.* Particle Technology Series. 2004: Springer Netherlands.

9.   *Studies in Surface Science and Catalysis*, in *Studies in Surface Science and Catalysis*, J.R.K.S.W.S. K.K. Unger and H. Kral, Editors. 1988, Elsevier. p. 643-645.

10.   Rouquerol, J., et al., *Recommendations For The Characterization Of Porous Solids* 1994, International Union of Pure and Applied Chemistry. p. 1739-1758.

11.   Leung, K., I.M.B. Nielsen, and L.J. Criscenti, *Elucidating the Bimodal Acid−Base Behavior of the Water−Silica Interface from First Principles.* Journal of the American Chemical Society, 2009. **131**(51): p. 18358-18365.

12.   Rahmat, N., A.Z. Abdullah, and A.R. Mohamed, *A review: Mesoporous Santa Barbara amorphous-15, types, synthesis and its applications towards biorefinery production.* American Journal of Applied Sciences, 2010. **7**(12): p. 1579-1586.

13.   Fellenz, N., et al., *Chromium (VI) removal from water by means of adsorption-reduction at the surface of amino-functionalized MCM-41 sorbents.* Microporous and Mesoporous Materials, 2017. **239**: p. 138-146.

14.   Ahmed, K., et al., *Aluminum doped mesoporous silica SBA-15 for the removal of remazol yellow dye from water.* Microporous and Mesoporous Materials, 2016. **236**: p. 167-175.

15.   Sadeghi, M., S. Yekta, and H. Ghaedi, *Synthesis and application of Pb-MCM-41/ZnNiO2 as a novel mesoporous nanocomposite adsorbent for the decontamination of chloroethyl phenyl sulfide (CEPS).* Applied Surface Science, 2017. **400**: p. 471-480.

16.   Dündar-Tekkaya, E. and Y. Yürüm, *Mesoporous MCM-41 material for hydrogen storage: A short review.* International Journal of Hydrogen Energy, 2016. **41**(23): p. 9789-9795.

17.   Martin, P.P., et al., *Zinc and Chromium elimination from complex aqueous matrices using a unique aminopropyl-modified MCM-41 sorbent: Temperature, kinetics and selectivity studies.* Journal of Environmental Chemical Engineering, 2017. **5**(1): p. 1210-1218.

18.   Dolatyari, L., M.R. Yaftian, and S. Rostamnia, *Removal of uranium(VI) ions from aqueous solutions using Schiff base functionalized SBA-15 mesoporous silica materials.* Journal of Environmental Management, 2016. **169**: p. 8-17.

19.   Meng, H., et al., *Engineered Design of Mesoporous Silica Nanoparticles to Deliver Doxorubicin and Pgp siRNA to Overcome Drug Resistance in a Cancer Cell Line.* ACS nano, 2010. **4**(8): p. 4539-4550.

20.   Cuello, N.I., et al., *Drug release profiles of modified MCM-41 with superparamagnetic behavior correlated with the employed synthesis method.* Materials Science and Engineering: C.

21.   Costa, J.A.S., et al., *Efficient adsorption of a mixture of polycyclic aromatic hydrocarbons (PAHs) by Si–MCM–41 mesoporous molecular sieve.* Powder Technology, 2017. **308**: p. 434-441.

22.   Shevade, S. and R.G. Ford, *Use of synthetic zeolites for arsenate removal from pollutant water.* Water Res, 2004. **38**(14-15): p. 3197-204.

23.   Zhang, L., et al., *Adsorptive and catalytic properties in the removal of volatile organic compounds over zeolite-based materials.* Chinese Journal of Catalysis, 2016. **37**(6): p. 800-809.

24.   Kobayashi, T., et al., *Decontamination of Extra-Diluted Radioactive Cesium in Fukushima Water Using Zeolite–Polymer Composite Fibers.* Industrial & Engineering Chemistry Research, 2016. **55**(25): p. 6996-7002.

25.   Sherman, J.D., *Synthetic zeolites and other microporous oxide molecular sieves.* Proceedings of the National Academy of Sciences, 1999. **96**(7): p. 3471-3478.

26.   Zuccato, E., S. Castiglioni, and R. Fanelli, *Identification of the pharmaceuticals for human use contaminating the Italian aquatic environment.* Journal of Hazardous Materials, 2005. **122**(3): p. 205-209.

27.   Pomati, F., et al., *Effects of a complex mixture of therapeutic drugs at environmental levels on human embryonic cells.* Environmental Science and Technology, 2006. **40**(7): p. 2442-2447.

28.   Aminov, R.I., *A Brief History of the Antibiotic Era: Lessons Learned and Challenges for the Future.* Frontiers in Microbiology, 2010. **1**: p. 134.

29.   Ungemach, F.R., *Figures on quantities of antibacterials used for different purposes in the EU countries and interpretation.* Acta Vet. Scand. Suppl., 2012. **93**(89-98): p. 111-117.

30.   Ogle, M. *Riots, Rage, and Resistance: A Brief History of How Antibiotics Arrived on the Farm*. 2013; In 1950, American farmers rejoiced at news from a New York laboratory: A team of scientists had discovered that adding antibiotics to livestock feed accelerated animals' growth and cost less than conventional feed supplements.]. Available from: https://blogs.scientificamerican.com/guest-blog/riots-rage-and-resistance-a-brief-history-of-how-antibiotics-arrived-on-the-farm/.

31.   McEwen, S.A. and P.J. Fedorka-Cray, *Antimicrobial Use and Resistance in Animals.* Clinical Infectious Diseases, 2002. **34**(Supplement_3): p. S93-S106.

32.   Tolls, J., *Sorption of veterinary pharmaceuticals in soils: A review.* Environmental Science and Technology, 2001. **35**(17): p. 3397-3406.

33.   Hamscher, G., et al., *Different behavior of tetracyclines and sulfonamides in sandy soils after repeated fertilization with liquid manure.* Environmental Toxicology and Chemistry, 2005. **24**(4): p. 861-868.

34.   Stoob, K., et al., *Exhaustive extraction of sulfonamide antibiotics from aged agricultural soils using pressurized liquid extraction.* Journal of Chromatography A, 2006. **1128**(1-2): p. 1-9.

35.   *Antibiotic Resistance: Implications for Global Health and Novel Intervention Strategies.* National Academies Press ed. 2011: Institute of Medicine, Board on Global Health, Forum on Microbial Threats. 496.

36.   Hruska, K. and M. Franek, *Sulfonamides in the environment: a review and a case report.* Veterinarni Medicina, 2012. **1**(57): p. 1-35.

37.   Hileman, B., *Troubled waters. EPA, USGS try to quantify prevalence, risks of compounds from drugs, personal care products.* Chem. Eng. News, 2001. **79**: p. 31-33.

38.   Thiele-Bruhn, S. and I.C. Beck, *Effects of sulfonamide and tetracycline antibiotics on soil microbial activity and microbial biomass.* Chemosphere, 2005. **59**(4): p. 457-465.

39.   Séveno, N.A., et al., *Occurrence and reservoirs of antibiotic resistance genes in the environment.* Reviews in Medical Microbiology, 2002. **13**(1): p. 15-27.

40.   Riesenfeld, C.S., R.M. Goodman, and J. Handelsman, *Uncultured soil bacteria are a reservoir of new antibiotic resistance genes.* Environmental Microbiology, 2004. **6**(9): p. 981-989.

41.   Pandey, S. and J. Musarrat, *Antibiotic resistant coliform bacteria in drinking water.* J. Environ. Biol., 1993. **14**: p. 267 - 274.

42.   Pathak, S.P., et al., *Incidence of transferable antibiotic resistance among enterotoxigenic Escherichia coli in urban drinking water.* J. Envir. Sci. Health., 1993. **A28**: p. 1445 -1455.

43.   Economou, V. and P. Gousia, *Agriculture and food animals as a source of antimicrobial-resistant bacteria.* Infection and Drug Resistance, 2015. **8**: p. 49-61.

44.   *Progress Report EU Action Plan against AMR Commission Staff Working Document.* 2015.

45.   *Antimicrobial Resistance Global Report on Surveillance* WHO, Editor. 2014, World Health Organization.

46.   Casey, J.A., et al., *High-density livestock operations, crop field application of manure, and risk of community-associated methicillin-resistant Staphylococcus aureus infection in Pennsylvania.* JAMA Internal Medicine, 2013. **173**(21): p. 1980-1990.

47.   Livermore, D.M., *Minimising antibiotic resistance.* Lancet Infectious Diseases, 2005. **5**(7): p. 450-459.

48.   *Antimicrobial resistance factsheet.* 2016 september 2016; Available from: http://www.who.int/mediacentre/factsheets/fs194/en/.

49.   *AMR factsheet.* 2015, European Commission.

50.   Sarmah, A.K., M.T. Meyer, and A.B.A. Boxall, *A global perspective on the use, sales, exposure pathways, occurrence, fate and effects of veterinary antibiotics (VAs) in the environment.* Chemosphere, 2006. **65**(5): p. 725-759.

51.   Acar, J. and B. Röstel, *Antimicrobial resistance: an overview.* OIE Revue Scientifique et Technique, 2001. **20**(3): p. 797-810.

52.   Haller, M.Y., et al., *Quantification of veterinary antibiotics (sulfonamides and trimethoprim) in animal manure by liquid chromatography-mass spectrometry.* J Chromatogr A, 2002. **952**(1-2): p. 111-20.

53.   Migliore, L., et al., *Toxicity of several important agricultural antibiotics to Artemia.* Water Research, 1997. **31**(7): p. 1801-1806.

54.   Berger, K.V., B. Petersen, and H. Bünung-Pfaue, *Persistenz von Gülle. Arzneistoffen in der Nahrungskette.* Arch Lebensmittelhyg, 1986(37): p. 85-108.

55. Qiang, Z. and C. Adams, *Potentiometric determination of acid dissociation constants (pKa) for human and veterinary antibiotics.* Water Res, 2004. **38**(12): p. 2874-90.

56. Thiele-Bruhn, S., et al., *Sorption of sulfonamide pharmaceutical antibiotics on whole soils and particle-size fractions.* J Environ Qual, 2004. **33**(4): p. 1331-42.

57. Burkhardt, M., et al., *Surface runoff and transport of sulfonamide antibiotics and tracers on manured grassland.* J Environ Qual, 2005. **34**(4): p. 1363-71.

58. Bajpai, A.K., M. Rajpoot, and D.D. Mishra, *Studies on the correlation between structure and adsorption of sulfonamide compounds.* Colloids and Surfaces A: Physicochemical and Engineering Aspects, 2000. **168**(3): p. 193-205.

59. Schwarz, J., et al., *Sorption of Sulfonamide Antibiotics to Soil Organic Sorbents: Batch Experiments with Model Compounds and Computational Chemistry.* ISRN Soil Science, 2012. **2012**: p. 10.

60. *Towards safe and effective use of chemicals in coastal aquaculture*, J.G.o.E.o.t.S.A.o.M.E.P. (GESAMP), Editor. 1997, FAO: Rome.

61. Serrano, P.H., *Responsible use of antibiotics in aquaculture* 2005: Food and agriculture organization of the united nations.

62. Cabello, F.C., *Heavy use of prophylactic antibiotics in aquaculture: a growing problem for human and animal health and for the environment.* Environ Microbiol, 2006. **8**(7): p. 1137-44.

63. Schmidt, A.S., et al., *Incidence, distribution, and spread of tetracycline resistance determinants and integron-associated antibiotic resistance genes among motile aeromonads from a fish farming environment.* Appl Environ Microbiol, 2001. **67**(12): p. 5675-82.

64. Mirand, C.D. and R. Zemelman, *Antimicrobial multiresistance in bacteria isolated from freshwater Chilean salmon farms.* Sci Total Environ, 2002. **293**(1-3): p. 207-18.

65. Ternes, T.A., *Occurrence of drugs in German sewage treatment plants and rivers.* Water Research, 1998. **32**(11): p. 3245-3260.

66. Michael, I., et al., *Urban wastewater treatment plants as hotspots for the release of antibiotics in the environment: A review.* Water Research, 2013. **47**(3): p. 957-995.

67. Martucci, A., et al., *Recent advances in clean-up strategies of waters polluted with sulfonamide antibiotics: A review of sorbents and related properties.* Mineralogical Magazine, 2014. **78**(5): p. 1115-1140.

68. Yang, S.-F., et al., *Sorption and biodegradation of sulfonamide antibiotics by activated sludge: Experimental assessment using batch data obtained under aerobic conditions.* Water Research, 2011. **45**(11): p. 3389-3397.

69. Gao, Y.Q., et al., *Ultraviolet (UV) light-activated persulfate oxidation of sulfamethazine in water.* Chemical Engineering Journal, 2012. **195-196**: p. 248-253.

70. Braschi, I., et al., *Removal of sulfonamide antibiotics from water: Evidence of adsorption into an organophilic zeolite Y by its structural modifications.* Journal of Hazardous Materials, 2010. **178**(1-3): p. 218-225.

71. Martucci, A., et al., *Adsorption and reaction of sulfachloropyridazine sulfonamide antibiotic on a high silica mordenite: A structural and spectroscopic combined study.* Microporous and Mesoporous Materials, 2013. **170**: p. 274-286.

72. Blasioli, S., et al., *Removal of sulfamethoxazole sulfonamide antibiotic from water by high silica zeolites: A study of the involved host-guest interactions by a combined structural, spectroscopic, and computational approach.* Journal of Colloid and Interface Science, 2014. **419**: p. 148-159.

73. Braschi, I., et al., *Effect of humic monomers on the adsorption of sulfamethoxazole sulfonamide antibiotic into a high silica zeolite Y: An interdisciplinary study.* Chemosphere, 2016. **155**: p. 444-452.

74. Laine, D.F. and I.F. Cheng, *The destruction of organic pollutants under mild reaction conditions: A review.* Microchemical Journal, 2007. **85**(2): p. 183-193.

75. Batchu, S.R., V.R. Panditi, and P.R. Gardinali, *Photodegradation of sulfonamide antibiotics in simulated and natural sunlight: Implications for their environmental fate.* Journal of Environmental Science and Health - Part B Pesticides, Food Contaminants, and Agricultural Wastes, 2014. **49**(3): p. 200-211.

76. Nahm, S.W., et al., *Thermal and chemical regeneration of spent activated carbon and its adsorption property for toluene.* Chemical Engineering Journal, 2012. **210**: p. 500-509.

77. Leardini, L., et al., *Regeneration of high-silica zeolites after sulfamethoxazole antibiotic adsorption: A combined in situ high-temperature synchrotron X-ray powder diffraction and thermal degradation study.* Mineralogical Magazine, 2014. **78**(5): p. 1141-1159.

78. Gao, P., M. Munir, and I. Xagoraraki, *Correlation of tetracycline and sulfonamide antibiotics with corresponding resistance genes and resistant bacteria in a conventional municipal wastewater treatment plant.* Science of the Total Environment, 2012. **421-422**: p. 173-183.

79. Khalid, M., et al., *Removal of phenol from water by adsorption using zeolites.* Industrial and Engineering Chemistry Research, 2004. **43**(17): p. 5275-5280.

80. Vignola, R., et al., *Zeolites in a permeable reactive barrier (PRB): One year of field experience in a refinery groundwater-Part 1: The performances.* Chemical Engineering Journal, 2011. **178**: p. 204-209.

81. Vignola, R., et al., *Zeolites in a permeable reactive barrier (PRB): One-year of field experience in a refinery groundwater. Part 2: Zeolite characterization.* Chemical Engineering Journal, 2011. **178**: p. 210-216.

82. Braschi, I., et al., *Sulfonamide antibiotics embedded in high silica zeolite Y: A combined experimental and theoretical study of host-guest and guest-guest interactions.* Langmuir, 2010. **26**(12): p. 9524-9532.

83. Braschi, I., et al., *Embedding monomers and dimers of sulfonamide antibiotics into high silica zeolite Y: An experimental and computational study of the tautomeric forms involved.* RSC Advances, 2013. **3**(20): p. 7427-7437.

84. Biedermann, M., K. Fiselier, and K. Grob, *Aromatic hydrocarbons of mineral oil origin in foods: method for determining the total concentration and first result.* Journal of Agricultural and Food Chemistry, 2009. **57**(19): p. 8711-8721.

85. Lorenzini, R., et al., *Saturated and aromatic mineral oil hydrocarbons from paperboard food packaging: Estimation of long-term migration from contents in the paperboard and data on boxes from the market.* Food Additives and Contaminants - Part A Chemistry, Analysis, Control, Exposure and Risk Assessment, 2010. **27**(12): p. 1765-1774.

86. Grob, K., *Chemical risks in foodstuffs.* Nachrichten aus der Chemie, 2010. **58**(9): p. 915-917.

87. Biedermann-Brem, S., et al., *Migration of polyolefin oligomeric saturated hydrocarbons (POSH) into food.* Food Additives and Contaminants - Part A Chemistry, Analysis, Control, Exposure and Risk Assessment, 2012. **29**(3): p. 449-460.

88. Bajpai, P., *Recycling and Deinking of Recovered Paper.* 2014: Elsevier Insights.

89. Biedermann, M. and K. Grob, *Is recycled newspaper suitable for food contact materials? Technical grade mineral oils from printing inks.* European Food Research and Technology, 2010. **230**(5): p. 785-796.

90.   Svendsen, K. and K.S. Rognes, *Exposure to organic solvents in the offset printing industry in Norway.* Ann Occup Hyg, 2000. **44**(2): p. 119-24.

91.   Jickells, S.M., et al., *Migration of contaminants by gas phase transfer from carton board and corrugated board box secondary packaging into foods.* Food Additives and Contaminants, 2005. **22**(8): p. 768-782.

92.   Nerín, C., E. Contín, and E. Asensio, *Kinetic migration studies using Porapak as solid-food simulant to assess the safety of paper and board as food-packaging materials.* Analytical and Bioanalytical Chemistry, 2007. **387**(6): p. 2283-2288.

93.   Lorenzini, R., et al., *Migration kinetics of mineral oil hydrocarbons from recycled paperboard to dry food: Monitoring of two real cases.* Food Additives and Contaminants - Part A Chemistry, Analysis, Control, Exposure and Risk Assessment, 2013. **30**(4): p. 760-770.

94.   Triantafyllou, V.I., K. Akrida-Demertzi, and P.G. Demertzis, *A study on the migration of organic pollutants from recycled paperboard packaging materials to solid food matrices.* Food Chemistry, 2007. **101**(4): p. 1759-1768.

95.   CEPI, *Key Statistics.* 2015, Confederation of European Paper Industries (CEPI): Brussels. p. 32.

96.   Aurela, B., H. Kulmala, and L. Söderhjelm, *Phthalates in paper and board packaging and their migration into Tenax and sugar.* Food Additives and Contaminants, 1999. **16**(12): p. 571-577.

97.   Fernandes, A.R., M. Rose, and C. Charlton, *4-Nonylphenol (NP) in food-contact materials: Analytical methodology and occurrence.* Food Additives and Contaminants - Part A Chemistry, Analysis, Control, Exposure and Risk Assessment, 2008. **25**(3): p. 364-372.

98.   Börjesson, M. and G. Westman, *Crystalline Nanocellulose — Preparation, Modification, and Properties*, in *Cellulose - Fundamental Aspects and Current Trends.* 2015, InTech: Rijeka. p. Ch. 0.

99.   Ragnar, M., et al., *Pulp*, in *Ullmann's Encyclopedia of Industrial Chemistry.* 2000, Wiley-VCH Verlag GmbH & Co. KGaA.

100.   Anderson, J.E., et al., *Composition and analysis of mineral oils and other organic compounds in metalworking and hydraulic fluids.* Critical Reviews in Environmental Science and Technology, 2003. **33**(1): p. 73-109.

101.   Ozaki, A., et al., *Chemical analysis and genotoxicological safety assessment of paper and paperboard used for food packaging.* Food and Chemical Toxicology, 2004. **42**(8): p. 1323-1337.

102.   Kurz, S., *Anzahl von Strukturisomeren der Alkane.* 2005, Universität Bayreuth, D-95440 Bayreuth, Deutschland.

103.   Grob, K., et al., *LC-GC analysis of the aromatics in a mineral oil fraction: Batching oil for jute bags.* J. High Resolut. Chromatogr., 1991. **14**: p. 33-39.

104.   Grob, K., et al., *Determination of food contamination by mineral oil from jute sacks using coupled LC-GC.* Journal of the Association of Official Analytical Chemists, 1991. **74**(3): p. 506-512.

105.   Biedermann, M. and K. Grob, *Comprehensive two-dimensional GC after HPLC preseparation for the characterization of aromatic hydrocarbons of mineral oil origin in contaminated sunflower oil.* Journal of Separation Science, 2009. **32**(21): p. 3726-3737.

106.   Biedermann, M. and K. Grob, *On-line coupled high performance liquid chromatography-gas chromatography for the analysis of contamination by mineral oil. Part 1: Method of analysis.* Journal of Chromatography A, 2012. **1255**: p. 56-75.

107.   Khan, S., et al., *Mechanisms of petroleum hydrocarbon toxicity: Studies on the response of rat liver mitochondria to Prudhoe Bay crude oil and its aliphatic, aromatic and heterocyclic fractions.* Toxicology, 1986. **42**(2-3): p. 131-142.

108. Mackerer, C.R., et al., *Petroleum Mineral Oil Refining and Evaluation of Cancer Hazard.* Applied Occupational and Environmental Hygiene, 2003. **18**(11): p. 890-901.

109. Kimber, I. and J.C. Carrillo, *Oral exposure to mineral oils: Is there an association with immune perturbation and autoimmunity?* Toxicology, 2016. **344-346**: p. 19-25.

110. Barp, L., et al., *Mineral oil in human tissues, Part I: Concentrations and molecular mass distributions.* Food and Chemical Toxicology, 2014. **72**: p. 312-321.

111. Concin, N., et al., *Mineral oil paraffins in human body fat and milk.* Food and Chemical Toxicology, 2008. **46**(2): p. 544-552.

112. Andreassen, M., et al., *Does dietary exposure to a broad MOSH mixture affect autoimmune arthritis in rats?* Toxicology Letters, 2016. **258, Supplement**: p. S233.

113. *59th Report of The Joint FAO/WHO Expert Committee On Food Additives*, in *WHO TRS n. 913*, J.F.W.E.C.o.F. Additives, Editor. 2002.

114. *Evaluation of certain food additives: seventy-sixth report of the Joint FAO/WHO Expert Committee on Food Additives*, in *Evaluation of certain food additives*, J.F.W.E.C.o.F. Additives, Editor. 2012.

115. *Summary and conclusions to the Seventy-sixth meeting.* 2012, Joint FAO/WHO Expert Committee on Food Additives. p. 16.

116. *IARC monographs on the evaluation of carcinogenic risks to human.* Available from: http://monographs.iarc.fr/ENG/Classification/latest_classif.php.

117. *Survey 4: Migration of selected ink components from printed packaging materials into foodstuffs and screening of printed packaging for the presence of mineral oils*, U.F.S. Agency, Editor. 2011.

118. *GRAS Notification for Use of Mineral Oil as a Direct Additive in Food Products* 2000, American Ingredients company, on behalf of U.S. Food and Drugs administration.

119. *Scientific opinion on mineral oil hydrocarbons in food*, in *CONTAM*, -.E.P.o.C.i.t.F.C. EFSA, Editor. 2012, EFSA: Parma, Italy.

120. *Questions and answers on the migration of mineral oil from packaging materials to foodstuffs* B.f. risikobewertung, Editor. 2010.

121. O'Keeffe, H., *Food-Contact Substances under the Spotlight in the European Union and the United States*, in *European Coatings Journal.* 2016.

122. Lommatzsch, M., et al., *Functional barriers or adsorbent to reduce the migration of mineral oil hydrocarbons from recycled cardboard into dry food.* European Food Research and Technology, 2016: p. 1-7.

123. Dima, G., A. Verzera, and K. Grob, *Migration of mineral oil from party plates of recycled paperboard into foods: 1. Is recycled paperboard fit for the purpose? 2. Adequate testing procedure.* Food Additives and Contaminants - Part A Chemistry, Analysis, Control, Exposure and Risk Assessment, 2011. **28**(11): p. 1619-1628.

124. Fiselier, K. and K. Grob, *Barriers against the migration of mineral oil from paperboard food packaging: experimental determination of breakthrough periods.* Packag Technol Sci, 2011.

125. Sacco, A., et al., *Toward quasi-solid state Dye-sensitized Solar Cells: Effect of γ-Al2O3 nanoparticle dispersion into liquid electrolyte.* Solar Energy, 2015. **111**: p. 125-134.

126. Costenaro, D., et al., *The effect of synthesis gel dilution on the physico-chemical properties of acid saponite clays.* Microporous and Mesoporous Materials, 2012. **162**: p. 159-167.

127. Zhao, D., et al., *Nonionic Triblock and Star Diblock Copolymer and Oligomeric Surfactant Syntheses of Highly Ordered, Hydrothermally Stable, Mesoporous Silica Structures.* Journal of the American Chemical Society, 1998. **120**(24): p. 6024-6036.

128. Chen, S.-Y., et al., *A Facile Route to Synthesizing Functionalized Mesoporous SBA-15 Materials with Platelet Morphology and Short Mesochannels.* Chemistry of Materials, 2008. **20**(12): p. 3906-3916.

129. Etgar, L., et al., *Enhancing the open circuit voltage of dye sensitized solar cells by surface engineering of silica particles in a gel electrolyte.* Journal of Materials Chemistry A, 2013. **1**(35): p. 10142-10147.

130. Batonneau-Gener, I., et al., *Tailoring the Hydrophobic Character of Mesoporous Silica by Silylation for VOC Removal.* Separation Science and Technology, 2010. **45**(6): p. 768-775.

131. Bradley, E.L., L. Castle, and D.R. Speck, *Model studies of migration from paper and board into fruit and vegetables and into Tenax™ as a food simulant.* Food Additives and Contaminants - Part A Chemistry, Analysis, Control, Exposure and Risk Assessment, 2014. **31**(7): p. 1301-1309.

132. *Commission Regulation (EU) No 10/2011 of 14 January 2011 on plastic materials and articles intended to come into contact with food.* 2011: Brussels.

133. Guazzotti, V., et al., *A study into the potential barrier properties against mineral oils of starch-based coatings on paperboard for food packaging.* Food Packaging and Shelf Life, 2015. **3**: p. 9-18.

134. Li, W., et al., *Physicochemical and structural properties of A- and B-starch isolated from normal and waxy wheat: Effects of lipids removal.* Food Hydrocolloids, 2016. **60**: p. 364-373.

135. Eggen, T. and C. Vogelsang, *Chapter 7 - Occurrence and Fate of Pharmaceuticals and Personal Care Products in Wastewater*, in *Comprehensive Analytical Chemistry*, Y.Z. Eddy, Editor. 2015, Elsevier. p. 245-294.

136. Hooda, P.S., *Trace Elements in Soils.* 2010.

137. Hawkes, S.J., *What is a "heavy metal"?* Journal of Chemical Education, 1997. **74**(11): p. 1374

138. Barker, A.V. and D.J. Pilbeam, *Handbook of Plant Nutrition.* 2 ed. 2015: CRC Press.

139. Tchounwou, P.B., et al., *Heavy Metals Toxicity and the Environment.* EXS, 2012. **101**: p. 133-164.

140. Halliwell, B. and J.M. Gutteridge, *Oxygen toxicity, oxygen radicals, transition metals and disease.* Biochemical Journal, 1984. **219**(1): p. 1-14.

141. *Framework for Metals risk assessment*, O.o.T.S. Advisor, Editor. 2007.

142. Baird, C. and M. Cann, *Environmental Chemistry.* 5th ed. 2012, New York: W. H. Freeman and Company.

143. Kozin, L.F. and S.C. Hansen, *Mercury Handbook: Chemistry, Applications and Environmental Impact.* 2013, Cambridge: RSC Publishing.

144. Murr, L.E., *A Brief History of Metals*, in *Handbook of Materials Structures, Properties, Processing and Performance.* 2015, Springer International Publishing: Cham. p. 3-9.

145. Khalil, M., et al., *Advanced nanomaterials in oil and gas industry: Design, application and challenges.* Applied Energy, 2017. **191**: p. 287-310.

146. Mattsson, M.-O. and M. Simkó, *The changing face of nanomaterials: Risk assessment challenges along the value chain.* Regulatory Toxicology and Pharmacology, 2017. **84**: p. 105-115.

147. Tansel, B., *From electronic consumer products to e-wastes: Global outlook, waste quantities, recycling challenges.* Environment International, 2017. **98**: p. 35-45.

148. Desjardins, J. *Rare earths elements, the technology metals.* 2012; Available from: http://www.visualcapitalist.com/rare-earth-elements-the-technology-metals/.

149.   Song, Q. and J. Li, *Environmental effects of heavy metals derived from the e-waste recycling activities in China: A systematic review.* Waste Management, 2014. **34**(12): p. 2587-2594.

150.   Fujimori, T. and H. Takigami, *Pollution distribution of heavy metals in surface soil at an informal electronic-waste recycling site.* Environmental Geochemistry and Health, 2014. **36**(1): p. 159-168.

151.   *Soil Contamination: Impacts on Human Health.*, in *Science for Environment Policy*, S.C. Unit, Editor. 2013, University of the West of England: Bristol.

152.   Cui, J.L., et al., *Speciation and leaching of trace metal contaminants from e-waste contaminated soils.* Journal of Hazardous Materials, 2017. **329**: p. 150-158.

153.   Shallari, S., et al., *Heavy metals in soils and plants of serpentine and industrial sites of Albania.* Sci Total Environ, 1998. **209**(2-3): p. 133-42.

154.   Arruti, A., I. Fernandez-Olmo, and A. Irabien, *Evaluation of the contribution of local sources to trace metals levels in urban PM2.5 and PM10 in the Cantabria region (Northern Spain).* J Environ Monit, 2010. **12**(7): p. 1451-8.

155.   He, Z.L., X.E. Yang, and P.J. Stoffella, *Trace elements in agroecosystems and impacts on the environment.* J Trace Elem Med Biol, 2005. **19**(2-3): p. 125-40.

156.   Hassanien, M.A., *Atmospheric heavy metals pollution: Exposure and prevention policies in mediterranean basin*, in *Environmental Heavy Metal Pollution and Effects on Child Mental Development: Risk Assessment and Prevention Strategies*, L.I. Simeonov, M.V. Kochubovski, and B.G. Simeonova, Editors. 2010. p. 287-307.

157.   Feng, M.H., et al., *A comparison of the rhizosphere-based method with DTPA, EDTA, CaCl2, and NaNO3 extraction methods for prediction of bioavailability of metals in soil to barley.* Environ Pollut, 2005. **137**(2): p. 231-40.

158.   Lindsay, W.L. and W.A. Norvell, *Development of a DTPA Soil Test for Zinc, Iron, Manganese, and Copper1.* Soil Science Society of America Journal, 1978. **42**(3): p. 421-428.

159.   Tessier, A., P.G.C. Campbell, and M. Blsson, *Sequential extraction procedure for the speciation of particulate trace metals.* Analytical Chemistry, 1979. **51**(7): p. 844-851.

160.   Okoro, H.K. and O.S. Fatoki, *A review of sequential extraction procedures for heavy metals speciation in soil and sediments.* J. Environ. Anal. Toxicol., 2012. **1**: p. 1-16.

161.   Moore, J.N., E.J. Brook, and C. Johns, *Grain size partitioning of metals in contaminated, coarse-grained river floodplain sediment: Clark Fork River, Montana, U.S.A.* Environmental Geology and Water Sciences, 1989. **14**(2): p. 107-115.

162.   Chon, H.S., D.G. Ohandja, and N. Voulvoulis, *The role of sediments as a source of metals in river catchments.* Chemosphere, 2012. **88**(10): p. 1250-1256.

163.   Felli, A., *Utilizzo sedimenti dragati, inquadramento normativo.* 2012, ISPRA.

164.   Fratini, M., *Tecnologie e costi della bonifica sedimenti.* 2008, ISPRA.

165.   Zapparoli, A.M., *Caratterizzazione dei sedimenti dei corpi idrici artificiali del territorio della Provincia di Bologna.* 2007, ARPA Emilia Romagna.

166.   del Giudice, C., A. Ricci, and T. Montanelli, *Movimentazione e Gestione dei Sedimenti.* 2010, ISPRA.

167.   *D. Lgs. 03/04/2006 n° 152 and further modifications - "Norme in materia ambientale" - G.U. 14/4/2006 N. 88.*

168.   Steinberg, R.V., *Contaminated soils: Environmental impact, disposal and treatment.* Contaminated Soils: Environmental Impact, Disposal and Treatment. 2011. 1-520.

169. Pulatsü, S. and A. Topçu, *Review of 15 Years of Research on Sediment Heavy Metal Contents and Sediment Nutrient Release in Inland Aquatic Ecosystems, Turkey.* . Journal of Water Resource and Protection, 2015. **7**: p. 16.

170. Plant, J.A., N. Voulvoulis, and Ragnarsdottir, *Pollutants, Human Health and the Environment: A Risk Based Approach.* Pollutants, Human Health and the Environment: A Risk Based Approach. 2012.

171. Sanz, L.H., *Heavy metal sediments.* Heavy Metal Sediments. 2011. 1-173.

172. Violante, A., P.M. Huang, and G.M. Gadd, *Biophysico-Chemical Processes of Heavy Metals and Metalloids in Soil Environments.* Biophysico-Chemical Processes of Heavy Metals and Metalloids in Soil Environments. 2007. 1-658.

173. Motuzova, G.V., et al., *Soil organic matter and their interactions with metals: Processes, factors, ecological significance.* Soil Organic Matter and their Interactions with Metals: Processes, Factors, Ecological Significance. 2012. 1-136.

174. Ehlken, S. and G. Kirchner, *Environmental processes affecting plant root uptake of radioactive trace elements and variability of transfer factor data: A review.* Journal of Environmental Radioactivity, 2002. **58**(2-3): p. 97-112.

175. Tack, P.M. and M.G. Verloo, *Metal contents in stinging nettle (Urtica dioica L.) as affected by soil characteristics.* Science of the Total Environment, 1996. **192**(1): p. 31-39.

176. Hooda, P.S., *Trace Elements in Soils.* Trace Elements in Soils. 2010.

177. Cline, S.R. and B.E. Reed, *Lead removal from soils via bench-scale soil washing techniques.* Journal of Environmental Engineering, 1995. **121**(10): p. 700-705.

178. EEC, *Council Directive 86/278/EEC of 12 June 1986 on the protection of the environment, and in particular of the soil, when sewage sludge is used in agriculture*, T.c.o.t.e. communities, Editor. 1986.

179. *Minister decree DM13/09/1999 Approval of "Official methods for chemical analysis on soil".* M.p.l.P. Agricole, Editor. 1999.

180. Standardization, I.O.f., *ISO 11466:1995 Extraction of trace elements soluble in aqua regia*, in *Soil quality*. 1995.

181. Standardization, I.O.f., *ISO 11047:1998 Determination of cadmium, chromium, cobalt, copper, lead, manganese, nickel and zinc -- Flame and electrothermal atomic absorption spectrometric methods*, in *Soil quality*. 1998.

182. Rulkens, W.H. and H. Bruning, *Cleanup technologies for dredged fine sediments: review and future challenges.* Remediation of Contaminated Sediments: Finding Achievable Risk Reduction Solutions, 2005: p. C6-01.

183. Dermont, G., et al., *Soil washing for metal removal: A review of physical/chemical technologies and field applications.* Journal of Hazardous Materials, 2008. **152**(1): p. 1-31.

184. Kumpiene, J., A. Lagerkvist, and C. Maurice, *Stabilization of As, Cr, Cu, Pb and Zn in soil using amendments - A review.* Waste Management, 2008. **28**(1): p. 215-225.

185. Juwarkar, A.A., S.K. Singh, and A. Mudhoo, *A comprehensive overview of elements in bioremediation.* Reviews in Environmental Science and Biotechnology, 2010. **9**(3): p. 215-288.

186. Bolan, N., et al., *Remediation of heavy metal(loid)s contaminated soils - To mobilize or to immobilize?* Journal of Hazardous Materials, 2014. **266**: p. 141-166.

187. Maejima, Y., et al., *Remediation of cadmium-contaminated paddy soils by washing with chemicals: Effect of soil washing on cadmium uptake by soybean.* Chemosphere, 2007. **67**(4): p. 748-754.

188. Ahmad, A., *Study on Effect of HCl and CaCl2 on Extraction of Heavy Metals From Contaminated Soils.* Asian Journal of Chemistry, 2009. **21**(3): p. 9.

189. Makino, T., et al., *Remediation of cadmium contamination in paddy soils by washing with chemicals: Selection of washing chemicals.* Environmental Pollution, 2006. **144**(1): p. 2-10.

190. Makino, T., et al., *Remediation of cadmium-contaminated paddy soils by washing with calcium chloride: Verification of on-site washing.* Environmental Pollution, 2007. **147**(1): p. 112-119.

191. Sastre-Conde, I., et al., *Remediation of saline soils by a two-step process: Washing and amendment with sludge.* Geoderma, 2015. **247-248**: p. 140150.

192. Gee, G.W. and J.W. Bauder, *Particle-size analysis*, in *Methods of soil analysis. Part I*, A. Klute, Editor. 1986, ASA and SSSA: Madison, WI, USA. p. 383-411.

193. *Soil Survey Manual*, S.S.D. Staff, Editor. 1993, Soil Conservation Service.

194. Kemper, W.D. and R.C. Rosenau, *Aggregate stability and size distribution*, in *Methods of soil analysis. Part I*, A. Klute, Editor. 1986, ASA and SSSA: Madison, WI, USA. p. 425-442.

195. van Reeuwijk, L.P., *Procedure for Soil Analysis - Technical paper 9*. 2002, FAO.

196. Kelderman, P. and A.A. Osman, *Effect of redox potential on heavy metal binding forms in polluted canal sediments in Delft (The Netherlands).* Water Res, 2007. **41**(18): p. 4251-61.

197. Saeki, K., M. Okazaki, and S. Matsumoto, *The chemical phase changes in heavy metals with drying and oxidation of the lake sediments.* Water Research, 1993. **27**(7): p. 1243-1251.

198. Zoumis, T., et al., *Contaminants in sediments: remobilisation and demobilisation.* Science of the Total Environment, 2001. **266**(1-3): p. 195-202.

199. Ferronato, C., G. Vianello, and L. Vittori Antisari, *Heavy metal risk assessment after oxidation of dredged sediments through speciation and availability studies in the Reno river basin, Northern Italy.* Journal of Soils and Sediments, 2015. **15**(5): p. 1235-1245.

200. Stevenson, F.J., *Humus Chemistry: Genesis, Composition, Reactions*. 2nd ed. 1994: John Wiley & Sons Ltd. 512.

201. Schulten, H.R., *Three-Dimensional Models for Humic Acids and Soil Organic Matter.* Naturwissenschaften, 1995. **82**(11): p. 12.

202. De Paolis, F. and J. Kukkonen, *Binding of organic pollutants to humic and fulvic acids: Influence of pH and the structure of humic material.* Chemosphere, 1997. **34**(8): p. 1693-1704.

203. Smilek, J., et al., *On the role of humic acids' carboxyl groups in the binding of charged organic compounds.* Chemosphere, 2015. **138**: p. 503-510.

204. Testa, M.L., et al., *Synthesis, characterization and environmental application of silica grafted photoactive substances isolated from urban biowaste.* RSC Advances, 2015. **5**(59): p. 47920-47927.

205. Schulten, H.R., *The three-dimensional structure of humic substances and soil organic matter studied by computational analytical chemistry.* Fresenius J Anal Chem, 1995. **351**(1): p. 12.

206. Schaumann, G.E. and S. Thiele-Bruhn, *Molecular modeling of soil organic matter: Squaring the circle?* Geoderma, 2011. **166**(1): p. 1-14.

207. Sutton, R. and G. Sposito, *Molecular Structure in Soil Humic Substances: The New View.* Environmental Science & Technology, 2005. **39**(23): p. 7.

208. Piccolo, A., *The supramolecular structure of humic substances: A novel understanding of humus chemistry and implications in soil science*, in *Advances in Agronomy*. 2002, Academic Press. p. 57-134.

209. de Melo, B.A.G., F.L. Motta, and M.H.A. Santana, *Humic acids: Structural properties and multiple functionalities for novel technological developments.* Materials Science and Engineering: C, 2016.

210. von Wandruszka, R., *Humic acids: Their detergent qualities and potential uses in pollution remediation.* Geochemical Transactions, 2000. **1**(2): p. 10-15.

211. Salati, S., G. Papa, and F. Adani, *Perspective on the use of humic acids from biomass as natural surfactants for industrial applications.* Biotechnology Advances, 2011. **29**(6): p. 913-922.

212. Fisher-Power, L.M., T. Cheng, and Z.S. Rastghalam, *Cu and Zn adsorption to a heterogeneous natural sediment: Influence of leached cations and natural organic matter.* Chemosphere, 2016. **144**: p. 1973-1979.

213. Kulikowska, D., et al., *Feasibility of using humic substances from compost to remove heavy metals (Cd, Cu, Ni, Pb, Zn) from contaminated soil aged for different periods of time.* Journal of Hazardous Materials, 2015. **300**: p. 882-891.

214. Helal, A.A., *Binding constant of thorium with gray humic acid.* Journal of Radioanalytical and Nuclear Chemistry, 2007. **274**(3): p. 575-580.

215. Tranvik, L.J. and E. von Wachenfeldt, *Interactions of Dissolved Organic Matter and Humic Substances*, in *Encyclopedia of Inland Waters*, G.E. Likens, Editor. 2009, Academic Press: Oxford. p. 754-760.

216. Senesi, N., V. D'Orazio, and T.M. Miano, *Adsorption mechanisms of s-triazine and bipyridylium herbicides on humic acids from hop field soils.* Geoderma, 1995. **66**(3–4): p. 273-283.

217. Koopal, L.K., et al., *Chemical immobilisation of humic acid on silica.* Colloids and Surfaces A: Physicochemical and Engineering Aspects, 1998. **141**(3): p. 385-395.

218. Klavins, M. and L. Eglte, *Immobilisation of humic substances.* Colloids and Surfaces A: Physicochemical and Engineering Aspects, 2002. **203**(1-3): p. 47-54.

219. Prado, A.G.S., B.S. Miranda, and J.A. Dias, *Attachment of two distinct humic acids onto a silica gel surface.* Colloids and Surfaces A: Physicochemical and Engineering Aspects, 2004. **242**(1–3): p. 137-143.

220. Klavins, M., L. Eglite, and A. Zicmanis, *Immobilized humic substances as sorbents.* Chemosphere, 2006. **62**(9): p. 1500-1506.

221. Dercová, K., et al., *Bioremediation of soil contaminated with pentachlorophenol (PCP) using humic acids bound on zeolite.* Chemosphere, 2007. **66**(5): p. 783-790.

222. Luo, D., et al., *Humic acid-bonded silica as a novel sorbent for solid-phase extraction of benzo[a]pyrene in edible oils.* Analytica Chimica Acta, 2007. **588**(2): p. 261-267.

223. Terbouche, A., et al., *Evaluation of adsorption capacities of humic acids extracted from Algerian soil on polyaniline for application to remove pollutants such as Cd(II), Zn(II) and Ni(II) and characterization with cavity microelectrode.* Journal of Environmental Sciences, 2011. **23**(7): p. 1095-1103.

224. Yang, Y.-H. and L.K. Koopal, *Immobilisation of humic acids and binding of nitrophenol to immobilised humics.* Colloids and Surfaces A: Physicochemical and Engineering Aspects, 1999. **151**(1–2): p. 201-212.

225. Bayrakci, M., et al., *Novel humic acid-bonded magnetite nanoparticles for protein immobilization.* Materials Science and Engineering: C, 2014. **42**: p. 546-552.

226. *Volatile Organic Compounds in the environment.* 1996: ASTM.

227. Sangster, J., *Octanol-Water Partition Coefficients of Simple Organic Compounds.* J. Phys. Chem. Ref. Data, 1989. **18**(3).

228. Sacchetto, V., et al., *Interactions of Toluene and n-Hexane on High Silica Zeolites: An Experimental and Computational Model Study.* Journal of Physical Chemistry C, 2015. **119**(44): p. 24875-24886.

229.   Weelink, S.A.B., M.H.A. van Eekert, and A.J.M. Stams, *Degradation of BTEX by anaerobic bacteria: Physiology and application.* Reviews in Environmental Science and Biotechnology, 2010. **9**(4): p. 359-385.

230.   *Groundwater Pollution, Aquifer Recharge and Vulnerability.* 1998, London: The Geological Society.

231.   Vasudevan, M., I.M. Nambi, and G. Suresh Kumar, *Scenario-based modelling of mass transfer mechanisms at a petroleum contaminated field site-numerical implications.* Journal of Environmental Management, 2016. **175**: p. 9-19.

232.   *Green Materials for Sustainable Water Remediation and Treatment.* RCS Green Chemistry. 2013: RCS Publishing.

233.   An, D., et al., *Sustainability assessment of groundwater remediation technologies based on multi-criteria decision making method.* Resources, Conservation and Recycling, 2017. **119**: p. 36-46.

234.   Cheremisinoff, N.P., *6 - Pump-and-Treat Remediation Technology*, in *Groundwater Remediation and Treatment Technologies.* 1997, William Andrew Publishing: Westwood, NJ. p. 203-258.

235.   Bulman, R.A. and G. Szabo, *Investigations of the interaction of transranic radionuclides with humic and fulvic acids chemically immobilized on silica gel*, in *Humic Substances in the Aquatic and Terrestrial Environment: Proceedings of an International Symposium Linköping, Sweden, August 21–23, 1989*, B. Allard, H. Borén, and A. Grimvall, Editors. 1991, Springer Berlin Heidelberg: Berlin, Heidelberg. p. 329-338.

236.   Szabo, G., S.L. Prosser, and R.A. Bulman, *Determination of the adsorption coefficient (KOC) of some aromatics for soil by RP-HPLC on two immobilized humic acid phases.* Chemosphere, 1990. **21**(6): p. 777-788.

237.   Szabó, G. and R.A. Bulman, *Comparison of Adsorption Coefficient (KOC) for Soils and HPLC Retention Factors of Aromatic Hydrocarbons Using a Chemically Immobilized Humic Acid Column in RP-HPLC.* Journal of Liquid Chromatography, 1994. **17**(12): p. 2593-2604.

238.   Colthup, N.B., L.H. Daly, and S.E. Wiberley, *Introduction to Infrared and Raman Spectroscopy.* third ed.

239.   Sardessai, S. and S. Wahidullah, *Structural characteristics of marine sedimentary humic acids by CP/MAS 13C NMR spectroscopy.* Oceanologica Acta, 1998. **21**(4): p. 543-550.

8.   ATTACHMENTS

LIST OF PUBLISHED AND ALMOST TO BE PUBLISHED PAPERS:

8.1.   Braschi, I., et al., *Physicochemical regeneration of high silica zeolite Y used to clean-up water polluted with sulfonamide antibiotics.* Journal of Environmental Sciences, 2016. **43**: p. 302-312.

8.2.   Braschi, I., et al., *Patent application No. 102016000072535, USE OF MESOPOROUS SILICA.* 2016: Ministero per lo Sviluppo Economico, Italy.

8.3.   Buscaroli, E., et al., *Stabilization of mineral oil hydrocarbons in recycled paper pulp by organo-functionalized mesoporous silicas and evaluation of migration to food.* European Food Research and Technology, 2017

8.4.   Buscaroli, E., et al., *Calcium chloride washing of wet calcareous sediments from fresh water canal: Effect on heavy metal removal and water aggregate stability.* Article submitted to Chemosphere

Physicochemical regeneration of high silica zeolite Y used to clean-up water polluted with sulfonamide antibiotics

I. Braschi[1,2,*], S. Blasioli[1], E. Buscaroli[1], D. Montecchio[1], A. Martucci[3]

1. Department of Agricultural Sciences, University of Bologna, Bologna 40127, Italy
2. NanoSiSTeMI Interdisciplinary Centre, Università del Piemonte Orientale A. Avogadro, Alessandria 15121, Italy
3. Department of Physics and Earth Sciences, University of Ferrara, Ferrara 44122, Italy

ARTICLE INFO

ABSTRACT

High silica zeolite Y has been positively evaluated to clean-up water polluted with sulfonamides, an antibiotic family which is known to be involved in the antibiotic resistance evolution. To define possible strategies for the exhausted zeolite regeneration, the efficacy of some chemico-physical treatments on the zeolite loaded with four different sulfonamides was evaluated. The evolution of photolysis, Fenton-like reaction, thermal treatments, and solvent extractions and the occurrence in the zeolite pores of organic residues eventually entrapped was elucidated by a combined thermogravimetric (TGA–DTA), diffractometric (XRPD), and spectroscopic (FT-IR) approach. The chemical processes were not able to remove the organic guest from zeolite pores and a limited transformation on embedded molecules was observed. On the contrary, both thermal treatment and solvent extraction succeeded in the regeneration of the zeolite loaded from deionized and natural fresh water. The recyclability of regenerated zeolite was evaluated over several adsorption/regeneration cycles, due to the treatment efficacy and its stability as well as the ability to regain the structural features of the unloaded material.

© 2015 The Research Center for Eco-Environmental Sciences, Chinese Academy of Sciences.
Published by Elsevier B.V.

Introduction

Adsorption of organic pollutants onto organic or inorganic sorbents is considered one of the most effective technologies for the wastewater treatment (Martucci et al., 2014; Rivera-Utrilla et al., 2013). After adsorption, exhausted materials should be regenerated and reused in order to avoid secondary environmental problems due to the disposal of contaminated materials. The sorbate characteristics, the nature of adsorption, and the regeneration costs affect the choice of the regeneration process (Leng and Pinto, 1996; Nahm et al., 2012).

The most common regeneration technique consists in thermal treatments, where adsorbed molecules are volatilized and/or oxidized by heating. Alternatively, the solvent extraction of entrapped molecules is considered another efficient technique. Other methods include photochemical, biological, vacuum, electrical/electrochemical, and supercritical fluid treatments, as well as microwave and ultrasounds.

Although activated carbons are the most widely used sorbents (Cooney, 1999) in wastewater treatment technology, zeolites are considered competitive materials in terms of cheapness, shape selectivity, and adsorption efficacy (Ahmaruzzaman, 2008). These sorbents are characterized by high surface area and excellent adsorption properties, and are largely applied for the removal of cations or organic compounds from effluents (Bish and Ming, 2001; Kesraoui-Ouki

et al., 1994; Martucci et al., 2012; Navalon et al., 2009; Rossner et al., 2009; Tsai et al., 2006). The capacity to retain different solutes mainly depends on the SiO_2/Al_2O_3 ratio that can be modulated in order to preferentially entrap hydrophilic or hydrophobic molecules.

High silica zeolites, namely hydrophobic zeolites with high affinity for organic molecules, have been recently applied for the removal of sulfonamide antibiotics (sulfa drugs) from water under laboratory conditions (Braschi et al., 2010a, 2013; Fukahori et al., 2011; Blasioli et al., 2014). Sulfonamides are a broad spectrum antibiotic class largely used in human and animal therapy and are known to contribute to the evolution of antibiotic resistance phenomena (van der Ven et al., 1994, 1995; Gao et al., 2012a). Sulfa drugs are potentially highly mobile in non-acidic soils, thus favoring their accumulation in water bodies due to their anionic nature (pK_a value in the range of 5.0–7.5) and are not completely transformed by activated sludge in wastewater treatment plants (Gao et al., 2012a). The occurrence of antibiotics in natural waters is one of the main reasons of the spreading of microbial antibiotic resistance which, in turn, makes the antibiotics less effective (Acar and Rostel, 2001).

A high silica zeolite Y ($SiO_2/Al_2O_3 = 200$) has been found to be able to clean up water polluted with sulfonamides (up to 28% of zeolite dry weight (dw)) with a very favorable kinetics (<1 min) (Braschi et al., 2010a, 2013; Blasioli et al., 2014). According to these studies, each zeolite cage (ca. 4×10^{20} cages/$g_{zeolite}$ (Braschi et al., 2010a)) is occupied by an antibiotic molecule, on average. In addition, the sulfa drug adsorption in the zeolite porosity has been found unaffected by the presence of dissolved organic matter.

Leardini et al. (2014) have recently investigated the thermal regeneration of high silica zeolites loaded with sulfamethox-azole sulfonamide by an *in situ* high-temperature synchrotron diffractometric (XRPD) study. The study has been carried out on samples treated at 575°C for 2 hr and, under these conditions, the degradation pathway of the embedded antibiotic has been defined. The architecture of treated zeolite was found unmodified, thus allowing the sorbent reuse for water depollution.

Four sulfa drugs were selected for this study because of their different structures as shown in Fig. 1, *i.e.*, a six membered diazine ring in sulfadiazine (SD) and sulfamethazine (SM), a six membered pyridazine ring in sulfachloropyridazine (SC), and a five membered isoxazole ring in sulfamethoxazole (SMX). Since the thermal treatment efficacy on exhausted zeolite Y can be affected by the chemical structure of embedded molecules, in this study the efficacy of the thermal treatment

was reconsidered on zeolite Y loaded with the four sulfa drugs and compared to the performance of solvent extractions. The development of chemical processes as Fenton and Fenton-like for soil, wastewater and manure decontamination (Rivas, 2006; Dec et al., 2007; Rivera-Utrilla et al., 2013), along with the well-known susceptibility of the sulfonamide moiety to photolytic cleavage (D'Souza and Day, 1968), prompted us to test photolysis and Fenton-like conditions for the regeneration of sulfonamide loaded-zeolite Y. The Fenton-like reaction in the presence of Fe^{3+} was preferred to Fenton reaction with Fe^{2+} owing to the ease of Fe(II) to be oxidized to Fe(III) during the reagent storage and handling.

The zeolite was loaded with the sulfonamides, chosen for their occurrence in water bodies and soils (Ungemach, 2012; Lindsey et al., 2001), in order to supply exhausted samples to be treated for regeneration purposes. The efficacy of the adopted regeneration techniques, the zeolite characterization before and after treatments, as well as the process evolution, were elucidated through a combined thermogravimetric, diffractometric, and spectroscopic analyses. Once the best regeneration conditions were identified, the treated zeolite Y was tested over several adsorption/regeneration cycles in both deionized and natural fresh water.

1. Materials and methods

1.1. Chemicals

Sulfadiazine (4-amino-2-N-pyrimidinyl-benzenesulfonamide, molar weight, MW, 250.3 g/mol; 99% purity), sulfamethazine (4-amino-N-(4,6-dimethyl-2-pyrimidinyl)benzenesulfonamide, MW 278.3 g/mol; 99% purity), sulfachloropyridazine (4-amino-N-(6-chloro-3-pyridazinyl)benzene sulfonamide, MW 284.7 g/mol; 98% purity) and sulfamethoxazole (4-amino-N-(5-methyl-isoxazol-3-yl)benzenesulfonamide, MW 253.3 g/mol; 99% purity) were purchased from Sigma-Aldrich (Saint Louis, MO, USA) in powder form. The chemical structure and the pK_a value of the antibiotics are reported in Fig. 1.

Stock solutions of each antibiotic at its maximal solubility were prepared by adding to Milli-Q® water (Merck KGaA, Darmstadt, Germany) an amount of sulfonamide exceeding the saturation concentration. Each drug suspension was then sonicated for 15 min at room temperature (RT) in order to speed up the dissolution process. Undissolved drug particles were then filtered through 0.45 μm Durapore® membrane (Merck KGaA, Darmstadt, Germany), and the antibiotic concentration of each supernatants evaluated by high performance liquid

Sulfadiazine (SD)
pK_a = 6.4

Sulfamethazine (SM)
pK_a = 7.5

Sulfachloropyridazine (SC)
pK_a = 5.5

Sulfamethoxazole (SMX)
pK_a = 5.7
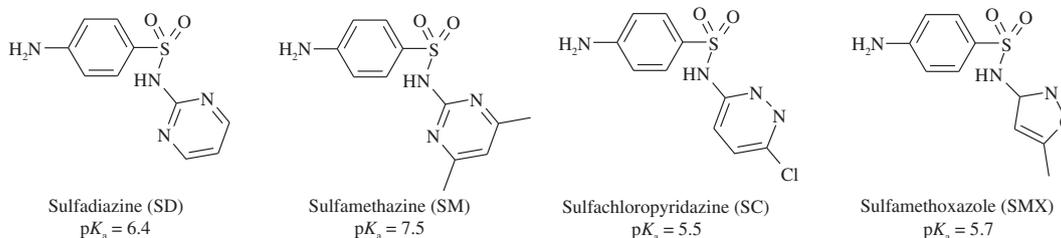
Fig. 1 – Chemical structures and pK_a of the four selected sulfonamides.

chromatography (HPLC). The maximal solubility of SD, SM, SC, and SMX were 71.9 ± 4.8, 138.5 ± 3.7, 176.3 ± 7.2, and 203.2 ± 2.4 mmol/L, respectively (Table 1). If needed, Milli-Q® water diluted solutions were prepared starting from stock solutions.

Y type faujasite zeolite powder with a 200 SiO_2/Al_2O_3 (mol/mol) ratio (code HSZ-390HUA) and with pore access window of $7.1 \text{ Å} \times 7.0 \text{ Å}$ was purchased (Tosoh Corporation, Minato, TKY, Japan).

1.2. Zeolite loading from deionized water

The maximal sulfonamide loading of zeolite was achieved by adding to the zeolite a volume of antibiotic aqueous solution at its maximal solubility which contained a drug amount slightly exceeding the loadable amount. The maximal adsorption capacity of zeolite Y toward SD, SM, SC, or SMX has been previously measured (ca. 15%, 21%, 26%, or 24% zeolite dw, respectively (Braschi et al., 2010a; Blasioli et al., 2014)). In the present study, 850 mL of aqueous SD solution at the maximal solubility (Table 1) was added to 100 mg of the zeolite, whereas 550 mL for SM or SC, and 500 mL for SMX were used. In accordance to the very favorable adsorption kinetics of sulfonamides by the zeolite Y (adsorption equilibrium < 1 min (Braschi et al., 2010a; Blasioli et al., 2014)), the suspensions were shaken on a magnetic stirrer for 30 min at RT and then filtered through 0.45 μm Durapore® membrane (Merck KGaA, Darmstadt, Germany). Once the adsorption was completed, the liquid phase was analyzed by HPLC to measure the residual antibiotic concentration, whereas the loaded zeolite samples were recovered, air dried and stored before the regeneration process. The same loading procedure was followed for the regenerated zeolite samples.

1.3. Zeolite loading from river water

Fresh natural water was collected from an Italian river (Reno) in Bologna municipality and filtered up to 0.22 μm (Millipore, Merck KGaA, Darmstadt, Germany) before use. The water was characterized for pH 8.8, conductivity 355.5 μS/cm by a CDM210 conductometer (CDM210, Radiometer Analytical, Villeurbanne Cedex, France), total organic carbon (TOC of 1.71 mg/L, method ISO 8245:1999 for water quality), and total nitrogen (TN of 0.47 mg/L, method CSN EN 12260 for water quality) by a Shimadzu TOC/TN analyzer (Kyoto, Kansai, Japan).

Zeolite Y (160 mg) was exposed for 30 min to 2 L of the 0.22 μm filtered river water spiked with a mixture of SD, SM,

SC, SMX (40 mg each). The entrapped amount of sulfa drugs was evaluated by HPLC, measuring the residual antibiotic concentration in the liquid phase. Under these conditions, SD (2.50% zeolite dw), SM (13.22% zeolite dw), SC (1.42% zeolite dw), and SMX (1.90% zeolite dw) were simultaneously retained by the zeolite. The loaded zeolite aliquot was therefore homogenized and split into two sub-samples which were used to evaluate the effectiveness of the thermal and solvent-assisted regeneration treatments (vide infra).

1.4. Regeneration treatments

1.4.1. Photolysis
The irradiation was realized by a handmade merry-go-round Rayonet photoreactor equipped with four low-pressure mercury lamps (RPR-2537 Å, Rayonet, Branford, Connecticut, USA). Owing to maximal absorbance at 271 nm for SC and 267 nm for the other sulfa drugs, photoexperiments were carried out by irradiating at a fixed wavelength of 254 nm on 10 mL of an aqueous suspension containing 20 mg of loaded Y zeolite placed into a tubular quartz reactor (average irradiation intensity of 110 mW/cm²). The suspension homogeneity was ensured by magnetic stirring and suspension overheating was avoided by ventilation (the temperature never exceeded 40°C). After 10, 30 and 60 min irradiation, each suspension was centrifuged at 14,000 r/min for 15 min and the zeolite pellet was recovered, air dried, and stored in a desiccator for further analysis. Photolysis experiments were also performed on aqueous solutions of pure sulfonamides (25 mmol/L) to evaluate their reactivity to the ultraviolet (UV) light.

1.4.2. Fenton-like reaction
The efficacy of Fenton-like reaction was tested at two different reagent concentrations (Dec et al., 2007), i.e., (1) 10 m mmol/L $FeCl_3$ (Carlo Erba Reagents, Cornaredo, Milano, Italy) and 200 m mmol/L H_2O_2 (40% M/V, Carlo Erba Reagents, Cornaredo, Milano, Italy) and (2) 40 m mmol/L $FeCl_3$ and 600 m mmol/L H_2O_2.

In both conditions, loaded zeolite samples (20 mg) were suspended in 10 mL $FeCl_3$ solution and shaken at 3000 r/min for 2 hr. H_2O_2 was then added drop by drop until the end of gas evolution. Under both the experimental conditions, both Fe^{3+} concentrations exceeded those of the sulfonamides entrapped into the zeolite (ca. 10 and 40 times) to favor the diffusion of the Fenton-like species in the zeolite cavities. The pH of suspension was monitored before and throughout the reaction at different

Table 1 – Solubility of the selected sulfonamides in solvent mixtures with different compositions.						
Sulfonamide	Solubility in $H_2O/CH_3CN/CH_3OH$ solution (mmol/L)					
	100/0/0	0/100/0	0/0/100	50/50/0	50/0/50	33/33/33
SD	0.072 (0.005)	3.9 (0.2)	4.4 (0.4)	8.7 (1.3)	1.9 (0.1)	7.7 (0.1)
SM	0.138 (0.004)	53.2 (3.0)	33.9 (11.1)	64.6 (5.6)	14.0 (2.7)	57.8 (2.5)
SC	0.176 (0.007)	158.8 (12.9)	43.7 (17.3)	100.8 (2.6)	12.7 (3.6)	90.5 (7.5)
SMX	0.203 (0.002)	73.9 (9.7)	28.0 (3.8)	22.2 (4.5)	11.4 (2.1)	275.5 (17.9)

Numbers in brackets are the standard deviation.
SD: sulfadiazine; SM: sulfamethazine; SC: sulfachloropyridazine; and SMX: sulfamethoxazole. $m/n/y$ (m, n, and y all ranging from 0 to 100) refer to $H_2O/CH_3CN/CH_3OH$ volume ratio.

times to avoid the iron hydroxide precipitation that occurs at pH > 2 at our concentrations (Pourbaix, 1949). The suspensions were left for additional 2 hr without further mixing, and then the zeolite was recovered through Whatman 42 filters (Whatman, Maidstone, United Kingdom), air dried, and stored in a desiccator for further analysis.

1.4.3. Thermal treatment

Samples (40 mg) of zeolite loaded with SD, SM, SC or SMX from both deionized and river water were treated in a Carlo Erba® static air furnace at different temperatures (400, 450, 500, 550, and 600°C) for different time durations (1–8 hr) and stored in a dessicator for further analysis.

1.4.4. Solvent extraction

Several combinations of miscible solvents as Milli-Q® water, acetonitrile (HPLC grade J. T. Baker, Avantor Performance Materials, Center Valley, Pennsylvania, USA), and methanol (HPLC grade Sigma-Aldrich®, Saint Louis, MO, USA), as well as pure solvents, were tested for their ability to remove the sulfonamides from loaded zeolite Y.

The solubility at RT of each sulfonamide in each solvent or desorption mixture was preliminarily determined by adding the antibiotics to each solvent/mixture in amount exceeding those required to saturate the solution. Each suspension was then shaken, sonicated for 5 min, filtered through a 0.45 μm Durapore membrane (Merck KGaA, Darmstadt, Germany) to eliminate the undissolved solute and the supernatant analyzed by HPLC. In Table 1 the solubility of the selected sulfonamides in the solvents/mixtures are reported. Then the volume required to solubilize the entire amount of sulfonamides loaded into the zeolite was calculated accordingly, to avoid saturation of the extractant mixtures.

Twenty milligrams of zeolite simultaneously loaded with SD, SM, SC, or SMX from deionized and river water was suspended in 5 mL of each solvent mixture. After 1, 5, 10, 20, and 30 min shaking (ca. 400 r/min) at RT, each suspension was centrifuged, and 1 mL of the liquid phase was brought to 100 mL with the same solvent mixture and analyzed by HPLC. The dilution was necessary to bring the sulfonamide concentration below the upper limit of the analytical calibration curve (20–200 mmol/L). The zeolite samples were then filtered, air dried, and stored in a desiccator for further analysis.

1.5. Fourier transform infrared (FT-IR) spectroscopy studies

Infrared spectra were collected on a spectrometer (Tensor27, Bruker, USA) with 4 cm^{-1} resolution. Self-supporting pellets (10 mg each) of loaded and treated zeolite were obtained with a mechanical press (SPECAC, Kent, UK) at ca. 6.5 ton/cm^2 and placed into an infrared spectroscopy (IR) cell equipped with KBr windows permanently attached to a vacuum line (residual pressure ~1 × 10^{-4} mbar), allowing sample dehydration *in situ*. Spectra of the bare zeolite were collected as a control.

1.6. XRPD analysis

XRPD patterns of thermally treated zeolites were measured on a Diffractometer (D8 Advance, Bruker, USA) equipped with a Sol-X detector, using Cu Kα1, α2 radiation. The spectra were collected in the 3–110° 2θ range with a counting time of 12 sec/step. Unit cell and structural parameters were determined by Rietveld profile fitting—using the GSAS package (Larson and Von Dreele, 2004) with the EXPGUI interface (Toby, 2001). The atomic coordinates and refinement details are given as supporting information in Table S1.

1.7. HPLC analysis

The sulfonamide solubility and their concentration in the extractant mixtures were determined by HPLC-Diodarray (Jasco Incorporation, USA). The chromatographic system consisted of a Jasco 880-PU Intelligent pump, a Jasco 875-UV UV–vis detector set at 271 nm for SC and 267 nm for the other antibiotics, a Jasco AS-2055 plus autosampler, Jasco ChromNAV 1.14.01 chromatography data software, a Jones Chromatography column heater 7971, and a 4.6 × 250 mm Waters Spherisorb® 5 μm C8 analytical column kept at 35°C. Acetonitrile and Milli-Q® water (23:77 by volume, pH 2.7 for H$_3$PO$_4$) at 1 mL/min was used as eluant mixture. Under these conditions, the retention times for SD, SM, SC, and SMX were 4.2, 5.6, 6.3, and 6.9 min, respectively.

1.8. Thermogravimetric analysis

Thermogravimetric and derivative thermogravimetric (TGA–DTG) analysis was performed with a TGDTA92 instrument (TGDTA92, SETARAM Instrumentation, France). Loaded or regenerated zeolite samples (20 mg) were placed into an alumina crucible and heated from 30 to 700°C at a 10°C/min rate under air flow (8 L/hr). The furnace was calibrated using a transition temperature of Indium. Bare zeolite Y was analyzed as a control.

2. Results and discussion

The selected zeolite Y has been found to be a sorbent suitable to clean up water from sulfonamides due to its ability to embed high antibiotic amount from water with a very favorable adsorption kinetics (Braschi et al., 2010a, 2013; Blasioli et al., 2014). This study is finalized to assess the most affordable technologies aiming at regenerating the zeolite once high amount of sulfonamides are entrapped into its pores and at evaluating its recyclability.

2.1. Photolysis

At first, the photodegradability at 254 nm of the pure sulfonamides in water solution was evaluated as a control, and the half-life times ($t_{1/2}$) of the antibiotics exposed to the treatment are reported in Table 2. It is of general knowledge that the sulfonamide moiety is susceptible to photolysis (D'Souza and Day, 1968). Under our conditions, the concentration of both SD and SC was halved in ca. 15 min whereas SM and SMX requested a longer exposition period (ca. 40 and 60 min, respectively). As reported by Gao et al. (2012b), SM in aqueous solution with a concentration slightly lower than that we used (20 and 25 μmol/L, respectively) has been found recalcitrant to UV-light-activated persulfate oxidation at 254 nm with 10% of SM transformed after 40 min treatment. Clearly, the different

Table 2 – Half-life times ($t_{1/2}$) of the selected sulfonamides in water solution (25 μmol/L) exposed to several chemical treatments.

Treatment	$t_{1/2}$ (min)			
	SD	SM	SC	SMX
Photolysis	12	39	16	60
Fenton-like[a]	<0.1	<0.1	<0.1	<0.1
Fenton-like[b]	<0.1	<0.1	<0.1	<0.1

[a] Reagent: 10 mmol/L $FeCl_3$ + 200 mmol/L H_2O_2.
[b] Reagent: 40 mmol/L $FeCl_3$ + 600 mmol/L H_2O_2.

photoreaction conditions reduced the SM degradation rate with respect to our conditions. Similar differences can be found in other studies (Batchu et al., 2014; Batista et al., 2014), where $t_{1/2}$ of several sulfonamide antibiotics treated at 254 nm spans from a few minutes to about half an hour, depending on the initial antibiotic concentration and adopted conditions.

As far as the photoreactivity of the entrapped sulfonamides is concerned, Table 3 shows the amount of organic residues that remained into the phototreated zeolite. TGA shows that more than 90% of the embedded amount was recovered unmodified after 1 hr treatment, making thus the method useless for regeneration purpose. The persistence of the sulfonamides into the irradiated zeolite Y was also confirmed by infrared spectroscopy. By way of example, Fig. 2 A–B shows the DTG and FTIR curves of SD-loaded zeolite before and after the UV treatment, respectively. Both the DTG curves of untreated and treated zeolites (Fig. 2A, curves a and b) present a similar profile at temperatures higher than 150°C, thus indicating the antibiotic preservation. The peak below 150°C is due to water release and is present in both samples. Also, the IR spectra of the same samples (Fig. 2B, curves a and b) show bands which are very similar in both the position and the intensity, thus confirming the unreactivity of the encapsulated antibiotic to UV treatment. Likely, the zeolite framework shielded the embedded species from the UV radiation and/or the photo-formed oxygenated species were not able to diffuse at the surface of the sulfonamide-loaded zeolite adduct.

2.2. Fenton-like reaction

The reactivity of the bare sulfonamides in water was evaluated under two different concentrations of Fe^{3+} ion and

H_2O_2. Under all the conditions, the antibiotics degraded very quickly ($t_{1/2}$ of a few seconds, Table 2), in full agreement with the findings of Gonzales and coworkers on Fenton-degraded sulfamethoxazole (González et al., 2007).

When the Fenton-like treatments were performed on the sulfonamide-loaded zeolite, the organic residue that remained into the sorbent accounted for 88%–100% of the initially loaded antibiotic amount (Table 3). DTG and IR spectra of the SD-zeolite system before and after the treatments are shown, by way of example, in Fig. 2. Only the IR region in the 1800–1300 cm^{-1} range is presented due to the absence of bands belonging to the zeolite Y, thus favoring the simple observation of features coming from the organic species. The DTG curves of the treated and untreated zeolites revealed different features, i.e., the treated samples (curves c and d) presented a new peak centered at about 430°C, which accounted for 8.6% of zeolite dw and was absent in the untreated one (curve a), thus indicating a partial formation of new more thermo-resistant species. No IR bands were clearly visible apart from those assignable to SD in the spectra of the treated zeolites (Fig. 2B, curves c and d) (Braschi et al., 2010b). In order to better observe the features of the more thermo-stable degradation product(s), the Fenton-like treated SD-zeolite sample was heated to 350°C in TGA environment. The simplified system was then newly analyzed by combined TGA and IR analysis (Fig. 2, curves e). The DTG results showed now a single peak centered at 430°C thus confirming the occurrence of entrapped degradation product(s). The related IR spectrum (Fig. 2B, curves e) revealed features typical of amorphous species which were formed by incomplete oxidation of the embedded sulfa drugs. The only partial degradation of the sulfonamides embedded into the zeolite exposed to Fenton-like treatments made these methods unsuitable for the zeolite regeneration. The adsorption of iron species by zeolite Y could be excluded because of the negligible cation exchange capacity of the sorbent with a SiO_2/Al_2O_3 ratio of 200. Likely, the radical oxygenated species (mainly ·OH and ·OOH, (Laine and Cheng, 2007)) cannot easily diffuse into the sulfonamide-loaded zeolite.

2.3. Thermal treatment

High silica zeolites are usually stable when thermally regenerated in air, thus preserving their adsorption properties (Khalid et al., 2004; Vignola et al., 2011a, 2011b). Due to the importance of discovering both the least time- and energy-consuming

Table 3 – Organic residue remained into the zeolite Y exposed to several regeneration chemical treatments with the exposition time of 60 min as determined by TGA.

Regeneration method	Percentage of organic residue referred to the loaded antibiotic amount			
	SD	SM	SC	SMX
Photolysis	95.3% (1.2%)	96.0% (1.6%)	93.0% (3.6%)	95.1% (1.0%)
Fenton-like[a]	100.0% (0.0%)	98.6% (0.1%)	98.1% (0.0%)	97.0% (0.1%)
Fenton-like[b]	89.7% (0.1%)	87.8% (0.0%)	96.9% (0.1%)	97.5% (0.4%)

Numbers in brackets are the absolute error.
TGA: thermogravimetric analysis.
[a] Reagent: 10 mmol/L $FeCl_3$ + 200 mmol/L H_2O_2.
[b] Reagent: 40 mmol/L $FeCl_3$ + 600 mmol/L H_2O_2.
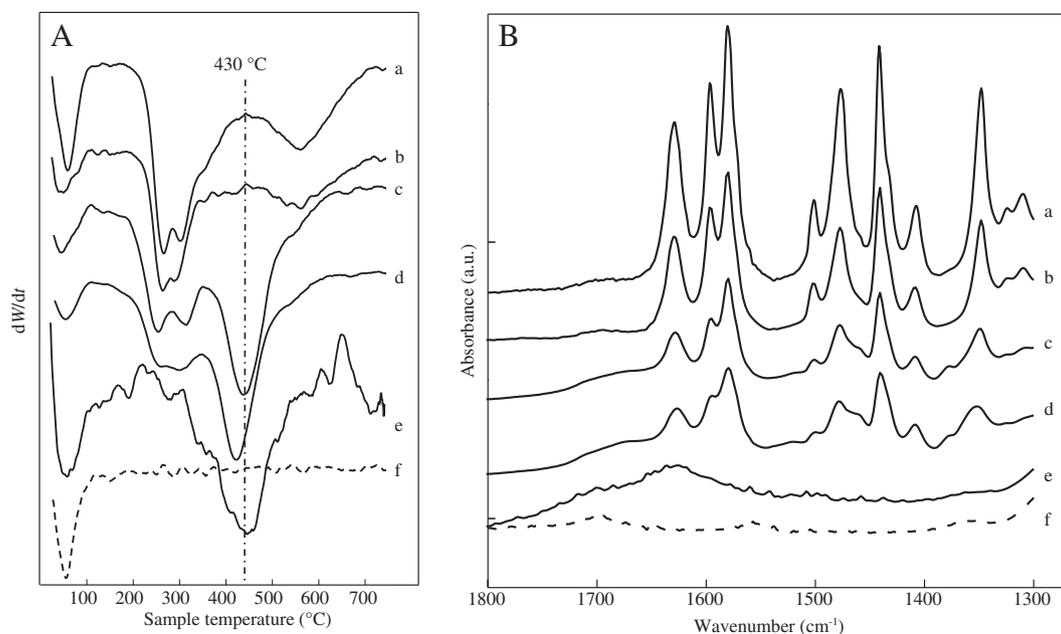
Fig. 2 – (A) DTG (derivative thermogravimetric) curves and (B) FT-IR (Fourier translation infrared spectroscopy) spectra of zeolite Y loaded with SD before (a) and after photolysis (b), Fenton-like treatment at 10 mmol/L FeCl$_3$ + 200 mmol/L H$_2$O$_2$ (c) and at 40 mmol/L FeCl$_3$ + 600 mmol/L H$_2$O$_2$ (d). DTG and IR features of (e) Fenton-like treated SD-loaded zeolite heated up to 350°C and of (f) bare zeolite are also reported. SD refers to sulfadiazine. dW/dt: first derivative of weight over time.

strategies to clean up zeolites used to clean up waters from sulfonamides, a detailed assessment devoted specifically to identifying the best thermal regeneration conditions is presented here. The amount of organic residues that remained into loaded zeolite samples exposed to different temperatures for different time durations was evaluated by TGA. For the sake of brevity, only the thermal regeneration of SMX-loaded zeolite is reported in Fig. 3. According to residual amount of sulfonamides in the treated zeolite, 4 hr at 500°C were identified as the best regeneration conditions for all the selected sulfonamides (organic residue = 0.18% zeolite dw, on average). The structural features of treated zeolites were evaluated by XRPD (Fig. 4). In the figure, the diffraction pattern from the same zeolite after
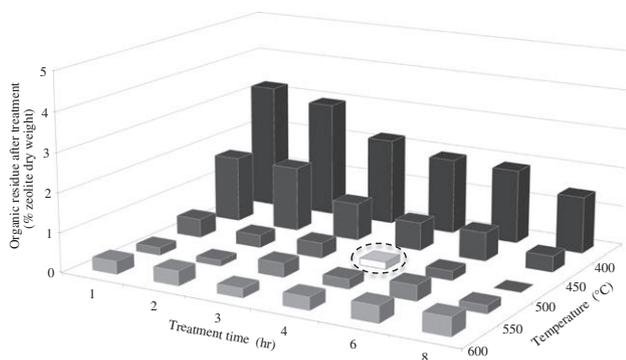
SMX adsorption (Leardini et al., 2014), which has been measured at the European Synchrotron Radiation Facility, is reported. In this last case, the X-ray beam wavelength was 0.653 Å, almost half of the Cu $K\alpha$ wavelength (1.544 Å) used for our XRD measurements. Consequently, for a better comparison all the diffraction patterns were reported as a function of the d-spacing:

$$2d \sin \theta = n \lambda$$

where, d is the interplanar distance related to the θ angle on the basis of the Bragg law, n is a positive integer and λ is the wavelength of incident wave. At the same time, the diffraction peak positions were quite similar among samples, and consequently, unit-cell parameters were not significantly modified, as shown in Table 4. The heating process did not affect the zeolite crystallinity and the diffraction patterns of regenerated samples regain almost perfectly the features of unloaded material. By virtue of its high flexibility and stability (Alberti and Martucci, 2005), the FAU framework is able to slightly distort and relieve the strain imposed by the regeneration as demonstrated by the crystallographic free area (CFA) (Baerlocher et al., 2007) and channel's ellipticity values, which are similar to those reported for the bare material (Table 4). These results highlighted the Y ability to modify the dimensions of the internal void volume for size and shape dependent sorption behavior.

The adsorption capacity of the thermally treated zeolite samples was tested through their application in several adsorption/regeneration cycles. In Fig. 5, three adsorption/regeneration cycles were performed on the zeolite toward SD, SM, and SC antibiotics whereas the recycle was repeated up to six times toward SMX.

Fig. 3 – Organic residues remained into SMX loaded-zeolite Y thermally treated under different temperatures and time durations. The least energy-consuming conditions are circled: 4 hr at 500°C. SMX refers to sulfamethoxazole.
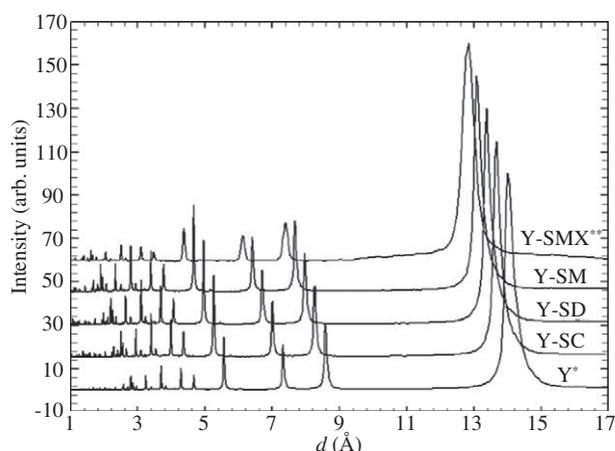
Fig. 4 – Normalized powder diffraction (XRPD) patterns of untreated zeolite Y (Y) and thermally treated (at 500°C for 4 hr) zeolite samples previously loaded with sulfonamides (Y-SM, Y-SD, Y-SC, Y-SMX). The stacked plots have been shifted for easy comparison. *As reported in Braschi et al. (2010a); **as reported in Leardini et al. (2014) after background subtraction (λ = 0.653 Å). SM, SD, SC and SMX refer to Fig. 1; d: interplanar distance which is related to the θ angle on the basis of the Bragg law.

For each investigated sulfonamides, the adsorption capacity of treated zeolite samples resulted very close to the initial loading capacity, thus making these conditions (4 hr at 500°C) suitable for zeolite regeneration. Interestingly, the first adsorption after regeneration was higher (+12%, on average) for three out of four sulfonamide-loaded systems. These findings can be explained by a partial modification of the zeolite silanol groups that are condensed by the thermal treatment (Braschi et al., 2012), thus making the sorbent more organophilic, as well as by a low reproducibility of such a complex multistep experiment.

Table 4 – Unit cell parameters, crystallographic free area (CFA) *sensu* Baerlocher et al. (2007) and channel's ellipticity (ε) for zeolite Y loaded with SD, SM, SC and SMX before and after 4 hr at 500°C.

Parameter	Y	Y-SD	Y-SM	Y-SC	Y-SMX
a (Å)	24.259 (1)	24.273 (1)	24.281 (1)	24.280 (1)	24.257 (1)
b (Å)	24.259 (1)	24.273 (1)	24.281 (1)	24.280 (1)	24.257 (1)
c (Å)	24.259 (1)	24.273 (1)	24.281 (1)	24.280 (1)	24.257 (1)
V (Å^3)	14,277.1 (1)	14,301.0 (9)	14,314.3 (3)	14,313.1 (3)	14,272.6 (4)
CFA (Å^2)	39.07	41.60	39.57	39.57	41.99
ε	1.01	1.01	1.02	1.02	1.02

Data of Y and Y-SMX were from Braschi et al. (2010a) and Leardini et al. (2014), respectively.
Numbers in brackets are the digit affected by error.
ε is defined as the ratio between the larger and the smaller O–O diameters.
a, b, and c are the dimensions along x, y, z directions of the crystal unit cell, and V refers to the unit cell volume.

When the treatment was applied to the zeolite exposed to the river water simultaneously spiked with the four sulfa drugs, the antibiotic adsorption was found at 83% of the initial loading capacity, on average, as shown by the HPLC data reported in Table 5. It should be noted that the HPLC data are specifically related to the sulfa drug loading, whereas the TGA measurements are referred to the total organic species embedded into the pores. The difference between TGA and HPLC data can be ascribed to the embedding into the pores of a small amount of organic species occurring in the natural water.

2.4. Solvent extraction

The sulfonamide-loaded zeolites were exposed to desorption treatments. Two protic solvents (water and methanol) as well as an aprotic one (acetonitrile) were selected for the molecular dimensions compatible with the cage access window dimension (7.0 Å × 7.1 Å) and for their different polarities. The pure solvents and their binary and ternary mixtures were evaluated to test their ability to displace antibiotics from the zeolite cages. In Table 6, the sulfonamides that remained into zeolite Y after 30 min extraction are reported as a percentage of the loaded amount. Some relevant error values (expressed as absolute error) are due to the complexity of the loading/extraction steps followed by the extractant dilution which is necessary to bring the sulfonamide concentration below the upper limit of the analytical calibration curve (20–200 mmol/L).

The amount of embedded sulfonamides was found almost unmodified after water extraction (94% of loaded sulfonamide, on average) in agreement with the irreversibility of the sulfonamide adsorption process by the zeolite Y (Braschi et al., 2010a; Blasioli et al., 2014). Similarly, when loaded zeolite samples were exposed to pure acetonitrile, SD, SM, and SC still recovered in high amounts (89% loaded sulfonamide, on average) after the treatment, whereas about 41% of SMX remained into the zeolite pores, thus making acetonitrile unsuitable for regeneration purpose. With pure methanol, the sulfonamide extraction efficiency was in the order of SD > SC > SM > SMX but still far to be acceptable. SD was more easily removed from the zeolite than SMX, regardless of the higher methanol solubility of the latter than SD (28.0 and 4.4 mmol/L, respectively, Table 1). Likely, the extraction efficacy depends not only on the solvation of guest molecules but also on the affinity between the extractant and zeolite framework as well. When sulfonamide-loaded zeolite samples were treated with water/acetonitrile or water/methanol binary mixtures, the amount that remained entrapped into the zeolite porosities was quite different among the sulfonamides, and still accounted for 16% and 26% of loaded sulfonamide on average, respectively. The best regeneration was obtained with the ternary H_2O/CH_3CN/CH_3OH mixture, which allowed the removal of the highest drug amount (8% of loaded sulfonamides remained entrapped, on average, roughly corresponding to 1.8% zeolite dw). Also the extraction power of water at pH 8.5 was evaluated as a component of the ternary mixture, due to the acidic nature of sulfonamides (pK_a values, Fig. 1). Surprisingly, under these conditions, the antibiotic amount that remained embedded into the zeolite increased to about 13% loaded amount, on average. Likely, with the exception of SM, the polarization of water molecules surrounding hydroxide ions affects the
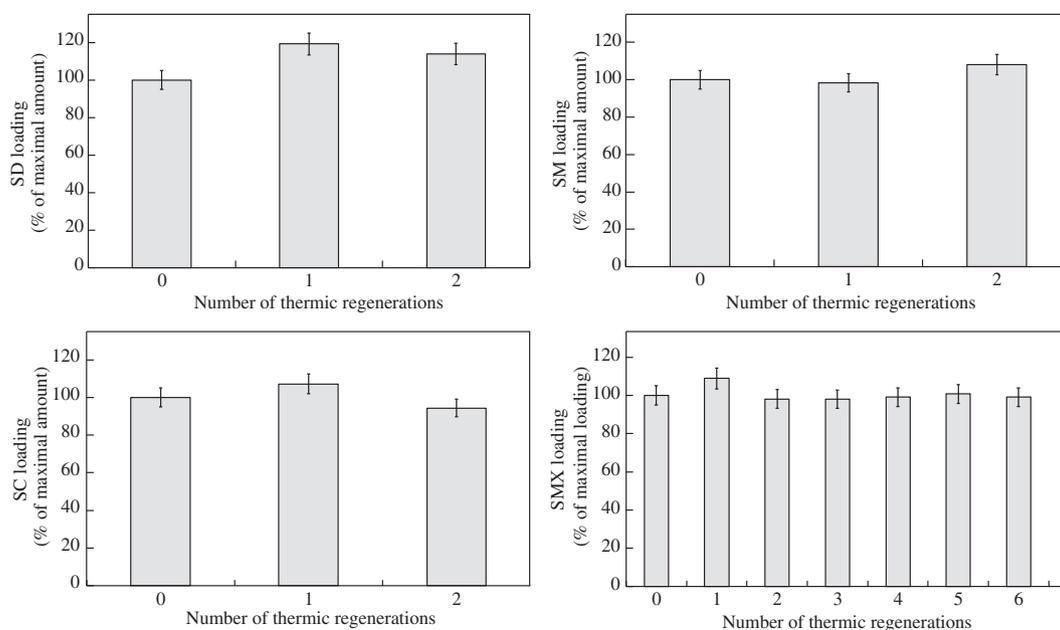
Fig. 5 – Adsorption capacity of zeolite Y toward sulfonamides after several adsorption/regeneration cycles. Regeneration conditions: at 500°C for 4 hr.

intermolecular interactions among the solvents with a reduction, as a general result, of the solvating and displacement properties toward the sulfonamides.

FT-IR spectra of sulfonamide loaded zeolite samples exposed to the neutral ternary mixture for different time durations were recorded to evaluate the desorption time needed to remove the sulfonamides from zeolite Y. This technique is not considered optimal to study the spectral features of low amount of matrix-dispersed organic compounds since it is generally accepted that amounts smaller than 1%–3% matrix dw cannot be appreciated. Nevertheless, due to the high drug loading, the technique was considered suitable to evaluate the extraction kinetics of the selected sulfonamides. In Fig. 6, IR spectra of sulfonamide-loaded zeolite Y samples (curves a), along with those of samples extracted for different time durations (b–e),

are reported. The IR absorptions of each single sulfonamide (spectra a) were well visible as expected by the high amount embedded (22% zeolite dw, on average) (Braschi et al., 2010a; Blasioli et al., 2014). The assignment of the main bands of the embedded antibiotics and related interactions with the zeolite adsorption sites have been detailed elsewhere (Blasioli et al., 2014; Braschi et al., 2010b). Already after 1 min extraction (curves b), no signal assignable to SM, SC or SMX structures could be observed, thus ensuring their complete removal from the zeolite matrix. Interestingly, in the case of SD-loaded zeolite, antibiotic bands were clearly visible after 1 and 5 min extraction (b and c, respectively) but disappeared after 10 min treatment (curve d). These findings indicate that the SD extraction kinetics is unfavoured if compared to those of the other sulfonamides. This can be explained through the occurrence of bulky SD

Table 5 – Evaluation of the loading capacity of zeolite Y toward a mixture of sulfa drugs added to a river water after thermal and solvent-assisted regeneration treatments by HPLC and TGA.

Regeneration treatment	Percentage of the loaded sulfa drug amount referred to the zeolite dry weight				
	SD	SM	SC	SMX	Total sulfa drugs
No treatment	2.5%	13.2%	1.4%	1.9%	19.1% (19.9%)
Thermally regenerated	1.9%	10.8%	0.7%	2.2%	15.7% (17.2%)
Desorbed with solvent	1.6%	11.1%	0.4%	1.6%	14.6% (18.1%)

Sulfa drug concentration was 40 mg/L each in fresh river water (pH 8.8).
Numbers in brackets are the TGA data.
HPLC: high performance liquid chromatography; TGA: thermogravimetric analysis.

Table 6 – Residual sulfonamides remained into the zeolite Y exposed to selected extractant mixtures obtained by HPLC analysis with the contact time of 30 min.

H_2O/ CH_3CN/ CH_3OH volume ratio	Percentage of residual sulfonamide referred to initial zeolite loading			
	SD	SM	SC	SMX
100/0/0	94.6% (0.3%)	93.8% (0.6%)	92.7% (0.4%)	96.1% (0.1%)
0/100/0	89.4% (0.4%)	87.6% (0.01%)	88.7% (0.5%)	40.8% (19.6%)
0/0/100	4.0% (3.1%)	18.8% (4.6%)	11.3% (3.5%)	31.4% (7.3%)
50/50/0	0.0% (0.9%)	13.8% (1.4%)	27.0% (1.9%)	23.8% (0.6%)
50/0/50	5.4% (4.3%)	14.8% (0.4%)	53.1% (1.7%)	31.9% (5.4%)
33/33/33	0.5% (4.5%)	10.4% (11.8%)	11.4% (0.3%)	8.8% (10.4%)
33/33/33 [a]	9.3% (5.0%)	3.7% (3.4%)	14.5% (3.0%)	22.7% (4.0%)

Numbers in brackets are the absolute error.
[a] Conditions: pH 9.5 for 0.1 mol/L KOH.

dimers embedded into the zeolite cage as recently reported for small sized sulfonamide antibiotics (Braschi et al., 2010b, 2013). The extra stabilization of the dimer inside the cage due to the occurrence of two medium strength H-bonds, along with the reduction of room available for solvent molecules to displace SD dimers from the cage wall, made this sulfonamide the last to be desorbed on a time scale. For this reason, at least 10 min of contact time has to be considered to completely regenerate sulfonamide-loaded zeolite Y by extraction. The absence of infrared signals assignable to organic species (Fig. 6) placed all the sulfonamide residues below 1%–3% zeolite dw, making thus this method suitable for zeolite Y regeneration.

When the treatment was applied to the zeolite exposed to the river water simultaneously spiked with sulfa drugs, the drug adsorption was found at 77% of the initial loading capacity, on average, as shown by the HPLC data reported in Table 5. Similar to what was already observed for the thermal treatment, the difference between TGA and HPLC data can be ascribed to the embedding into the zeolite pores of a small amount of organic species occurring in the natural water.

3. Conclusions

A high silica zeolite Y loaded with sulfadiazine, sulfamethazine, sulfachloropyridazine, and sulfamethoxazole was exposed to several regeneration techniques. Chemical processes (photolysis,

Fenton-like reaction) did not allow the regeneration of sulfonamide-loaded zeolite Y. In particular, the adopted photolysis conditions affected neither the quantity nor the structure of the embedded sulfonamides, whereas Fenton-like process only partially transformed the entrapped antibiotic molecules with no significant reduction of the loaded amount.

On the contrary, both the thermal treatment and solvent extraction were successful in the complete regeneration of loaded zeolite samples. As far as the thermal regeneration is considered, the best results were obtained when loaded zeolite samples were exposed to 500°C for 4 hr. Thermogravimetric analysis (TGA/DTG) and infrared (FT-IR) spectroscopy were used to monitor the evolution of guest transformations, if present, and changes in the loaded amount. The ability of zeolite Y to regain its original structural features was defined by XRPD investigations on thermally treated and untreated samples, regardless of the sulfonamide considered. The high flexibility and thermal stability of the zeolite Y was confirmed by its reuse in several adsorption/thermal treatment cycles with no significant changes in the loading capacity.

A feasibility study on solvent extraction of sulfonamides from zeolite pores was also conducted with solvent mixtures of different composition and pH. Several combinations of water, acetonitrile, and methanol were used to remove all the four sulfonamides from the loaded zeolite samples. In general, the mixture with the best affinity for the zeolite and with the best solving properties for the sulfonamides was composed by equal amounts of acetonitrile, methanol and
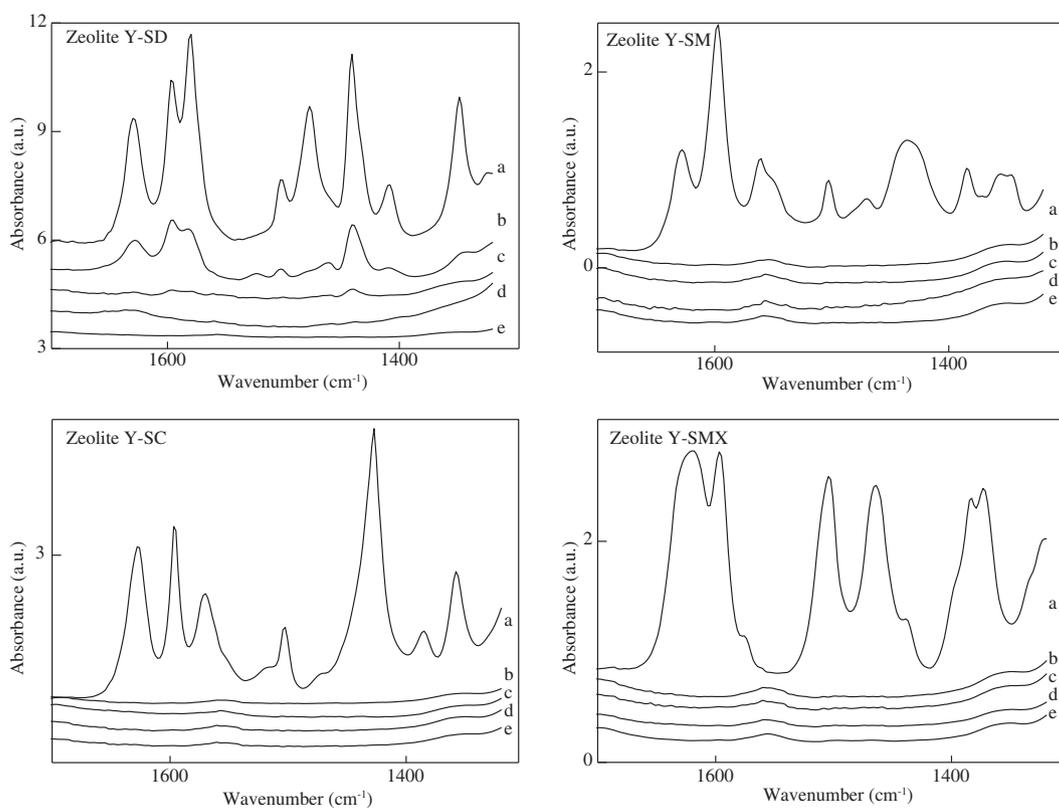

Fig. 6 – FT-IR spectra of high silica zeolite Y loaded with sulfadiazine (SD), sulfamethazine (SM), sulfachloropyridazine (SC), and sulfamethoxazole (SMX) before (a) and after extraction with $CH_3CN/CH_3OH/H_2O$ = 33/33/33 (V/V/V) ratio with the extraction durations for (b) 1, (c) 5, (d) 10, and (e) 20 min. FT-IR: Fourier translation infrared.

water at pH 7. The extraction from the zeolite cage of singly embedded sulfonamide molecules (as in the case of sulfamethazine, sulfachloropyridazine, and sulfamethoxazole) was immediate (1 min contact was enough to completely remove the antibiotics) whereas a contact time of at least 10 min was requested to displace those retained as dimeric species (as in the case of sulfadiazine).

Due to the good recyclability of the exhausted sorbent, even when applied to clean up natural river water spiked with a mixture of the four sulfa drugs, the zeolite-based water treatment presented here can be considered an affordable technology.

Although nowadays great efforts have to be done to develop environmental strategies alternative to solvent-based or energy-consuming processes, a problem as the world-wide diffusion of bacterial antibiotic resistance induced by antibiotics still needs to be addressed. The thermal treatment and the solvent extraction presented here allow a full recyclability of a sorbent material with an excellent ability to entrap sulfonamides from water. This zeolite-based technology can be easily adopted to reduce the point source sulfonamide pollution as that represented by wastewaters coming from fish farms and hospitals.

Acknowledgments

Appendix A. Supplementary data

Supplementary data to this article can be found online at http://dx.doi.org/10.1016/j.jes.2015.07.017.

REFERENCES

Acar, J., Rostel, B., 2001. Antimicrobial resistance: an overview. Rev. Sci. Tech. 20 (3), 797–810.

Ahmaruzzaman, M., 2008. Adsorption of phenolic compounds on low-cost adsorbents: a review. Adv. Colloid Interf. Sci. 143 (1-2), 48–67.

Alberti, A., Martucci, A., 2005. Phase transformations and structural modifications induced by heating in microporous materials. In: Gamba, A., Colella, C., Coluccia, S. (Eds.), Studies in Surface Science and Catalysis vol. 155. Elsevier, Amsterdam, pp. 19–43.

Baerlocher, C., McCusker, L.B., Olson, D.H., 2007. Atlas of Zeolite Framework Types. 6th ed. Elsevier, Amsterdam.

Batchu, S.R., Panditi, V.R., Gardinali, P.R., 2014. Photodegradation of sulfonamide antibiotics in simulated and natural sunlight: implications for their environmental fate. J. Environ. Sci. Health B 49 (3), 200–211.

Batista, A.P.S., Pires, F.C.C., Teixeira, A.C.S.C., 2014. Photochemical degradation of sulfadiazine, sulfamerazine and sulfamethazine: relevance of concentration and heterocyclic aromatic groups to degradation kinetics. J. Photochem. Photobiol. A Chem. 286, 40–46.

Bish, D.L., Ming, D.W., 2001. Natural Zeolites: Occurrence, Properties, Applications, Reviews in Mineralogy & Geochemistry. Mineralogical Society of America and the Geochemical Society, Washington, DC.

Blasioli, S., Martucci, A., Paul, G., Gigli, L., Cossi, M., Johnston, C.T., et al., 2014. Removal of sulfamethoxazole sulfonamide antibiotic from water by high silica zeolites: a study of the involved host–guest interactions by a combined structural, spectroscopic, and computational approach. J. Colloid Interface Sci. 419, 148–159.

Braschi, I., Blasioli, S., Gigli, L., Gessa, C.E., Alberti, A., Martucci, A., 2010a. Removal of sulfonamide antibiotics from water: evidence of adsorption into an organophilic zeolite Y by its structural modifications. J. Hazard. Mater. 178 (1-3), 218–225.

Braschi, I., Gatti, G., Paul, G., Gessa, C.E., Cossi, M., Marchese, L., 2010b. Sulfonamide antibiotics embedded in high silica zeolite Y: a combined experimental and theoretical study of host–guest and guest–guest interactions. Langmuir 26 (12), 9524–9532.

Braschi, I., Gatti, G., Bisio, C., Berlier, G., Sacchetto, V., Cossi, M., et al., 2012. The role of silanols in the interactions between methyl tert-butyl ether and high silica faujasite Y: an infrared spectroscopy and computational model study. J. Phys. Chem. C 116 (12), 6943–6952.

Braschi, I., Paul, G., Gatti, G., Cossi, M., Marchese, L., 2013. Embedding monomers and dimers of sulfonamide antibiotics into high silica zeolite Y: an experimental and computational study of the tautomeric forms involved. RSC Adv. 3 (20), 7427–7437.

Cooney, D.O., 1999. Adsorption Design for Wastewater Treatment. Lewis Publishers, London, England, UK.

D'Souza, L., Day, R.A., 1968. Photolytic cleavage of sulfonamide bonds. Science 160 (3830), 882–883.

Dec, J., Bruns, M.A., Cai, L.S., Koziel, J.A., Snyder, E.M., Kephart, K.B., et al., 2007. Removal of odorants from animal waste using Fenton's reaction. Proceedings of the International Symposium on Air Quality and Waste Management for Agriculture. Broomfield, Colorado, USA (Sep 16-19).

Fukahori, S., Fujiwara, T., Ito, R., Funamizu, N., 2011. pH-Dependent adsorption of sulfa drugs on high silica zeolite: modeling and kinetic study. Desalination 275 (1-3), 237–242.

Gao, Y.Q., Gao, N.Y., Deng, Y., Yang, Y.Q., Ma, Y., 2012a. Ultraviolet (UV) light-activated persulfate oxidation of sulfamethazine in water. Chem. Eng. J. 195–196, 248–253.

Gao, P., Munir, M., Xagoraraki, I., 2012b. Correlation of tetracycline and sulfonamide antibiotics with corresponding resistance genes and resistant bacteria in a conventional municipal wastewater treatment plant. Sci. Total Environ. 421-422, 173–183.

González, O., Sans, C., Esplugas, S., 2007. Sulfamethoxazole abatement by photo-Fenton: toxicity, inhibition and biodegradability assessment of intermediates. J. Hazard. Mater. 146 (3), 459–464.

Kesraoui-Ouki, S., Cheeseman, C.R., Perry, R., 1994. Natural zeolite utilization in pollution control: a review of applications to metals' effluents. J. Chem. Technol. Biotechnol. 59 (2), 121–126.

Khalid, M., Joly, G., Renaud, A., Magnoux, P., 2004. Removal of phenol from water by adsorption using zeolites. Ind. Eng. Chem. Res. 43 (17), 5275–5280.

Laine, D.F., Cheng, I.F., 2007. The destruction of organic pollutants under mild reaction conditions: a review. Microchem. J. 85 (2), 183–193.

Larson, A.C., Von Dreele, R.B., 2004. General Structure Analysis System (GSAS). Los Alamos National Laboratory Report LAUR86-748.

Leardini, L., Martucci, A., Braschi, I., Blasioli, S., Quartieri, S., 2014. Regeneration of high-silica zeolites after sulfamethoxazole antibiotic adsorption: a combined in situ high-temperature

synchrotron powder X-ray diffraction and thermal degradation study. Mineral. Mag. 78 (5), 1141–1159.

Leng, C.C., Pinto, N.G., 1996. An investigation of the mechanisms of chemical regeneration of activated carbon. Ind. Eng. Chem. Res. 35 (6), 2024–2031.

Lindsey, M.E., Meyer, M., Thurman, E.M., 2001. Analysis of trace levels of sulfonamide and tetracycline antimicrobials in groundwater and surface water using solid-phase extraction and liquid chromatography/mass spectrometry. Anal. Chem. 73 (19), 4640–4646.

Martucci, A., Pasti, L., Marchetti, N., Cavazzini, A., Dondi, F., Alberti, A., 2012. Adsorption of pharmaceuticals from aqueous solutions on synthetic zeolites. Microporous Mesoporous Mater. 148 (1), 174–184.

Martucci, A., Braschi, I., Marchese, L., Quartieri, S., 2014. Recent advances in clean-up strategies of waters polluted with sulfonamide antibiotics: a review of sorbents and related properties. Mineral. Mag. 78 (5), 1115–1140.

Nahm, S.W., Shim, W.G., Park, Y.K., Kim, S.C., 2012. Thermal and chemical regeneration of spent activated carbon and its adsorption property for toluene. Chem. Eng. J. 210, 500–509.

Navalon, S., Alvaro, M., Garcia, H., 2009. Highly dealuminated Y zeolite as efficient adsorbent for the hydrophobic fraction from wastewater treatment plants effluents. J. Hazard. Mater. 166 (1), 553–560.

Pourbaix, M., 1949. Thermodynamics of Dilute Aqueous Solutions. Edward Arnold and Co., London, England, UK, pp. 1–136.

Rivas, F.J., 2006. Polycyclic aromatic hydrocarbons sorbed on soils: a short review of chemical oxidation based treatments. J. Hazard. Mater. 138 (2), 234–251.

Rivera-Utrilla, J., Sánchez-Polo, M., Ferro-García, M.Á., Prados-Joya, G., Ocampo-Pérez, R., 2013. Pharmaceuticals as emerging contaminants and their removal from water. A review. Chemosphere 93 (7), 1268–1287.

Rossner, A., Snyder, S.A., Knappe, D.R.U., 2009. Removal of emerging contaminants of concern by alternative adsorbents. Water Res. 43 (15), 3787–3796.

Toby, B.H., 2001. EXPGUI, a graphical user interface for GSAS. J. Appl. Crystallogr. 34 (2), 210–213.

Tsai, W.T., Hsu, H.C., Su, T.Y., Lin, K.Y., Lin, C.M., 2006. Adsorption characteristics of bisphenol-A in aqueous solutions onto hydrophobic zeolite. J. Colloid Interface Sci. 299 (2), 513–519.

Ungemach, F.R., 2012. Figures on quantities of antibacterials used for different purposes in the EU countries and interpretation. Acta Vet. Scand. Suppl. 93 (89–98), 111–117.

van der Ven, A.J.A.M., Mantel, M.A., Vree, T.B., Koopmans, P.P., van der Meer, J.W.M., 1994. Formation and elimination of sulphamethoxazole hydroxylamine after oral administration of sulphamethoxazole. Br. J. Clin. Pharmacol. 38 (2), 147–150.

van der Ven, A.J.A.M., Vree, T.B., van Ewijk-Benken Kolmer, E.W., Koopmans, P.P., van der Meer, J.W.M., 1995. Urinary recovery and kinetics of sulphamethoxazole and its metabolites in HIV-seropositive patients and healthy volunteers after a single oral dose of sulphamethoxazole. Br. J. Clin. Pharmacol. 39 (6), 621–625.

Vignola, R., Bagatin, R., De Folly D'Auris, A., Flego, C., Nalli, M., Ghisletti, D., et al., 2011a. Zeolites in a permeable reactive barrier (PRB): one year of field experience in a refinery groundwater — part 1: the performances. Chem. Eng. J. 178, 204–209.

Vignola, R., Bagatin, R., De Folly D'Auris, A., Previde Massara, E., Ghisletti, D., Millini, R., et al., 2011b. Zeolites in a permeable reactive barrier (PRB): one-year of field experience in a refinery groundwater. part 2: zeolite characterization. Chem. Eng. J. 178, 210–216.

TITLE: "USE OF MESOPOROUS SILICA"

CLAIMS

1.- A use of organofunctionalized mesoporous silica for the production of a paper material; the organofunctionalized mesoporous silica comprises a base mesoporous silica having, on its surface, groups having the following general formula (I):

$$\equiv Si^1\!-\!O\!-\!\underset{\underset{R^2}{|}}{\overset{\overset{R^3}{|}}{Si^A}}\!-\!R^1 \qquad (I),$$
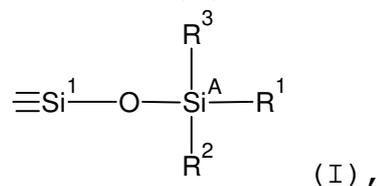
wherein Si^1 is a silicon atom of the base mesoporous silica; R^1 is a C_1-C_5 aliphatic, R^2 is chosen in the group consisting of: a C_1-C_5 aliphatic and an oxygen atom bound with a silicon atom of the base mesoporous silica; R^3 is chosen in the group consisting of: a hydroxyl, a C_1-C_5 aliphatic and an oxygen atom bound with a silicon atom of the base mesoporous silica.

2.- A use according to claim 1, wherein the base mesoporous silica is chosen in the group consisting of: MCM-41, SBA-15 and a combination thereof.

3.- A use according to claim 1 or 2, wherein R^1 is an alkyl; R^2 and R^3 are chosen, each independently of one another, in the group consisting of: an alkyl and an oxygen atom bound with a silicon atom of the base mesoporous silica.

Simone MANGINI
(Iscrizione Albo N.1001/BM)

4.- A use according to any of the preceding claims, wherein R^1, R^2 and R^3 are, each independently of one another, a C_1–C_5 aliphatic, in particular a C_1–C_5 alkyl.

5.- A use according to any of the preceding claims, wherein R^1, R^2 and R^3 are C_1–C_3 alkyls, in particular they each are a methyl.

6.- A use according to any of the preceding claims and comprising a mixing step, during which the organofunctionalized mesoporous silica and paper pulp are mixed so as to obtain a work mixture.

7.- A use according to claim 6 and comprising a slushing step, during which paper is slushed with water so as to obtain the paper pulp; a washing step, which is at least partially subsequent to the mixing step and during which the work mixture is caused to come into contact with water so as to obtain a washed pulp; and a forming step, during which the washed pulp is used for the production of products made of paper material (in particular paper or cardboard sheets).

8.- A use according to claim 7 and comprising a recovery step, during which at least part of the organofunctionalized mesoporous silica is separated from the pulp after the mixing step and prior to the forming step.

9.- A use according to any of the preceding claims and

Simone MANGINI
(Iscrizione Albo N.1001/BM)

having a mixing step, during which particles (in particular, pellets and/or monoliths) having dimensions greater than 1 mm are caused to come into contact with cellulose pulp; said particles (in particular, the pellets and/or the monoliths) comprising the organofunctionalized mesoporous silica.

10.- A use according to claim 8 or 9 and comprising a regeneration step, which is subsequent to the recovery step and during which at least part of the MOHs are removed from the organofunctionalized mesoporous silica that was previously separated from the pulp.

Simone MANGINI
(Iscrizione Albo N.1001/BM)

Ministero dello Sviluppo Economico

Ricevuta di presentazione

per

Brevetto per invenzione industriale

Domanda numero: 102016000072535

Data di presentazione: 12/07/2016

DATI IDENTIFICATIVI DEL DEPOSITO

Ruolo	Mandatario
Data di compilazione	12/07/2016
Titolo	USO DI SILICE MESOPOROSA
Carattere domanda	Ordinaria
Esenzione	NO
Accessibilità al pubblico	NO
Numero rivendicazioni	10
Autorità depositaria	

RICHIEDENTE/I

Natura giuridica	Persona giuridica
Denominazione	UNIVERSITA' DEGLI STUDI DEL PIEMONTE ORIENTALE "A. AVOGADRO"
Partita IVA	01943490027
Nazione sede legale	Italia
Tipo Società	le universita'

Natura giuridica	Persona giuridica
Denominazione	ALMA MATER STUDIORUM - UNIVERSITA' DI BOLOGNA
Partita IVA	01131710376
Nazione sede legale	Italia
Tipo Società	le universita'

DOMICILIO ELETTIVO

Cognome/R.sociale	Studio Torta S.p.A.
Indirizzo	via Viotti 9
CAP	10121
Comune	Torino

Ministero dello Sviluppo Economico - Ufficio Italiano Brevetti e Marchi
Atto non firmato digitalmente in quanto completamente prodotto da sistema informativo automatizzato (decreto legislativo 39/93 art.3)

pagina 2 di 5

Telefono	011 - 5611320
Fax	011 - 5622102
Indirizzo Email	info@studiotorta.it
Indirizzo PEC	
Riferimento depositante	IT0153-16-UNIVERSITA' DEGLI STUDI DEL-SMG

MANDATARI/RAPPRESENTANTI

Cognome	Nome
Mangini	Simone

INVENTORI

Cognome	Nome	Nazione residenza
BRASCHI	ILARIA	
BISIO	CHIARA	
BUSCAROLI	ENRICO	
BUSSINI	DANIELE	
ELEGIR	GRAZIANO	
MARCHESE	LEONARDO	

CLASSIFICAZIONI

Sezione	Classe	Sottoclasse	Gruppo	Sottogruppo
D	21	D		

NUMERO DOMANDE COLLEGATE

Ministero dello Sviluppo Economico - Ufficio Italiano Brevetti e Marchi
Atto non firmato digitalmente in quanto completamente prodotto da sistema informativo automatizzato (decreto legislativo 39/93 art.3)

pagina 3 di 5

DOCUMENTAZIONE ALLEGATA

Tipo documento	Riserva	Documento
Lettera di Incarico	NO	LETTERA INCARICO 0153-16 UNIBO-UNIV. DEL PIEMONTE.pdf.p7m hash: dbbc31e9b341da9929c0d597743ebc66
Rivendicazioni	NO	RIVENDICAZIONI ITALIANE 0153-16 UNIBO-UNIV. DEL PIEMONTE.pdf.p7m hash: d6c449044346a71789e057d9c7210e56
Rivendicazioni in inglese	NO	RIVENDICAZIONI INGLESI 0153-16 UNIBO-UNIV. DEL PIEMONTE.pdf.p7m hash: 44705e7d8b87843971096f8a6055bbbe
Descrizione in italiano*	NO	DESCRIZIONE ITALIANA 0153-16 UNIBO-UNIV. DEL PIEMONTE.pdf.p7m hash: eca7d3eea07c638b8963083f4b736656
Disegni	NO	TAVOLE ITALIANE 0153-16 UNIBO-UNIV. DEL PIEMONTE.pdf.p7m hash: 8cb36bbddff6189beaa9d17ebd10b7da
Designazione d'inventore	NO	DESIGNAZIONE 0153-16 UNIBO-UNIV. DEL PIEMONTE.pdf.p7m hash: 1c5ddb346a7ee433cbfe0fef784e2bfe
Riassunto	NO	RIASSUNTO ITALIANO 0153-16 UNIBO-UNIV. DEL PIEMONTE.pdf.p7m hash: 88ffd68c0956a3f01f4946ff5b3842ee

PAGAMENTI

Tipo	Identificativo	Data
Bollo	01140061153302	11/07/2016

ESENZIONI INDICATE

Ministero dello Sviluppo Economico - Ufficio Italiano Brevetti e Marchi
Atto non firmato digitalmente in quanto completamente prodotto da sistema informativo automatizzato (decreto legislativo 39/93 art.3)

pagina 4 di 5

Esenzione su diritti e tasse	DM 02/04/2007 - art. 2: esonero dal pagamento dei diritti di deposito e di trascrizione relativamente ai brevetti per invenzioni industriali, e modelli di utilita' a vantaggio di: Universita'; Amministrazioni Pubbliche aventi fra i loro scopi istituzionali finalita' di ricerca; Amministrazioni della Difesa; Amministrazioni delle Politiche Agricole, alimentari e forestali.

Ministero dello Sviluppo Economico - Ufficio Italiano Brevetti e Marchi
Atto non firmato digitalmente in quanto completamente prodotto da sistema informativo automatizzato (decreto legislativo 39/93 art.3)

pagina 5 di 5

CrossMark

ORIGINAL PAPER

Stabilization of mineral oil hydrocarbons in recycled paper pulp by organo-functionalized mesoporous silicas and evaluation of migration to food

Buscaroli Enrico[1] · Bussini Daniele[2] · Bisio Chiara[3,4] · Montecchio Daniela[1] ·
Elegir Graziano[2] · Garbini Davide[5] · Marchese Leonardo[3,4] · Braschi Ilaria[1,4]

Abstract The occurrence of mineral oil hydrocarbons (MOH) in cellulose-based packaging is mainly due to the offset printing process where MOH are used as a ink pigments' solvent. The MOH migration from paper/paperboard to food is matter of concern for EFSA, members state authorities, consumers, and food industry. In this study, the feasibility to stabilize MOH by adding a sorbent into recycled paper obtained through a common washing process was investigated and the migration to wheat flour/Tenax® assessed. Among several white/pale yellow porous materials, organo-modified powder silica MCM-41-Si(CH$_3$)$_3$ showed the best combination between affinity for MOH (184% dw) and stability to thermal regeneration. A freshly issued newspaper with >3000 mg MOH kg^{-1} was used to produce recycled paper at a laboratory-scale plant. MCM-41-Si(CH$_3$)$_3$ was added at the pulping step (1% dw) and the sorbent-enriched pulp handled according to a washing paper production process with no effect on the paper optical brightness. The MOH content of the wheat flour in contact with the sorbent-enriched paper under accelerated migration conditions (15 days at 40 °C) resulted 20% of that contacted with control paper (4.3 ± 1.1 and 20.4 ± 5.5 mg kg^{-1}, respectively), despite its contamination was 24% higher than the control. On the contrary, Tenax® contamination resulted 56.0 ± 10.0 and 47 ± 14.0 mg kg^{-1} when exposed to sorbent-enriched and control paper, respectively.

Keywords MOSH · MOAH · Paper-based packaging · Food contact · Paper production

✉ Braschi Ilaria
   ilaria.braschi@unibo.it

1 Department of Agricultural Sciences, University of Bologna, Viale G. Fanin 44, 40127 Bologna, Italy

2 INNOVHUB-SSI, Pulp and Paper Business Area, Milan, Italy

3 Department of Science and Technological Innovation, University of Eastern Piedmont A. Avogadro, Alessandria, Italy

4 Interdisciplinary Nano-SiSTeMI Centre, University of Eastern Piedmont A. Avogadro, Alessandria, Italy

5 Coop Italia s.c.a.r.l., Casalecchio di Reno, BO, Italy

Introduction

Cellulose is worldwide considered a multipurpose, economical, and reliable material. Recovered paper represents the most important raw material for the European paper industry helping to keep the correct balance between virgin and recycled fibres, thus maintaining a very high recycling rate (71.5%) and a sustainable loop [1, 2]. Recycling suitability can be considered one of its most important properties, making paper products a largely sustainable commodity. Nevertheless, the quality of paper/paperboard used for food packaging and the level of contaminants can vary significantly, depending on the raw starting material and the industrial procedures adopted for its production [3].

Only during the last decades, a toxicological risk assessment and a characterization of contaminants occurring in recycled paper have been addressed [4]. Among paper contaminants reported in the literature (e.g., phthalates, photo initiators, and diisopropylnaphthalenes [5, 6]), the most abundant ones are revealed to be a mixture of both linear and branched aliphatic and aromatic hydrocarbons at different composition [4, 7, 8].

 Springer

Mineral oil hydrocarbons (MOH) are commonly used as a solvent for ink pigments in the offset printing process [9] as well as in processing aids and lubricants. Recently, health safety of recycled paper and paperboard has been questioned by the European Food Safety Agency (EFSA), with particular concern about cellulose-based packaging for food contact [10].

Several studies have identified the volatile fraction with 12–24 carbon atoms of both aliphatic (mineral oil saturated hydrocarbons: MOSH) and aromatic hydrocarbons (mineral oil aromatic hydrocarbons: MOAH) as possible food contaminants [11–17] migrating through gas phase from both paper-based packaging and tertiary transport packaging (i.e., corrugated cardboard). It has been demonstrated that MOSH and MOAH can eventually migrate into food [11–13, 18]. Technical grade mineral oil contains a MOAH percentage of 15–35%, which is minimised in food grade mineral oil (white oil): MOAH may be mutagenic and carcinogenic and, therefore, of serious health concern [19, 20]. MOSH accumulates into human body tissues [21–23] and their oral exposition is related to inflammations and necrosis in rats' liver and mesenteric lymph nodes [24, 25]. Due to the molecular composition complexity of mineral oils and their effects still unclear on human health [26, 27], a satisfactory risk assessment of mineral oil exposition is still unavailable; (FAO/WHO revoked in 2012 their daily Acceptable Dose Intakes—ADI—for white mineral oil previously released in 2002, JECFA 2012); hence, regulation is far from fulfilment. The European Food Safety Authority (EFSA) expressed concern on exposure risk [10], but no regulatory discussions followed. Among European countries, Germany's Federal Ministry of Food, Agriculture and Consumer Protection issued in late 2014 the 3rd draft ordinance, proposing to limit the concentration of MOSH and MOAHS in food contact products; still, no actual law issuing followed.

Since the contamination risk of recycled paperboard has been raised, many different strategies to deal with this issue have been adopted through the packaging value chain. The main approaches suitable to face the MOH migration from paper to food consist in: (1) limiting the percentage of recycled fibres in paper-based packaging coming into contact with food; (2) selecting proper high-quality paper for recycling grades; (3) substituting recovered paper with virgin paper; and (4) use of functional barriers.

Recently, an evaluation of the ability of different layered barriers, placed internally or externally to the paper section, to prevent MOH migration from cardboard box to food has been done [29, 30]. Here, among the cellulose-based packaging available on the market, only the cardboard produced by Smurfit Kappa internally containing an activated carbon (AC) layer and coated with

an additional polyvinyl alcohol layer prevented the MOH migration below the limit of detection (LOD) to wheat flakes, thus underlying the feasibility to disperse MOH sorbents into recycled/virgin paper for food safety [30]. The producer guarantees the recyclability of the AC-enriched paperboard, although a grey colored cellulose-based recycled material could be obtained, in case the AC layer is not previously detached from the paper.

With the exception of the last mentioned AC-enriched cardboard coated with a plastic layer, most of the solutions available on the market nowadays do not ensure an acceptable food protection [29] and appear sometimes eco-unfriendly strategies. In fact, composite cellulose-based materials, as those with oil-based plastic barriers, are non-renewable materials and de facto additional post-consumer wastes of the paper recycling process which request the development of alternative approaches.

Paper and paperboard are made of cellulose pulp mixed with different amounts of minerals (usually kaolin and/or calcium carbonate) to give them improved mechanical and surface properties. Our research findings (internal unpublished data) have shown that MOH are retained mainly by the mineral fraction rather than cellulose fibres. These evidences have prompted us to develop several white/pale yellow organo-modified mesoporous silicas with an excellent affinity for MOH and suitable for being used under paper mill conditions as recoverable and regenerable MOH sorbents.

An Italian patent application has recently been filed [31] with the aim to provide stakeholders (e.g., packaging factories, paper mills, and food industry) alternative solutions to produce recycled paper at low MOH content for food contact in the absence of additional internal or external plastic layer or barrier. The patented solutions are based on the use of organo-functionalized mesoporous silicas in the form of powder or pellets/monolites for fast adsorption of MOH from water-based paper production steps. The suitability of silica materials to be produced in the form of pellets and monolites [32–35] for an easy recovery from aqueous solutions and thermal regeneration is of general knowledge.

In the present study, the most relevant results on the selection of MOH sorbents and their feasibility to be thermally regenerated are described. The material with the best combination between MOH retention from water and thermal stability profile was added to the first step of a paper production chain (i.e., pulping unit) and left along the entire paper production process up to its contact with food/food simulant. This simple experimental design was adopted to define its effect on the paper and food MOH content as well as the production steps ideal for its addition and removal of the paper production chain.

Materials and methods

Mineral oil

Paraset 32H mineral oil standard mixture (Petrochem Carless, Leatherhead-UK) with a density of 0.836 g ml^{-1} at 15 °C, a boiling point at 278–315 °C and a vapour pressure <0.04 kPa at 20 °C, was selected because of its mixed composition in terms of aliphatic and aromatic hydrocarbons (87.5 and 12.5% w/w, respectively).

Porous silica-based sorbents

Sorbents were selected among silica-based layered and porous materials because of their known water stability and their high specific surface area (SSA: 216–1040 m^2 g^{-1}) suitable to host hydrocarbons. Moreover, the white/pale yellow color of the sorbents was a strong decision point for selecting them. In fact, any change in paper color had to be avoided for eventual marketing purposes. The list of sorbents, as well as their particle and pore size, is reported in Table 1.

Davisil silica was purchased by Sigma-Aldrich, whereas the other sorbents were synthesized according to the methods reported in the literature and cited in Table 1.

Synthesis of SBA-15-*iso*butyl

The material was synthesized by adapting the method described by Etgar et al. [36]. Briefly, the as-prepared SBA-15 sample [37] was functionalized to introduce *iso*butyl groups on the surface using post-synthesis grafting procedure. About 1 g of SBA-15 silica was treated in vacuum at 200 °C for 2 h for removing adsorbed water. After this activation treatment, the sample was kept under N$_2$ flow and then dispersed in 100 ml of anhydrous toluene before the addition of the organic silane. Specifically, 0.50 ml of *iso*butyl (trimethoxy)silane [(CH$_3$)$_2$CHCH$_2$Si(OCH$_3$)$_3$] (97%, Sigma-Aldrich) was added drop-by-drop to the SBA-15 suspension and then it was left for 20 h at 50 °C under magnetic stirring. The sample was then recovered by filtering, and the powder washed accurately with toluene and then with ethyl ether to remove the unreacted silane. The percentage of organic grafted on silica was determined by thermogravimetric (TG) analysis with a TGDTA92 thermobalance (SETARAM, France). About 20 mg of each material was weighed in an alumina crucible and heated from 30 to 800 °C at a 10 °C min^{-1} under airflow of 8 l h^{-1}. Calcined kaoline was used as a reference material. The furnace was calibrated using the indium transition temperature. TG analysis of not functionalized materials was performed as a control.

Synthesis of SBA-15-Si(CH$_3$)$_3$ and MCM-41-Si(CH$_3$)$_3$

The materials were synthesized by adapting the procedure described by Batonneau and coworkers [38]. The following procedure was adopted for the surface functionalization of both MCM-41 and SBA-15 materials. Two grams of each solid were put in a three-neck round-bottom flask and heated at 200 °C for 2 h. After the thermal treatment, the material was cooled down at room temperature (RT) in nitrogen gas flow and then contacted with 40 ml of anhydrous toluene (Carlo Erba, analytical grade). Finally, 2 × 10^{-3} mol of hexamethyldisilazane corresponding to ca. 420 µl (99.9%, Sigma–Aldrich) were added drop-by-drop and the reaction mixture was maintained at 110 °C for 3 h. Subsequently, the derivatized material was recovered and dried at 40 °C for 24 h in an oven. Sililated SBA-15 and MCM-41 were named SBA-15-Si(CH$_3$)$_3$

Table 1 Physical characteristics of selected materials and their MOH adsorption measured by TG/DTG analysis

Sorbent materials	Source or synthesis method	Particle size (µm)	Pore size (nm)	SSA (m^2 g^{-1})	MOH adsorption (% dw)
SiO$_2$-Davisil	Sigma–Aldrich	150–250	6.0	605	<1
Porous Al$_2$O$_3$	[41]	5–10	3–8	450	<1
SAP-20	[42]	<2	0.10–10	216	2.0
SAP-110	[42]	<2	0.1–10	369	≥1
SAP-150	[42]	<2	0.1–10	314	≥1
SBA-15	[37]	0.5–0.6	8	757	<1
Platelet SBA-15	[43]	0.2–0.3	~8.5	733	≥1
SBA-15-*iso*butyl	[36]	<1	8.1	659	137
SBA-15-Si(CH$_3$)$_3$	[38]	<1	6.5–15	690–1040	318
MCM-41-Si(CH$_3$)$_3$	[38]	<1	2.5	729	184

SSA specific surface area, *dw* dry weight

and MCM-41-Si(CH$_3$)$_3$, respectively (Table 1). Qualitative and quantitative information of succeeded grafting was provided by FTIR and TG analysis performed on the derivatised materials compared to the silicas with no derivatisation.

Recovered paper

Five fresh copies of an Italian newspaper ("Il Giornale" issued on October 22, 2014) containing a consistent amount of MOH (>3000 mg kg^{-1} dw, Table 2) were used as a starting material to produce highly contaminated recycled paper. To maximize the MOH level occurring in the pulp/paper sheet eventually produced, a selection of pages with the largest extension of colored parts was done, and the selected material was processed immediately to reduce the MOH loss due to evaporation. The pages were finally chopped into pieces of about 2 cm × 2 cm dimension by a office Paper shredder (GBC, USA) before pulp manipulation and paper production. The same selection of newspaper pages was used to produce recycled paper in the presence or in the absence of the additive.

Adsorption and regeneration screening

The materials listed in Table 1 were screened for their ability to retain MOH from water. Samples of each material (ca. 50 mg) were placed into 2 ml Eppendorf® Safe-Lock microcentrifuge tubes. MilliQ® water (1.5 ml) and mineral oil (350 μl) were then added to each vial. The suspension appeared roughly dived in three phases: the sorbent as a solid phase, the aqueous solution containing the MOH soluble portion, and the mineral oil as distinct liquid phases. The suspensions were thoroughly mixed under magnetic stirring at RT overnight. This simple experimental setting allowed to maximize the contact among the sorbent, the mineral oil dissolved in water, and the oily phase. Once the stirring was stopped, the residual mineral oil supernatant was removed with a cotton swab and the remaining suspension centrifuged at 15,000 rpm for 15 min. The aqueous solution was then removed from each centrifuge tube by a Pasteur pipette, whereas the sorbent remained into the tube was dried at

40 °C for 24 h in an oven. Control tests on bare materials (i.e., in the absence of mineral oil) were also performed for comparison.

The nature of MOH species adsorbed on SBA-15-Si-(CH$_3$)$_3$ and MCM-41-Si-(CH$_3$)$_3$ was investigated by infrared spectroscopy (FTIR) using a Tensor27 spectrometer (Bruker, USA) equipped with a KBr cell permanently connected to a vacuum line (residual pressure ≤1 × 10^{-4} mbar). Before analysis, a weight corresponding to 5 mg of each sorbent was mixed with 20 mg of KBr (Sigma–Aldrich) and pelletized with a SPECAC (UK) mechanical press at a pressure of 5 tons cm^{-2}. The pellet was then placed into the IR cell and exposed at about 2 × 10^{-2} mbar for 10 s for further dehydration. IR spectra were collected with 4 cm^{-1} resolution. Control sorbent samples were analyzed as a control. Spectra were normalized to each sorbent weight.

The adsorption capacity of each sorbent for MOH and the thermal regeneration conditions were determined by thermogravimetric (TG) analysis and its derivative (DTG) using a TGDTA92 instrument (SETARAM, France) on the loaded material and compared to that performed on the material as a control. About 20 mg of samples were weighed into an aluminum crucible and heated continuously from 30 to 800 °C at a heating rate of 10 °C min^{-1} under airflow of 8 l h^{-1}. Calcined kaolinite was used as a reference material. The weight loss was referred to the weight of air dried sample.

Production of recycled paper

Recycled paper sheets were produced in the presence of MCM-41-Si(CH$_3$)$_3$ because of its high affinity for MOH combined to favourable regeneration profile (*vide infra*) among the sorbents investigated. The process selected to produce recycled paper is sketched in Scheme 1.

Here, the chopped newspaper is added into a pulping unit where it is slashed and the fibres homogenized in the presence of the organo-functionalized silica. The pulp suspension produced is subsequently washed into a washing unit. The washed pulp is collected and paper handsheets prepared in a typical laboratory handsheets former.

Table 2 Content of mineral oil hydrocarbons (MOH) with a number of C atoms >12 of recovered (freshly issued newspaper) and recycled cellulose-based samples determined by GC-FID analysis (EPA 8015D 2003)

	Recovered newspaper paper	Pulp		Washed pulp		Paper sheets	
		Enriched	Control	Enriched	Control	Enriched	Control
MOH (mg kg^{-1} dw)	3125	961.5	638.5	615.8	502.7	286.0	236.1

Analytical error <25%

Scheme 1 Sketch of the process adopted for the production of recycled paper sheet with an indication of the main production steps: pulping unit for pulp production, washing unit for pulp cleaning, and forming unit for paper sheet production. Particles <105 μm diameter: pigments, inorganic particles, and soluble substances
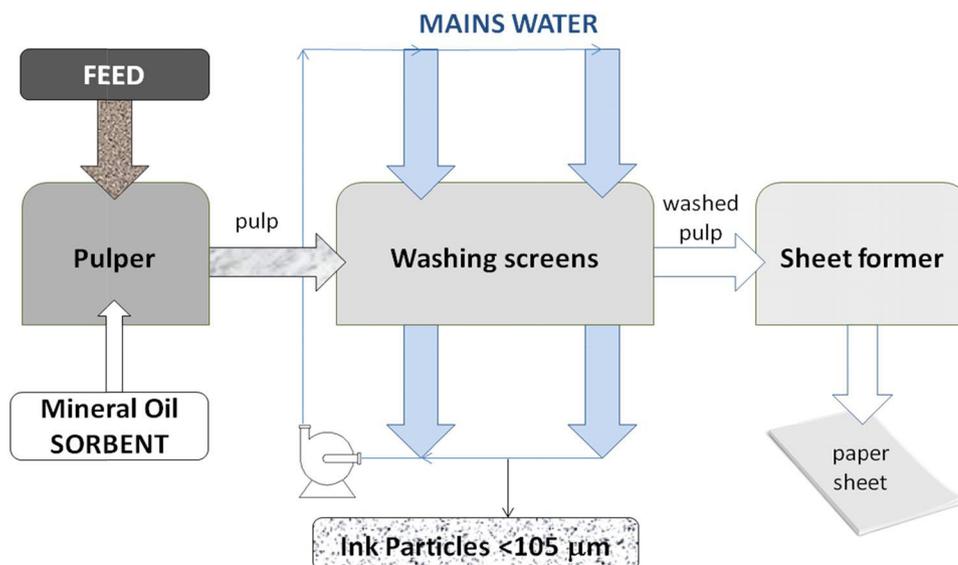
Pulper step

50 grams (dw) of chopped newspaper and 0.5 g of MCM-41-Si(CH$_3$)$_3$ were placed in a standard laboratory disintegrator (called pulper from now on) according to the requirements of ISO 5263 (Enrico Toniolo, Italy) and mashed with 1200 ml of mains water (pH 7.2) at 40 °C for 10 min. The pulping process was conducted twice to produce as a whole 100 g of sorbent-enriched recycled pulp (from here on called enriched pulp). A similar amount of pulp was also produced without the sorbent as a control. Both the enriched and control pulp samples were analyzed for their MOH content.

Washing step

Enriched pulp aliquots (50 g each) were dispersed in ca. 1200 ml of mains water and placed in a standard Sommerville type Fractionator (Lorentzen & Wettre, Sweden) (called washing unit from here on). The washing unit was equipped with a 150-mesh wire screen (105 μm of holes diameter) at the bottom and was operated as a washing machinery able to retain cellulose fibres. The unit was fed with water at a flow of 4.7 l min^{-1} for 15 min. Control pulp was washed under the same conditions. The washing of both the enriched and control pulp samples was conducted in duplicate and analyzed for their MOH content.

Optical properties (ISO brightness and Ink Elimination) were measured on filter pads with a basis weight of 225 g m^{-2}, obtained by filtrating the proper amount of washed pulp samples on a Buchner funnel. ISO Brightness is the measurement of diffuse blue reflectance factor according to ISO 2470-1:2009 (CIE Illuminant C). The Ink Elimination (IE 700) was calculated as a ratio of the reflectance factors at 700 nm of filter pads obtained from the pulp before and after the washing step according to INGEDE Method 2:2014. All the optical measurements were carried out using an Elrepho 3000 Spectrophotometer (Datacolor International, USA) in accordance with ISO 2470-1:2009.

Recycled paper sheet production

About 50 g of both enriched and control washed pulp was diluted in about 5 l of mains water, homogenized, and used for the preparation of recycled paper sheets using the standard Rapid–Kothen equipment (Estanit GmbH, Germany) (called sheet former from here on) according to ISO 5269-2. Recycled paper sheets with a 140 g m^{-2} basis weight were hence vacuum-dried at 93 °C and 63 mbar for 10 min. The forming procedure to produce sorbent-enriched and control paper sheets was repeated twice.

MOH analysis on cellulose-based materials (EPA 8015D 2003 method)

The MOH content of recycled cellulose-based materials obtained at each step of the paper production process (i.e. newspaper, pulp, washed pulp and paper sheet) was determined on extracting solutions of samples at different humidity content as reported by Lorenzini and coworkers [12]. Briefly, wet samples (namely, pulp and washed pulp) corresponding to about 1 g dw were placed in a 100 ml amber flasks with frosted glass caps and added with 25 ml ethanol (95% HPLC grade, J.T. Baker). The flasks were then placed onto an Intercontinental Suprema horizontal shaker at RT. After 1 h shaking, 20 ml n-hexane (analytical grade, Carlo Erba PA) were added to each

flask and the sample shaken again overnight. Samples were hence left to sediment for 1 h and subsequently, about 10 ml of MilliQ® water were added to allow a better separation between the ethanol and *n*-hexane phases. Dry samples (namely, newspaper and paper sheet) did undergo the same procedure described above for wet samples but using 5 ml of ethanol and 5 ml of *n*-hexane. Finally, a 5 ml aliquot of *n*-hexane was withdrawn and analyzed for its MOH content (expressed as the fraction with a carbon number >12) by GC-FID analysis according to the EPA 8015D 2003 method for nonhalogenated organics using GC-FID (see https://www.epa.gov/sites/production/files/2015-12/documents/8015d_r4.pdf and references here reported). No sample pre-treatment was done and a direct injection was adopted for MOH analysis. Although the extracts of recovered and recycled paper may contain other substances beside MOH (i.e., phthalates and diisopropylnaphtalenes) and those substances might be present in the GC chromatograms in addition to the signals of MOH, the results obtained by GC-FID analysis can be safely compared each other.

Accelerated migration test of MOH from paper sheet to food/food simulant

Durum wheat course flour (also known as semolina) was selected as a model to evaluate the MOH migration from recycled paper sheet to dry low fat food. In fact, its high surface area could maximize the adsorption of volatile hydrocarbons eventually released from food-packagings. Tenax® (Supelco) with surface area of 35 m² g⁻¹ was used as a simulant of dry food as well. Tenax is often used as a food simulant for testing the migration of contaminants from packaging of different origin/composition [39].

Flour or Tenax® samples (20 g) and chopped enriched recycled paper sheet (4 g) were placed into 500 ml jars. The jars were tightly closed by a screw cap with an aluminum foil between the jar and cap internal part, and placed into a thermal chamber at 40 °C for 15 days. Though 10 days at 40 °C are indicated for the MOH migration to Tenax® according to the EU Commission Regulation 10/2011, in this study, a period of 15 days was preferred to magnify the effect of sorbent-enriched paper on the MOH migration to food/food simulant. The same experimental setting was used in the presence of recycled paper sheet obtained in the absence of the additive as a control. Once 15 days had passed, the paper sheet and food or food simulant were collected and analyzed to evaluate their MOSH and MOAH content. Each migration trial (flour on sorbent-enriched or control paper and Tenax® on sorbent-enriched or control paper) was conducted in duplicate.

MOSH and MOAH analysis of paper sheet and food/Tenax® (Silliker 004 MPP FCM040 Rev 2 2012 method)

The mineral oil saturated hydrocarbons (MOSH) and aromatic hydrocarbons (MOAH) analysis were performed by Coop Italia at Mérieux NutriSciences Italia (Accredia Lab No. 0144, Tuscany Lab 016) following the LC-GC-FID internal method 004 MPP FCM040 Rev 2 2012. Before their use in the food migration study, durum wheat course flour and Tenax® were certified with a MOSH and MOAH content lower than their limit of quantification (LOQ = 0.5 ppm).

Briefly, mineral oils were extracted from the control and sorbent-enriched paper by treatment with a mixture *n*-hexane/ethanol (1:1 V:V). The extract was then added with water and centrifuged. The upper organic phase was then injected into an online HPLC-GC-FID system, in which the fractions containing MOSH and MOAH were pre-separated through HPLC purification on a silica gel column. The MOSH and MOAH fractions were then separately transferred to the GC, with partial evaporation of the solvent, and revealed using a FID, which provides a virtually equal response factor per unit of mass for all hydrocarbons. The quantification is performed by means of appropriate internal standards added to samples.

Flour samples and Tenax® were extracted with pure *n*-hexane. The extract was centrifuged and injected in the on-line HPLC-GC-FID system after concentration. The analytical approach was the same already reported for the paper samples.

Results and discussion

Table 1 reports the list of sorbents with different specific surface area (SSA) and pore size, which were screened for their ability to retain Paraset 32H mineral oil standard mixture from water. The saponite samples (SAP-20; SAP-110 and SAP-150) belong to trioctahedral layered mineral of the smectite group, whereas the other sorbents are classified as mesoporous materials (2 nm> pore width <50 nm according to the IUPAC classification).

Adsorption and regeneration screening

Information about the MOH adsorption of the selected sorbents was obtained by TG/DTG analysis as reported in Table 1. According to the data, the MOH adsorption was significant only for the organo-functionalized mesoporous silicas in the order:

SBA-15-Si(CH$_3$)$_3$ > MCM-41-Si(CH$_3$)$_3$ > SBA-15-*iso*butyl with 318, 184, and 137% sorbent dw, respectively.

The nature of Paraset 32H mineral oil standard mixture retained by screened SBA-15-Si(CH$_3$)$_3$ and MCM-41-Si(CH$_3$)$_3$ samples was investigated by FTIR analysis and compared to the spectra of the control sorbents as reported in Fig. 1.

For both control SBA-15-Si(CH$_3$)$_3$ and MCM-41-Si(CH$_3$)$_3$ samples, bands characteristics of asymmetric and symmetric stretching of anchored methyl groups were visible at 2966 and 2909 cm^{-1}, respectively [38]. In both MOH loaded sorbents, strong complex signals became visible in the region of the asymmetric and symmetric stretching of aliphatic moieties (<3000 cm^{-1}). The other bands at 1462 and 1377 cm^{-1} were mainly assigned to bending modes of –CH$_2$– and –CH$_3$ moieties, respectively [40]. With the exception of a small band at 1608 cm^{-1} related to aromatic C=C stretching, no net signal in the region of aromatic CH stretching (>3000 cm^{-1}) was revealed in the spectrum of Paraset 32H mineral oil mixture (MOH in CCl$_4$, Fig. 1) as well as in both MOH loaded silicas. As the oil mixture used in the adsorption screening is declared to contain 12.5% weight of MOAH, it was possible to speculate that the aromatic rings of the mixture were highly substituted and/or partially lost by hydration.

Interestingly, the IR spectrum of MOH in CCl$_4$ showed an additional broad, strong, and complex band peaked at 1551 cm^{-1} that was not visible in the spectra of the MOH loaded silicas. The signal could be related to the occurrence of specific components with a polar character higher than those of hydrocarbons, owing to their low affinity for the organo-functionalized silicas. The identification of these components was not conducted, because it was considered beyond the scope of the study.

The TG/DTG curves of SBA-15-Si(CH$_3$)$_3$ and MCM-41-Si(CH$_3$)$_3$ samples before (control) and after the MOH adsorption screening (exhausted sorbent) are shown in Fig. 2.

Concerning the control sample of SBA-15-Si(CH$_3$)$_3$ (Fig. 2a), the weight loss in the RT-150 °C range of temperature (−3.6%) was ascribed to adsorbed water owing to the mild conditions adopted to dehydrate the sample (40 °C overnight). A further weight loss of −4.5% at higher temperature (negative peak centred at ca. 425 °C in the DT curve) was mainly related to the cleavage of the methyl groups anchored to the silica, thus revealing about 4.7% of organic grafted on the dehydrated material even if a small amount of water coming from the condensation of silanol groups could not be excluded (SBA-15 weight loss of 2.8% in the 150–800 °C range of temperature, internal data).

As far as the MOH loaded SBA-15-Si(CH$_3$)$_3$ sample was concerned (Fig. 2a′), a net weight loss of 77.2% was observed between 100 and 300 °C (negative broad peak centred at ca. 250 °C in the DTG curve) due to the MOH release. The MOH adsorbed by dry SBA-15-Si(CH$_3$)$_3$ was approximately calculated by subtracting the weight loss of the control silica up to 300 °C (ca. −4.5%) to that of the MOH loaded material (−77.2% dw) and the MOH loading referred to the weight of dry silica (318% silica dw).

Concerning the MCM-41-Si(CH$_3$)$_3$ control sample, no release of adsorbed water was observed in the TG (Fig. 2b), whereas the weight loss of 2.7% at temperature higher than 300 °C indicated the cleavage of organic grafted on the

Fig. 1 FTIR spectra of Paraset 32 H mineral oil standard mixture in CCl$_4$ (MOH in CCl$_4$), SBA-15-Si(CH$_3$)$_3$ and MCM-41-Si(CH$_3$)$_3$ before (*dotted curve*) and after MOH adsorption (*solid curve*)
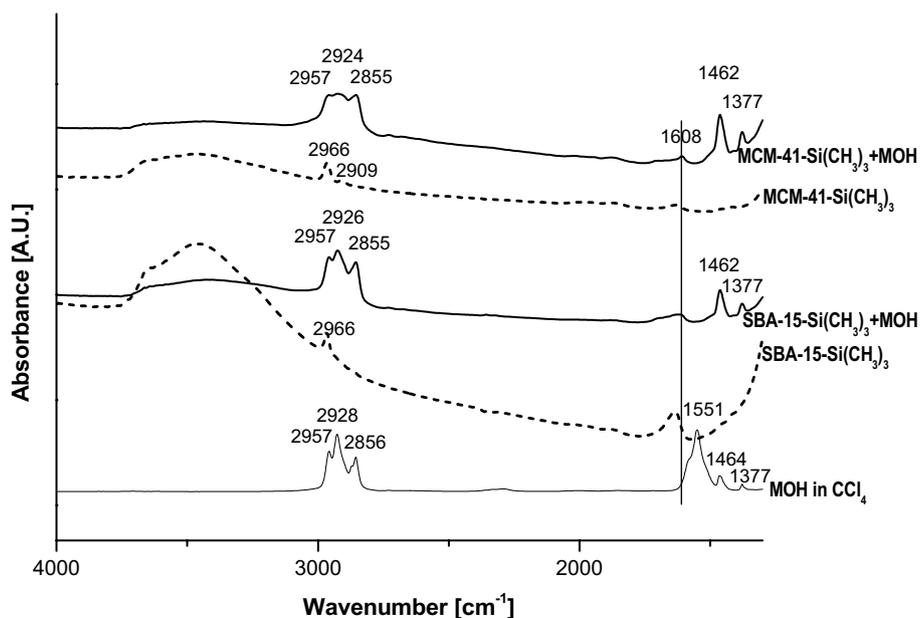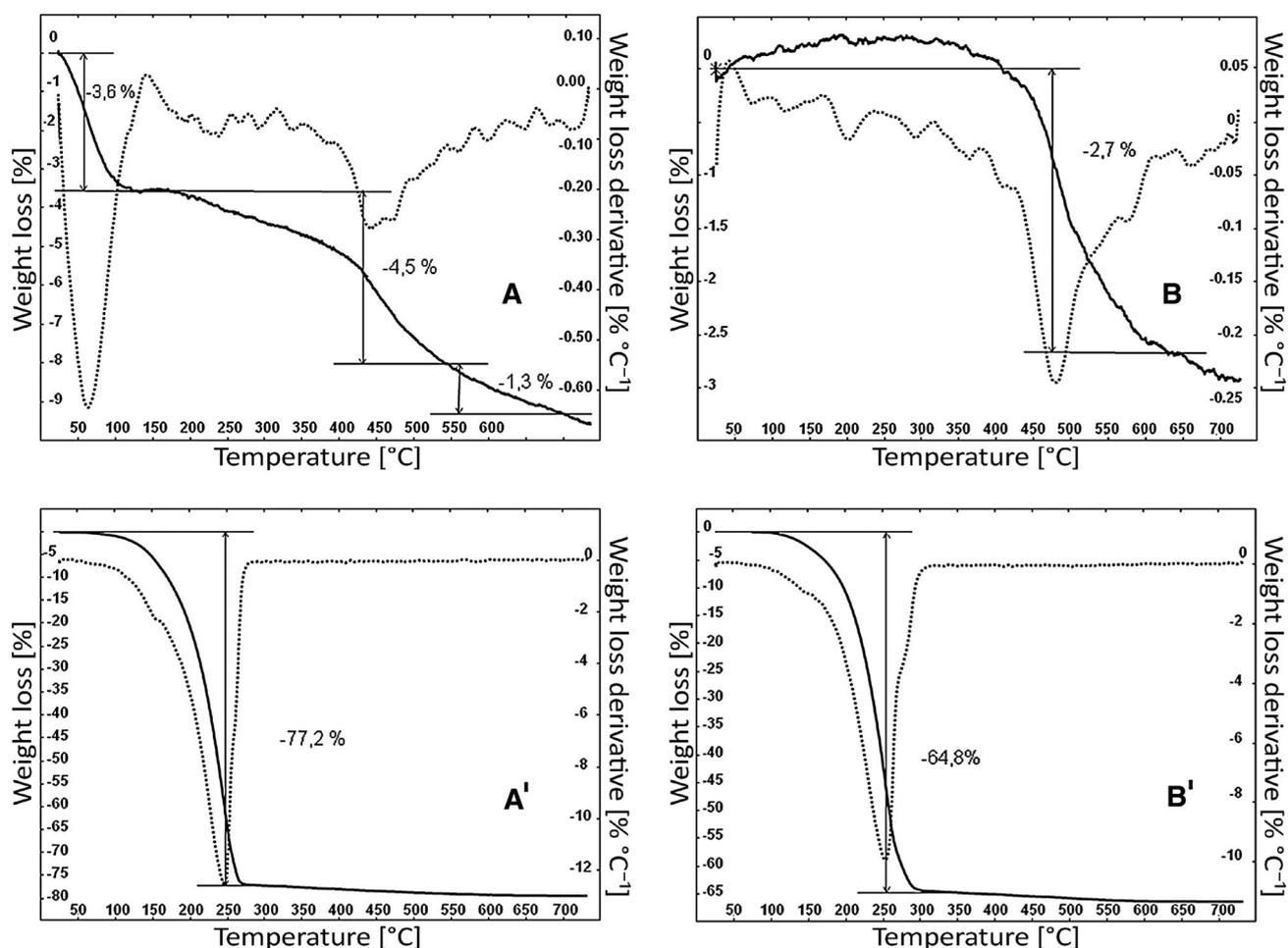
Fig. 2 Thermograms (TG, *solid line*) and derivative profiles (DTG, *dotted line*) of: SBA-15-Si(CH$_3$)$_3$ before (**a**) and after MOSH adsorption (**a′**); MCM-41-Si(CH$_3$)$_3$ before (**b**) and after MOH adsorption (**b′**). Before analysis, the wet samples were kept at 40 °C overnight

silica. The weight loss of 64.8% below 300 °C of the MOH loaded silica (Fig. 2b′) was, therefore, ascribed entirely to adsorbed MOH that resulted 184% silica dw.

Although this is a study preliminary to the definition of the operational conditions suitable for the recovery/regeneration/reuse of the exhausted sorbent, from a practical point of view, the chance to regenerate exhausted sorbents is necessary to be in line with the zero-waste EU policy. This demand can be easily satisfy by silicas in general, and specifically by MCM-41, owing to their well-known suitability to be produced in the form of recoverable/reusable pellets/monolites with medium-to-limited loss of specific surface area (40–5%) [32–35]. In this context, preliminary information concerning the feasibility to thermally regenerate exhausted SBA-15-Si(CH$_3$)$_3$ and MCM-41-Si(CH$_3$)$_3$ could be obtained by comparing the profile of the TG/DTG curves of control and exhausted sorbents (Fig. 2).

To select the best material suitable for MOH adsorption as well as for its eventual recovery and thermal

regeneration, the temperature range for MOH desorption has to be as far as possible from the range where the cleavage of the grafted methyl groups occurs. Despite the excellent MOH adsorption shown by SBA-15-Si(CH$_3$)$_3$, the material was not considered optimal owing to the partial overlapping between the temperature ranges for MOH release (≤300 °C) and that observed for the grafted organic cleavage (250–500 °C) (Fig. 2a′, a). MCM-41-Si(CH$_3$)$_3$ released the organic grafting in a temperature range (negative peak centred at 480 °C in the TDG curve) higher than SBA-15-Si(CH$_3$)$_3$ (ca. 425 °C). Thus MCM-41-Si(CH$_3$)$_3$ was selected as the additive to be added to recycled paper, owing to its favourable adsorption and better stability when exposed to thermal regeneration.

MOH stabilization in MCM-41-Si(CH$_3$)$_3$-enriched recycled paper

Table 2 reports the MOH content of the recovered paper (freshly issued "Il Giornale" newspaper) used to produce recycled paper as determined by GC-FID. The adopted method of analysis (EPA 8015D 2003) allowed to evaluate the content of MOH fraction with a number of C atoms > 12 with no discrimination between the aliphatic and aromatic components.

According to the data reported in Table 2, the recovered paper contained a MOH level higher than 3000 mg kg^{-1} dw. Such an amount was high enough to maximize the effect of each step of the paper production on the contamination level of the cellulose-based material produced. In addition, it would be given a "worst case" scenario to test the retention capacity of MCM-41-Si(CH$_3$)$_3$ toward MOH along the entire paper production process adopted and eventual food contamination.

Scheme 1 shows the main steps of the paper production process adopted in the study: (1) the pulper was fed with recovered paper in the presence of MCM-41-Si(CH$_3$)$_3$; (2) meshed paper enriched with the additive was washed in the washing unit; and (3) sorbent-enriched washed pulp was used for sheet forming. The same procedure was followed in the absence of additive to produce pulp, washed pulp, and paper sheets as control samples.

In the initial stages of paper recycling process, commonly, coarse screens are used to retain large non-paper contaminants (mainly large plastic fragments), while fine screens are subsequently used for the separation of smaller contaminant particles, such as adhesives or highly fragmented plastics, from pulp. On the contrary, the washing step is less common in the recycling process being normally used to eliminate very small ink particles, inorganic fillers, and the soluble fraction of contaminants eventually occurring in the pulp.

In our case, after pulping the newspaper sample, coarse and fine screens were not necessary owing to the absence of large non-paper components, whereas the washing step was performed to verify the extent of MOH released in the water circuit or retained by the sorbent-enriched pulp. Under the adopted washing conditions, the main components of cellulose fibres were retained, whereas only small particles as ink pigments and fibres with dimension lower than 105 μm (i.e., dimension of the wire screen holes) were flushed away.

The evolution of MOH content was evaluated along the paper production process: in Table 2, the MOH content of the pulp, washed pulp and paper sheet samples produced with the additive are reported along with the controls.

The MOH content of the control (638.5 mg kg^{-1} dw) and sorbent-enriched pulp samples (961.5 mg kg^{-1} dw)

was 20 and 31%, respectively, of that found in the newspaper (3125 mg kg^{-1}). These features indicate the mechanical disintegration of the recovered paper carried out at 40 °C in the pulping unit (see Scheme 1) responsible for the strong reduction of hydrocarbons. Such a decreasing was somehow expected given that the newspapers selected as recovered paper were printed a few hours before being collected and immediately processed. It is of common experience that freshly issued newspapers have a solvent fragrance due to the release of the most labile fraction of MOH. A loss of the volatile part of MOH can be directly visualized within the GC chromatograms reported as supporting information (Figure SI1). Here, it is possible to observe a reduction of the area at the volatile edge (left part) of the MOH hump of both the control and sorbent-enriched pulp samples compared to the hump detected in the newspaper. The MOH loss from the pulp samples could be ascribed to their desorption from cellulose fibre and volatilization from water both sped up by the mechanical mixing action conducted at 40 °C.

Interestingly, the pulp sample produced in the presence of the additive showed a MOH content which was 50% higher than the control pulp: this feature could be easily related to the affinity of MCM-41-Si(CH$_3$)$_3$ for hydrocarbons as revealed by the adsorption screening (Table 1). In the light of these findings, it seems reasonable to add the sorbent at the final stage or at the end of the pulping step to let the highest amount of labile MOH fraction be released from the pulp before to immobilize the remaining one.

The MOH content of the washed control and enriched pulp further decreased to 16 and 20% (503 and 616 mg kg^{-1} dw, respectively) of the amount found in the recovered paper. The floating behavior (i.e., the high hydrophobicity) of the non-wettable MCM-41-Si(CH$_3$)$_3$ particles limited its loss through the water released from the bottom of the washing chamber and allowed its blending with the washed pulp. In fact, most of the additive revealed to be utterly mixed within the pulp, making it extremely hard to be flushed away. However, the loss of a minor portion of the additive (ca. 15%) through the screen wire holes along with washing water could not be avoided. From an operational point of view, the chance to pelletize the sorbent would eventually allow to recover the entire amount of sorbent for subsequent regeneration and reuse.

Finally, both the washed control and sorbent-enriched samples were processed under vacuum (63 mbar) and 93 °C to form sheets whose final MOH contents were further decreased below 50% of the amount contained in the corresponding washed pulp samples.

Paper optical properties

The effect of the additive on the optical properties (namely, ink elimination—IE—and ISO brightness) of washed pulp samples was evaluated. The Ink Elimination value, calculated as a percentage of the reflectance factors of pulp pads before and after the washing, represents the level of ink removal during the washing step. At washing step, no significant difference of IE between active and control samples was found (75.0 and 74.3%).

ISO Brightness can be affected by the amount of ink pigments as well as inorganic particles contained in the pulp. The index was evaluated on active and control pulp before and after the washing process. As shown by results, no difference of ISO Brightness resulted between the samples at both the pulping (46.6 and 46.8% for control and sorbent-enriched paper, respectively) and washing steps (56.8 and 56.8% for control and sorbent-enriched washed pulp, respectively). Owing to the very similar optical characteristics (IE and ISO Brightness) between the control and sorbent-enriched samples, it was possible to conclude that the presence of the additive in the washed pulp does not affect its optical features.

Evaluation of MOSH and MOAH migration from paper sheet to food

The recycled paper sheet produced in the presence or in the absence of MCM-41-Si(CH$_3$)$_3$ was placed in contact with durum wheat course flour or Tenax® and an accelerated migration test was conducted at 40 °C for 15 days. Table 3 reports the level of MOH, as well as the saturated (MOSH) and aromatic components (MOAH), revealed in the paper sheet and food samples before and after the migration text. Only the hydrocarbons with C ≤ 24 are reported, because, according to the recent literature [13, 44], the migration to food of the MOH fraction with C ≥ 25 is not likely.

As far as the starting materials are concerned (initial concentration at day 0, Table 3), the MOH content of the enriched paper sheet (272 mg kg^{-1} dw) was 25% higher than the control (220 mg kg^{-1} dw), in good accordance with the MOH analysis conducted by EPA 8015D 2003 method according to which the MOH level of enriched sheet was ca. 20% higher than the control (286.0 and 236.1 mg kg^{-1} dw, respectively, Table 2). As the two methods consider different fractions of hydrocarbons (the fraction with C > 12 the former and with C ≤ 24 the latter), the comparison among the results is not allowed, although numerically quite similar.

Interestingly, the ratio between the saturated (MOSH) and aromatic (MOAH) components of mineral oil hydrocarbons in both the sorbent-enriched and control sheets was similar (3/1). This finding indicates a similar affinity of MCM-41-Si-(CH$_3$)$_3$ for both the aliphatic and aromatic components of hydrocarbons usually occurring in waste paper. In other words, MCM-41-Si-(CH$_3$)$_3$ did not selectively retain one component with respect to the other as it adsorbs MOSH and MOAH proportionally to their relative amount in the control.

At day 15 of migration, the control sheet reduced its MOH content (92.0 mg kg^{-1} dw) to 40% of the initial amount and a consistent amount was recovered on the flour (20.4 mg kg^{-1} dw). The mass balance of MOH on control sheet and flour at day 15 of migration is represented

Table 3 Concentration (mg kg^{-1} dw) of mineral oil saturated (MOSH) and aromatic hydrocarbons (MOAH) of paper sheet and durum wheat course flour or Tenax® exposed to an accelerated migration test (40 °C for 15 days)

Samples	MOSH C ≤ 24	MOAH C ≤ 24	MOH C ≤ 24
Initial concentration (day 0)			
Enriched paper sheet	210.0 ± 37.0	62.0 ± 15.0	272.0 ± 52.0
Control paper sheet	168.0 ± 28.0	52.0 ± 10.0	220.0 ± 38.0
Migration at day 15			
On durum wheat course flour			
Enriched paper sheet	188.0 ± 33.0	51.0 ± 12.0	239.0 ± 45.0
Control paper sheet	70.0 ± 12.0	22.0 ± 5.0	92.0 ± 17.0
Flour on enriched paper sheet	3.1 ± 0.8	1.2 ± 0.3	4.3 ± 1.1
Flour on control paper sheet	15.9 ± 4.3	4.5 ± 1.2	20.4 ± 5.5
On Tenax®			
Enriched paper sheet	40.0 ± 6.0	16.0 ± 4.0	56.0 ± 10.0
Control paper sheet	32.0 ± 10.0	15.0 ± 4.0	47.0 ± 14.0
Tenax® on enriched paper sheet	23.5 ± 6.3	9.9 ± 2.7	33.4 ± 9.0
Tenax® on control paper sheet	18.3 ± 5.0	5.8 ± 1.6	24.1 ± 6.6

Mineral oil hydrocarbons (MOH = MOSH + MOAH). Expanded uncertainty of data calculated by a metrological approach from data validation (Silliker method 004 MPP FCM040 Rev 2 2012)

Fig. 3 Mass balance of mineral oil hydrocarbons (MOH) on paper sheet and durum wheat course flour (**a**) or Tenax® (**b**), both exposed to accelerated migration test at 40 °C for 15 days (paper/food or simulant = 4 g/20 g)
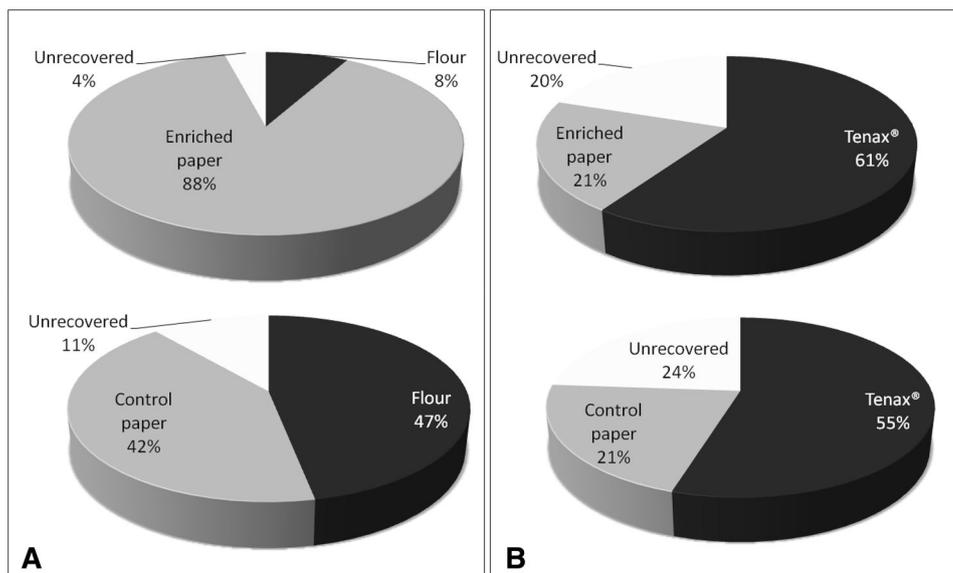
in Fig. 3. Here, the hydrocarbons initially belonging to the sheet were found almost equally distributed between the paper sheet (42%) and flour (47%).

Differently, when the migration test was conducted in the presence of the additive, the sheet revealed an MOH level equal to 88% of initial amount at day 0 and 8% the flour (Fig. 3). The MOH content of the flour (4.3 mg kg^{-1} dw) was 20% of the amount found when contacted with the control sheet (Table 3). This positive result is even more interesting considering the higher initial MOH amount of the sorbent-enriched sheet than the control (272.0 and 220.0 kg^{-1} dw, respectively), thus undoubtedly indicating a preferential MOH adsorption by the organo-modified silica than the cellulose fibres.

As far as the migration on Tenax® is concerned, the scenario was quite different from what observed on the flour. At day 15 of migration, the MOH levels measured in both sorbent-enriched and control sheet were 21% of the related starting amount in each paper sample (56.0 and 47.0 mg kg^{-1} dw respectively) and Tenax® contamination resulted very high after contacting both enriched and control paper (33.4 and 24.1 mg kg^{-1} dw, respectively, Table 3). According to the MOH mass balance (Fig. 3), Tenax® resulted contaminated with 59 and 55% of the MOH initial amount when contacted to the enriched and control sheets, respectively.

The MOH migration from control sheet to the food simulant could be explained by comparing the Tenax® and flour composition. In fact, Tenax® is a poly(2,6-diphenyl-*p*-phenylene oxide) resin with well-known high affinity for volatile and nonpolar compounds as hydrocarbons. Though the use of Tenax® remains questionable owing to its chemical composition which is far away from any food component [45], it is used as a food simulant of dry food. Its use

to assess the content of compounds potentially harmful in food packaging is valuable especially when migration assessment into food is technically difficult, if not impossible, to perform.

Wheat flour has a more complex composition with starches, a subset of complex carbohydrates also known as polysaccharides, as the main components [46]. As a result, the affinity of wheat flour for MOH is necessarily lower than Tenax®, owing to the polar hydroxylated structure of its carbohydrate aliphatic chains.

As far as the MOH migration at day 15 from sorbent-enriched paper to Tenax® is concerned (Table 3; Fig. 3), even in this case, the affinity of the food simulant for MOH revealed much higher than that of the silica organic grafting [–Si–(CH$_3$)$_3$]. It is matter of fact that the adsorption is a physical phenomenon acting at the sorbent surface: in our case, the affinity of MOH for Tenax® was higher than for the sorbent-enriched paper despite the 20-fold lower surface area of the former (35 m^2 g^{-1}) with respect to the latter (727 m^2 g^{-1}).

Finally, the missing percentage of MOH reported in the mass balance of Fig. 3 might be mainly due to their escape from the jar head space at the jar opening and/or during the entire experimental period. In fact, although the jars were tightly closed by a screw cap with an aluminum foil between the jar and cap internal part, the treatment at 40 °C for 15 days might have forced the MOH escape from the jar.

Conclusions

The present study is intended as a preliminary investigation to provide innovative solutions against the migration of

mineral oil hydrocarbons (MOH) from paper/paperboard-based packaging to food in the absence of additional internal layer or barrier. With the future perspective to remove MOH from paper/paperboard by adsorption on a recoverable, thermally regenerable, and reusable material, in this study, an MOH sorbent was identified, added to the pulping step of a washing-based process and never removed from the pulp to evaluate its ability to retain MOH in the pulp/paper samples obtained along all the paper production steps up to the food contact.

Among the several materials screened for their ability to retain MOH from water, MCM-41-Si(CH$_3$)$_3$ was selected because of the best combination between its MOH adsorption capacity and thermal stability. The sorbent was added to waste paper (1% dw) containing a relevant amount of MOH (>3000 mg kg^{-1}) for recycled paper production according to a washing-based process. Its ability to retain MOH was proved by their higher concentration in the sorbent-enriched pulp/paper samples, with respect to the control, at any production step up to the food contact: +51% MOH after pulping, +22% after washing, +21% after sheet forming ; +169% after 15 days of accelerated migration at 40 °C on durum wheat course flour. A low MOH migration to the flour was observed, resulting 8% (4.3 mg/kg) of the amount initially contained in the enriched paper (day 0 of migration), whereas a relevant percentage of MOH migrated to Tenax® (59%). The relevant MOH migration from the sorbent-enriched paper to Tenax® confirmed, if further necessary, the general need to remove the sorbent from the pulp before food contact.

In this context, a list of relevant considerations based on additional findings could be reported as follows: (1) the pulping and washing steps were identified as the two points of the paper production chain suitable for the sorbent addition and removal, owing to the lowest and highest water/pulp ratios, respectively. Nevertheless, due to the strong MOH abatement (−69%) observed in the control pulp as a consequence of pulping, it is preferable to add the sorbent to the pulper at the end of the pulping procedure; (2) the proved MCM-41-Si(CH$_3$)$_3$ stability in the range of temperature suitable for the removal of adsorbed MOH (<300 °C) supports its suitability to be thermally regenerated and reused in the paper production process with considerable reduction of costs and waste materials; (3) the similar technological properties of the sorbent-enriched paper with respect to the control in terms of brightness, texture uniformity, and graininess rules out any effect of silica particles eventually detached from the sorbent, once recovered, on the optical features of the produced recycled paper.

In conclusion, the proved MOH stabilization by the silica along the paper production chain, as well as the well-known feasibility of porous silicas to be formed as pellets/monolites, pave the way to produce MCM-41-Si(CH$_3$)$_3$ in recoverable forms in line with the EU zero-waste policy. The exploitation of recoverable MOH sorbents for the production of white/natural color paper at low MOH content without additional plastic layers or barriers will represent the natural evolution of this innovative approach.

Compliance with ethical standards

Conflict of interest The authors declare that they have no conflict of interest.

Compliance with ethics requirements This article does not contain any studies with human or animal subjects.

References

1. Runte S, Putz HJ, Bussini D, Limongi L, Elegir G (2015) Recyclability criteria for paper based packaging products. Cellul Chem Technol 49(7–8):667–676
2. CEPI (2015) Key statistics. Confederation of European Paper Industries (CEPI), Brussels
3. Bajpai P (2014) Recycling and deinking of recovered paper. Elsevier Insights. doi:10.1016/B978-0-12-416998-2.00018-0
4. Song YS, Park HJ, Komolprasert V (2000) Analytical procedure for quantifying five compounds suspected as possible contaminants in recycled paper/paperboard for food packaging. J Agric Food Chem 48(12):5856–5859. doi:10.1021/jf000512x
5. Aurela B, Kulmala H, Söderhjelm L (1999) Phthalates in paper and board packaging and their migration into Tenax and sugar. Food Addit Contam 16(12):571–577
6. Fernandes AR, Rose M, Charlton C (2008) 4-Nonylphenol (NP) in food-contact materials: Analytical methodology and occurrence. Food additives and contaminants—Part A chemistry, analysis, control, exposure and risk. Assessment 25(3):364–372. doi:10.1080/02652030701564548
7. Droz C, Grob K (1997) Determination of food contamination by mineral oil material from printed cardboard using on-line coupled LC-GC-FID. Eur Food Res Technol 205(3):239–241
8. Summerfield W, Cooper I (2001) Investigation of migration from paper and board into food—development of methods for rapid testing. Food Addit Contam 18(1):77–88. doi:10.1080/02652030010004674
9. Biedermann M, Grob K (2010) Is recycled newspaper suitable for food contact materials? Technical grade mineral oils from printing inks. Eur Food Res Technol 230(5):785–796. doi:10.1007/s00217-010-1223-9
10. CONTAM (2012) Scientific opinion on mineral oil hydrocarbons in food. EFSA Journal, vol 10. EFSA, Parma
11. Biedermann M, Uematsu Y, Grob K (2011) Mineral oil contents in paper and board recycled to paperboard for food packaging. Packag Technol Sci 24(2):61–73. doi:10.1002/pts.914
12. Lorenzini R, Fiselier K, Biedermann M, Barbanera M, Braschi I, Grob K (2010) Saturated and aromatic mineral oil hydrocarbons from paperboard food packaging: estimation of long-term migration from contents in the paperboard and data on boxes from the market. Food additives and contaminants—Part A chemistry, analysis, control, exposure and risk. Assessment 27(12):1765–1774. doi:10.1080/19440049.2010.517568
13. Lorenzini R, Biedermann M, Grob K, Garbini D, Barbanera M, Braschi I (2013) Migration kinetics of mineral oil hydrocarbons from recycled paperboard to dry food: monitoring of two real cases. Food additives and contaminants—Part A chemistry,

analysis, control, exposure and risk. Assessment 30(4):760–770. doi:10.1080/19440049.2013.766765

14. Choi JO, Jitsunari F, Asakawa F, Park HJ, Lee DS (2002) Migration of surrogate contaminants in paper and paperboard into water through polyethylene coating layer. Food Addit Contam 19(12):1200–1206. doi:10.1080/02652030210151877

15. Binderup ML, Pedersen GA, Vinggaard AM, Rasmussen ES, Rosenquist H, Cederberg T (2002) Toxicity testing and chemical analyses of recycled fibre-based paper for food contact. Food Addit Contam 19(SUPPL.):13–28. doi:10.1080/02652030110089878

16. Nerín C, Contín E, Asensio E (2007) Kinetic migration studies using Porapak as solid-food simulant to assess the safety of paper and board as food-packaging materials. Anal Bioanal Chem 387(6):2283–2288. doi:10.1007/s00216-006-1080-3

17. Poças MDF, Oliveira JC, Pereira JR, Brandsch R, Hogg T (2011) Modelling migration from paper into a food simulant. Food Control 22(2):303–312. doi:10.1016/j.foodcont.2010.07.028

18. Biedermann M, Ingenhoff JE, Barbanera M, Garbini D, Grob K (2011) Migration of mineral oil into noodles from recycled fibres in the paperboard box and the corrugated board transport box as well as from printing inks: a case study. Packag Technol Sci 24(5):281–290. doi:10.1002/pts.937

19. Brown-Woodman PDC, Webster WS, Picker K, Huq F (1994) In vitro assessment of individual and interactive effects of aromatic hydrocarbons on embryonic development of the rat. Reprod Toxicol 8(2):121–135. doi:10.1016/0890-6238(94)90019-1

20. Khan S, Rahman AM, Payne JF, Rahimtula AD (1986) Mechanisms of petroleum hydrocarbon toxicity: studies on the response of rat liver mitochondria to Prudhoe Bay crude oil and its aliphatic, aromatic and heterocyclic fractions. Toxicology 42(2–3):131–142. doi:10.1016/0300-483X(86)90004-1

21. Barp L, Kornauth C, Wuerger T, Rudas M, Biedermann M, Reiner A, Concin N, Grob K (2014) Mineral oil in human tissues, Part I: concentrations and molecular mass distributions. Food Chem Toxicol 72:312–321. doi:10.1016/j.fct.2014.04.029

22. Biedermann M, Barp L, Kornauth C, Würger T, Rudas M, Reiner A, Concin N, Grob K (2015) Mineral oil in human tissues, Part II: characterization of the accumulated hydrocarbons by comprehensive two-dimensional gas chromatography. Sci Total Environ 506–507:644–655. doi:10.1016/j.scitotenv.2014.07.038

23. Concin N, Hofstetter G, Plattner B, Tomovski C, Fiselier K, Gerritzen K, Fessler S, Windbichler G, Zeimet A, Ulmer H, Siegl H, Rieger K, Concin H, Grob K (2008) Mineral oil paraffins in human body fat and milk. Food Chem Toxicol 46(2):544–552. doi:10.1016/j.fct.2007.08.036

24. Carlton WW, Boitnott JK, Dungworth DL, Ernst H, Hayashi Y, Mohr U, Parodi AL, Pattengale PK, Rittinghausen S, Ward JM (2001) Assessment of the morphology and significance of the lymph nodal and hepatic lesions produced in rats by the feeding of certain mineral oils and waxes. Exp Toxicol Pathol 53(4):247–255

25. Scotter MJ, Castle L, Massey RC, Brantom PG, Cunninghame ME (2003) A study of the toxicity of five mineral hydrocarbon waxes and oils in the F344 rat, with histological examination and tissue-specific chemical characterisation of accumulated hydrocarbon material. Food Chem Toxicol 41(4):489–521. doi:10.1016/S0278-6915(02)00279-X

26. Tarnow P, Hutzler C, Grabiger S, Schön K, Tralau T, Luch A (2016) Estrogenic activity of mineral oil aromatic hydrocarbons used in printing inks. PLoS One 11(1. doi:10.1371/journal.pone.0147239

27. Kimber I, Carrillo JC (2016) Oral exposure to mineral oils: is there an association with immune perturbation and autoimmunity?. Toxicology 344–346:19–25. doi:10.1016/j.tox.2016.01.008

28. Additives JFWECoF (2012) Summary and conclusions to the seventy-sixth meeting. Food and Agriculture Organization of the United Nations. World Health Organization, Genewa

29. Lommatzsch M, Richter L, Biedermann-Brem S, Biedermann M, Grob K, Simat TJ (2016) Functional barriers or adsorbent to reduce the migration of mineral oil hydrocarbons from recycled cardboard into dry food. Eur Food Res Technol:1–7. doi:10.1007/s00217-016-2672-6

30. Grob K (2010) Chemical risks in foodstuffs. Nachricht Chem 58(9):915–917

31. Braschi I, Bisio C, Buscaroli E, Bussini D, Elegir G, Marchese L (2016) (Application No. 102016000072535) Use of mesoporous silica 12/07/2016. Italy Patent

32. Topka P, Karban J, Soukup K, Jirátová K, Šolcová O (2011) Preparation of Al-SBA-15 pellets with low amount of additives: effect of binder content on texture and mechanical properties. Application to Friedel–Crafts alkylation. Chem Eng J 168(1):433–440. doi:10.1016/j.cej.2010.12.079

33. Han Y, Choi J, Tong M, Kim H (2014) Synthesis and characterization of high-surface-area millimeter-sized silica beads with hierarchical multi-modal pore structure by the addition of agar. Mater Char 90:31–39. doi:10.1016/j.matchar.2014.01.018

34. Sharma P, Seong JK, Jung YH, Choi SH, Park SD, Yoon Y II, Baek IH (2012) Amine modified and pelletized mesoporous materials: synthesis, textural-mechanical characterization and application in adsorptive separation of carbondioxide. Powder Technol 219:86–98. doi:10.1016/j.powtec.2011.12.023

35. Lind A, du Fresne von Hohenesche C, Smått JH, Lindén M, Unger KK (2003) Spherical silica agglomerates possessing hierarchical porosity prepared by spray drying of MCM-41 and MCM-48 nanospheres. Microporous Mesoporous Mater 66(2–3):219–227. doi:10.1016/j.micromeso.2003.09.011

36. Etgar L, Schuchardt G, Costenaro D, Carniato F, Bisio C, Zakeeruddin SM, Nazeeruddin MK, Marchese L, Graetzel M (2013) Enhancing the open circuit voltage of dye sensitized solar cells by surface engineering of silica particles in a gel electrolyte. J Mater Chem A 1(35):10142–10147. doi:10.1039/C3TA11436H

37. Zhao D, Huo Q, Feng J, Chmelka BF, Stucky GD (1998) Nonionic triblock and star diblock copolymer and oligomeric surfactant syntheses of highly ordered, hydrothermally stable, mesoporous silica structures. J Am Chem Soc 120(24):6024–6036. doi:10.1021/ja974025i

38. Batonneau-Gener I, Yonli A, Trouvé A, Mignard S, Guidotti M, Sgobba M (2010) Tailoring the hydrophobic character of mesoporous silica by silylation for VOC removal. Sep Sci Technol 45(6):768–775. doi:10.1080/01496391003609155

39. Bradley EL, Castle L, Speck DR (2014) Model studies of migration from paper and board into fruit and vegetables and into Tenax™ as a food simulant. Food additives and contaminants—Part A chemistry, analysis, control, exposure and risk. Assessment 31(7):1301–1309. doi:10.1080/19440049.2014.914633

40. Sacchetto V, Bisio C, Olivas Olivera DF, Paul G, Gatti G, Braschi I, Berlier G, Cossi M, Marchese L (2015) Interactions of toluene and n-hexane on high silica zeolites: an experimental and computational model Study. J Phys Chem C 119(44):24875–24886. doi:10.1021/acs.jpcc.5b08380

41. Sacco A, Lamberti A, Gerosa M, Bisio C, Gatti G, Carniato F, Shahzad N, Chiodoni A, Tresso E, Marchese L (2015) Toward quasi-solid state dye-sensitized solar cells: effect of γ-Al$_2$O$_3$ nanoparticle dispersion into liquid electrolyte. Sol Energy 111:125–134. doi:10.1016/j.solener.2014.10.034

42. Costenaro D, Gatti G, Carniato F, Paul G, Bisio C, Marchese L (2012) The effect of synthesis gel dilution on the physico-chemical properties of acid saponite clays. Microporous Mesoporous Mater 162:159–167. doi:10.1016/j.micromeso.2012.06.023

43. Chen S-Y, Tang C-Y, Chuang W-T, Lee J-J, Tsai Y-L, Chan JCC, Lin C-Y, Liu Y-C, Cheng S (2008) A facile route to synthesizing functionalized mesoporous SBA-15 materials with platelet morphology and short mesochannels. Chem Mater 20(12):3906–3916. doi:10.1021/cm703500c

44. Guazzotti V, Limbo S, Piergiovanni L, Fengler R, Fiedler D, Gruber L (2015) A study into the potential barrier properties against mineral oils of starch-based coatings on paperboard for food packaging. Food Packag Shelf Life 3:9–18. doi:10.1016/j.fpsl.2014.09.003

45. Zurfluh M, Biedermann M, Grob K (2013) Simulation of the migration of mineral oil from recycled paperboard into dry foods by Tenax®? Food Addit Contam Part A 30(5):909–918. doi:10.1080/19440049.2013.790089

46. Li W, Gao J, Wu G, Zheng J, Ouyang S, Luo Q, Zhang G (2016) Physicochemical and structural properties of A- and B-starch isolated from normal and waxy wheat: effects of lipids removal. Food Hydrocoll 60:364–373. doi:10.1016/j.foodhyd.2016.04.011

Corresponding Author: Dr. ilaria braschi, Ph.D. Assistant Professor

Corresponding Author's Institution: University of Bologna

First Author: Enrico Buscaroli, PhD

Order of Authors: Enrico Buscaroli, PhD; Luigi Sciubba, PhD; Gloria Falsone, Assistant Professor; Luciano Cavani, Assistant Professor; Emanuele Argese, Full Professor; Claudio Marzadori, Associate Professor; Bertrand Pourrut, Assistant Professor; ilaria braschi, Ph.D. Assistant Professor

Suggested Reviewers: Tomoyuki Makino
National Institute for Agro-Environmental Sciences, National Institute for Agro-Environmental Sciences
t_makino@affrc.go.jp
It is an expert of soil restoration by saline washing

Filip M. G. Tacka
Applied Analytical and Physical Chemistry, Ghent University
Filip.Tack@UGent.be
He is an expert in cycling and ecosystem impact of metals

Oliver Schramel
Institute for Ecological Chemistry, GSF-National Research Centre for Environment and Health
oliver.schramel@gsf.de
He is an expert of metal extraction procedures

Rodrigo Navia
Professor, Nucleo Científico Tecnologico en Biorrecursos, Universidad de La Frontera
rnavia@ufro.cl
He is an expert of waste management

Adel Reyhanitabar

Department of Soil Science, Faculty of Agriculture
areyhani@tabrizu.ac.ir
He is an expert of metal bioavailability

Zhaolong Zhu
State Key Laboratory of Soil Erosion and Dryland Farming on the Loess
Plateau, State Key Laboratory of Soil Erosion and Dryland Farming on the
Loess Plateau
zhu_zl@nwsuaf.edu.cn
Expert of soil aggragates stability

Cover Letter

DEPARTMENT OF AGRICULTURAL SCIENCES

Ilaria Braschi, Ph.D.

Assistant Professor

Department of Agricultural Sciences - University of Bologna

Viale G. Fanin 44, 40127 Bologna (Italy)

E-mail: ilaria.braschi@unibo.it

Phone: +39.051.2096208; Mobile: +39.329.9731940, Fax: +39.051.2096203

Bologna, March 30, 20017

Dear Editor,

I am submitting a manuscript entitled "Calcium chloride washing of wet calcareous sediments from fresh water canal: Effect on heavy metal removal and water aggregate stability" authored by Enrico Buscaroli, Luigi Sciubba, Gloria Falsone, Luciano Cavani, Emanuele Argese, Claudio Marzadori, Bertrand Pourrut, and myself for publication on Chemosphere Journal.

The ability of $CaCl_2$ washing to remediate acidic soils from heavy metals, along with the proved feasibility to reuse the treated soils for agriculture purpose, has been widely addressed in the literature. On the contrary, the effect of $CaCl_2$ on different environmental contexts as calcareous soils/sediments has not been investigated yet. In this study, the ability of $CaCl_2$ washing to restore a calcareous sediment polluted with Cu and Zn excavated from a calcareous fresh water canal was evaluated and the water stability of the washed sediment was assessed with the aim to use the treated sediment for on-site bank shaping of water channel.

The $CaCl_2$ washing operated on the dredged wet calcareous sediment successfully decreased its Cu and Zn content with the highest efficiency in the most polluted sediment sample (-26% and -10% of pseudo-total content, respectively) with copper mainly removed from the sulfide-organic matter fraction and zinc from the carbonates and, to a lesser extent, from the sulfide-organic matter component. The increased flocculation of the clay fraction due to the occurrence of calcium ion negatively affected the water macroaggregate stability of washed sediment.

The washing had different effect on the potential bioavailability of the metals, lowering the DTPA extractable amount of Cu and increasing that of Zn with respect to the control. Nevertheless, after one year of dry storage, both metals showed a potential bioavailability in washed sediment much lower than the corresponding air dry control.

These preliminary findings indicate the $CaCl_2$ washing as a valuable method to strongly abate the total amount of Cu and, to a minor extent, Zn in wet calcareous sediment dredged from fresh water canals with an associated drop of their potential bioavailable fraction in a time period of one year after dredging.

The use of slightly acidic pH values in association to $CaCl_2$ washing to tune the removal of Zn from the carbonates phase, followed by the correction of the decreased water aggregate stability of washed sediments by good quality organic amendments will represent the natural evolution of this preliminary investigation.

We believe that the manuscript is suitable for publication on Chemosphere Journal, in that the obtained results can be applied to relevant environmental issues.

Best regards,
Ilaria Braschi

Highlights

- Cu and Zn speciation in polluted calcareous sediment from fresh water canal

- O*n-site* 0.5 M CaCl$_2$ washing of sediment

- Removal of Cu and Zn from the most polluted washed sediment

- Water aggregate stability of washed sediment

- DTPA extractable fraction of trace metals in washed sediment

1   **Calcium chloride washing of wet calcareous sediments from fresh water canal: Effect on heavy metal**

2   **removal and water aggregate stability**

3

4   Enrico Buscaroli [1], Luigi Sciubba [1], Gloria Falsone [1], Luciano Cavani [1], Emanuele Argese [2], Claudio

5   Marzadori [1], Bertrand Pourrut [3], Ilaria Braschi [1, *]

6

7   [1] Department of Agricultural Sciences, University of Bologna, I-40127 Bologna, Italy

8   [2] Department of Molecular Sciences and Nanosystems, University Ca' Foscari, I-30123 Venezia, Italy

9   [3] ISA [3] Yncrea Hauts de France - ISA Lille, LGCgE, F-59046 Lille, France

10

11   * Corresponding author: ilaria.braschi@unibo.it, phone: +330512096208, fax +330512096203

12

13   **Highlights**

14   • Cu and Zn speciation in polluted calcareous sediment from fresh water canal

15   • O*n-site* 0.5 M CaCl$_2$ washing of sediment

16   • Removal of Cu and Zn from the most polluted washed sediment

17   • Water aggregate stability of washed sediment

18   • DTPA extractable fraction of trace metals in washed sediment

19

20   **Abstract**

21   Anthropic heavy metals contamination is one of the most concerning pollution that sediments of water canals

22   may suffer from. Canal dredging and shaping tend to produce huge amounts of contaminated sediments with

23   high associated costs for their disposal. Therefore the development of on-site sediment treatments able to

24   remove heavy metals and preserve sediments to water erosion for eventual channel embankments is of

utmost importance. In this study, the ability of a 0.5 M CaCl2 washing to remove Cu and Zn from polluted

calcareous sediment samples dredged from a fresh water canal and the aggregate water stability of the

washed samples were assessed. Samples differed for texture and pseudo-total metal content with the most

polluted sample (ca. 200 and 500 mg/kg of Cu and Zn, respectively) close to the waste water treatment plant

affluent to the water canal. In the sample, the washing decreased Cu pseudo-total amount of approx -26%

mainly in the sulfide/organic fraction, whereas Zn was lowered of -10% mainly in the carbonates phase. A

decreased dispersivity of clay fraction was observed in washed samples due to the flocculation effect of Ca

ions. At large size scale, the aggregates formed by the interaction between large particles and flocculated

clay presented lower water stability with respect to the control. Interestingly, the average percentage of Cu

and Zn potentially bioavailable sensibly dropped (23 and 13% of pseudo-total amount, respectively) with

respect to the control (40 and 19%) and carbonates phases increased (+33%) in the washed sediment after

one year dry storage

Keywords: Cupper removal, Zinc removal, Metal speciation, CaCl$_2$ washing, Water aggregate stability

index, DTPA extractable metal content

Introduction

Heavy metals are generally considered concerning environmental pollutants which largely affect

industrialized areas (Sanz, 2011; Plant et al., 2012). They can be transferred and accumulated along the food

chain with an associated toxic effects on *biocoenosis* (Steinberg, 2011). Heavy metals are commonly

discharged from sewage treatment plants to superficial waters where they subsequently precipitate and/or are

adsorbed on sediments transported by water flow (Pulatsü and Topçu, 2015).

Metal species in soil, sediment, and water are more or less mobile, soluble, exchangeable or bioavailable to

organisms according to their nature, chemical framework, pH conditions, redox potential and availability of

specific enzymes (Violante et al., 2007; Motuzova et al., 2012). As a matter of fact, a high total

concentration of these pollutants in environmental matrices does not necessarily result in a high

bioavailability or in a high *biota* uptake (Tack and Verloo, 1996; Hooda, 2010). Owing to the intrinsic

complexity of the equilibria supporting the bioavailability of heavy metals in soil, sediment and water

1   bodies, in general, policy-makers consider metal hazardousness as a sole function of their total or pseudo-

2   total amount. This is also the case of Italy, where the risk assessment policies request the total metal analysis

3   on soil (Standardization, 1995, 1998; 1999).

4   The management of artificial water canals is onerous, as they need to be reshaped from time to time in order

5   to maintain them functional. This produces large amount of excavated materials, whose possible on-site

6   reuse often depends on their heavy metals content. The directive 2000/60/CE does not report any limit for

7   heavy metal content in water sediments: in the absence of a specific European regulation to refer, member

8   states usually adopt the local limits reported for soil. Even in case water channel sediments slightly exceed

9   the soil heavy metals' limits for a few of them, excavated material cannot be reused for their bank shaping or

10   spread on neighbouring fields and, in countries where it is still allowed, are actually disposed in landfill.

11   In accordance to the European guidelines (EEC, 1986), the soil/sediment consumption needs to be restricted

12   as much as possible. For these reasons, the chance to develop on-site environmentally friendly treatments to

13   be performed on excavated wet sediments characterized by medium-low heavy metal pollution has to be

14   thoroughly considered.

15   Several soil/sediment treatments aimed at removing or immobilizing metals and heavy metals are available

16   in the literature (Rulkens and Bruning, 2005; Dermont et al., 2008; Kumpiene et al., 2008; Peng et al., 2009;

17   Juwarkar et al., 2010). Those based on extractants consist in exposing polluted matrices to aqueous solution

18   at different pH and extraction ability. On a pH scale, the strong acidic treatments and the use of saline

19   solutions can be considered poles apart. In fact, the strong pH drop provoked by the formers removes the

20   highest amount of heavy metals by decreasing the matrix negative charge and disaggregating or dissolving

21   some of its components. On the contrary, the latters are able to displace the exchangeable fraction of metal

22   cations with minimal effect on the matrix pH (Maejima et al., 2007). In this context, the suitability of $CaCl_2$

23   treatments followed by the addition of organic amendments for the correction of alkaline-sodic soils is well

24   known (Sastre-Conde et al., 2015). Alternatively, acidic pH can be also combined to $CaCl_2$ to improve the

25   displacement of heavy metals from soil exchange sites (Ahmad, 2009).

26   The ability of $CaCl_2$ washing to remediate acidic soils from heavy metals, along with the proved feasibility to

27   reuse the treated soils for agriculture purpose, has been widely addressed in the literature. The effect of

28   $CaCl_2$ on the restoration of soils polluted with Cd has been examined in depth (Makino et al., 2006; Maejima

1 et al., 2007; Makino et al., 2007). Among several acidic and saline treatments, 0.1 M $CaCl_2$ washing has

2 been proved as optimal to remove Cd from polluted acidic paddy fields in Japan (Maejima et al., 2007).

3 Though the removal mainly affected the Cd exchangeable fraction, a significant Cd decrease was observed in

4 rice grains grown on the washed fields (Makino et al., 2006). In addition, the reduced soil fertility in the

5 washed paddy fields could be corrected with no effect on the plant growth (Makino et al., 2006). An even

6 lower Cd content was observed in soybean once the washed acidic paddy fields were converted to upland

7 fields (Makino et al., 2007).

8 On the contrary, the effect of $CaCl_2$ on different environmental contexts as calcareous soils/sediments has not

9 been investigated yet. In this study, the ability of $CaCl_2$ washing to restore a calcareous sediment polluted

10 with Cu and Zn excavated from an Italian fresh water canal was evaluated and the water stability of the

11 washed sediment was assessed with the aim to use the treated sediment for on-site bank shaping of water

12 channel.

13

14 **Materials and Methods**

15

16 *Sediment sampling*

17 Sediment samples were collected from a fresh water canal of Padanian Plain (Northern Italy) during summer

18 2013 in three different spots: S1 (11°13'10.5"E 44°42'57.2"N), S2 (11°12'55.5"E 44°43'04.3"N) and S3

19 (11°12'38.7"E 44°43'12.5"N). The samples were kept at the distance of 50, 390 and 840 m from a urban

20 wastewater treatment plant (WWTP) affluent to the canal and built to supply 7000 population equivalent.

21 The canal section was 1.5 m at the bottom, 5.5 m at the upper mouth and 2.5 m deep. At the sampling, the

22 water depth was about 30 cm. At each position, about 30 kg of canal bed sediment were collected from the 0-

23 20 cm layer. All the wet samples were then sieved at 2 mm, homogenized and separately stored at 4°C.

24 About one half of each sample underwent $CaCl_2$ washing, while the rest was used as a control.

25

26 *$CaCl_2$ washing*

27 $CaCl_2 \cdot 2H_2O$ (Merck) and milliQ water were used to prepare a 0.5 M calcium chloride solution. Fresh

28 sediment aliquots equivalent to 100 g dry mass (dm) were contacted with 250 mL of 0.5 M $CaCl_2$ solution

1 into 500 mL Nalgene^{TM} centrifuge tubes. The tubes were then placed on a horizontal shaker (Continental

2 Instruments VDR) for 6 h at room temperature (RT). Finally, sediment samples were rinsed with milliQ

3 water up to restore their original EC value. All trials were repeated twice.

4 Control trials were conducted following the same procedures described above in the presence of 25 mL of

5 milliQ water in the place of $CaCl_2$ solution.

6

7 *Sediment characterization*

8 With the exception of the moisture content which was obtained as a mass loss at 105 °C overnight of fresh

9 and homogenized samples, the physico-chemical characterizations were performed on sediment samples air-

10 dried, milled through a ball mill (Retsch, Haan, Germany) and sieved at 2 mm.

11 Volatile solids were determined as a mass loss at 550 °C for 4 h. The pH (ISO 10390) was determined with a

12 Crison pH-probe (Spain) in deionized water or 10 mM $CaCl_2$ aqueous solution. Electrical conductivity (EC-

13 ISO 11265) was measured by a Radiometer conductivity meter (Denmark). Total organic carbon (TOC-ISO

14 14235) and total nitrogen (TN-ISO 11261) were determined using an organic elemental Thermo Scientific

15 Flash 2000 CHNS-O analyzer (USA). Total carbonates were determined according to ISO 10693 procedure.

16 All the analyses were performed in triplicate.

17

18 *Pseudo-total metal content*

19 Pseudo-total trace metals of sediment samples were determined through wet acid digestion (ISO 12914, ISO

20 22036). Digested samples were filtered through Whatman no.42 paper filters and analyzed by a Spectro

21 Arcos ICP-OES (Ametek, Germany). The determination was done in triplicate and a certified BRC-145R

22 external standard was used.

23

24 *DTPA extractable fraction of trace metals*

25 A diethylentriaminopentaacetic acid (DTPA) extraction was used in order to estimate the potentially

26 bioavailable fraction of trace metals. Sediment samples were contacted with a DTPA solution (1.97 g/L

27 DTPA, 1.46 g/L $CaCl_2$, 14.92 g/L triethanolamine) at pH 7.3 at 1:2 w:v ratio, shaken for 2 h, filtered through

28 Whatman no. 42 paper filters and analyzed by ICP-OES. The analyses were performed in triplicate.

1

Metal speciation

3 About 2 g of air dry sediment samples were lyophilized and then subjected to five step sequential extraction

4 based on Tessier's protocol (Tessier et al., 1979) modified as already described by Argese and co-workers

5 (Argese et al., 2003). The sequential extraction allowed to discriminate the distribution of heavy metals

6 among the following geochemical phases: (1) Exchangeable metals; (2) Metals bound to carbonates; (3)

7 Metals bound to the most labile amorphous Mn and Fe oxides/hydroxides; (4) Metals bound to less labile

8 low crystallinity grade Mn and Fe oxides/hydroxides; (5) Metals bound to sulfides-organic matter; (6)

9 Residual fraction.

10 After each extraction step, the residue was washed again with the extractant then twice with Milli-Q water.

11 The extraction solutions and milliQ washings were pooled together, filtrated at 0.45 μm with cellulose

12 acetate filters (2.5 cm diameter, Axiva Sichem Biotech, Delhi, India) before ICP-OES analysis. All the

13 determinations were performed in triplicate.

14

Particle size distribution and dispersivity of clay fraction

16 The particle size distribution was determined by the pipette method (Gee and Bauder, 1986) using two

17 different dispersants: *(i)* sodium hexametaphosphate [$(NaPO_3)_6$] and *(ii)* deionised water. For each dispersion

18 procedures, five particle size classes were determined (Staff, 1993): coarse sand (2.0-0.2 mm), fine sand

19 (0.20-0.05 mm), coarse silt (0.05-0.02 mm), fine silt (0.02 mm-2 μm), and clay (<2 μm). The samples

20 textural class was defined on the basis of the sodium hexametaphosphate data (Soil Survey Division Staff,

21 1993).

22 The <2 μm fractions obtained by the two dispersion procedures were labelled as sodium-dispersible clay

23 (SDC) and water-dispersible clay (WDC). The dispersivity of clay fraction was evaluated by the WDC/SDC

24 ratio (i.e., clay dispersion ratio – CDR).

25 The particle size distribution and dispersivity of clay fraction were performed on control and $CaCl_2$-trated

26 samples.

27

Wet aggregate stability of sediment samples

1   The wet aggregate stability (Kemper and Rosenau, 1986) was evaluated on rewetted sediment samples by 1 d

2   incubation at their original water content (63.7, 62.9 and 54.1% for S1, S2 and S3, respectively), in order to

3   simulate the field condition. Then, 10 g of each rewetted sample were wet sieved at 0.2 mm for 10 and 60

4   min using an automatic shaker at 60 cycles min^{-1}. The material remaining on the sieves was then dried and

5   weighed. The amount of stable samples (i.e. the fraction that maintained its size >0.2 mm) was corrected for

6   the content of coarse sand determined after H_2O_2 oxidation and subsequent $(NaPO_3)_6$ dispersion according to

7   van Reeuwijk LP (2002) (van Reeuwijk, 2002) and skeleton grains obtained after further samples wet

8   sieving to 2 mm. The wet aggregate stability index (WAS%) was calculated as follows:

$$WAS\% = \frac{weight\ retained - weight\ of\ coarse\ sand - weight\ of\ skeleton\ grains}{total\ sample\ weight - wieght\ of\ coarse\ sand - weight\ of\ skeleton\ grains} \cdot 100 \qquad (1)$$

9   Water aggregate stability was determined on control and $CaCl_2$-treated samples.

10

11   **Results and Discussion**

12

13   This study explores the ability of on-site 0.5 M $CaCl_2$ washing to lower the content of heavy metals

14   accumulated in wet calcareous sediment samples collected from a fresh water canal and the effect on the

15   aggregate water stability of the washed sediment. The washing was intended to be performed on wet dredged

16   sediments to exploit the maximal expansion of their hydrated internal surfaces, as those of expandable clay

17   and organic matter components (Dal Ferro et al., 2012; Zhang et al., 2016) to maximize the eventual

18   displacement of cationic metals by calcium ions.

19

20   *Physico-chemical properties and heavy metal content of control sediments*

21   The physico-chemical characteristics of fresh sediment samples are reported in Table 1. The sediment

22   moisture differed among the samples in the range 54.1-63.7 % fm. The content of volatile solids, that is

23   related to the amount of thermally unstable organic compounds, spaced between 7.2 to 14.1% dm. The sub-

24   alkaline pH-$_{H_2O}$ values of samples (7.5-8.2) decreased by -0.4 pH unit, on average, when measured in 10

25   mM $CaCl_2$ solution, thus revealing a certain exchange acidity. The sediment samples presented moderate

electrical conductivity (EC) between 0.55 and 1.09 dS m^{-1} whereas the TOC was quite consistent and varied from 9.62 to 5.52 % dm. The carbonates content ranged between 13.4 and 9.04 % dm.

The volatile solids, EC and TOC decreased in the samples by increasing the sampling distance from the WWTP (from S1 to S3; Table 1), thus enlightening the treatment plant contribute to the input of organic matter and ions into the water canal.

Among samples, the pH of 8.2 was found at the maximal sampling distance from the WWTP (S3): such a pH value is typical of carbonates phase at equilibrium with the sediment solid phases (Chesworth et al., 2008b). On the contrary, the lowest pH values measured in the sediment samples closer to the WWTP associated to higher TOC (9.62 and 8.22% dm, respectively) are typical conditions of carbonates dissolution. However, the dissolution of carbonates was not yet complete and the presence of $CaCO_3$ in S1 and S2 maintained sediment pH between 7 and 8, as often reported (Chesworth et al., 2008a).

The sediment samples showed a different texture, having S1 and S2 silt loam and S3 clay textural class, respectively. The difference observed between S1-S2 and S3 samples was related to the presence of a weir immediately after the S3 sampling position and connecting the sampled canal perpendicularly to another one. The hydraulic device partially limited the water flowing into the receiving water canal, thus creating a physical barrier to the transport of suspended particles and allowing the sedimentation of clay components at S3 site.

The current Italian legislation Dlgs 152/2006 indicates two thresholds for contaminants concentration in soil on the basis of its use (namely, limits A and B). According to the legislation, in case all contaminants are lower than their A limit, soils and, owing to the lack of specific legislation for sediments, sediments can be re-used in green/residential areas. If the amount of each contaminant is between A and B thresholds, the material can be used in industrial sites only. Finally, in case the B limit is exceeded by at least one contaminant, the soil/sediment must be removed and, when allowed, conferred to a landfill. The metal regulated by Dlgs 152/2006 and their content in the sediment samples are reported in Table 2.

In the sediment samples, the content of the metals is below their A limit with the exception of Cu in S1 and S2, and Sn and Zn with values between A and B limits in all the samples.

Copper and zinc are commonly found to exceed the admitted limits in sediments of fresh water canals and rivers of industrialized areas(Rauret et al., 1988; Kelderman and Osman, 2007; Ferronato et al., 2015).

1   In our samples, the level of copper and zinc decreased with respect to the sampling distance from the WWTP

2   (Table 2). The observed trend indicates the WWTP as a point source of Cu and Zn pollution as confirmed by

3   their background values in neighbouring soils of ≤60 and 76-150 mg/kg, respectively (Marchi et al., 2016).

4   On the contrary, the Sn background value >1.5 mg/kg was in the range of value reported for Padanian Plain

5   (Saeki et al., 1993) and its trend in the sediment samples ruled out its anthropic origin.

6

7   *CaCl$_2$ washing: effect on Cu and Zn content of sediment samples*

8   A significant removal of Cu and Zn was observed in all the washed sampleswith respect to the control. For

9   Cu -25.8±2.3% in S1, -20.7±2.4 in S2 and -29.8±2.0% in S3 was found. A similar trend was observed for Zn,

10   although a lower percentage was removed from the samples with respect to Cu: -10±2.1% in S1, -7.7±1.2 in

11   S2 and -3.7±0.9% in S3. To our knowledge, such a high removal of the two heavy metals by CaCl$_2$ washing

12   has never been observed in calcareous sediment.

13   Interestingly, when the washing was performed on the sediment samples air dry stored for one year, no

14   decrease of Cu and Zn content was observed, although their displacement was facilitated by rewetting the

15   samples for one week before washing. The washing ineffectiveness indicated the oxidizable sulfide-organic

16   matter fraction of fresh sediment as the component where Cu and Zn are mainly removed from by calcium

17   ion and the exploitation of the anoxic conditions of wet freshly dredged sediments for their removal.

18   To better understand which sediment components underwent Cu and Zn depletion, the distribution of the two

19   metals among the geochemical phases of sediment was evaluated and compared to the control. The metal

20   speciation was performed on the highest polluted sediment sample S1 in order to minimize the measure

21   uncertainty associated to the complexity of sequential extraction and the results are reported in Table 3.

22   The goodness of the extraction is indicated in Table 3 as a percentage of recovery with respect to the pseudo-

23   total amount (Ure et al., 1993; Sepahvand and Forghani, 2012; Samourgiannidis and Matsi, 2013). In the

24   case of Cu, the extraction recovery in the S1 control and washed sample resulted 84 and 97% of their

25   pseudo-total amount whereas for Zn the recovery was 103 and 107%. In the light of the experimental

26   complexity of each step of the sequential extraction, the metals recovery resulted largely acceptable and the

27   produced speciation data could be safely considered in the following.

1   In the control sample (Table 3), Cu was found mainly concentrated in the sulfide-organic matter fraction and,

2   to a minor extent, in the residual fraction, whereas Zn was found distributed among the phases in the order:

3   amorphous Fe/Mn-oxihydroxides > carbonates > sulfide-organic matter > low crystallinity grade Fe/Mn-

4   oxihydroxides fractions > exchangeable fraction.

5   The ability of the sulfide-organic matter fraction of water sediments to retain copper and zinc is well known

6   (Peng et al., 2009). In the fraction, the accumulation of a high proportion of heavy metals is mainly due to

7   volatile hydrogen sulfide (Hansen et al., 1996) as well as to sulfide minerals. Cu and Zn can easily

8   accumulate by displacing metals from the sulfide minerals surfaces (Peng et al., 2009). Zinc has a more

9   complex chemistry in anaerobic environments and it is generally found distributed among the solid phases of

10 calcareous sediments (Kelderman and Osman, 2007; Tack and Vandecasteele, 2008).

11 After washing, a strong Cu depletion in the sulfides-organic matter phase, passing from 113 to 81.8 mg/kg

12 was revealed. In parallel, a general redistribution of the exchanged metal was observed among the other

13 phases. Zn was displaced by $CaCl_2$ washing mainly from carbonates and, to a lesser extent, from the sulfides-

14 organic matter fraction and a redistribution was observed in both the amorphous and low crystallinity grade

15 Fe/Mn-oxides-hydroxides, as well as in the residual fraction.

16

17 *Effect of $CaCl_2$ washing on particle size distribution and wet aggregate stability of sediment samples*

18 The particle size distribution of control sediments obtained after $(NaPO_3)_6$-dispersion reflected the textural

19 class reported for each sample, and, as visible in Table 4, the amount of clay in S3 sample was 57.1% (i.e.,

20 clay textural class) while it was 12.7 and 19.9% for S1 and S2 samples (silt loam textural class). The silt

21 content (sum of coarse and fine silt) was 51.0, 60.4 and 38.0% and the sand content (sum of coarse and fine

22 sand) was 36.3, 19.7 and 4.9% in S1, S2 and S3, respectively. After water dispersion, in all control samples

23 the amount of clay particles was lower than after $(NaPO_3)_6$-dispersion, and the water dispersible clay (WDC)

24 amount was 12.1, 9.8 and 9.3% in S1, S2 and S3 samples, respectively (Table 4). The calculated clay

25 dispersion ratio (CDR, Table 4) suggested a decrease in clay dispersivity from S1 to S3 samples.

26 After $CaCl_2$ washing, a slight increase of sodium-dispersible clay and a consequent decrease in sand (both

27 coarse and fine sodium-dispersible) were found in the samples (Table 4). The WDC fraction was again lower

28 than the sodium-dispersible clay and the calculated CDR was 86.1, 29.2 and 5.6% in S1, S2 and S3,

respectively. Comparing the CDR of control and CaCl$_2$ washed samples, it was thus visible that the washing reduced the dispersivity of clay fraction in all samples. The ability of bivalent calcium ion to reduce the interparticle electrical repulsion allowing to the colloidal phase to flocculate is well known (Sposito, 1989).

The wet aggregate stability data indicated that S2 and S3 control samples contained a higher proportion of water stable particles than S1, as stability indexes after 10 minutes of wet sieving (WAS$_{10}$) were 88.1-81.8 *vs* 60.5%, respectively (Table 5). The high stability of S2 was confirmed also after 60 minutes of wet sieving (WAS$_{60}$: 67.0%) while S3 was the most fragile.

From the WAS indexes the negative effect of the CaCl$_2$-treatment on the aggregate stability was evident. For each sample and each sieving time, the WAS indexes in fact always decreased (Table 5). This was probably due to the flocculation Ca^{2+} effect, that produced new aggregates formed by large particles, such as sand or already formed smaller aggregates, linked to the flocculated clay phase and characterised by a low water resistance (Attou et al., 1998; Falsone et al., 2007).

In order to improve the water resistance of the washed sediment, the addition of organic amendments should be taken into account. The use of organic amendments can have in fact profound effects on aggregation, increasing aggregate stability through the formation of strong bonding involving Ca^{2+} bridges (Bronick and Lal, 2005; Sastre-Conde et al., 2015).

Effect of CaCl$_2$ washing on possible metal bioavailability of sediment samples

An evaluation of the potentially bioavailable metal fractions of washed calcareous sediment was assessed by DTPA extraction and compared with the control as reported in Table 6 (left side). Clearly, in fresh control samples, among the trace metals, copper and zinc showed the highest DTPA extractable contents. The washing of sediment samples differently affected the potential bioavailability of Cu and Zn with respect to the control and a decrease and an increase in their DTPA extractable amounts were observed, respectively.

The effect of the redox potential change associated to the wet-to-dry gradient on the metal bioavailability was evaluated in the washed sediment after one year of air dry storage and compared to the control kept under same conditions (Table 6 right side). In the control samples, both the Cu and Zn potential bioavailability sensibly increased after air dry storage (e.g. from 24.6 to 68.2 mg/kg and from 60.6 to 101 mg/kg for Cu and Zn, respectively, in S1). The combined effect of drying/oxidizing conditions on the

enhancement of metal bioavailability in sediments is well known (Saeki et al., 1993; Zoumis et al., 2001; Kelderman and Osman, 2007). Briefly, the oxidation of sulfides to sulphates and the accelerated degradation rate of the organic matter with a consequent acidification of the sediment induce an increase of metal bioavailability (Peng et al., 2009). In accordance to the mentioned mechanism, a slight pH decrease was revealed in control samples after air dry storage: from 7.5 to 7.2 (S1), from 7.8 to 7.5 (S2), and from 8.2 to 7.8 (S3).

Interestingly, in the washed samples air dry stored for one year, the DTPA extractable percentage of Cu and Zn contents still increased with respect to the fresh washed samples (e.g. from 20.0 to 36.3 mg/kg and from 68.9 to 74.8 mg/kg for Cu and Zn, respectively, in S1) but with a less pronounced effect than what already described for the dry stored control samples. Since no significant pH change was observed in the washed samples after air dry storage with respect to the air dried control samples, it was possible to conclude that the oxidizing conditions were less effective in the presence of calcium ion. In addition, an increase of carbonates content was observed: from 13.4 to 16.9 in S1, from 11.7 to 13.0 in S2, and from 10.6 to 10.9 in S3. These findings highlighted the ability of newly formed carbonates phase to buffer the acidity increase due to the oxidation of the sulfide-organic matter fraction of the washed sediment.

Conclusions

The $CaCl_2$ washing operated on the dredged wet calcareous sediment successfully decreased its Cu and Zn content with the highest efficiency in the most polluted sediment sample (-26% and -10% of pseudo-total content, respectively) with copper mainly removed from the sulfide-organic matter fraction and zinc from the carbonates and, to a lesser extent, from the sulfide-organic matter component. The increased flocculation of the clay fraction due to the occurrence of calcium ion negatively affected the water macroaggregate stability of washed sediment.

The washing had different effect on the potential bioavailability of the metals, lowering the DTPA extractable amount of Cu and increasing that of Zn with respect to the control. Nevertheless, after one year of dry storage, both metals showed a potential bioavailability in washed sediment much lower than the corresponding air dry control.

These preliminary findings indicate the $CaCl_2$ washing as a valuable method to strongly abate the total amount of Cu and, to a minor extent, Zn in wet calcareous sediment dredged from fresh water canals with an associated drop of their potential bioavailable fraction in a time period of one year after dredging.

The use of slightly acidic pH values in association to $CaCl_2$ washing to tune the removal of Zn from the carbonates phase, followed by the correction of the decreased water aggregate stability of washed sediments by good quality organic amendments will represent the natural evolution of this preliminary investigation.

References

1999. Minister decree DM13/09/1999 Approval of "Official methods for chemical analysis on soil". in: Agricole, M.p.l.P. (Ed.).

Ahmad, A., 2009. Study on Effect of HCl and CaCl2 on Extraction of Heavy Metals From Contaminated Soils. Asian Journal of Chemistry 21, 9.

Argese, E., Bettiol, C., Cedolin, A., Bertini, S., Delaney, E., 2003. Speciation of heavy metals in sediments of the lagoon of Venice collected in the industrial area. ANNALI DI CHIMICA 93.

Attou, F., Bruand, A., Le Bissonnais, Y., 1998. Effect of clay content and silt—clay fabric on stability of artificial aggregates. European Journal of Soil Science 49, 569-577.

Bronick, C.J., Lal, R., 2005. Soil structure and management: a review. Geoderma 124, 3-22.

Chesworth, W., Camps Arbestain, M., Macías, F., 2008a. Calcareous Soils. in: Chesworth, W. (Ed.). Encyclopedia of Soil Science. Springer Netherlands, Dordrecht, pp. 77-79.

Chesworth, W., Camps Arbestain, M., Macías, F., Spaargaren, O., Spaargaren, O., Mualem, Y., Morel- Seytoux, H.J., Horwath, W.R., Almendros, G., Chesworth, W., 2008b. Carbonates. in: Chesworth, W. (Ed.). Encyclopedia of Soil Science. Springer Netherlands, Dordrecht, pp. 99-101.

Dal Ferro, N., Berti, A., Francioso, O., Ferrari, E., Matthews, G.P., Morari, F., 2012. Investigating the effects of wettability and pore size distribution on aggregate stability: the role of soil organic matter and the humic fraction. European Journal of Soil Science 63, 152-164.

1 Dermont, G., Bergeron, M., Mercier, G., Richer-Laflèche, M., 2008. Soil washing for metal removal: A
2 review of physical/chemical technologies and field applications. Journal of Hazardous Materials 152, 1-31.

3 EEC, 1986. Council Directive 86/278/EEC of 12 June 1986 on the protection of the environment, and in
4 particular of the soil, when sewage sludge is used in agriculture. in: communities, T.c.o.t.e. (Ed.).

5 Falsone, G., Celi, L., Bonifacio, E., 2007. AGGREGATE FORMATION IN CHLORITIC AND
6 SERPENTINITIC ALPINE SOILS. Soil Science 172, 1019-1030.

7 Ferronato, C., Vianello, G., Vittori Antisari, L., 2015. Heavy metal risk assessment after oxidation of
8 dredged sediments through speciation and availability studies in the Reno river basin, Northern Italy. Journal
9 of Soils and Sediments 15, 1235-1245.

10 Gee, G.W., Bauder, J.W., 1986. Particle-size analysis. in: Klute, A. (Ed.). Methods of soil analysis. Part I.
11 ASA and SSSA, Madison, WI, USA, pp. 383-411.

12 Hansen, D.J., Berry, W.J., Boothman, W.S., Pesch, C.E., Mahony, J.D., Di Toro, D.M., Robson, D.L.,
13 Ankley, G.T., Ma, D., Yan, Q., 1996. Predicting the toxicity of metal-contaminated field sediments using
14 interstitial concentration of metals and acid-volatile sulfide normalizations. Environmental Toxicology and
15 Chemistry 15, 2080-2094.

16 Hooda, P.S., 2010. Trace Elements in Soils.

17 Juwarkar, A.A., Singh, S.K., Mudhoo, A., 2010. A comprehensive overview of elements in bioremediation.
18 Reviews in Environmental Science and Biotechnology 9, 215-288.

19 Kelderman, P., Osman, A.A., 2007. Effect of redox potential on heavy metal binding forms in polluted canal
20 sediments in Delft (The Netherlands). Water Res 41, 4251-4261.

21 Kemper, W.D., Rosenau, R.C., 1986. Aggregate stability and size distribution. in: Klute, A. (Ed.). Methods
22 of soil analysis. Part I. ASA and SSSA, Madison, WI, USA, pp. 425-442.

23 Kumpiene, J., Lagerkvist, A., Maurice, C., 2008. Stabilization of As, Cr, Cu, Pb and Zn in soil using
24 amendments - A review. Waste Management 28, 215-225.

25 Maejima, Y., Makino, T., Takano, H., Kamiya, T., Sekiya, N., Itou, T., 2007. Remediation of cadmium-
26 contaminated paddy soils by washing with chemicals: Effect of soil washing on cadmium uptake by soybean.
27 Chemosphere 67, 748-754.

28 Makino, T., Kamiya, T., Takano, H., Itou, T., Sekiya, N., Sasaki, K., Maejima, Y., Sugahara, K., 2007.
29 Remediation of cadmium-contaminated paddy soils by washing with calcium chloride: Verification of on-
30 site washing. Environmental Pollution 147, 112-119.

31 Makino, T., Sugahara, K., Sakurai, Y., Takano, H., Kamiya, T., Sasaki, K., Itou, T., Sekiya, N., 2006.
32 Remediation of cadmium contamination in paddy soils by washing with chemicals: Selection of washing
33 chemicals. Environmental Pollution 144, 2-10.

34 Marchi, N., Guermandi, M., Amorosi, A., Sammartino, I., 2016. Carta del fondo naturale dei metalli pesanti
35 della pianura emiliano-romagnola. Servizio Geologico, Sismico e dei Suoli.

Motuzova, G.V., Makarychev, I.P., Dergham, H.M., Stepanov, A.A., Barsova, N.U., 2012. Soil organic matter and their interactions with metals: Processes, factors, ecological significance.

Nazif, W., Marzouk, E.R., Perveen, S., Crout, N.M., Young, S.D., 2015. Zinc solubility and fractionation in cultivated calcareous soils irrigated with wastewater. The Science of the total environment 518-519, 310-319.

Peng, J.f., Song, Y.h., Yuan, P., Cui, X.y., Qiu, G.l., 2009. The remediation of heavy metals contaminated sediment. Journal of Hazardous Materials 161, 633-640.

Plant, J.A., Voulvoulis, N., Ragnarsdottir, 2012. Pollutants, Human Health and the Environment: A Risk Based Approach.

Pulatsü, S., Topçu, A., 2015. Review of 15 Years of Research on Sediment Heavy Metal Contents and Sediment Nutrient Release in Inland Aquatic Ecosystems, Turkey. . Journal of Water Resource and Protection 7, 16.

Rauret, G., Rubio, R., López-Sánchez, J.F., Casassas, E., 1988. Determination and speciation of copper and lead in sediments of a Mediterranean river (River Tenes, Catalonia, Spain). Water Research 22, 449-455.

Rulkens, W.H., Bruning, H., 2005. Cleanup technologies for dredged fine sediments: review and future challenges. Remediation of Contaminated Sediments: Finding Achievable Risk Reduction Solutions, C6-01.

Saeki, K., Okazaki, M., Matsumoto, S., 1993. The chemical phase changes in heavy metals with drying and oxidation of the lake sediments. Water Research 27, 1243-1251.

Samourgiannidis, G., Matsi, T., 2013. Comparison of Two Sequential Extraction Methods and the DTPA Method for the Extraction of Micronutrients from Acidic Soils. Communications in Soil Science and Plant Analysis 44, 38-49.

Sanz, L.H., 2011. Heavy metal sediments.

Sastre-Conde, I., Carmen Lobo, M., Icela Beltrán-Hernández, R., Poggi-Varaldo, H.M., 2015. Remediation of saline soils by a two-step process: Washing and amendment with sludge. Geoderma 247-248, 140150.

Sepahvand, H., Forghani, A., 2012. Comparison of two sequential extraction procedures for the fractionation of zinc in agricultural calcareous soils. Chemical Speciation & Bioavailability 24, 13-22.

Sposito, G., 1989. The Chemistry of Soils. Oxford University Press, New York.

Staff, S.S.D., 1993. Soil Survey Manual. in: Agriculture, U.S.D.o. (Ed.). Soil Conservation Service.

Standardization, I.O.f., 1995. ISO 11466:1995 Extraction of trace elements soluble in aqua regia. Soil quality.

Standardization, I.O.f., 1998. ISO 11047:1998 Determination of cadmium, chromium, cobalt, copper, lead, manganese, nickel and zinc -- Flame and electrothermal atomic absorption spectrometric methods. Soil quality.

1   Steinberg, R.V., 2011. Contaminated soils: Environmental impact, disposal and treatment.

2   Tack, F.M., Vandecasteele, B., 2008. Cycling and ecosystem impact of metals in contaminated calcareous
3   dredged sediment-derived soils (Flanders, Belgium). The Science of the total environment 400, 283-289.

4   Tack, P.M., Verloo, M.G., 1996. Metal contents in stinging nettle (Urtica dioica L.) as affected by soil
5   characteristics. Science of the Total Environment 192, 31-39.

6   Tessier, A., Campbell, P.G.C., Blsson, M., 1979. Sequential extraction procedure for the speciation of
7   particulate trace metals. Analytical Chemistry 51, 844-851.

8   Ure, A.M., Quevauviller, P., Muntau, H., Griepink, B., 1993. Speciation of Heavy Metals in Soils and
9   Sediments. An Account of the Improvement and Harmonization of Extraction Techniques Undertaken Under
10   the Auspices of the BCR of the Commission of the European Communities. International Journal of
11   Environmental Analytical Chemistry 51, 135-151.

12   van Reeuwijk, L.P., 2002. Procedure for Soil Analysis - Technical paper 9. FAO.

13   Violante, A., Huang, P.M., Gadd, G.M., 2007. Biophysico-Chemical Processes of Heavy Metals and
14   Metalloids in Soil Environments.

15   Zhang, L., Lu, X., Liu, X., Yang, K., Zhou, H., 2016. Surface Wettability of Basal Surfaces of Clay
16   Minerals: Insights from Molecular Dynamics Simulation. Energy & Fuels 30, 149-160.

17   Zoumis, T., Schmidt, A., Grigorova, L., Calmano, W., 2001. Contaminants in sediments: remobilisation and
18   demobilisation. Science of the Total Environment 266, 195-202.

19

1   **Table 1.** Physical and chemical characterization of fresh sediment samples.

	Sediment samples		
Parameter (unit)	**S1**	**S2**	**S3**
Moisture (% fm)	63.7	62.9	54.1
Volatile solids (% dm)	14.1	13.9	7.2
pH-$_{H_2O}$	7.5	7.8	8.2
pH-$_{CaCl_2}$	7.3	7.3	7.8
EC (dS m^{-1})	1.09	0.56	0.55
TOC (% dm)	9.62	8.22	5.52
Total carbonates (% dm)	13.3	13.4	9.04
Textural class	silt loam	silt loam	clay

2   fm: fresh mass; dm: dry mass

3

1 **Table 2.** Pseudo-total metal content (mg kg^{-1}) of sediment samples. The error is expressed as STD. Italian

2 current threshold limits (Dlgs 152/2006) are also reported for comparison (limit A: for public and private

3 green areas; limit B: for commercial and industrial sites).

Metal	Sediment sample			Dlgs 152/2006 threshold limits	
	S1	S2	S3	A	B
As	4.60 ± 0.06	4.76±0.28	4.83±0.17	20	50
Be	1.12±0.11	1.44±0.11	2.00±0.23	2	10
Cd	0.56±0.00	0.56±0.00	0.24±0.00	2	15
Co	10±0.06	11.9±0.34	15.5±0.06	20	250
Cr	73.2±2.26	82.9±5.99	96.6±11.3	150	800
Cr(VI)	n.d.	n.d.	n.d.	2	15
Cu	197±1.13	174±4.53	69.8±1.81	120	600
Hg	0.48±0.00	0.48±0.00	<LOQ	1	5
Ni	46.6±0.17	52.6±1.53	63.3±0.34	120	500
Pb	85.2±1.70	94.7±2.83	30.5±2.15	100	1000
Sb	2.68±0.06	2.16±0.23	1.64±0.06	10	30
Se	1.44±0.00	1.08±0.04	<LOQ	3	15
Sn	1.62±0.09	1.70±0.07	1.51±0.05	1	350
Tl	0.79±0.02	0.96±0.68	0.89±0.19	1	10
V	57.3±4.35	72.7±6.62	94.6±16.4	90	250
Zn	494±2.83	481±5.09	166±1.70	150	1500

4 n.d. not determined; LOQ: limit of quantification

5

1 **Table 3**: Five step metal speciation (mg/kg) of Cu and Zn in sediment sample S1 washed with water (as a

2 control) and with 0.5 M $CaCl_2$. The pseudo-total content of each metal is reported for comparison.

Metal fraction	Cu	Zn	Cu	Zn
Sediment sample S1	*Control*		*CaCl₂ Washed*	
Exchangeable	0.62	16.5	0.91	15.3
Carbonates	11.5	140	14.3	103
Amorphous Fe/Mn-oxihydroxides	10.2	153	10.5	155
Low crystallinity grade Fe/Mn-oxihydroxides	4.59	67.4	7.75	70.0
Sulfides and Organic matter	113	75.3	81.8	67.3
Residual	26.4	42.3	35.4	64.2
Sum of the above	166	495	151	475
Pseudo-total content	197	494	146	444
Recovery	84%	100%	103%	107%

3

Table 4. Particle size distribution* of control and CaCl$_2$ washed sediment samples by dispersion in water and (NaPO$_3$)$_6$ and the calculated clay dispersible ratio (CDR). All the values are reported as a percentage. The error is expressed as STD.

Sample	Dispersant	Coarse sand	Fine sand	Coarse silt	Fine silt	Clay	CDR
Control sediment samples							
S1	(NaPO$_3$)$_6$	4.2±0.5	32.1±4.2	14.5±1.8	36.5±2.6	12.7±0.7	-
S2	(NaPO$_3$)$_6$	1.7±0.2	18.0±1.5	18.5±1.7	41.9±2.2	19.9±1.3	-
S3	(NaPO$_3$)$_6$	0.2±0.1	4.7±0.7	2.8±0.4	35.2±2.2	57.1±3.0	-
S1	H$_2$O	3.8±0.8	29.7±1.2	29.3±0.7	25.2±1.9	12.0±0.8	95.1
S2	H$_2$O	1.2±0.2	41.0±3.9	23.1±1.1	24.9±0.8	9.8±1.1	49.7
S3	H$_2$O	0.3±0.1	9.8±1.0	11.1±0.9	69.5±3.2	9.3±1.2	16.3
CaCl$_2$-washed sediment samples							
S1	(NaPO$_3$)$_6$	2.8±0.4	28.2±1.3	12.3±1.1	37.7±2.3	19.0±1.1	-
S2	(NaPO$_3$)$_6$	1.0±0.3	20.3±1.4	9.0±1.5	42.6±3.2	27.1±1.8	-
S3	(NaPO$_3$)$_6$	0.5±0.2	0.5±0.1	1.8±0.7	36.1±1.6	61.1±2.3	-
S1	H$_2$O	2.8±0.7	27.4±2.7	25.0±2.4	28.4±0.2	16.4±0.9	86.1
S2	H$_2$O	2.3±0.5	12.4±0.3	35.5±2.8	41.9±2.1	7.9±0.7	29.2
S3	H$_2$O	0.9±0.2	7.1±0.5	8.2±1.5	80.3±3.3	3.5±0.3	5.6

*Coarse (2-0.2 mm) and fine sand (0.2-0.05 mm); coarse (0.05-0.02 mm) and fine silt (0.02 mm-2 µm); clay (<2 µm). CDR: water dispersible clay/hexametasphosphate dispersible clay x 100

1 **Table 5.** Evaluation of wet aggregate stability (WAS) of control and $CaCl_2$ washed sediment samples at 10

2 and 60 minutes of wet sieving

Sediment	$WAS_{10'}$		$WAS_{60'}$	
Sample	*Control*	*CaCl₂ washed*	*Control*	*CaCl₂ washed*
S1	60.5 ± 9.2	33.3 ± 10.9	42.4 ± 7.6	36.9 ± 4.9
S2	88.1 ± 6.8	52.0 ± 9.9	67.0 ± 3.8	47.7 ± 3.4
S3	81.8 ± 8.6	60.5 ± 0.2	23.4 ± 1.8	10.3 ± 4.5

3

4

Table 6. DTPA extractable trace metal content (mg kg^{-1}) of control and washed sediment samples with

2   associated error expressed as STD. In brackets the potential bioavailability expressed as percentage of the

3   pseudo-total metal content. The bioavailability was also tested on washed sediment samples after one year of

4   air dry storage. DTPA: diethylentriaminopentaacetic acid. LOQ: limit of quantification.

	S1	S2	S3	S1	S2	S3
Trace			**Control Sediment samples**			
Metal		*Fresh*			*One year air dry stored*	
Cd	0.21 ± 0.00	0.21 ± 0.00	0.15 ± 0.01	0.18 ± 0.01	0.16 ± 0.03	0.03 ± 0.01
	(38%)	(38%)	(63%)	(31%)	(26%)	(10%)
Co	0.57 ± 0.06	0.56 ± 0.05	0.50 ± 0.04	0.58 ± 0.01	0.51 ± 0.02	0.40 ± 0.01
	(6%)	(5%)	(3%)	(5%)	(4%)	(2%)
Cr	0.14 ± 0.01	0.14 ± 0.01	0.14 ± 0.01	<LOQ	<LOQ	<LOQ
	(<1%)	(<1%)	(<1%)			
Cu	24.6±1.01	26.4±1.10	18.7±0.50	68.2±0.8	71.4±1.2	27.5±0.5
	(12%)	(15%)	(27%)	(35%)	(41%)	(39%)
Ni	2.14±0.02	1.80±0.01	1.61±0.01	2.70±0.05	2.10±0.07	1.79±0.06
	(5%)	(3%)	(3%)	(6%)	(4%)	(3%)
Pb	11.9 ± 0.50	14.5 ± 0.2	7.90 ± 0.10	13.8 ± 0.1	16.9 ± 0.01	9.84 ± 0.03
	(14%)	(14%)	(26%)	(16%)	(18%)	(26%)
Zn	60.6 ± 2.20	44.6 ± 2.10	10.8 ± 0.50	101.0 ± 0.2	71.8 ± 0.2	17.9 ± 0.2
	(12%)	(9%)	(7%)	(20%)	(15%)	(12%)
			CaCl$_2$ washed sediment samples			
		Fresh			*One year air dry stored*	
Cd	0.08 ± 0.01	0.09 ± 0.01	0.03 ± 0.01	0.10 ± 0.01	0.08 ± 0.01	0.03 ± 0.01
	(38%)	(38%)	(63%)	(20%)	(18%)	(11%)
Co	0.45 ± 0.06	0.44 ± 0.04	0.33 ± 0.04	0.30 ± 0.01	0.29 ± 0.01	0.27 ± 0.01

	(6%)	(5%)	(3%)	(3%)	(2%)	(2%)
Cr	<LOQ	<LOQ	<LOQ	<LOQ	<LOQ	<LOQ
Cu	20.0 ± 1.01	23.3 ± 1.21	10.3 ± 0.50	36.3 ± 0.1	39.8 ± 0.1	13.2 ± 0.1
	(14%)	(15%)	(17%)	(25%)	(23%)	(22%)
Ni	2.14 ± 0.02	1.82 ± 0.03	1.57 ± 0.01	1.90 ± 0.09	1.60 ± 0.05	1.10 ± 0.01
	(5%)	(3%)	(3%)	(4%)	(3%)	(2%)
Pb	13.3 ± 0.5	14.1 ± 0.3	6.76 ± 0.10	17.8 ± 0.1	21.9 ± 0.1	8.14 ± 0.08
	(14%)	(14%)	(26%)	(21%)	(24%)	(21%)
Zn	68.9 ± 2.51	53.1 ± 1.97	15.6 ± 0.75	74.8 ± 0.2	61.9 ± 0.2	14.3 ± 0.2
	(15%)	(13%)	(10%)	(17%)	(13%)	(9%)

1

Graphical Abstract

Cu 25%   Zn 17%

Wet Aggregate Stability (60')
36.9%   42.4%

Zn 20%   Cu 35%

CaCl$_2$-washed sediment
Cu 146 mg/kg
Zn 445 mg/kg

Control sediment
Cu 197 mg/kg
Zn 494 mg/kg

FRESH WATER CANAL